UNIVERSITY OF AMSTERDAM

UvA-DARE (Digital Academic Repository)

Advanced head and neck cancer treatment: A basic step forward

Dohmen, A.J.C.

Publication date
2018
Document Version
Final published version
License
Other

Link to publication

Citation for published version (APA):
Dohmen, A. J. C. (2018). *Advanced head and neck cancer treatment: A basic step forward*. [Thesis, externally prepared, Universiteit van Amsterdam].

General rights
It is not permitted to download or to forward/distribute the text or part of it without the consent of the author(s) and/or copyright holder(s), other than for strictly personal, individual use, unless the work is under an open content license (like Creative Commons).

Disclaimer/Complaints regulations
If you believe that digital publication of certain material infringes any of your rights or (privacy) interests, please let the Library know, stating your reasons. In case of a legitimate complaint, the Library will make the material inaccessible and/or remove it from the website. Please Ask the Library: https://uba.uva.nl/en/contact, or a letter to: Library of the University of Amsterdam, Secretariat, Singel 425, 1012 WP Amsterdam, The Netherlands. You will be contacted as soon as possible.

UvA-DARE is a service provided by the library of the University of Amsterdam (https://dare.uva.nl)

Download date:09 Mar 2023

Advanced head and neck cancer treatment

A basic step forward

Advanced head and neck cancer treatment - A basic step forward

Amy J.C. Dohmen

2013

Amy J.C. Dohmen

ADVANCED HEAD AND NECK CANCER TREATMENT

A BASIC STEP FORWARD

Amy J.C. Dohmen

COLOFON

© 2018 by Amy J.C. Dohmen. All rights reserved.
PhD thesis, Head and Neck Oncology & Surgery and Cell Biology, The Netherlands Cancer Institute – Antoni van Leeuwenhoek
Amsterdam, The Netherlands

This research was funded by the Riki Stichting.

Printing and defense of this thesis were financially supported by:
NKI, Riki Stichting, ALK, PerkinElmer, Pfizer bv, Allergy Therapeutics Netherlands BV, ChipSoft and Dos Medical.

Cover: Cindy Cheung
Print and lay-out: Nauka Amsterdam

ISBN: 978-94-91688-11-9
Online: http://dare.uva.nl

ADVANCED HEAD AND NECK CANCER TREATMENT

A BASIC STEP FORWARD

ACADEMISCH PROEFSCHRIFT

ter verkrijging van de graad van doctor

aan de Universiteit van Amsterdam

op gezag van de Rector Magnificus prof. dr. ir. K.I.J. Maex

ten overstaan van een door het College voor Promoties ingestelde commissie,

in het openbaar te verdedigen in de Agnietenkapel

op donderdag 13 december 2018, te 14:00 uur

door

Amy Johanna Cornelia Dohmen

geboren te Eindhoven

Promotiecommissie:

Promotor(es):	Prof. dr. J.J.C. Neefjes	Universiteit Leiden
	Prof. dr. M.W.M. van den Brekel	Universiteit van Amsterdam
Copromotor(es):	Dr. C.L. Zuur	Universiteit van Amsterdam
	Prof. dr. H. Ovaa	Universiteit Leiden
Overige leden:	Prof. dr. A.J.M. Balm	Universiteit van Amsterdam
	Prof. dr. L.E. Smeele	Universiteit van Amsterdam
	Prof. dr. E. Bloemena	Vrije Universiteit Amsterdam
	Prof. dr. R.H. Brakenhoff	Vrije Universiteit Amsterdam
	Prof. dr. C.R.N. Rasch	Universiteit van Amsterdam
	Dr. C. Vens	Nederlands Kanker Instituut - Antoni van Leeuwenhoek
	Dr. S.M. Willems	Universitair Medisch Centrum Utrecht
Faculteit:	Tandheelkunde	

"*If you want to go fast, go alone.*
If you want to go far, go together."

Old African proverb

TABLE OF CONTENTS

CHAPTER 1

General introduction and thesis outline

GENERAL INTRODUCTION

Head and Neck Cancer

Before elaborating on head and neck cancer, let's start with cancer itself. Simplistically, cancer is defined as an uncontrolled growth of abnormal cells, with the potential to invade and spread to other parts of the body. This is in contrast to normal cells, which have a regulated cell cycle with controlled proliferation and cell death, maintaining healthy tissue homeostasis. In cancer however, this balance is disrupted via a very complex variety of biological features[1-3], which I will explain briefly. One of the most fundamental traits of cancer is that cancer cells can acquire the capability to sustain chronic proliferation, usually via growth factors. Additionally, cancer cells must circumvent anti-proliferation actions regulated by tumor suppressor genes. Inactivation or defects in these genes permits persistent tumor growth. Besides continuous cell proliferation, cancer cells must escape or be resistant to programmed cell death (i.e. apoptosis) and senescence (an irreversible state in which cells can no longer replicate and remain non-proliferative but metabolically active). This enables unlimited replicative potential in order to generate macroscopic tumors. Tumors require their own energy metabolism program, and they also need nutrients and oxygen to sustain this expanding growth. These latter needs are addressed through the formation of a vasculature of new blood vessels (angiogenesis). Furthermore, cancer cells have the ability to invade surrounding tissue and migrate to distant sites to form secondary tumor growths (metastases), via a complex cascade of events. Metastatic disease is responsible for over 90% of cancer-related deaths. All these mentioned cancer features[1-3] are facilitated by the development of genomic instability and by evading immunological attack and destruction. These core hallmarks of cancer (*Figure 1*) illustrate the complexity of cancer and also how challenging it is to treat cancer.

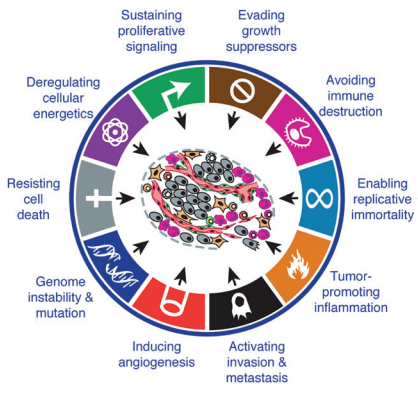

Figure 1. Hallmarks of Cancer. (With permission from Hanahan and Weinberg, Hallmarks of cancer: the next generation, Cell, 144(5):646-74, Elsevier, 2011, adapted from figure 6.)

The tumor microenvironment (TME) also plays an important role in cancer development. The TME is the cellular environment in which the tumor exists, and consists of multiple cell types, including stromal cells, endothelial cells, fibroblasts, immune cells (lymphocytes, macrophages, dendritic cells) and extracellular matrix. Cancer cells interact with the TME and can change this environment, thereby enabling primary, invasive and metastatic growth[2]. Sustaining tumor progression, the TME is also responsible for therapy resistance and prognosis[4].

Head and neck cancer is in 90% of the cases originating from mucosa squamous cells, known as head and neck squamous cell carcinoma (HNSCC). HNSCC comprises a range of malignant tumors of soft tissue originating from the mucosa of the oral cavity (mouth, including the lips), nasal cavity, paranasal sinuses, pharynx and larynx (*Figure 2*). Worldwide, HNSCC accounts for more than 809.000 incident cases and 316.000 deaths annually in 2015, ranking it the 7th cancer type globally[5]. Males are affected significantly more than females with a ratio ranging from 2:1 to 4:1, respectively[5].

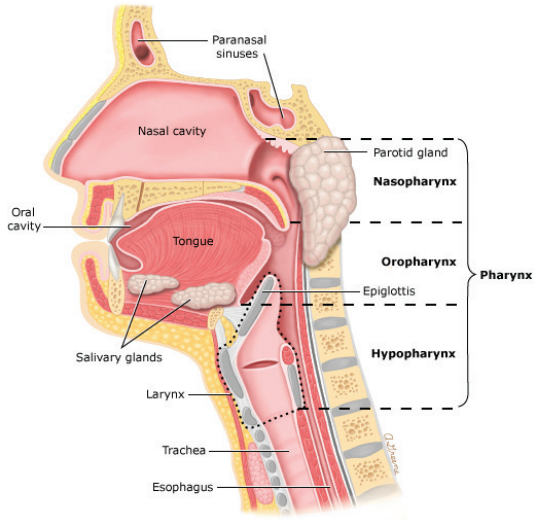

Figure 2. Anatomy of the head and neck. (With permission from: Brockstein BE, Overview of treatment for head and neck cancer, UpToDate, accessed on May 2018, Copyright, www.uptodate.com)

In 80% of the patients, HNSCC is strongly associated with tobacco use and alcohol consumption[6]. Besides this, HNSCC is increasingly associated with certain viruses, such as the sexually transmitted human papillomavirus (HPV, 25%) and the Epstein-Barr virus (EBV)[7,8]. HPV is in particularly associated with oropharyngeal cancer; the most common subtype is HPV16, accounting for around 80% of HPV positive HNSCC[9,10]. EBV infection

is mainly associated with nasopharyngeal cancer[8,10]. Chronic exposure of the upper aerodigestive tract to all factors mentioned above, can result in premalignant lesions of the mucosa and ultimately in HNSCC. Beside these factors, there is only a modest inherited familial susceptibility for HNSCC[11]. Patients with Fanconi anemia, a rare inherited disease, have an increased overall risk of 700-fold for developing HNSCC, compared to the general population[12,13]. Furthermore, HNSCC is known as a remarkably heterogeneous cancer with high intra-tumor genetic heterogeneity (high degree of genetic alterations in genomic DNA sequences between cells within an individual tumor)[14]. Commonly described genetic alterations are in the TP53, CDKN2A (p16), PIK3CA, PTEN, NOTCH and HRAS pathways[15-18].

General treatment options and prognosis

Current treatment selection relies on clinical, histopathologic and radiologic parameters to determine the stage of disease using the tumor-node-metastasis (TNM) classification[19]. This system indicates clinical outcome in general and assists the clinician in making appropriate treatment decision.

Approximately 30% of HNSCC patients presents with early stage disease (stage I or II). Approximately 80-90% of these patients are cured with surgery or radiotherapy (RT) alone[20-22]. However, the majority of patients presents with advanced stage disease (stage III or IV; 70% of HNSCC patients). For these patients, more challenging multi-modality treatment approaches are often indicated, including (a combination of) chemotherapy (CT), RT and surgery. However, their prognosis, showing an average 5-year survival of 46%, is relatively poor[20,21] due to a high local recurrence rate (around 30%) or development of a second primary tumor. Patients with a recurrent or metastatic (R/M) HNSCC have a poor 3- and 5-year survival of 7% and 3.6% respectively, with a median overall survival of 7.8 months[23]. Novel immunotherapy treatment for R/M HNSCC with Nivolumab shows, in a phase III trial, a 1-year survival of 36% (compared to 16.6% after standard of care) with a median survival of 7.5 months (compared to 5.1 months)[24]. A distinct clinical identity are patients with HPV related oropharyngeal SCC. They usually show an improved overall survival when compared to HPV negative oropharyngeal SCC[25,26]. TP53 is frequently mutated in HPV negative tumors and this is associated with reduced survival and resistance to therapy[27,28].

Advanced HNSCC: radiotherapy and chemoradiotherapy

70% of the patients suffer advanced stage HNSCC, in which (chemo-)radiotherapy is a key treatment modality. Radiotherapy works by exposing tissue to ionizing radiation (IR), a process called irradiation. IR damages the DNA inside cells, if these damages are

left unrepaired this could lead to cell death via distinct mechanisms such as apoptosis, senescence, necrosis and autophagy[29,30]. Both normal and cancer cells will be damaged by IR. Cancer cells could be eradicated by maximizing the radiation dose, however normal tissue will then inevitably be exposed to irradiation as well, leading to unacceptable toxicity. Therefore, a balance between tumor control and normal tissue damage must be kept, known as the therapeutic window[29]. By giving the total radiation dose in multiple fractions and therefore lower doses, normal tissues are given the opportunity to (partly) recover between the fractions[31].

Tumors have also mechanisms to resist radiation damage. TME, hypoxia and inherent resistance by mutations and repopulation are the main causes of treatment resistance[31]. Despite the high doses in which RT is given in HNSCC (up to 70 Gray (Gy) and boosts sometimes over 80 Gy) and the technical advances over the past years, the cure rate in advanced HNSCC is still relatively limited. Besides this, the high doses of RT cause considerable morbidity because normal cells receive radiation as well, leading to loss of organ integrity and impaired function, such as dysphonia and dysphagia.

In an effort to improve cure rates of locally advanced HNSCC, RT is combined with chemotherapy (CRT). For advanced HNSCC, standard of care chemotherapies are cisplatin and cetuximab. The conventional cisplatin chemotherapeutic has been combined with RT (CCRT) since 1978[32,33] and is still the most commonly used CRT for advanced HNSCC. Cisplatin forms DNA adducts (crosslinks between the two DNA strands) which alter the DNA structure and thereby inhibits DNA replication. A meta-analysis of randomized trials, comparing CCRT with RT alone, unfortunately proved only a moderate absolute overall survival benefit of 6.5% at 5 years[34]. Furthermore, CCRT is associated with a high local recurrence rate in more than 50% of patients and with a substantial increase in severe toxicity (nausea, mucositis, dysphagia, nephrotoxicity and hematologic toxicity)[35]. Cisplatin, as a radiosensitizer, dose intensifies the radiation dose in normal tissue, thereby increasing toxicity. As a result, concomitant cisplatin treatment is only given to patients with normal renal function and a good performance status.

In 2006, cetuximab, a humanized monoclonal antibody targeted against the epidermal growth factor receptor (EGFR), became the first major drug for HNSCC to gain Food and Drug Administration (FDA) approval since cisplatin[33]. In HNSCC, EGFR is frequently overexpressed, driving cellular division, angiogenesis, invasion and metastasis, resulting in radioresistant tumors with unfavourable clinical outcome[36]. By binding to EGFR, cetuximab alters these effects. Another anti-tumor effect of cetuximab is to initiate an immune response by activating natural killer and dendritic cells[37]. Combined with irradiation, cetuximab redistributes DNA-PK from the nucleus to the cytoplasm which inhibits the repair of DSB induced by radiation[38,39]. Additionally, it causes cells to accumulate in G1

and G2 cell cycle phase resulting in more radiosensitive cancer cells[39]. To date, only one trial reported efficacy of cetuximab-RT in HNSCC[40], while a recent phase II randomized trial, comparing RT with concomitant cisplatin versus cetuximab, showed that cetuximab increased acute toxicity rates without a corresponding clinical benefit[41]. Therefore, CCRT is presently still favoured over cetuximab-RT in routine care[42]. When renal function and performance state of a patient are not good, cetuximab is the first choice of treatment at the moment. In addition to these standard of care treatments, cetuximab CRT is now combined with immunotherapy (bioimmunoradiotherapy) in clinical trials (clinicaltrials.gov.: REACH, N16BIR).

Drug resistance (intrinsic or acquired), regardless of RT, is one of the main challenges in the current therapy of advanced HNSCC[43]. To handle this problem, extensive efforts have been made to find reliable predictive biomarkers to better select (sub)groups of patients who are likely to benefit from the currently used drugs, thereby trying to predict patients' response. The only clinical established biomarkers to predict prognosis are p16 overexpression for HPV association (and thereby favorable outcome) and plasma EBV which is associated with nasopharyngeal cancer and deteriorated outcome[44,45]. Prognostic factors associated with unfavorable prognosis are EGFR, PI3K/AKT activation, loss of PTEN and TP53, cyclin D1 overexpression and HIF-alpha (hypoxia)[44,45]. However, these well-established prognostic biomarkers are not predictive for prediction and selection of individualized treatment. Some suggest that these potential predictive markers are unlikely to improve prediction of outcome due to the high genetic mutational heterogeneity in HNSCC. In this view, it is unlikely for a single targeted inhibitor to benefit a large percentage of patients[43]. For example, although EGFR is highly expressed in HNSCC, the majority of tumors will develop primary resistance against cetuximab (targeting EGFR) and eventually manifest disease progression, which implies acquired resistance[46]. PD-L1/2 is maybe a potential immune biomarker to be correlated with response to immunotherapy in R/M HNSCC[47,48]. The extensive efforts in biomarker research have not resulted in individualized treatment decision making yet, resulting in a persistent need for an individualized treatment prediction model.

Irradiation and DNA damage repair

Given the limitations of radiosensitizers currently administered in the clinic and the urgent need for new RT compatible therapies, currently there is a substantial interest, within the radiosensitizing field, to target DNA repair processes as a potential source of novel targeted anticancer treatments[49-53]. As mentioned earlier, IR works by directly damaging the DNA inside cells. This is for example manifested by single (SSB) and double-strand breaks (DSB)

and by base damage, which are leading to cell death. These DNA breaks trigger DNA damage response and repair (DDR) mechanisms, including the non-homologous-end joining (NHEJ), homologous recombination (HR) and base excision repair (BER) pathways (*Figure 3*). If IR-induced DNA damage is repaired, cells will survive better. Fortunately, many tumors have defects in their repair mechanisms because of various mutations, limiting them to repair the damage. If cancer cells with repair deficiencies are treated with IR, they become more sensitive to IR, resulting in cell death. Having an excess of DNA repair pathways, normal cells are able to repair DNA damage more effectively[54].

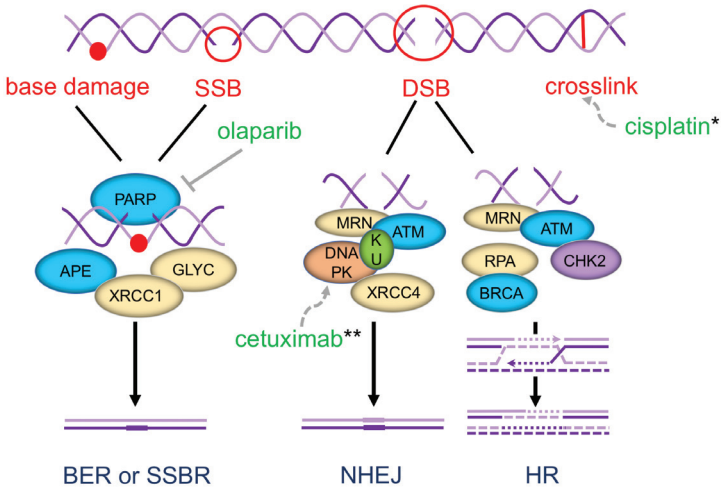

Figure 3. Simplified overview of types of DNA damage and repair mechanisms. (*cisplatin forms crosslinks between DNA strands, **cetuximab redistributes DNA-PK from the nucleus to the cytoplasm)

Targeting the DDR, olaparib is emerging as a novel drug in HNSCC to be combined with RT. Olaparib inhibits Poly(ADP-ribose)polymerase (PARP), which is an important enzyme in BER and in SSB DNA repair. By inhibiting PARP, olaparib alters these DNA repair mechanisms and thereby enhances the efficacy of radiation. As monotherapy, olaparib shows low to high toxicity profiles, depending on the cancer type[55-57]. Pre-clinical studies show efficient sensitization to IR in various tumor types[58-61]. A Phase I trial in 16 patients with locally advanced HNSCC and heavy smoking histories, treated with the combination of olaparib with cetuximab and radiation, showed that the most common grade 3-4 side effects were mucositis (69%) and radiation dermatitis (38%). When combined with other treatments, olaparib radiosensitizes at much lower doses than for monotherapy. 5 patients were treated with the lowest dose, 25 mg olaparib, and experienced grade 3 dermatitis and dysphagia in 40% and grade 3 mucositis in 60%. Two-year overall survival, progression

free survival, local control and distant control rates were 72%, 63%, 72%, 79%, respectively. The combination of olaparib with only RT is currently being tested in clinical trials, also for HNSCC (clinicaltrials.gov.: N13ORH).

Despite these promising developments in RT treatment regimens, the routine HNSCC care is still characterized by high ablative RT doses with relatively poor survival and high toxicity rates. This highlights an urgent need for novel, cancer cell specific radiosensitizers.

Need for novel radiosensitizers – Robotic drug screen assay

To improve clinical outcome and to decrease toxicity in HNSCC patients treated with RT, radiosensitizing drugs are needed that enhance the sensitivity of cancer cells while protecting normal tissue. To search for radiosensitizers, automated robotic drug screens can be used. These facilitate a rapid high-throughput testing of so-called libraries, consisting of multiple drugs or compounds (chemical molecules) with a broad range of targets. Importantly, a screen can be performed for a phenotypic biological activity (for example cell viability) without the upfront need of knowledge of the drug target. This allows for unbiased drug discovery and facilitates the identification of critical targets[62]. In order to identify radiosensitizers, one should treat cells with IR and compare this to non-irradiated cells and cells treated with 'IR + drug'. Our goal is to identify novel radiosensitizing drugs by comparing them to currently used clinical drugs (*i.e.* cisplatin, cetuximab or olaparib). Each drug will be tested by comparing 'drug' to 'drug + IR'.

Our radiosensitizer identification screening assay consists of cell culture plates in which HNSCC cell lines are seeded. As controls, DMSO (dimethyl sulfoxide, vehicle drug, high viability, negative control) or PAO (phenylarsine oxide, toxic, low viability, positive control) is used. One plate is treated with drugs only (IRneg), the other (identical) plate is treated with drugs + 4 Gy IR (IRpos) (*Figure 4*). Hence, four experimental situations exist: 1) cells only (DMSO, IRneg); 2) IR only (DMSO, IRpos); 3) drug only (drug, IRneg) and 4) a combination of drug + IR (drug, IRpos). Using CellTiter-Blue®, chemosensitivity is determined by measuring cell viability. This is done by adding a reagent to the cells which can be converted into a fluorescent product through the general metabolism of living viable cells. This fluorescent signal, measured by a plate reader instrument, is proportional to the number of viable cells present[63]. In order to compare viability of cells in the IRneg plates to the IRpos plates, we performed a per-plate normalization to controls (controls set to 0 and 1), which ensures correction for plate-to-plate variability (pipette effects, robotic errors, unintended variation in concentrations, compound evaporation and incubation fluctuations). When normalizing drugs on the IRpos plate to their DMSO controls, the effect of IR will be set to 1, which enables us to compare the drug effect to the effect of the drug + IR. By calculating the difference

between the two dose-response curves at every tested concentration, an enhanced effect (loss of viability) of the drug + IR is hypothesized to be a potential radiosensitizing effect. Importantly, to prove radiosensitization, the (more laborious) gold standard colony forming 'growth' assay is needed. Instead of measuring viability, this assay defines survival as the proliferative capacity of a single cell to form a colony (at least 6 cell divisions and 50 cells per colony, to determine capacity for continued proliferation) after several weeks[64]. To do so, firstly, from the prior cell viability assay, a specific drug concentration is selected that shows the highest difference between IRneg and IRpos; with ideally no toxicity in IRneg (*Figure 4,**). With this drug concentration a colony forming assay, comparing IR only to IR + drugs (with increasing IR-doses), should be performed.

In addition, when hits of the primary compound screen and validation experiments are confirmed, these hits can be chemically optimized by analysis of the structure-activity relationship (SAR). Adaptations to the chemical structure may change the biological activity, ideally to improve the potency of the compound and thereby transforming a screening 'hit' compound into a 'lead candidate'. After identifying the 'leads', *in vivo* animal experiments will test for biodistribution, pharmacokinetics and efficacy. This will eventually be followed by clinical phase I, II and III trials in patients after which a compound may be labeled as a real anti-cancer 'drug'. This process will take years of persistent translational research.

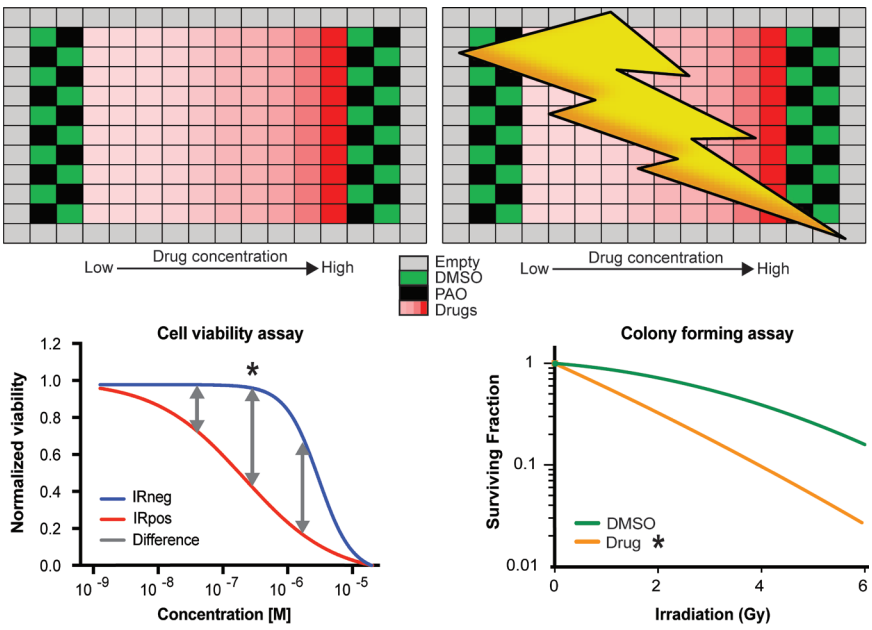

Figure 4. Radiosensitizing screening method

Preclinical short-term fresh tumor cultures to screen drugs and to predict individual cancer treatment response

When testing and identifying novel drug leads, one needs a preclinical model that resembles human HNSCC as closely as possible, to maximize translation of the *in vitro* effect to the effect in clinical patients. In our drug screens, we used cell lines, one of the most common methods to study tumor characteristics and potential drugs *in vitro*. This is a two-dimensional (2D) culture system, of immortalized cells once isolated from a human tumor, which divide continuously on a rigid surface to form a confluent monolayer of cells. Important advantages are the availability, indefinite growth, ease of use, usage in high-throughput screens and low costs[65-67]. However, limitations are a lack of cell type diversity, genotypic and phenotypic differentiation from the original tumor, no supporting TME (non-cancer cell types, such as stroma, fibroblasts, immune cells, mesenchymal cells and endothelial cells), no distinctive tissue-specific architecture (flat monolayer) and the phenomenon that usually only highly aggressive cancer cells are able to form a cell line[65-67]. To confirm *in vitro* findings for usage in patients, the usual common approach is to do *in vivo* animal experiments. Here, human cancer cell lines are injected in (usually) mice. Advantages of mice research are the ability of collecting pharmacological and biodistributional drug data. However, there are many concerns using this 'model': practical and ethical concerns, compromised immune systems, limited ability to mimic the extremely complex human carcinogenesis and mice experiments are costly and time-consuming[67-70]. Successful translation from animal models to clinical trials remains challenging illustrated by the fact that as little as 8% of drugs pass phase I trials[68,69,71].

To develop more advanced *ex vivo* preclinical models, resembling the human tumor as closely as possible, preclinical 3D fresh human tumor histoculture models were developed. In HNSCC, the sponge-gel-supported 3D histoculture method showed successful culture rates and best clinical correlations so far[72]. Benefits of this technique when compared to cell lines are: 1) preservation of the 3D histological structure by using tumor tissue from biopsies, 2) no requirement for additional enzymatic digestion, maintaining cell-cell interactions within the tumor tissue[73,74], 3) hindering clonal evolution of tumor cell (sub) populations[75-78], 4) co-culturing of all cells together (benign, malignant, TME), maintaining tumor heterogeneity, and 5) mimicking the human situation as closely as possible (tumor fragments are attached to a sponge drenched in medium, surrounded by air, preserving the air-mucosa interface of head and neck tumors in humans). These are prerequisites needed for a preclinical culture model to be comparable to the *in vivo* tumor, in order to test novel drugs more reliably[73].

In addition to testing novel drugs, patient-derived 3D tumor cultures could also be of great importance to individualized medicine. It is known that the currently available treatments for HNSCC patients result in a great variety in clinical outcome, where cancer treatment response varies from patient to patient. This diversity in individual clinical response reflects a tumors' individual intrinsic sensitivity to treatment. Extensive research efforts to predict treatment response have not resulted in a routinely used and reliable individual predictive biomarker yet. Maybe a patient-derived 3D histoculture model could be beneficial in this research field.

With our research we aimed to optimize the sponge-gel-supported histoculture for its potential use as a model for testing novel drugs and as individual preclinical model to select the best treatment regimen.

THESIS AIM AND OUTLINE

Part I of this thesis describes the search for a preclinical short-term fresh 3D tumor culture model to use for future drug testing and to assist individualized treatment decision-making. In Chapter 2 an overview of all preclinical culture models available in HNSCC is presented, from cell lines to animal experiments. In Chapter 3 we report our results of a narrative literature review, describing the various *in vitro* fresh tumor culture models to identify the best model following culture success rates and translation of treatment sensitivity into the clinic. Chapter 4 will describe novel adaptations and insights into this best selected *in vitro* tumor culture model.

Part II of the thesis focuses on identifying novel cancer-specific radiosensitizers for HNSCC treatment to improve the survival rates of advanced HNSCC patients while minimizing treatment toxicity. This was done by performing high-throughput drug screens in combination with radiation. Chapter 5 addresses the screening of various drug 'libraries, namely the FDA-approved oncology drugs, Roche kinase inhibitors and DUB inhibitors. Chapter 6 describes the screening of GSK kinase inhibitors.

Finally, in Chapter 7 the results obtained in this thesis are summarized and discussed, and suggestions for future research are given.

REFERENCES

1 Fouad, Y. A. & Aanei, C. Revisiting the hallmarks of cancer. *Am J Cancer Res* **7**, 1016-1036 (2017).

2 Hanahan, D. & Weinberg, R. A. Hallmarks of cancer: the next generation. *Cell* **144**, 646-674, doi:10.1016/j.cell.2011.02.013 (2011).

3 Sonnenschein, C. & Soto, A. M. The aging of the 2000 and 2011 Hallmarks of Cancer reviews: a critique. *J Biosci* **38**, 651-663 (2013).

4 Schmitz, S. & Machiels, J. P. Targeting the Tumor Environment in Squamous Cell Carcinoma of the Head and Neck. *Curr Treat Options Oncol* **17**, 37, doi:10.1007/s11864-016-0412-6 (2016).

5 Global Burden of Disease Cancer, C. *et al.* Global, Regional, and National Cancer Incidence, Mortality, Years of Life Lost, Years Lived With Disability, and Disability-Adjusted Life-years for 32 Cancer Groups, 1990 to 2015: A Systematic Analysis for the Global Burden of Disease Study. *JAMA Oncol* **3**, 524-548, doi:10.1001/jamaoncol.2016.5688 (2017).

6 Hashibe, M. *et al.* Interaction between tobacco and alcohol use and the risk of head and neck cancer: pooled analysis in the International Head and Neck Cancer Epidemiology Consortium. *Cancer Epidemiol Biomarkers Prev* **18**, 541-550, doi:10.1158/1055-9965.EPI-08-0347 (2009).

7 Kreimer, A. R., Clifford, G. M., Boyle, P. & Franceschi, S. Human papillomavirus types in head and neck squamous cell carcinomas worldwide: a systematic review. *Cancer Epidemiol Biomarkers Prev* **14**, 467-475, doi:10.1158/1055-9965.EPI-04-0551 (2005).

8 Lung, M. L. *et al.* The interplay of host genetic factors and Epstein-Barr virus in the development of nasopharyngeal carcinoma. *Chin J Cancer* **33**, 556-568, doi:10.5732/cjc.014.10170 (2014).

9 Spence, T., Bruce, J., Yip, K. W. & Liu, F. F. HPV Associated Head and Neck Cancer. *Cancers (Basel)* **8**, doi:10.3390/cancers8080075 (2016).

10 Brumbaugh, J., Ferris, R. L. & Hu, S. in *Head and Neck Cancer* (ed J. Bernier) Ch. 8, 163-179 (Springer, 2016).

11 Johnson, N. W. & Amarasinghe, H. K. in *Head and Neck Cancer: Multimodality Management* (ed J. Bernier) 1-58 (Springer International Publishing, 2016).

12 Alter, B. P. Fanconi's anemia, transplantation, and cancer. *Pediatr Transplant* **9 Suppl 7**, 81-86, doi:10.1111/j.1399-3046.2005.00440.x (2005).

13 Rosenberg, P. S., Alter, B. P. & Ebell, W. Cancer risks in Fanconi anemia: findings from the German Fanconi Anemia Registry. *Haematologica* **93**, 511-517, doi:10.3324/haematol.12234 (2008).

14 Mroz, E. A. & Rocco, J. W. Intra-tumor heterogeneity in head and neck cancer and its clinical implications. *World J Otorhinolaryngol Head Neck Surg* **2**, 60-67, doi:10.1016/j.wjorl.2016.05.007 (2016).

15 Agrawal, N. *et al.* Exome sequencing of head and neck squamous cell carcinoma reveals inactivating mutations in NOTCH1. *Science* **333**, 1154-1157, doi:10.1126/science.1206923 (2011).

16 Stransky, N. *et al.* The mutational landscape of head and neck squamous cell carcinoma. *Science* **333**, 1157-1160, doi:10.1126/science.1208130 (2011).

17 The Cancer Genome Atlas, N. Comprehensive genomic characterization of head and neck squamous cell carcinomas. *Nature* **517**, 576, doi:10.1038/nature14129 https://www.nature.com/articles/nature14129#supplementary-information (2015).

18 Chung, C. H. *et al.* Genomic alterations in head and neck squamous cell carcinoma determined by cancer gene-targeted sequencing. *Ann Oncol* **26**, 1216-1223, doi:10.1093/annonc/mdv109 (2015).

19 Huang, S. H. & O'Sullivan, B. Overview of the 8th Edition TNM Classification for Head and Neck Cancer. *Curr Treat Options Oncol* **18**, 40, doi:10.1007/s11864-017-0484-y (2017).

20 Surveillance, E., and End Results (SEER) Program from the United States. *Cancer Stat Facts: Oral Cavity and Pharynx Cancer*, <https://seer.cancer.gov/statfacts/html/oralcav.html> (Research data (2007-2013)).

21 Surveillance, E., and End Results (SEER) Program from the United States. *Cancer Stat Facts: Larynx Cancer*, <https://seer.cancer.gov/statfacts/html/laryn.html> (Research data (2007-2013)).

22 Lavaf, A., Genden, E. M., Cesaretti, J. A., Packer, S. & Kao, J. Adjuvant radiotherapy improves overall survival for patients with lymph node-positive head and neck squamous cell carcinoma. *Cancer* **112**, 535-543, doi:10.1002/cncr.23206 (2008).

23 Argiris, A., Li, Y. & Forastiere, A. Prognostic factors and long-term survivorship in patients with recurrent or metastatic carcinoma of the head and neck. *Cancer* **101**, 2222-2229, doi:10.1002/cncr.20640 (2004).

24 Ferris, R. L. *et al.* Nivolumab for Recurrent Squamous-Cell Carcinoma of the Head and Neck. *N Engl J Med* **375**, 1856-1867, doi:10.1056/NEJMoa1602252 (2016).

25 O'Rorke, M. A. *et al.* Human papillomavirus related head and neck cancer survival: a systematic review and meta-analysis. *Oral Oncol* **48**, 1191-1201, doi:10.1016/j.oraloncology.2012.06.019 (2012).

26 Ang, K. K. *et al.* Human papillomavirus and survival of patients with oropharyngeal cancer. *N Engl J Med* **363**, 24-35, doi:10.1056/NEJMoa0912217 (2010).

27 Poeta, M. L. *et al.* TP53 mutations and survival in squamous-cell carcinoma of the head and neck. *N Engl J Med* **357**, 2552-2561, doi:10.1056/NEJMoa073770 (2007).

28 Zhou, G., Liu, Z. & Myers, J. N. TP53 Mutations in Head and Neck Squamous Cell Carcinoma and Their Impact on Disease Progression and Treatment Response. *J Cell Biochem* **117**, 2682-2692, doi:10.1002/jcb.25592 (2016).

29 Zeman, E. M. in *Clinical Radiation Oncology (Fourth Edition)* (ed Joel E. Tepper) 2-40.e45 (Elsevier, 2016).

30 Wouters, B. G. in *Basic clinical radiobiology* (eds M. Joiner & A. van der Kogel) Ch. 3, 27 - 40 (Hodder Arnold, 2009).

31 Baskar, R., Dai, J., Wenlong, N., Yeo, R. & Yeoh, K. W. Biological response of cancer cells to radiation treatment. *Front Mol Biosci* **1**, 24, doi:10.3389/fmolb.2014.00024 (2014).

32 Al-Sarraf, M. Treatment of locally advanced head and neck cancer: Historical and critical review. *Cancer Control* **9**, 387-399 (2002).

33 Blasco, M. A. *et al.* Systemic therapy for head and neck squamous cell carcinoma: Historical perspectives and recent breakthroughs. *Laryngoscope* **127**, 2565-2569, doi:10.1002/lary.26629 (2017).

34 Pignon, J. P., le Maitre, A., Maillard, E., Bourhis, J. & Group, M.-N. C. C. Meta-analysis of chemotherapy in head and neck cancer (MACH-NC): an update on 93 randomised trials and 17,346 patients. *Radiotherapy and oncology: journal of the European Society for Therapeutic Radiology and Oncology* **92**, 4-14, doi:10.1016/j.radonc.2009.04.014; 10.1016/j.radonc.2009.04.014 (2009).

35 Adelstein, D. J. *et al.* An intergroup phase III comparison of standard radiation therapy and two schedules of concurrent chemoradiotherapy in patients with unresectable squamous cell head and neck cancer. *Journal of clinical oncology: official journal of the American Society of Clinical Oncology* **21**, 92-98, doi:10.1200/JCO.2003.01.008 (2003).

36 Maiti, G. P. *et al.* Overexpression of EGFR in head and neck squamous cell carcinoma is associated with inactivation of SH3GL2 and CDC25A genes. *PLoS One* **8**, e63440, doi:10.1371/journal.pone.0063440 (2013).

37 Srivastava, R. M. *et al.* Cetuximab-activated natural killer and dendritic cells collaborate to trigger tumor antigen-specific T-cell immunity in head and neck cancer patients. *Clin Cancer Res* **19**, 1858-1872, doi:10.1158/1078-0432.CCR-12-2426 (2013).

38 Dittmann, K., Mayer, C. & Rodemann, H. P. Inhibition of radiation-induced EGFR nuclear import by C225 (Cetuximab) suppresses DNA-PK activity. *Radiother Oncol* **76**, 157-161, doi:10.1016/j.radonc.2005.06.022 (2005).

39 Huang, S. M. & Harari, P. M. Modulation of radiation response after epidermal growth factor receptor blockade in squamous cell carcinomas: inhibition of damage repair, cell cycle kinetics, and tumor angiogenesis. *Clin Cancer Res* **6**, 2166-2174 (2000).

40 Bonner, J. A. *et al.* Radiotherapy plus cetuximab for locoregionally advanced head and neck cancer: 5-year survival data from a phase 3 randomised trial, and relation between cetuximab-induced rash and survival. *Lancet Oncol* **11**, 21-28, doi:10.1016/S1470-2045(09)70311-0 (2010).

41 Magrini, S. M. *et al.* Cetuximab and Radiotherapy Versus Cisplatin and Radiotherapy for Locally Advanced Head and Neck Cancer: A Randomized Phase II Trial. *J Clin Oncol* **34**, 427-435, doi:10.1200/JCO.2015.63.1671 (2016).

42 Gyawali, B., Shimokata, T., Honda, K. & Ando, Y. Chemotherapy in locally advanced head and neck squamous cell carcinoma. *Cancer Treat Rev* **44**, 10-16, doi:10.1016/j.ctrv.2016.01.002 (2016).

43 Wen, Y. & Grandis, J. R. Emerging drugs for head and neck cancer. *Expert Opin Emerg Drugs* **20**, 313-329, doi:10.1517/14728214.2015.1031653 (2015).

44 Eze, N., Lo, Y.-C. & Burtness, B. Biomarker driven treatment of head and neck squamous cell cancer. *Cancers of the Head & Neck* **2**, 6, doi:10.1186/s41199-017-0025-1 (2017).

45 Suh, Y., Amelio, I., Guerrero Urbano, T. & Tavassoli, M. Clinical update on cancer: molecular oncology of head and neck cancer. *Cell Death Dis* **5**, e1018, doi:10.1038/cddis.2013.548 (2014).

46 Wheeler, D. L., Dunn, E. F. & Harari, P. M. Understanding resistance to EGFR inhibitors-impact on future treatment strategies. *Nat Rev Clin Oncol* **7**, 493-507, doi:10.1038/nrclinonc.2010.97 (2010).

47 Chow, L. Q. M. *et al.* Antitumor Activity of Pembrolizumab in Biomarker-Unselected Patients With Recurrent and/or Metastatic Head and Neck Squamous Cell Carcinoma: Results From the Phase Ib KEYNOTE-012 Expansion Cohort. *J Clin Oncol* **34**, 3838-3845, doi:10.1200/JCO.2016.68.1478 (2016).

48 Muller, T. *et al.* PD-L1: a novel prognostic biomarker in head and neck squamous cell carcinoma. *Oncotarget* **8**, 52889-52900, doi:10.18632/oncotarget.17547 (2017).

49 Curtin, N. J. DNA repair dysregulation from cancer driver to therapeutic target. *Nat Rev Cancer* **12**, 801-817, doi:10.1038/nrc3399 (2012).

50 Goldstein, M. & Kastan, M. B. The DNA damage response: implications for tumor responses to radiation and chemotherapy. *Annu Rev Med* **66**, 129-143, doi:10.1146/annurev-med-081313-121208 (2015).

51 Lord, C. J. & Ashworth, A. The DNA damage response and cancer therapy. *Nature* **481**, 287-294, doi:10.1038/nature10760 (2012).

52 O'Connor, M. J. Targeting the DNA Damage Response in Cancer. *Mol Cell* **60**, 547-560, doi:10.1016/j.molcel.2015.10.040 (2015).

53 Raleigh, D. R. & Haas-Kogan, D. A. Molecular targets and mechanisms of radiosensitization using DNA damage response pathways. *Future Oncol* **9**, 219-233, doi:10.2217/fon.12.185 (2013).

54 Moding, E. J., Kastan, M. B. & Kirsch, D. G. Strategies for optimizing the response of cancer and normal tissues to radiation. *Nat Rev Drug Discov* **12**, 526-542, doi:10.1038/nrd4003 (2013).

55 Matulonis, U. A. *et al.* Olaparib monotherapy in patients with advanced relapsed ovarian cancer and a germline BRCA1/2 mutation: a multistudy analysis of response rates and safety. *Ann Oncol* **27**, 1013-1019, doi:10.1093/annonc/mdw133 (2016).

56 Zhou, J. X., Feng, L. J. & Zhang, X. Risk of severe hematologic toxicities in cancer patients treated with PARP inhibitors: a meta-analysis of randomized controlled trials. *Drug Des Devel Ther* **11**, 3009-3017, doi:10.2147/DDDT.S147726 (2017).

57 Tutt, A. *et al.* Oral poly(ADP-ribose) polymerase inhibitor olaparib in patients with BRCA1 or BRCA2 mutations and advanced breast cancer: a proof-of-concept trial. *Lancet* **376**, 235-244, doi:10.1016/S0140-6736(10)60892-6 (2010).

58 Senra, J. M. *et al.* Inhibition of PARP-1 by olaparib (AZD2281) increases the radiosensitivity of a lung tumor xenograft. *Mol Cancer Ther* **10**, 1949-1958, doi:10.1158/1535-7163.MCT-11-0278 (2011).

59 Powell, C. *et al.* Pre-clinical and clinical evaluation of PARP inhibitors as tumour-specific radiosensitisers. *Cancer Treat Rev* **36**, 566-575, doi:10.1016/j.ctrv.2010.03.003 (2010).

60 Nowsheen, S., Bonner, J. A. & Yang, E. S. The poly(ADP-Ribose) polymerase inhibitor ABT-888 reduces radiation-induced nuclear EGFR and augments head and neck tumor response to radiotherapy. *Radiother Oncol* **99**, 331-338, doi:10.1016/j.radonc.2011.05.084 (2011).

61 Chatterjee, P. *et al.* PARP inhibition sensitizes to low dose-rate radiation TMPRSS2-ERG fusion gene-expressing and PTEN-deficient prostate cancer cells. *PLoS One* **8**, e60408, doi:10.1371/journal.pone.0060408 (2013).

62 Macarron, R. *et al.* Impact of high-throughput screening in biomedical research. *Nat Rev Drug Discov* **10**, 188-195, doi:10.1038/nrd3368 (2011).

63 Riss, T. L. *et al.* in *Assay Guidance Manual* (eds G. S. Sittampalam *et al.*) (2004).

64 Franken, N. A., Rodermond, H. M., Stap, J., Haveman, J. & van Bree, C. Clonogenic assay of cells in vitro. *Nat Protoc* **1**, 2315-2319, doi:10.1038/nprot.2006.339 (2006).

65 Kaur, G. & Dufour, J. M. Cell lines: Valuable tools or useless artifacts. *Spermatogenesis* **2**, 1-5, doi:10.4161/spmg.19885 (2012).

66 Masters, J. R. Human cancer cell lines: fact and fantasy. *Nat Rev Mol Cell Biol* **1**, 233-236, doi:10.1038/35043102 (2000).

67 Zuur, C. L., Dohmen, A. J. C., van den Brekel, M. W. M., Wang, X. J. & Malkosky, S. P. in *Head and Neck Cancer: Multimodality Management* (ed J. Bernier) Ch. 10, 205-213 (Springer International Publishing, 2016).

68 Mak, I. W., Evaniew, N. & Ghert, M. Lost in translation: animal models and clinical trials in cancer treatment. *Am J Transl Res* **6**, 114-118 (2014).

69 Voskoglou-Nomikos, T., Pater, J. L. & Seymour, L. Clinical predictive value of the in vitro cell line, human xenograft, and mouse allograft preclinical cancer models. *Clin Cancer Res* **9**, 4227-4239 (2003).

70 Hoarau-Vechot, J., Rafii, A., Touboul, C. & Pasquier, J. Halfway between 2D and Animal Models: Are 3D Cultures the Ideal Tool to Study Cancer-Microenvironment Interactions? *Int J Mol Sci* **19**, doi:10.3390/ijms19010181 (2018).

71 Johnson, J. I. *et al.* Relationships between drug activity in NCI preclinical in vitro and in vivo models and early clinical trials. *Br J Cancer* **84**, 1424-1431, doi:10.1054/bjoc.2001.1796 (2001).

72 Dohmen, A. J. *et al.* Feasibility of Primary Tumor Culture Models and Preclinical Prediction Assays for Head and Neck Cancer: A Narrative Review. *Cancers (Basel)* **7**, 1716-1742, doi:10.3390/cancers7030858 (2015).

73 Leighton, J. A sponge matrix method for tissue culture; formation of organized aggregates of cells in vitro. *Journal of the National Cancer Institute* **12**, 545-561 (1951).

74 Sherwin, R. P., Richters, A., Yellin, A. E. & Donovan, A. J. Histoculture of human breast cancers. *Journal of surgical oncology* **13**, 9-20 (1980).

75 Ragin, C. C., Reshmi, S. C. & Gollin, S. M. Mapping and analysis of HPV16 integration sites in a head and neck cancer cell line. *International journal of cancer. Journal international du cancer* **110**, 701-709, doi:10.1002/ijc.20193 (2004).

76 Worsham, M. J. *et al.* Chromosomal aberrations identified in culture of squamous carcinomas are confirmed by fluorescence in situ hybridisation. *Molecular pathology: MP* **52**, 42-46 (1999).

77 Shapiro, J. R. & Shapiro, W. R. The subpopulations and isolated cell types of freshly resected high grade human gliomas: their influence on the tumor's evolution in vivo and behavior and therapy in vitro. *Cancer metastasis reviews* **4**, 107-124 (1985).

78 Bjerkvig, R. *Spheroid Culture in Cancer Research*. First edit edn, (CRC Press, 1992).

PART I

Preclinical fresh tumor histoculture models of HNSCC

CHAPTER 2

Preclinical models of head and neck squamous cell carcinoma

C.L. Zuur

A.J.C. Dohmen

M.W.M. van den Brekel

X.J. Wang

S. Malkosky

Head and Neck Cancer: Multimodality Management Book:

J. Bernier, Chapter 10. 2016; 2nd edition, p 205-2013

ABSTRACT

Head and neck squamous cell carcinoma (HNSCC) is characterized by a broad genetic diversity, likely from prolonged carcinogen exposure and high levels of genetic instability. To date, this high genetic heterogeneity of HNSCC has hampered the development of targeted therapy, and routine use of molecular markers for treatment selection is not established. This chapter reviews preclinical models of HNSCC as a critical tool for exploring tumor initiation and progression, cancer genetics, novel therapeutic approaches, and predictors of clinical response. HNSCC model systems including cancer cell lines derived from human HNSCC, primary human fresh tumor cultures, animals exposed to oral carcinogens, genetically engineered mouse models (GEMMs), and various combinations of these systems are discussed.

INTRODUCTION

Head and neck squamous cell carcinoma (HNSCC) represents 3-5% of newly diagnosed cancers and has a 5-year survival between 25-95% depending on disease site and stage. This indicates both the need for novel treatment strategies as well as the variable response to treatment. Currently, therapy selection is based on data derived from a combination of randomized controlled trials, meta-analyses, and retrospective case series. Although in HNSCC the routine use of molecular markers for treatment selection is not established yet, in several other tumor types such as breast, colon, lung and melanoma, this molecular knowledge has already been translated into important predictive assays used in treatment selection[1-4].

HNSCCs are characterized by a broad genetic diversity, likely from prolonged carcinogen exposure and high levels of genetic instability[5,6]; however, several signaling pathways are commonly involved in HSNCC carcinogenesis, including p16, p53, CyclinD1 and PTEN (phosphate and tensin homolog)[7-9]. The high genetic heterogeneity of HNSCC has hampered the development of targeted therapy, and to date only anti-epidermal growth factor receptor (EGFR) therapy has demonstrated clinical efficacy in locally advanced HNSCC[10]. Nonetheless, targeting other pathways including phosphoinositide 3-Kinase (PI3K)-AKT, insulin-like growth receptor, B-cell lymphoma 2 (Bcl-2), and c-met has shown promise in preclinical models[11-16].

Human papilloma virus (HPV) oncogenes E6 and E7 bind and inactivate tumor suppressors p53 and retinoblastoma (Rb)[17]. Although HPV has been thought to promote HNSCC development for decades[18], it has only more recently been appreciated that HPV-positive and HPV-negative HNSCC are biologically distinct. HPV-associated HNSCCs tend to occur at a younger age, are less related to smoking and alcohol exposure, and do not typically exhibit p53 mutations or p16 (INK4a) alterations. Moreover, HPV status predicts both responses to radiation therapy and improved outcome[19-21]. However, as stated above, at the moment we lack the knowledge and reliable trials to personalize treatment regimens in HNSCC.

Because studying cancer in humans poses ethical, financial and practical hurdles, preclinical models are a critical tool for exploring tumor initiation and progression, cancer genetics, novel therapeutic approaches, and predictors of clinical response. HNSCC model systems include cancer cell lines derived from human HNSCC, primary human tumor cultures, animals exposed to oral carcinogens, genetically engineered mouse models (GEMMs) and various combinations of these systems. Each system has strengths and weaknesses that are important to interpreting data derived from these models. To maximize clinical relevance, model systems should resemble human HNSCC as closely

as possible. For example, cell lines should harbor the genetic and epigenetic alterations common to HNSCC, and carcinogen exposures should mimic the routes and chemicals associated with human HNSCC. Similarly, GEMMs or primary tumor models should examine the genetic alterations observed in human HNSCC. To overcome the limitations of a given model, results should be validated by multiple approaches in different systems; however, ultimately, all results obtained in model systems must be validated in human samples or subjects.

HNSCC Cell Lines

Cultured HNSCC cells are a versatile model system that can be characterized by genetic mutation, anatomic site of origin, and *in vitro* behavior[22]. Genetic manipulation of cultured cells can be used to elucidate the role of specific molecules on behaviors relevant to cancer development and progression in view of clinical treatment response[23]. HPV 16 E6-E7-immortalized mouse tonsil epithelial cells (MTECs) have been used to define the viral genes required for immortalization, anchorage-independent growth, and, eventually, malignant growth *in vivo*[24]. In addition, differences in response were attributed to differences in the genetic makeup of HNSCC cell lines, being either HPV-positive or HPV-negative[12,25]. A major advantage of HNSCC lines is that the low cost permits high-throughput approaches that allow screening of novel compounds (alone or in combination), treatment modalities (e.g., drugs plus radiation therapy), and resistance to targeted treatment. For example, cell lines have been used to demonstrate that resistance to anti-EGFR therapy may be overcome through simultaneous targeting of EGFR and either Src kinase[26] or HER3[27]. Similarly, cell lines have been used to demonstrate that hypoxia and DNA repair are important in radioresistance[28-30], and studying DNA repair after radiation treatment may facilitate the development of strategies that increase the therapeutic window of chemoradiotherapy (CRT) in HNSCC patients[31].

However, cancer cell lines have critical limitations. They are a homogeneous clonal population capable of growing *in vitro* without the supporting tumor stroma (fibroblasts, immune cells, or vasculature) and typically fail to reflect the genetic heterogeneity of the native tumor from which they were derived. Although the majority of individual tumor cells are incapable of growing in culture, patients whose tumors can establish cell lines have worse clinical prognosis, suggesting that characteristics supporting *in vitro* growth are indicative of aggressive tumor behavior *in vivo*[32]. Furthermore, as cells are passaged, there is selective pressure for *in vitro* growth and a lack of standardized tissue culture techniques can limit reproducibility[33-39]. Culture conditions can also influence the responses to cytotoxic therapies as cells grown as anchorage-independent spheroids can have

different responses to cytotoxic agents than the same cells grown as monolayers[40]. Also, passaged lines may exhibit different chemosensitivity patterns over time[41-43]. Therefore, cell lines are poor predictors of treatment response in individual patients[44,45]. Many of these issues may have been accentuated in HNSCC secondary to the relative paucity of well-characterized lines[32,46].

Despite these limitations, much of our basic mechanistic understanding of the roles of specific molecules has been derived from cell culture experiments. Perhaps the most successful example of this is identification and subsequent inhibition of the bcr-abl fusion protein in chronic myelogenous leukemia[47,48]. Unfortunately, like most solid tumors, HNSCC is not uniformly sensitive to inhibition of a single oncogenic driver[6], and combinations of inhibitors or targeting of specific tumor subsets will be required to improve disease control. Currently, inhibitors of EGFR, PI3Kinase-AKT pathway, insulin-like growth factor receptor (IGFR), Bcl-2 and cMET are being studied in preclinical HNSCC models [11-16].

Although cell lines are the optimal system to study pathways and the role of specific genes, it has proven difficult to identify reliable markers of treatment response using cell lines. We generated a radiosensitivity profile using HNSCC cell lines[30,45], but this profile was not predictive of clinical local control after radiotherapy in laryngeal cancer patients. Nevertheless, other profiles like the Chung high-risk profile and the Slebos HPV-negative expression profile have been useful in predicting local recurrence in HPV-negative HNSCC after CRT[49-51].

Short-Term Primary Tumor Cultures

As cell lines are difficult to establish and are poor predictors of *in vivo* responsiveness, short-term cultures of primary HNSCC specimens have also been used to predict therapeutic responsiveness. Soft agar culture of primary digested HNSCC cells was first described over 40 years ago[52], and colonies of 20 to 50 cells can be established from 33 to 74% of HNSCC biopsies within a few weeks[53-56]. This system has been used to assess chemosensitivity[54] and radiosensitivity[53], both of which correlated with clinical tumor behavior. The approach is limited by a relatively small number of available tumor cells, low clonal growth (presumably secondary to a limited number of cells capable of forming colonies), and high contamination with non-epithelial cells. Intrinsic radiosensitivity of fresh HNSCC cell cultures has also been tested in a cell adhesive monolayer that better restores cell-cell contact and thus may better predict treatment response[57-59]. Contamination with stromal cells can impact both chemo- and radiosensitivity where drug- or radiation-resistant stromal cells can mask selective epithelial sensitivity patterns[60-63].

To overcome these limitations, the histoculture drug response assay (HDRA) was developed to improve the predictive ability of primary cultures[64]. In this technique, tumor fragments are cultured without digestion to maintain cell-cell adhesions and tumor heterogeneity and potentially protect a limited number of tumor stem cells. This markedly improves culture success as well as the ability of the culture to predict clinical responsiveness[65-68]. The improved predictive value may be related to the three-dimensional structure and relatively inaccessibility of the hypoxic tumor interior to chemotherapeutic agents, which better models the actual *in vivo* tumor environment. Several groups have also grown HNSCC "spheres" or "organoids" to better mimic the three-dimensional configuration of tumor cells *in vivo*[69-73]. When benign and malignant "spheres" were generated from HNSCC tumor fragments in agar-coated culture flasks, the importance of the immune system was illustrated as increased cytokine production (stimulated by contact between monocytes and tumor cells) was predictive of an unfavorable clinical prognosis[69,70]. Unfortunately, the low culture success rate (6%) limits the clinical applicability of this technique[71]. To date, no phase II or III studies have demonstrated added predictive value of preclinical short-term fresh HNSCC chemosensitivity or radiosensitivity assays.

Xenograft Mouse Models

A variety of approaches are available to study HNSCC tumor behavior *in vivo:* one of the most common is xenografting of established human HNSCC cell lines into immunocompromised mice. Depending on the desired application, xenografts can be established heterotopically in the flank, or orthotopically in the buccal mucosa, floor of mouth or tongue. Xenografts can be used to assess the response to drug or radiation therapy[74-76], or to define the role of specific molecules during head and neck cancer development[77,78]. In addition, these models can be used to study other processes critical for HNSCC development and progression, including lymphatic metastasis[79], bone invasion[80], interactions between cancer-associated fibroblasts and cancer epithelial cells[81], and tumor cell invasion[82]. The major limitations of this technique are an inability to study tumor-immune interactions, the poor ability of xenografts to predict drug activity against human cancers[83] and the cost compared to *in vitro* cell culture experiments.

Murine HNSCC cells can also be grafted into syngeneic immunocompetent hosts, and although the number of murine-derived lines is limited, these models can facilitate the study of advanced tumor behavior and tumor-immune system interactions. Oral SCC VII/SF cells were derived from C3H/HeJ mice[84], while the PAM-LY and B4B8 cells were derived from BALB/c mice[85-87]; these cell lines have been used to study bone invasion, metastasis, and tumor recurrence[88-92].

Xenografts of primary human HNSCCs can also be established in the flanks of immunocompromised animals either after a short-term passage *in vitro* or from primary human HNSCC samples[93,94]. Direct patient xenografts can amplify tumor material for downstream molecular or cellular analysis and can provide a platform for *in vivo* testing of therapeutic compounds[95]. Direct xenografts are genetically stable over multiple passages in mice[95] and preserve some features that cultured cells irreversibly lose[96]. Moreover, these systems may be better suited for studying invasiveness and metastases than cell culture systems[97] secondary to the preservation of tumor stromal cells that are important for these processes[98]. Since this model implants developed human tumors into immunocompromised mice, it is unsuitable for studying tumor initiation, chemoprevention, or tumor immunology.

Chemical Carcinogenises Models

Oral cancers can also be induced by exposing rodents to carcinogens. Because specific mutagens produce characteristic genetic lesions [99,100], carcinogen-induced tumors tend to be more homogeneous than their human counterparts, but because these models have a long latency and exhibit premalignant lesions, they are useful for studying tumor initiation and chemoprevention.

One well-characterized approach is the hamster buccal pouch model in which HNSCC are induced by prolonged oral application of the H-ras mutagen DMBA (7,12-dimethylbenz(a) anthracene)[99,101]. This produces squamous cell carcinomas in the majority of animals, and animals develop lymph node metastases if observed long enough[102]. This model has been used to study the chemopreventive activity of a variety of natural compounds[103,104], as well as inhibitors of EGFR and cyclooxygenase-2 (COX2) signalling[105,106]. However, the utility of this model is somewhat limited by the relative paucity of hamster-specific tools and reagents, especially compared to mice.

Similarly, prolonged oral exposure to another H-ras mutagen 4-NQO (4-nitroquinoline N-oxide) induces both oral and esophageal SCC in mice[100,107,108], and cervical lymph node metastasis can be observed with a more prolonged observation period[109]. This model has been used to test chemoprevention by inhibitors of mammalian target of rapamycin (mTOR), vascular endothelial growth factor (VEGF), and EGFR[110-112]. Although DMBA and 4-NQO are not tobacco-derived carcinogens, they provide a convenient way of inducing a clinically relevant tumor-initiating event[113].

Genetically Engineered Mouse Models (GEMMs)

GEMMs have been an enormous step forward for cancer modeling and allow evaluation of discrete genetic alterations in specific organs *in vivo* in an immunocompetent animal. Additional benefits of GEMMs include the ability to evaluate how multiple genetic defects interact to promote or inhibit cancer, and the opportunity to evaluate whether specific targeted therapies are active against tumors with a defined genetic composition. Drawbacks are that human cancers are more genetically complex and heterogeneous than tumors produced in mouse models, and differences in the human and mouse immune systems may complicate studies of tumor immunology.

Targeted mutagenesis of the mouse germ line by homologous recombination in embryonic stem cells can be used to create classic "knockout" mice, and, if the genetic modification is not embryonic lethal, heterozygotes can be crossed to create mice homozygous for a particular gene deletion. While knockout mice can be used to study tumor suppressor loss if combined with HNSCC carcinogens[114-116], there are critical limitations to this approach. First, global deletion of putative tumor suppressors is frequently embryonic lethal, thus it is difficult, if not impossible, to study combinations of genetic modifications using this technique[117]. In addition, because the genetic modification is present in all tissues, tumors can develop in multiple anatomic locations and gene deletion in tumor stromal cells can impact both animal phenotype and tumor behaviour in unanticipated ways. To overcome these issues and target genetic manipulations to specific tissue compartments, several approaches have been taken. One of the first strategies was to target oncogene overexpression with a promoter that restricts transgene expression to the oral epithelium. For example, when the Epstein-Barr virus ED-L2 promoter was used to target cyclin D1 to oral-esophageal epithelium, mice developed dysplasia that progressed to SCC when this transgene is crossed into a $p53^{-/-}$ background[118]. Second generation systems provided another layer of control of genetic manipulations through an ability to induce transgene expression. For example, when a keratin 5 (K5)-targeted, doxycycline-inducible system was used to induce expression of a tet-responsive $Kras^{G12D}$ oncogene, animals developed tumors of the oral mucosa and esophagus; however, because these animals also developed skin and urogenital lesions (secondary to broad K5 expression and systemic doxycycline treatment), the applicability of this system to HNSCC has been limited[119].

Most current GEMMs combine promoter-mediated tissue targeting and ligand induction to achieve organ specificity and temporal control of genetic alterations. In these systems, conditional genetic deletion is achieved by placing loxP restriction sites around a target gene; the target gene is excised upon Cre recombination activation[120]. By placing a loxP-

flanked stop codon upstream of an oncogene (e.g., $Kras^{G12D}$), this approach can also be used to "knock-in" oncogenes[121]. Tissue specificity is achieved by placing Cre recombinase expression under the control of an epithelial-specific promoter (typically keratin 5 or keratin 14); however, an additional layer of control is required to restrict Cre recombinase expression to the oral epithelium as keratins are robustly expressed in other epithelial tissues including the skin and mammary gland. This control is achieved through a ligand-inducible Cre recombinase fusion protein; the two most common are the tamoxifen-inducible truncated estrogen receptor (ER) fusions ($K14CreER^T$ and $K5CreER^{T2}$) and RU486-inducible truncated progesterone receptor (PR) fusions (K14CrePR or K5Cre*PR)[122,123]. The advantage of these systems is tissue-specific, spatial and temporal control of recombination and the ability to introduce multiple genetic alterations simultaneously. Disadvantages of this system are that most inducible Cre recombinase systems have some level of background activity and there may be variability in recombination efficiency for different genes which may be related to the distance between LoxP sites[124,125].

When the K5Cre*PR construct and oral RU486 are used to target oncogenic $K\text{-}ras^{G12D}$ expression, mice develop oral papillomas that progress to HNSCC with the simultaneous activation of mutant $p53^{R172F}$, but not with conditional p53 deletion[122,126]. Similarly, deletion of transforming growth factor beta type II receptor (TGFßRII) in conjunction with $Kras^{G12D}$ activation causes full penetrance HNSCC with frequent metastases[127]. As deletion of TGFßRII alone does not cause tumor formation, it appears that $Kras^{G12D}$ functions as a tumor initiator while TGFßRII loss functions to promote tumor development and progression. In contrast to TGFßRII, Smad4 deletion in the oral epithelium targeted by K14CrePR or K5Cre*PR and oral RU486 causes HNSCC in the absence of Kras activation, perhaps secondary to the genomic instability that characterizes $Smad4^{-/-}$ HNSCC[128].

The $K14CreER^T$ construct and oral tamoxifen have been used to simultaneously target conditional deletion of TGFß receptor type I (TGFßRII) and PTEN; this model exhibits full penetrance in HNSCC and has been used to study chemoprevention by rapamycin and treatment with inhibitors of PI3K/mTOR and interleukin-13 receptor[129-131].

Chemoprevention by rapamycin was also seen in a model that used $K14CreER^T$ to target $Kras^{G12D}$ and conditional p53 deletion to oral mucosa[132]; it is unclear why conditional p53 deletion promoted SCC development in this model but not when these same genetic alterations were targeted by K5Cre*PR[126]. In a more complex model, conditional p53 deletion targeted by $K14CreER^T$ caused malignant conversion of dysplasias produced by a K5-targeted constitutively active Akt construct[133]. Finally, $K14CreER^T$ targeting of TGFßRII and E-cadherin deletion results in both oral and esophageal SCC formation[134]. In sum, the current HNSCC GEMM models offer a wide array of options for both examining the role of

a specific gene during HNSCC development as well as testing the efficacy of therapeutic interventions on genetically defined tumors.

Genetic and carcinogenesis models have also been combined to study the effects of oncogenes and tumor suppressors on HNSCC initiation, progression, and metastasis. For example, a single dose of oral DMBA produces HNSCC in 100% of mice with K5-targeted TGFßRII deletion[127] and 45% of mice with a K14-targeted TGFßRI deletion[135]. Interestingly, cervical lymph node metastases were observed in both models, but no tumors were observed without DMBA tumor initiation[127,135]. A single submandibular DMBA injection has also been used to induce salivary gland sarcomas in $p53^{-/-}$ mice[114], while chronic oral DMBA treatment has been used to demonstrate that nude mice develop HNSCC more rapidly than immunocompetent C57BL6 animals[136]. Similarly, deletion or mutation of tumor suppressors, such as p53 or xeroderma pigmentosa A, renders mice more susceptible to 4NQO carcinogenesis[115,116] while overexpression of oncogenes like HPV proteins E6/E7 and cyclin D1 has a similar effect[137-139].

Imaging Techniques

A number of imaging techniques are also now being coupled with *in vivo* models. The most common is the stable introduction of the firefly luciferase gene into cancer cells prior to grafting; this allows *in vivo* serial imaging of tumor growth by bioluminescence (IVIS)[76,140,141]. Organs can also be imaged by bioluminescence *ex vivo* at the time of euthanasia to detect regional and distant metastases[142]. HPV targeted luciferase reporters can also be combined with genetic models to track tumor response to treatment over time[143]. Cancer cells can also be engineered to express mCherry and then tumor growth and metastasis is tracked by two-photon microscopy[144]. Other imaging techniques have also been used to improve the applicability of animal HNSCC models. Ultrasound can be used to monitor growth of cervical lymph node metastases as well as to guide fine needle sampling of these nodes[145]. This approach may prove powerful for serially tracking lymph node metastases over time. Rigid confocal endoscopy has been used to monitor the growth of carcinogen-induced oral lesions[146]; this may be helpful in modelling the progression of mucosal lesions from dysplasia to cancer. These imaging techniques will likely improve the utility of many HNSCC mouse models by facilitating the monitoring of tumor growth and metastases as well as the response to therapy without needing to euthanize the animal.

REFERENCES

1 Zwart, W. *et al.* Classification of anti-estrogens according to intramolecular FRET effects on phospho-mutants of estrogen receptor alpha. *Molecular cancer therapeutics* **6**, 1526-1533, doi:10.1158/1535-7163.MCT-06-0750 (2007).

2 Gerber, D. E. EGFR Inhibition in the Treatment of Non-Small Cell Lung Cancer. *Drug development research* **69**, 359-372, doi:10.1002/ddr.20268 (2008).

3 Rodriguez-Antona, C. & Taron, M. Pharmacogenomic biomarkers for personalized cancer treatment. *Journal of internal medicine*, doi:10.1111/joim.12321 (2014).

4 Long, G. V. *et al.* Combined BRAF and MEK inhibition versus BRAF inhibition alone in melanoma. *The New England journal of medicine* **371**, 1877-1888, doi:10.1056/NEJMoa1406037 (2014).

5 Gaykalova, D. A. *et al.* Novel insight into mutational landscape of head and neck squamous cell carcinoma. *PloS one* **9**, e93102, doi:10.1371/journal.pone.0093102 (2014).

6 Reshmi, S. C., Saunders, W. S., Kudla, D. M., Ragin, C. R. & Gollin, S. M. Chromosomal instability and marker chromosome evolution in oral squamous cell carcinoma. *Genes, chromosomes & cancer* **41**, 38-46, doi:10.1002/gcc.20064 (2004).

7 Leng, K., Schlien, S. & Bosch, F. X. Refined characterization of head and neck squamous cell carcinomas expressing a seemingly wild-type p53 protein. *Journal of oral pathology & medicine: official publication of the International Association of Oral Pathologists and the American Academy of Oral Pathology* **35**, 19-24, doi:10.1111/j.1600-0714.2005.00365.x (2006).

8 Perez-Ordonez, B., Beauchemin, M. & Jordan, R. C. Molecular biology of squamous cell carcinoma of the head and neck. *Journal of clinical pathology* **59**, 445-453, doi:10.1136/jcp.2003.007641 (2006).

9 Forastiere, A., Koch, W., Trotti, A. & Sidransky, D. Head and neck cancer. *The New England journal of medicine* **345**, 1890-1900, doi:10.1056/NEJMra001375 (2001).

10 Bonner, J. A. *et al.* Radiotherapy plus cetuximab for squamous-cell carcinoma of the head and neck. *The New England journal of medicine* **354**, 567-578, doi:10.1056/NEJMoa053422 (2006).

11 Wilsbacher, J. L. *et al.* Insulin-like growth factor-1 receptor and ErbB kinase inhibitor combinations block proliferation and induce apoptosis through cyclin D1 reduction and Bax activation. *The Journal of biological chemistry* **283**, 23721-23730, doi:10.1074/jbc.M708360200 (2008).

12 Gupta, A. K. *et al.* Radiation response in two HPV-infected head-and-neck cancer cell lines in comparison to a non-HPV-infected cell line and relationship to signaling through AKT. *International journal of radiation oncology, biology, physics* **74**, 928-933, doi:10.1016/j.ijrobp.2009.03.004 (2009).

13 Young, N. R. *et al.* Molecular phenotype predicts sensitivity of squamous cell carcinoma of the head and neck to epidermal growth factor receptor inhibition. *Molecular oncology* **7**, 359-368, doi:10.1016/j.molonc.2012.11.001 (2013).

14 Martin, D. *et al.* The head and neck cancer cell oncogenome: A platform for the development of precision molecular therapies. *Oncotarget* **5**, 8906-8923 (2014).

15 Dok, R. *et al.* p16INK4a impairs homologous recombination-mediated DNA repair in human papillomavirus-positive head and neck tumors. *Cancer research* **74**, 1739-1751, doi:10.1158/0008-5472.can-13-2479 (2014).

16 Li, R. *et al.* Inhibition of STAT3 by niclosamide synergizes with erlotinib against head and neck cancer. *PloS one* **8**, e74670, doi:10.1371/journal.pone.0074670 (2013).

17 Chung, C. H. & Gillison, M. L. Human papillomavirus in head and neck cancer: its role in pathogenesis and clinical implications. *Clinical cancer research: an official journal of the American Association for Cancer Research* **15**, 6758-6762, doi:10.1158/1078-0432.CCR-09-0784 (2009).

18 Park, N. H., Li, S. L., Xie, J. F. & Cherrick, H. M. In vitro and animal studies of the role of viruses in oral carcinogenesis. *European journal of cancer. Part B, Oral oncology* **28b**, 145-152 (1992).

19 Friedman, J. M., Stavas, M. J. & Cmelak, A. J. Clinical and scientific impact of human papillomavirus on head and neck cancer. *World journal of clinical oncology* **5**, 781-791, doi:10.5306/wjco.v5.i4.781 (2014).

20 Ang, K. K. *et al.* Human papillomavirus and survival of patients with oropharyngeal cancer. *The New England journal of medicine* **363**, 24-35, doi:10.1056/NEJMoa0912217 (2010).

21 O'Sullivan, B. *et al.* Deintensification candidate subgroups in human papillomavirus-related oropharyngeal cancer according to minimal risk of distant metastasis. *Journal of clinical oncology: official journal of the American Society of Clinical Oncology* **31**, 543-550, doi:10.1200/JCO.2012.44.0164 (2013).

22 Lin, C. J. *et al.* Head and neck squamous cell carcinoma cell lines: established models and rationale for selection. *Head & neck* **29**, 163-188 (2007).

23 Crowe, D. L. & Sinha, U. K. p53 apoptotic response to DNA damage dependent on bcl2 but not bax in head and neck squamous cell carcinoma lines. *Head & neck* **28**, 15-23, doi:10.1002/hed.20319 (2006).

24 Hoover, A. C. *et al.* The role of human papillomavirus 16 E6 in anchorage-independent and invasive growth of mouse tonsil epithelium. *Archives of otolaryngology--head & neck surgery* **133**, 495-502, doi:10.1001/archotol.133.5.495 (2007).

25 Olthof, N. C. *et al.* Viral load, gene expression and mapping of viral integration sites in HPV16-associated HNSCC cell lines. *International journal of cancer. Journal international du cancer*, doi:10.1002/ijc.29112 (2014).

26 Li, C., Iida, M., Dunn, E. F., Ghia, A. J. & Wheeler, D. L. Nuclear EGFR contributes to acquired resistance to cetuximab. *Oncogene* **28**, 3801-3813, doi:10.1038/onc.2009.234 (2009).

27 Huang, S. *et al.* Dual targeting of EGFR and HER3 with MEHD7945A overcomes acquired resistance to EGFR inhibitors and radiation. *Cancer research* **73**, 824-833, doi:10.1158/0008-5472.CAN-12-1611 (2013).

28 Begg, A. C., van der Kolk, P. J., Dewit, L. & Bartelink, H. Radiosensitization by cisplatin of RIF1 tumour cells in vitro. *International journal of radiation biology and related studies in physics, chemistry, and medicine* **50**, 871-884 (1986).

29 Begg, A. C. & Vens, C. Genetic manipulation of radiosensitivity. *International journal of radiation oncology, biology, physics* **49**, 367-371 (2001).

30 Eschrich, S. A. *et al.* A gene expression model of intrinsic tumor radiosensitivity: prediction of response and prognosis after chemoradiation. *International journal of radiation oncology, biology, physics* **75**, 489-496, doi:10.1016/j.ijrobp.2009.06.014 (2009).

31 Vens, C. & Begg, A. C. Targeting base excision repair as a sensitization strategy in radiotherapy. *Seminars in radiation oncology* **20**, 241-249, doi:10.1016/j.semradonc.2010.05.005 (2010).

32 Pekkola, K. *et al.* Permanent in vitro growth is associated with poor prognosis in head and neck cancer. *Acta oto-laryngologica* **124**, 192-196 (2004).

33 Masuda, N., Fukuoka, M., Takada, M., Kudoh, S. & Kusunoki, Y. Establishment and characterization of 20 human non-small cell lung cancer cell lines in a serum-free defined medium (ACL-4). *Chest* **100**, 429-438 (1991).

34 Verschraegen, C. F. *et al.* Establishment and characterization of cancer cell cultures and xenografts derived from primary or metastatic Mullerian cancers. *Clinical cancer research: an official journal of the American Association for Cancer Research* **9**, 845-852 (2003).

35 Liu, B. *et al.* Anticancer effect of tetrandrine on primary cancer cells isolated from ascites and pleural fluids. *Cancer letters* **268**, 166-175, doi:10.1016/j.canlet.2008.03.059 (2008).

36 Inagaki, T. *et al.* Establishment of human oral-cancer cell lines (KOSC-2 and -3) carrying p53 and c-myc abnormalities by geneticin treatment. *International journal of cancer. Journal international du cancer* **56**, 301-308 (1994).

37 Ince, T. A. *et al.* Transformation of different human breast epithelial cell types leads to distinct tumor phenotypes. *Cancer cell* **12**, 160-170, doi:10.1016/j.ccr.2007.06.013 (2007).

38 Lam, D. C. *et al.* Establishment and expression profiling of new lung cancer cell lines from Chinese smokers and lifetime never-smokers. *Journal of thoracic oncology: official publication of the International Association for the Study of Lung Cancer* **1**, 932-942 (2006).

39 Mouriquand, J., Mouriquand, C., Petitpas, E. & Mermet, M. A. Long-term tissue cultures of human pleural effusions: a cytological follow-up. *In vitro* **14**, 591-600 (1978).

40 Griffon-Etienne, G., Merlin, J. L. & Marchal, C. Evaluation of Taxol in head and neck squamous carcinoma multicellular tumor spheroids. *Anti-cancer drugs* **8**, 48-55 (1997).

41 Engelholm, S. A. *et al.* Genetic instability of cell lines derived from a single human small cell carcinoma of the lung. *European journal of cancer & clinical oncology* **21**, 815-824 (1985).

42 Ferguson, P. J. & Cheng, Y. C. Phenotypic instability of drug sensitivity in a human colon carcinoma cell line. *Cancer research* **49**, 1148-1153 (1989).

43 Kruczynski, A. & Kiss, R. Evidence of a direct relationship between the increase in the in vitro passage number of human non-small-cell-lung cancer primocultures and their chemosensitivity. *Anticancer research* **13**, 507-513 (1993).

44 Johnson, J. I. *et al.* Relationships between drug activity in NCI preclinical in vitro and in vivo models and early clinical trials. *British journal of cancer* **84**, 1424-1431, doi:10.1054/bjoc.2001.1796 (2001).

45 Grenman, R. *et al.* In vitro radiation resistance among cell lines established from patients with squamous cell carcinoma of the head and neck. *Cancer* **67**, 2741-2747 (1991).

46 Spiegel, J., Carey, T. E., Shimoura, S. & Krause, C. J. In vitro sensitivity and resistance of cultured human squamous carcinoma cells to cis-platinum and methotrexate. *Otolaryngology--head and neck surgery: official journal of American Academy of Otolaryngology-Head and Neck Surgery* **92**, 524-531 (1984).

47 Cohen, M. H. *et al.* Approval summary for imatinib mesylate capsules in the treatment of chronic myelogenous leukemia. *Clinical cancer research: an official journal of the American Association for Cancer Research* **8**, 935-942 (2002).

48 O'Brien, S. G. *et al.* Antisense BCR-ABL oligomers cause non-specific inhibition of chronic myeloid leukemia cell lines. *Leukemia* **8**, 2156-2162 (1994).

49 Chung, C. H. *et al.* Molecular classification of head and neck squamous cell carcinomas using patterns of gene expression. *Cancer cell* **5**, 489-500 (2004).

50 de Jong, M. C. *et al.* HPV and high-risk gene expression profiles predict response to chemoradiotherapy in head and neck cancer, independent of clinical factors. *Radiotherapy and oncology: journal of the European Society for Therapeutic Radiology and Oncology* **95**, 365-370, doi:10.1016/j.radonc.2010.02.001 (2010).

51 Slebos, R. J. *et al.* Gene expression differences associated with human papillomavirus status in head and neck squamous cell carcinoma. *Clinical cancer research: an official journal of the American Association for Cancer Research* **12**, 701-709, doi:10.1158/1078-0432.CCR-05-2017 (2006).

52 Courtenay, V. D. & Mills, J. An in vitro colony assay for human tumours grown in immune-suppressed mice and treated in vivo with cytotoxic agents. *British journal of cancer* **37**, 261-268 (1978).

53 Bjork-Eriksson, T., West, C., Karlsson, E. & Mercke, C. Tumor radiosensitivity (SF2) is a prognostic factor for local control in head and neck cancers. *International journal of radiation oncology, biology, physics* **46**, 13-19 (2000).

54 Johns, M. E. The clonal assay of head and neck tumor cells: results and clinical correlations. *The Laryngoscope* **92**, 1-26 (1982).

55 Mattox, D. E., Von Hoff, D. D., Clark, G. M. & Aufdemorte, T. B. Factors that influence growth of head and neck squamous carcinoma in the soft agar cloning assay. *Cancer* **53**, 1736-1740 (1984).

56 Stausbol-Gron, B. & Overgaard, J. Relationship between tumour cell in vitro radiosensitivity and clinical outcome after curative radiotherapy for squamous cell carcinoma of the head and neck. *Radiotherapy and oncology: journal of the European Society for Therapeutic Radiology and Oncology* **50**, 47-55 (1999).

57 Brock, W. A., Baker, F. L., Wike, J. L., Sivon, S. L. & Peters, L. J. Cellular radiosensitivity of primary head and neck squamous cell carcinomas and local tumor control. *International journal of radiation oncology, biology, physics* **18**, 1283-1286 (1990).

58 Eschwege, F. *et al.* Predictive assays of radiation response in patients with head and neck squamous cell carcinoma: a review of the Institute Gustave Roussy experience. *International journal of radiation oncology, biology, physics* **39**, 849-853 (1997).

59 Girinsky, T. *et al.* In vitro parameters and treatment outcome in head and neck cancers treated with surgery and/or radiation: cell characterization and correlations with local control and overall survival. *International journal of radiation oncology, biology, physics* **30**, 789-794 (1994).

60 Dollner, R., Granzow, C., Tschop, K. & Dietz, A. Ex vivo responsiveness of head and neck squamous cell carcinoma to vinorelbine. *Anticancer research* **26**, 2361-2365 (2006).

61 Horn, I. S. *et al.* Heterogeneity of epithelial and stromal cells of head and neck squamous cell carcinomas in ex vivo chemoresponse. *Cancer chemotherapy and pharmacology* **65**, 1153-1163, doi:10.1007/s00280-009-1124-4 (2010).

62 Stausbol-Gron, B., Nielsen, O. S., Moller Bentzen, S. & Overgaard, J. Selective assessment of in vitro radiosensitivity of tumour cells and fibroblasts from single tumour biopsies using immunocytochemical identification of colonies in the soft agar clonogenic assay. *Radiotherapy and oncology: journal of the European Society for Therapeutic Radiology and Oncology* **37**, 87-99 (1995).

63 Dollner, R. *et al.* The impact of stromal cell contamination on chemosensitivity testing of head and neck carcinoma. *Anticancer research* **24**, 325-331 (2004).

64 Robbins, K. T., Connors, K. M., Storniolo, A. M., Hanchett, C. & Hoffman, R. M. Sponge-gel-supported histoculture drug-response assay for head and neck cancer. Correlations with clinical response to cisplatin. *Archives of otolaryngology--head & neck surgery* **120**, 288-292 (1994).

65 Ariyoshi, Y., Shimahara, M. & Tanigawa, N. Study on chemosensitivity of oral squamous cell carcinomas by histoculture drug response assay. *Oral oncology* **39**, 701-707 (2003).

66 Hasegawa, Y. *et al.* Evaluation of optimal drug concentration in histoculture drug response assay in association with clinical efficacy for head and neck cancer. *Oral oncology* **43**, 749-756, doi:10.1016/j.oraloncology.2006.09.003 (2007).

67 Pathak, K. A. *et al.* In vitro chemosensitivity profile of oral squamous cell cancer and its correlation with clinical response to chemotherapy. *Indian journal of cancer* **44**, 142-146 (2007).

68 Singh, B. *et al.* Prediction of survival in patients with head and neck cancer using the histoculture drug response assay. *Head & neck* **24**, 437-442, doi:10.1002/hed.10066 (2002).

69 Heimdal, J., Aarstad, H. J. & Olofsson, J. Monocytes secrete interleukin-6 when co-cultured in vitro with benign or malignant autologous fragment spheroids from squamous cell carcinoma patients. *Scandinavian journal of immunology* **51**, 271-278 (2000).

70 Kross, K. W., Heimdal, J. H., Olsnes, C., Olofsson, J. & Aarstad, H. J. Co-culture of head and neck squamous cell carcinoma spheroids with autologous monocytes predicts prognosis. *Scandinavian journal of immunology* **67**, 392-399, doi:10.1111/j.1365-3083.2008.02072.x (2008).

71 Lim, Y. C. *et al.* Cancer stem cell traits in squamospheres derived from primary head and neck squamous cell carcinomas. *Oral oncology* **47**, 83-91, doi:10.1016/j.oraloncology.2010.11.011 (2011).

72 Lim, Y. C., Oh, S. Y. & Kim, H. Cellular characteristics of head and neck cancer stem cells in type IV collagen-coated adherent cultures. *Experimental cell research* **318**, 1104-1111, doi:10.1016/j.yexcr.2012.02.038 (2012).

73 Kopf-Maier, P. & Kolon, B. An organoid culture assay (OCA) for determining the drug sensitivity of human tumors. *International journal of cancer. Journal international du cancer* **51**, 99-107 (1992).

74 Adachi, M., Cui, C., Dodge, C. T., Bhayani, M. K. & Lai, S. Y. Targeting STAT3 inhibits growth and enhances radiosensitivity in head and neck squamous cell carcinoma. *Oral oncology* **48**, 1220-1226, doi:10.1016/j.oraloncology.2012.06.006 (2012).

75 Galer, C. E. *et al.* Hyaluronic acid-paclitaxel conjugate inhibits growth of human squamous cell carcinomas of the head and neck via a hyaluronic acid-mediated mechanism. *Oral oncology* **47**, 1039-1047, doi:10.1016/j.oraloncology.2011.07.029 (2011).

76 Martin, C. K. *et al.* Zoledronic acid reduces bone loss and tumor growth in an orthotopic xenograft model of osteolytic oral squamous cell carcinoma. *Cancer research* **70**, 8607-8616, doi:10.1158/0008-5472.CAN-10-0850 (2010).

77 Huang, W. C. *et al.* miRNA-491-5p and GIT1 serve as modulators and biomarkers for oral squamous cell carcinoma invasion and metastasis. *Cancer research* **74**, 751-764, doi:10.1158/0008-5472.CAN-13-1297 (2014).

78 Sano, D. *et al.* Disruptive TP53 mutation is associated with aggressive disease characteristics in an orthotopic murine model of oral tongue cancer. *Clinical cancer research: an official journal of the American Association for Cancer Research* **17**, 6658-6670, doi:10.1158/1078-0432.CCR-11-0046 (2011).

79 Szaniszlo, P. *et al.* Temporal characterization of lymphatic metastasis in an orthotopic mouse model of oral cancer. *Head & neck* **36**, 1638-1647, doi:10.1002/hed.23500 (2014).

80 Hwang, Y. S., Zhang, X., Park, K. K. & Chung, W. Y. An orthotopic and osteolytic model with a newly established oral squamous cell carcinoma cell line. *Archives of oral biology* **58**, 218-225, doi:10.1016/j.archoralbio.2012.04.023 (2013).

81 Li, X. *et al.* A CCL2/ROS autoregulation loop is critical for cancer-associated fibroblasts-enhanced tumor growth of oral squamous cell carcinoma. *Carcinogenesis* **35**, 1362-1370, doi:10.1093/carcin/bgu046 (2014).

82 Smirnova, T. *et al.* In vivo invasion of head and neck squamous cell carcinoma cells does not require macrophages. *The American journal of pathology* **178**, 2857-2865, doi:10.1016/j.ajpath.2011.02.030 (2011).

83 Kelland, L. R. Of mice and men: values and liabilities of the athymic nude mouse model in anticancer drug development. *European journal of cancer* **40**, 827-836, doi:10.1016/j.ejca.2003.11.028 (2004).

84 O'Malley, B. W., Jr., Cope, K. A., Johnson, C. S. & Schwartz, M. R. A new immunocompetent murine model for oral cancer. *Archives of otolaryngology--head & neck surgery* **123**, 20-24 (1997).

85 Yuspa, S. H., Hawley-Nelson, P., Koehler, B. & Stanley, J. R. A survey of transformation markers in differentiating epidermal cell lines in culture. *Cancer research* **40**, 4694-4703 (1980).

86 Chen, Z., Smith, C. W., Kiel, D. & Van Waes, C. Metastatic variants derived following in vivo tumor progression of an in vitro transformed squamous cell carcinoma line acquire a differential growth advantage requiring tumor-host interaction. *Clinical & experimental metastasis* **15**, 527-537 (1997).

87 Thomas, G. R., Chen, Z., Oechsli, M. N., Hendler, F. J. & Van Waes, C. Decreased expression of CD80 is a marker for increased tumorigenicity in a new murine model of oral squamous-cell carcinoma. *International journal of cancer. Journal international du cancer* **82**, 377-384 (1999).

88 Behren, A. *et al.* Development of an oral cancer recurrence mouse model after surgical resection. *International journal of oncology* **36**, 849-855 (2010).

89 Dong, G. *et al.* Molecular profiling of transformed and metastatic murine squamous carcinoma cells by differential display and cDNA microarray reveals altered expression of multiple genes related to growth, apoptosis, angiogenesis, and the NF-kappaB signal pathway. *Cancer research* **61**, 4797-4808 (2001).

90 Lee, J. K. *et al.* KITENIN represents a more aggressive phenotype in a murine model of oral cavity squamous carcinoma. *Otolaryngology--head and neck surgery: official journal of American Academy of Otolaryngology-Head and Neck Surgery* **142**, 747-752 e741-742, doi:10.1016/j.otohns.2009.12.032 (2010).

91 Takayama, Y., Mori, T., Nomura, T., Shibahara, T. & Sakamoto, M. Parathyroid-related protein plays a critical role in bone invasion by oral squamous cell carcinoma. *International journal of oncology* **36**, 1387-1394 (2010).

92 Vigneswaran, N., Wu, J., Song, A., Annapragada, A. & Zacharias, W. Hypoxia-induced autophagic response is associated with aggressive phenotype and elevated incidence of metastasis in orthotopic immunocompetent murine models of head and neck squamous cell carcinomas (HNSCC). *Experimental and molecular pathology* **90**, 215-225, doi:10.1016/j.yexmp.2010.11.011 (2011).

93 Anderson, R. T. *et al.* The dual pathway inhibitor rigosertib is effective in direct patient tumor xenografts of head and neck squamous cell carcinomas. *Molecular cancer therapeutics* **12**, 1994-2005, doi:10.1158/1535-7163.MCT-13-0206 (2013).

94 Law, J. H. *et al.* Human-in-mouse modeling of primary head and neck squamous cell carcinoma. *The Laryngoscope* **119**, 2315-2323, doi:10.1002/lary.20607 (2009).

95 Rubio-Viqueira, B. *et al.* An in vivo platform for translational drug development in pancreatic cancer. *Clinical cancer research: an official journal of the American Association for Cancer Research* **12**, 4652-4661, doi:10.1158/1078-0432.CCR-06-0113 (2006).

96 Daniel, V. C. *et al.* A primary xenograft model of small-cell lung cancer reveals irreversible changes in gene expression imposed by culture in vitro. *Cancer research* **69**, 3364-3373, doi:10.1158/0008-5472.CAN-08-4210 (2009).

97 Langdon, S. P. *et al.* Preclinical phase II studies in human tumor xenografts: a European multicenter follow-up study. *Annals of oncology: official journal of the European Society for Medical Oncology / ESMO* **5**, 415-422 (1994).

98 De Wever, O. & Mareel, M. Role of tissue stroma in cancer cell invasion. *The Journal of pathology* **200**, 429-447, doi:10.1002/path.1398 (2003).

99 Gimenez-Conti, I. B., Bianchi, A. B., Stockman, S. L., Conti, C. J. & Slaga, T. J. Activating mutation of the Ha-ras gene in chemically induced tumors of the hamster cheek pouch. *Molecular carcinogenesis* **5**, 259-263 (1992).

100 Yuan, B., Heniford, B. W., Ackermann, D. M., Hawkins, B. L. & Hendler, F. J. Harvey ras (H-ras) point mutations are induced by 4-nitroquinoline-1-oxide in murine oral squamous epithelia, while squamous cell carcinomas and loss of heterozygosity occur without additional exposure. *Cancer research* **54**, 5310-5317 (1994).

101 Shklar, G., Schwartz, J., Grau, D., Trickler, D. P. & Wallace, K. D. Inhibition of hamster buccal pouch carcinogenesis by 13-cis-retinoic acid. *Oral surgery, oral medicine, and oral pathology* **50**, 45-52 (1980).

102 Take, Y., Umeda, M., Teranobu, O. & Shimada, K. Lymph node metastases in hamster tongue cancer induced with 9,10-dimethyl-1,2-benzanthracene: association between histological findings and the incidence of neck metastases, and the clinical implications for patients with tongue cancer. *The British journal of oral & maxillofacial surgery* **37**, 29-36, doi:10.1054/bjom.1998.0271 (1999).

103 Letchoumy, P. V. *et al.* In vitro antioxidative potential of lactoferrin and black tea polyphenols and protective effects in vivo on carcinogen activation, DNA damage, proliferation, invasion, and angiogenesis during experimental oral carcinogenesis. *Oncology research* **17**, 193-203 (2008).

104 Manoharan, S., Balakrishnan, S., Menon, V. P., Alias, L. M. & Reena, A. R. Chemopreventive efficacy of curcumin and piperine during 7,12-dimethylbenz[a]anthracene-induced hamster buccal pouch carcinogenesis. *Singapore medical journal* **50**, 139-146 (2009).

105 Feng, L. & Wang, Z. Chemopreventive effect of celecoxib in oral precancers and cancers. *The Laryngoscope* **116**, 1842-1845, doi:10.1097/01.mlg.0000233778.41927.c7 (2006).

106 Sun, Z. *et al.* Chemoprevention of 7,12-dimethylbenz[a]anthracene (DMBA)-induced oral carcinogenesis in hamster cheek pouch by topical application of a dual inhibitor of epidermal growth factor receptor (EGFR) and ErbB2 tyrosine kinases. *Oral oncology* **44**, 652-657, doi:10.1016/j.oraloncology.2007.08.006 (2008).

107 Schoop, R. A., Noteborn, M. H. & Baatenburg de Jong, R. J. A mouse model for oral squamous cell carcinoma. *Journal of molecular histology* **40**, 177-181, doi:10.1007/s10735-009-9228-z (2009).

108 Tang, X. H., Knudsen, B., Bemis, D., Tickoo, S. & Gudas, L. J. Oral cavity and esophageal carcinogenesis modeled in carcinogen-treated mice. *Clinical cancer research: an official journal of the American Association for Cancer Research* **10**, 301-313 (2004).

109 Li, J., Liang, F., Yu, D., Qing, H. & Yang, Y. Development of a 4-nitroquinoline-1-oxide model of lymph node metastasis in oral squamous cell carcinoma. *Oral oncology* **49**, 299-305, doi:10.1016/j.oraloncology.2012.10.013 (2013).

110 Czerninski, R., Amornphimoltham, P., Patel, V., Molinolo, A. A. & Gutkind, J. S. Targeting mammalian target of rapamycin by rapamycin prevents tumor progression in an oral-specific chemical carcinogenesis model. *Cancer prevention research* **2**, 27-36, doi:10.1158/1940-6207.CAPR-08-0147 (2009).

111 Leeman-Neill, R. J. *et al.* Inhibition of EGFR-STAT3 signaling with erlotinib prevents carcinogenesis in a chemically-induced mouse model of oral squamous cell carcinoma. *Cancer prevention research* **4**, 230-237, doi:10.1158/1940-6207.CAPR-10-0249 (2011).

112 Zhou, G. *et al.* Dual inhibition of vascular endothelial growth factor receptor and epidermal growth factor receptor is an effective chemopreventive strategy in the mouse 4-NQO model of oral carcinogenesis. *Cancer prevention research* **3**, 1493-1502, doi:10.1158/1940-6207.CAPR-10-0135 (2010).

113 Saranath, D. *et al.* High frequency mutation in codons 12 and 61 of H-ras oncogene in chewing tobacco-related human oral carcinoma in India. *British journal of cancer* **63**, 573-578 (1991).

114 Ide, F., Kitada, M., Sakashita, H. & Kusama, K. Reduction of p53 dosage renders mice hypersensitive to 7, 12-dimethylbenz(alpha) anthracene-induced salivary gland tumorigenesis. *Anticancer research* **23**, 201-204 (2003).

115 Ide, F. *et al.* p53 haploinsufficiency profoundly accelerates the onset of tongue tumors in mice lacking the xeroderma pigmentosum group A gene. *The American journal of pathology* **163**, 1729-1733, doi:10.1016/S0002-9440(10)63531-6 (2003).

116 Zhang, Z. *et al.* p53 Transgenic mice are highly susceptible to 4-nitroquinoline-1-oxide-induced oral cancer. *Molecular cancer research: MCR* **4**, 401-410, doi:10.1158/1541-7786.MCR-06-0028 (2006).

117 Berns, A. Cancer. Improved mouse models. *Nature* **410**, 1043-1044, doi:10.1038/35074238 (2001).

118 Opitz, O. G. *et al.* A mouse model of human oral-esophageal cancer. *The Journal of clinical investigation* **110**, 761-769, doi:10.1172/JCI15324 (2002).

119 Vitale-Cross, L., Amornphimoltham, P., Fisher, G., Molinolo, A. A. & Gutkind, J. S. Conditional expression of K-ras in an epithelial compartment that includes the stem cells is sufficient to promote squamous cell carcinogenesis. *Cancer research* **64**, 8804-8807, doi:10.1158/0008-5472.CAN-04-2623 (2004).

120 Akagi, K. *et al.* Cre-mediated somatic site-specific recombination in mice. *Nucleic acids research* **25**, 1766-1773 (1997).

121 Jackson, E. L. *et al.* Analysis of lung tumor initiation and progression using conditional expression of oncogenic K-ras. *Genes & development* **15**, 3243-3248, doi:10.1101/gad.943001 (2001).

122 Caulin, C. *et al.* Inducible activation of oncogenic K-ras results in tumor formation in the oral cavity. *Cancer research* **64**, 5054-5058, doi:10.1158/0008-5472.CAN-04-1488 (2004).

123 Vasioukhin, V., Degenstein, L., Wise, B. & Fuchs, E. The magical touch: genome targeting in epidermal stem cells induced by tamoxifen application to mouse skin. *Proceedings of the National Academy of Sciences of the United States of America* **96**, 8551-8556 (1999).

124 Higashi, A. Y. *et al.* Direct hematological toxicity and illegitimate chromosomal recombination caused by the systemic activation of CreERT2. *Journal of immunology* **182**, 5633-5640, doi:10.4049/jimmunol.0802413 (2009).

125 Leonhard, W. N., Roelfsema, J. H., Lantinga-van Leeuwen, I. S., Breuning, M. H. & Peters, D. J. Quantification of Cre-mediated recombination by a novel strategy reveals a stable extra-chromosomal deletion-circle in mice. *BMC biotechnology* **8**, 18, doi:10.1186/1472-6750-8-18 (2008).

126 Acin, S. *et al.* Gain-of-function mutant p53 but not p53 deletion promotes head and neck cancer progression in response to oncogenic K-ras. *The Journal of pathology* **225**, 479-489, doi:10.1002/path.2971 (2011).

127 Lu, S. L. *et al.* Loss of transforming growth factor-beta type II receptor promotes metastatic head-and-neck squamous cell carcinoma. *Genes & development* **20**, 1331-1342, doi:10.1101/gad.1413306 (2006).

128 Bornstein, S. *et al.* Smad4 loss in mice causes spontaneous head and neck cancer with increased genomic instability and inflammation. *The Journal of clinical investigation* **119**, 3408-3419, doi:10.1172/JCI38854 (2009).

129 Sun, Z. J. *et al.* Chemopreventive and chemotherapeutic actions of mTOR inhibitor in genetically defined head and neck squamous cell carcinoma mouse model. *Clinical cancer research: an official journal of the American Association for Cancer Research* **18**, 5304-5313, doi:10.1158/1078-0432.CCR-12-1371 (2012).

130 Hall, B. *et al.* Targeting of interleukin-13 receptor alpha2 for treatment of head and neck squamous cell carcinoma induced by conditional deletion of TGF-beta and PTEN signaling. *Journal of translational medicine* **11**, 45, doi:10.1186/1479-5876-11-45 (2013).

131 Herzog, A. *et al.* PI3K/mTOR inhibitor PF-04691502 antitumor activity is enhanced with induction of wild-type TP53 in human xenograft and murine knockout models of head and neck cancer. *Clinical cancer research: an official journal of the American Association for Cancer Research* **19**, 3808-3819, doi:10.1158/1078-0432.CCR-12-2716 (2013).

132 Raimondi, A. R., Molinolo, A. & Gutkind, J. S. Rapamycin prevents early onset of tumorigenesis in an oral-specific K-ras and p53 two-hit carcinogenesis model. *Cancer research* **69**, 4159-4166, doi:10.1158/0008-5472.CAN-08-4645 (2009).

133 Moral, M. *et al.* Akt activation synergizes with Trp53 loss in oral epithelium to produce a novel mouse model for head and neck squamous cell carcinoma. *Cancer research* **69**, 1099-1108, doi:10.1158/0008-5472.CAN-08-3240 (2009).

134 Andl, T. *et al.* Concerted loss of TGFbeta-mediated proliferation control and E-cadherin disrupts epithelial homeostasis and causes oral squamous cell carcinoma. *Carcinogenesis* **35**, 2602-2610, doi:10.1093/carcin/bgu194 (2014).

135 Bian, Y. *et al.* Progressive tumor formation in mice with conditional deletion of TGF-beta signaling in head and neck epithelia is associated with activation of the PI3K/Akt pathway. *Cancer research* **69**, 5918-5926, doi:10.1158/0008-5472.CAN-08-4623 (2009).

136 Ku, T. K. & Crowe, D. L. Impaired T lymphocyte function increases tumorigenicity and decreases tumor latency in a mouse model of head and neck cancer. *International journal of oncology* **35**, 1211-1221 (2009).

137 Sarkar, J., Dominguez, E., Li, G., Kusewitt, D. F. & Johnson, D. G. Modeling gene-environment interactions in oral cavity and esophageal cancers demonstrates a role for the p53 R72P polymorphism in modulating susceptibility. *Molecular carcinogenesis* **53**, 648-658, doi:10.1002/mc.22019 (2014).

138 Strati, K., Pitot, H. C. & Lambert, P. F. Identification of biomarkers that distinguish human papillomavirus (HPV)-positive versus HPV-negative head and neck cancers in a mouse model. *Proceedings of the National Academy of Sciences of the United States of America* **103**, 14152-14157, doi:10.1073/pnas.0606698103 (2006).

139 Wilkey, J. F. *et al.* Cyclin D1 overexpression increases susceptibility to 4-nitroquinoline-1-oxide-induced dysplasia and neoplasia in murine squamous oral epithelium. *Molecular carcinogenesis* **48**, 853-861, doi:10.1002/mc.20531 (2009).

140 Paolini, F., Massa, S., Manni, I., Franconi, R. & Venuti, A. Immunotherapy in new pre-clinical models of HPV-associated oral cancers. *Human vaccines & immunotherapeutics* **9**, 534-543 (2013).

141 Sanjiv, K. *et al.* The novel DNA alkylating agent BO-1090 suppresses the growth of human oral cavity cancer in xenografted and orthotopic mouse models. *International journal of cancer. Journal international du cancer* **130**, 1440-1450, doi:10.1002/ijc.26142 (2012).

142 Martin, C. K. *et al.* Characterization of bone resorption in novel in vitro and in vivo models of oral squamous cell carcinoma. *Oral oncology* **48**, 491-499, doi:10.1016/j.oraloncology.2011.12.012 (2012).

143 Zhong, R., Pytynia, M., Pelizzari, C. & Spiotto, M. Bioluminescent imaging of HPV-positive oral tumor growth and its response to image-guided radiotherapy. *Cancer research* **74**, 2073-2081, doi:10.1158/0008-5472.CAN-13-2993 (2014).

144 Gatesman Ammer, A. *et al.* Multi-photon imaging of tumor cell invasion in an orthotopic mouse model of oral squamous cell carcinoma. *Journal of visualized experiments: JoVE*, doi:10.3791/2941 (2011).

145 Walk, E. L., McLaughlin, S., Coad, J. & Weed, S. A. Use of high frequency ultrasound to monitor cervical lymph node alterations in mice. *PloS one* **9**, e100185, doi:10.1371/journal.pone.0100185 (2014).

146 Farahati, B. *et al.* Rigid confocal endoscopy for in vivo imaging of experimental oral squamous intra-epithelial lesions. *Journal of oral pathology & medicine: official publication of the International Association of Oral Pathologists and the American Academy of Oral Pathology* **39**, 318-327, doi:10.1111/j.1600-0714.2009.00841.x (2010).

CHAPTER 3

Feasibility of primary tumor culture models and preclinical prediction assays for head and neck cancer a narrative review

A.J.C. Dohmen
J.E. Swartz
M.W.M. van den Brekel
S.M. Willems
R. Spijker
J. Neefjes
C.L. Zuur

Cancers. Aug 2015, 7(3), 1716-174

ABSTRACT

Primary human tumor culture models allow for individualized drug sensitivity testing and are therefore a promising technique to achieve personalized treatment for cancer patients. This would especially be of interest for patients with advanced stage head and neck cancer. They are extensively treated with surgery, usually in combination with high-dose cisplatin chemoradiation. However, adding cisplatin to radiotherapy is associated with an increase in severe acute toxicity, while conferring only a minor overall survival benefit. Hence, there is a strong need for a preclinical model to identify patients that will respond to the intended treatment regimen and to test novel drugs. One of such models is the technique of culturing primary human tumor tissue. This review discusses the feasibility and success rate of existing primary head and neck tumor culturing techniques and their corresponding chemo- and radiosensitivity assays. A comprehensive literature search was performed and success factors for culturing *in vitro* are debated, together with the actual value of these models as preclinical prediction assay for individual patients. With this review, we aim to fill a gap in the understanding of primary culture models from head and neck tumors, with potential importance for other tumor types as well.

INTRODUCTION

Seventy percent of all patients with head and neck squamous cell carcinoma (HNSCC) present with advanced staged disease and are characterized by an overall 5-year survival rate of approximately 35-60% in case of surgical treatment with or without chemotherapy (CT) and radiotherapy (RT)[1-3]. From around 1980 onward, the addition of high-dose cisplatin to RT (CCRT) has become the routine treatment for locally advanced disease[4]. Nevertheless, a meta-analysis of randomized trials in 2009 indicated that there is only a moderate absolute overall survival benefit of 6.5% at 5 years when adding CT to loco-regional treatment[5]. A subgroup of head and neck cancer (HNC) patients with HPV-positive oropharynx carcinomas usually shows better prognosis after CCRT[6]. A similar analysis in laryngeal cancer patients also described no survival benefit from the addition of CT to RT[7]. Moreover, the addition of high-dose cisplatin to RT is accompanied with a substantial increase in grade three or worse toxicity of 52% to 89%[8]. A more personalized patient selection for this treatment should improve the quality-of-life of the non-responding patient population.

More effective and less toxic targeted therapies have not (yet) penetrated in the treatment of patients with HNC. In recent years, only cetuximab has been registered as a radiosensitizer to improve treatment for advanced HNSCC. Literature, however, shows inconclusive results for survival benefit of this treatment compared to CCRT[9,10]. Unfortunately, this leaves CCRT the mainstream of therapy with rather variable individual clinical outcome.

It therefore remains a major challenge in HNSCC to develop novel drugs for improved survival and to reveal patients prior to therapy that will actually benefit from the intended treatment regimen. Consequently, there is a strong need for a preclinical model to identify those tumors of patients that will respond to a particular treatment. One of such models is the technique of culturing primary tumor tissue and testing drugs prior to treatment. In order for a culture model to be feasible as a preclinical treatment prediction tool, it should be a short-term culture technique, resembling the patient's tumor as closely as possible and it should be low in costs.

Xenograft mouse models can be used to assess therapy response as well. However, they are in fact long-term assays in which the patient's tumor cells adjust to the murine environment, leading to genetic drift of the tumor cells. These models are not optimal, expensive and difficult for multiple drug testing. For these reasons, we excluded xenograft mouse models from our literature search.

With this review, we aim to study feasibility and success percentages of previously described fresh primary HNSCC culturing techniques and their preclinical chemo- and radiosensitivity assays.

MATERIALS AND METHODS

A narrative review was performed via a systematic literature search in Pubmed searching for primary HNSCC tumor culturing techniques (Research Question 1) and their *in vitro* sensitivity assays with clinical correlation (Research Question 2) (*Supplemental Data*). We screened title and abstracts of the identified literature using preformulated criteria (*Figure 1A* and *1B*). Thereafter, a full text screen of the selected articles was done. Included were studies that described any technique for tissue culturing fresh primary tumor tissue of HNSCC patients, except for techniques involving only cultures using xenografts models. The search includes papers using cell lines. Only papers considering primary tumor tissue to establish fresh cell lines were included. Studies describing the use of purchased or already established cell lines, while not reporting the technique of its establishment, were excluded. Also included were fresh HNSCC culture studies regarding *in vitro* versus *in vivo* chemosensitivity or radiosensitivity assays. Additionally, references of the included studies were screened and added to the literature list when relevant. Final selection was based on consensus of all authors.

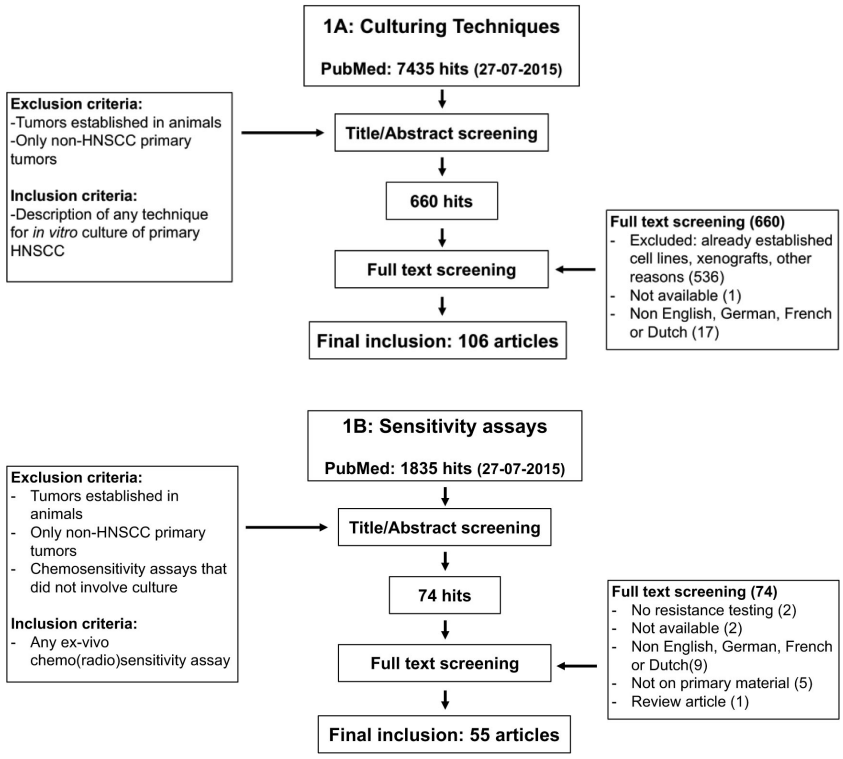

Figure 1. Flow diagram of the systematic literature review process. Literature selection of various culturing techniques concerning Research Question 1 (**A**) and of chemo- and radiosensitivity assays concerning Research Question 2 (**B**), used in head and neck cancer.

RESULTS

An overview of key publications for fresh primary tumor cell culture of HNSCC is presented in Table 1, representing the culturing techniques, and Table 2, showing the clinical correlation.

HNSCC cell lines

The first attempts to establish HNSCC monolayer cell lines were performed in the 1950's on a variety of tumors (sarcoma, leukemia, Hodgkin, myeloma, kidney, breast, lung, pharynx, larynx, rectum, melanoma and ovary)[11]. From the 1980's onward, several groups, including those of Carey and Grenman[12], Rheinwald and Beckett[13], and Easty[14], were among the earliest to be able to establish HNSCC cell lines, achieving success rates of around 30%[12]. Nowadays, a myriad of HNSCC cell lines are available for *in vitro* experiments, as summarized by Carey in 1994[12], Sacks in 1996[15] and Lin in 2007[16]. Also, tumor cell lines from particular patient cases are available, such as very young patients or patients with Fanconi anemia-associated HNSCC[17,18]. It is not exactly known why certain tumors may be cultured indefinitely, while others cannot, although culture success rates have improved by taking biopsies under aseptic conditions from non-necrotic and uninfected tumor areas.
In all studies, HNSCC cell lines were established through the "explant technique", described extensively in 1994 by Carey[12]. In this technique, fresh tumor specimens were mechanically minced into fragments. Samples may be further dispersed enzymatically using trypsin, DNase, collagenase or a combination thereof[19]. The cell suspension was then placed into a rich culture medium, such as DMEM or RPMI-1640 with additional fetal bovine serum (FBS) and transferred to petri-dishes or culture flasks[20-22]. A combination of antibiotics and antimycotics was added to prevent bacterial or fungal overgrowth, and fibroblast overgrowth was managed through selective trypsinization or cell scraping[12]. The cells were then cultured at 37 °C in an air mixture with 5% CO_2. When cells grew to confluency, they were passaged. According to Carey, a cell line may be considered established after the 20th passage (e.g., several months, depending on growth rate), as about 15% of tumor cells initially show growth but then stop growing or die. Success percentages of 11% to 33% have been described for establishment of cell lines from HNSCC in this fashion[13,23,24]. Recently, Owen et al. described higher success rates of 50%. They used fluorescence associated cell sorting to separate fibroblasts from tumor cells. This appeared to be a promising technique to reduce fibroblast overgrowth and to improve the success rate of cell line establishment[25].

Regarding *in vitro* to *in vivo* correlation, no significant difference was found between radiosensitivity of HNSCC cell lines established from 7 patients with recurrent disease

after RT, and cell lines derived from 13 patients without prior RT. Moreover, two patients with unfavorable clinical response to RT, provided cell lines with good irradiation response *in vitro*[26]. However, these preclinical assays did not consider fresh tumor specimens but cell regrowth from previously established cell lines up to 22 passages, conditions that may have selected cells with reasonable radiosensitivity.

Unfortunately, while assays using HNSCC cell lines have been proven essential for experiments concerning molecular biology, they seem not useful as a preclinical prediction model for the individual cancer patient. It is critical to establish cells in culture that best resemble the patient's tumor. This implies that the selection on the fast growing stable cells, surviving under culture conditions, should be prevented. Short tissue cultures, where various cells are still present and not out-selected, would be critical to arrive at patient-relevant culture conditions for the testing of various treatment conditions.

Single cell cultures

One essential way of culturing is by starting off with single cell suspensions from tumor biopsies. This is usually done by mechanical and enzymatic digestion. The first part of *Table 1* describes studies using this technique.

The cell-adhesive matrix (CAM) assay

The cell adhesive matrix (CAM) assay is a monolayer culture system developed by Baker *et al*. that uses a fibronectin and fibrinopeptides coated dish for optimized cell adhesion[27]. Cell growth was stimulated through hormone- and growth factor-supplemented medium. Fresh primary tumor biopsies (melanoma, sarcoma, lung, colon, ovarian and renal) were mechanically and enzymatically digested and plated as single cells. After 24 hours of incubation, irradiation or drugs were administered. After 2 weeks, the cultures were fixed for quantification of cell growth and survival. Baker *et al*.[27] successfully cultured 75% to 90% of tumors using this technique. The articles reviewed, reached culture success rates of 60%, within 14 to 21 days of culturing, in studies with a large number of patients (*Table 1*).

Table 1. Overview of the various culturing techniques from HNSCC tissue.

Authors, year	Assay	Read-out	Result	Corrected for stroma	Days	Patient (n)	Success (%)
Single cell cultures after enzyme digest							
Brock 1990	CAM monolayer	SF2	SF2 0.33 (0.1 1–0.91)	No	14	121	60
Girinsky 1993	CAM monolayer	SF2, alpha	SF2 0.39 (0.37–0.42), alpha 0.18 (0.13–0.24)	No	14–21	96	60
Girinsky 1994	CAM monolayer	SF2, alpha	SF2 0.39 (0.37–0.41). alpha 0.19 (0.14–0.25)	No	14–21	156	60
Eschwege 1997	CAM monolayer	SF2	SF2 0.41 (0.21-0.88)	-	-	92	-
Mattox 1980a	Soft-agar clonogenic	CE (>20 cells), 3-Th	CE 0.006 (0.001–0.08)	No	10–14	36	64
Mattox 1980b	Soft-agar clonogenic	CE (>20 cells)	CE 0.001–0.19	-	14–21	73	45
Johns 1982	Soft-agar clonogenic	CE (≥30 cells, ≥5 colonies)	CE 0.005	No	7–14	73	49
Mattox 1984	Soft-agar clonogenic	CE (≥6 colonies)	CE -	No	14–21	158	36
Cobleigh 1984	Soft-agar clonogenic	CE (≥30 cells. >50 ≥m, >5 colonies)	Growth observation	No	7–14	51	0
Schiff 1984	Soft-agar and agarose	CE (>20 cells)	CE 0.002–0.08	No	7–21	19	56/90**
Rofstad 1987	Soft-agar clonogenic	PE (>50 cells), SF2	SF2 ±0.18–0.45. PE 0.6-2.2	No	28–35	4	33
Stausbøl-Grøn 1995	Soft-agar clonogenic	PE (>50 cells, >60 µm), SF2	SF2 0.36 (0.19–0.88). PE 0.02–0.75	Yes	28	15	-
Stausbø/-Grøn 1999a	Soft-agar clonogenic	PE (>60 µm). SF2	SF2 0.50 (0.11–1.00). PE 0.052 (0.005–1.60)	Yes	28	105	70
Stausbøl-Grøn 1999b	Soft-agar clonogenic	PE (>50 cells/>60 µm), SF2	SF2 0.50 (0.19–1.00). PE 0.043 (0.005–1.03)	Yes	28	105	68
Björk-Eriksson 1998	Soft-agar clonogenic	CE (>50 cells/>60 µm), SF2	SF2 0.48 (0.10–1.00). CE 0.093 (0.002–1.30)	Yes	28	140	74
Björk-Eriksson 2000	Soft-agar clonogenic	CE (>50 cells), SF2	SF2 0.40(0.10–1.00). CE-	Yes	28	156	70
Dollner 2004a	Colony forming (flavin free)	CE (> 16 cells); C100		Yes	4	13	92
Dollner 2004b	Colony forming (flavin free)	CE (> 16 cells); C100		Yes	4	19	85
Dollner 2006a	Colony forming (flavin free)	CE (> 16 cells); C100		Yes	4	13	-
Dollner 2006b	Colony forming (flavin free)	CE (> 16 cells); C100		Yes	4	12	-

Authors, year	Assay	Read-out	Result	Corrected for stroma	Days	Patient (n)	Success (%)
Histocultures							
Robbins 1994	HDRA	3-Th	Sensitivity: ≥84%IR	Yes	3–15	26	88
Singh 2002	HDRA	MTT, DNA	Sensitivity: >30% IR	No	2	42	98
Ariyoshi 2003	HDRA	MTT	Sensitivity: >40%–60% IR, depending on drug	No	7	19	100
Hasegawa 2007	HDRA	MTT	Sensitivity: >40%–60% IR	No	7	49	-
Pathak 2007	HDRA	MTT	Sensitivity: >50% IR	No	8	57	91
Gerlach 2014	Slice culture on membrane	IHC	Cytotoxic effect	No	5 h–7 days	12	-
Heimdal 2000a	Fragment spheroids	IHC	Viability, cytokine	No	10–28	18	90
Kross 2005	Fragment spheroids	ELISA, IHC	IL-6, MCP-],TNF-*	Yes/No	>7	31	-
Kross 2008	Fragment spheroids	ELISA	IL-6, MCP-1*	Yes/No	10–28	65	-
Lim 2011	Squamospheres	Tumor differentiation, stemcell traits	PCR, IHC, FACS, xenograft	No	>14	47	6
Lim 2012	Squamospheres	Tumor differentiation, stemcell traits	PCR, IHC, FACS, western blot, xenograft	No	>14	-	-

*CAM = cell adhesive matrix; ELISA = enzyme-linked immuno sorbent assay; HDRA = histoculture drug response assay; IR = inhibition rate; SF2 = surviving fraction at 2 Gray; PCR = polymerase chain reaction; CE or PE = cloning or plating efficiency; FACS = fluorescence-activated cell sorting; C100 = complete suppression of colony formation; * cytokines and chemokine; MTT = yellow tetrazole is reduced to purple formazan in living cells; ** 56% soft-agar. 90% agarose; IHC = immunohistochemistry.*

The CAM assay in HNSCC has only been used to assess radiosensitivity. Brock *et al*. first reported on radiosensitivity using the CAM assay in 1990, in which 72 of 121 HNSCC patients were evaluable (60% success rate) (*Table 2*)[28,29]. Radiosensitivity was determined by comparing the cell-covered surface to the total surface of 24-well plates after irradiation with 2 Gray (surviving fraction at 2 Gray, SF2). The SF2 was 0.40 in 12 patients with recurrent disease and 0.30 in 60 patients with local tumor control ($p > 0.05$).
In 1994, Girinsky *et al*. described the CAM assay in 156 HNSCC biopsies. SF2 data were available for 76 HNSCC patients[30,31]. SF2 values were not predictive for long-term local control (cut-off 0.50; 66% versus 63%). On the other hand, a significantly higher local control rate ($p = 0.04$) was obtained for patients with higher alpha values (which illustrates the rate of cell kill by a single dose of irradiation; cut-off 0.07 Gy^{-1}; 69% versus 38% at 2 years). The third group to work with the CAM assay was Eschwege *et al*.[32]. They studied 92 HNSCC patients with mainly oropharyngeal carcinomas treated with RT and found both SF2 and alpha value not to be prognostic factors for local control and overall survival.

Soft-agar clonogenic assays

Clonogenic assays, in which single tumor cells were cultured on agar-coated plates, were first described by Puck and Marcus on HeLa cervical tumors[33,34]. In 1977, Salmon and Hamburger utilized an adaptation of this technique as an *in vitro* clonogenic assay of anticancer drugs on tumor cells (myeloma, lymphoma, leukemia, lung, ovary, melanoma and neuroblastoma)[35]. Later, it was used for human pancreatic and colon tumor cells grown in immune-suppressed mice, popularized by Courtenay and Mills and referred to as the Courtenay-Mills clonogenic assay[36]. The main feature of this agar method is its selection for stem cells or transformed cells[37,38]. Although agar cultures also support benign tumors and anchorage-dependent cells, if supplemented with high serum levels or transforming growth factors, soft-agar is still a broadly accepted method for tumor cell selection based on their anchorage-independent growth behavior.
The successful use of the Courtenay-Mills soft-agar clonogenic assay with biopsies of HNSCC was first described by Mattox and Von Hoff[39-41], Johns[37] and Schiff[42] (*Table 1*). Primary HNSCC samples were washed, minced with scalpels and further disaggregated, as in the "explant" technique described by Carey[12]. The cell suspensions were placed in culture plates covered with a feeding layer containing agar, culture medium, FBS and a variety of other nutrients, and then incubated with a chemotherapeutic drug for one hour[41]. After that, cells were washed, plated and incubated, along with untreated controls. After 7 to 21 days, the cultures can be evaluated for colony formation (clumps of more than 20 to 40 cells). Plating efficiency (number of colonies compared to number of plated cells) was generally low, around 0.005, meaning only 1 in 200 cells will grow out as a colony. Cultures

were regarded successful if six or more colonies form in untreated control plates[37,39-41]. The survival fraction was calculated from the number of colonies formed in treated, compared to untreated plates. Survival rates of 30% or less, compared to untreated controls, were considered an *in vitro* indicator of chemosensitivity[37,39-41]. We reviewed several studies using soft-agar clonogenic assays, showing overall success rates of 50% (0% to 74%), where colonies of 20 to 50 cells form within a time span of 1 to 5 weeks[37,39-49]. These studies were done on a reasonably number of patients (*Table 1*). More poorly differentiated tumors had higher overall culture success rates than well-differentiated tumors[39,42].

These authors also did *in vivo* correlations with this assay (*Table 2*). However, chemosensitivity testing was often not possible due to low tumor cell count. Mattox and Johns showed that a higher cloning efficiency (>0.02% and >0.05%) was associated with a higher likelihood of recurrence[37] and early mortality[37,40]. However, a follow-up study of 158 attempted fresh HNSCC cultures did not confirm this correlation[41]. Cobleigh attempted a soft-agar assay on HNSCC in 1984 as well, with no success[45]. Finally, Schiff tried to culture tumors from 19 HNSCC patients[42]. Samples from nine patients were cultured in agar and 10 in agarose. Culture success was higher in agarose-cultured samples (56% versus 90%).

With respect to radiosensitivity correlations done with this clonogenic assay, Rofstad, in 1987, studied various tumors (including four head and neck tumors) with a 33% culture success rate[46]. The SF2 differed considerably among individual tumors of the same histological type. In 1995, Stausbøl-Grøn cultured biopsies of 15 HNSCC patients prior to irradiation[48]. In 12 tumor biopsies 2% to 33% of the colonies were tumor and 83% to 100% of the colonies were fibroblasts. The overall SF2 correlated significantly to the fibroblast SF2 but not to tumor cell SF2. In 1999, the same group assessed radiosensitivity in 105 HNSCC patients. Culture was successful in 70%. Data were described from 38 patients who were treated with RT[47,49]. The majority of the colonies obtained from the biopsies were again fibroblast-marker positive. No significant correlations were found between overall or tumor SF2 and T/N-class and disease stage. Neither tumor cell SF2, overall SF2, nor plating efficiency predicted the locoregional tumor control probability.

Bjork-Eriksson determined the intrinsic radiosensitivity of primary HNSCC on data collected over 5 years for 140 patients using a soft-agar clonogenic assay[44]. Care was taken to ensure that only colonies from malignant cells were scored by morphology and staining. Colonies with a radius of more than 60 µm (>50 cells) after 4 weeks of culture were quantified. A culture success rate of 74% (104/140) was reached with a colony-forming efficiency (CFE) of 0.093 and SF2 data from 63% of the patients was obtained with a mean of 0.48 (0.10–1.00). Interestingly, these authors observed that approximately 0% to 10% of cultured colonies

Table 2. Overview of the various assays and their chemo- and radiosensitivity correlations.

Authors, year	Assay	*In vitro* treatment	*In vivo* treatment	Read-out	Correlation	Outcome correlation	FU (months)
Single cell cultures after enzyme digest							
Brock 1990	CAM monolayer	RT	Post-op RT	SF2	Yes	Local control, SF2: recurrent 0.40 (n = 12), not yet recurred 0.30 (n = 60). Not significant.	24
Girinsky 1993	CAM monolayer	RT	70% RT, 30% post-op RT	SF2, alpha	Yes	Local control: alpha value. Not for survival	15 (1–29)
Girinsky 1994	CAM monolayer	RT	62% RT, 38% post-op RT	SF2, alpha	Yes	Local control: alpha value	24 (9–47)
Eschwege 1997	CAM monolayer	RT	RT	SF2	No	Local control, survival	68 (45–80)
Mattox 1980a	Soft-agar clonogenic	CT	-	CE, 3-Th	-	-	-
Mattox 1980b	Soft-agar clonogenic	CT	-	CE	Yes	Early mortality: CE > 0.02%	-
Johns 1982	Soft-agar clonogenic	CT	-	CE	Yes	Stage, N-class and survival: high CE (n = 29) No correlation positive culture with stage,	-
Mattox 1984	Soft-agar clonogenic	CT	-	CE	No	N-class, recurrence, No difference in survival for high (>0.02%) and low (<0.02%) CE	24
Cobleigh 1984	Soft-agar clonogenic	-	-	CE	-	-	-
Schiff 1984	Soft-agar and agarose	-	-	CE	-	-	-
Rofstad 1987	Soft-agar clonogenic	RT	-	PE, SF2	-	-	-
Stausbøl-Grøn 1995	Soft-agar clonogenic	RT	RT	PE, SF2	-	-	-
Stausbøl-Grøn 1999a	Soft-agar clonogenic	RT	-	PE, SF2	No	Overall/tumor SF2 were not correlated with T/N and stage	-
Stausbøl-Grøn 1999b	Soft-agar clonogenic	RT	RT	PE, SF2	No	Overall/tumor SF2 and PE did not predict local-regional control (n = 38)	42 (16-70)
Björk-Eriksson 1998	Soft-agar clonogenic	RT	-	CE, SF2	No	SF2 did not correlate with tumor grade, T/N class Tumor SF2 (0.40) prognostic for local control, not for overall survival. SF2: recurrent 0.53 (n = 14), not yet recurrent 0.38 (n = 70)	25 (7-65)
Björk-Eriksson 2000	Soft-agar clonogenic	RT	RT/CT/ Surgery	CE, SF2	Yes		
Dollner 2004a	Colony forming (flavin free)	CT	-	CE, C100	-	-	-
Dollner 2004b	Colony forming (flavin free)	CT	-	CE, C100	-	-	-
Dollner 2006a	Colony forming (flavin free)	CT	-	CE, C100	-	-	-
Dollner 2006b	Colony forming (flavin free)	CT	-	CE, C100	-	-	-

Authors, year	Assay	*In vitro* treatment	*In vivo* treatment	Read-out	Correlation	Outcome correlation	FU (months)
			Histocultures				
Robbins 1994	HDRA	CT	CT	3-Th	Yes	Clinical response. PPV 83%, NPV 64%. Sensitivity 71%, specificity 78%	-
Singh 2002	HDRA	CT	Surgery/(C) RT/CT	MTT, DNA	Yes	Clinical response. Chemosensitivity is a significant prognostic variable for 2 year cause specific survival Clinical response. CRT: PPV 87%, NPV 50%.	30
Ariyoshi 2003	HDRA	CT	CT and CRT	MTT	Yes	Sensitivity 87%, specificity 50% (patients received RT, *in vitro* no RT)	-
"	"					CT: PPV 90%, NPV 100%. Sensitivity 100%, specificity 67%	
Hasegawa 2007	HDRA	CT	CT then surgery	MTT	Yes	Clinical response. PPV 77%, NPV 80%. Sensitivity 91%, specificity 57%.	>4 weeks
"	"					Significant correlation between cisplatin sensitivity *in vitro* (50% cut-off) and clinical response. No correlation for 5-FU.	
Pathak 2007	HDRA	CT	Surgery/(C) RT/CT	MTT	Yes	Clinical response. PPV 69%, NPV 80%. Sensitivity 79%, specificity 71%.	2 weeks
"	"					Significant correlation between *in vitro* chemosensitivity and clinical response	
Gerlach 2014	Slice culture on membrane	CT	-	IHC	-	-	-
Heimdal 2000a	Fragment spheroids	-	-	IHC	-	-	-
Kross 2005	Fragment spheroids	-	-	ELISA, IHC	-	-	-
Kross 2008	Fragment spheroids	-	-	ELISA	Yes	Increased IL-6 levels predict recurrence and survival	30
Lim 2011	Squamospheres	CT	-	Differentiation	-	-	-
Lim 2012	Squamospheres	CT	-	Differentiation	-	-	-

CAM = cell adhesive matrix; C100 = complete suppression of colony formation; HDRA = histoculture drug response assay; MTT = a yellow tetrazole, is reduced to purple formazan in living cells; RT = radiotherapy/irradiation; ELISA = enzyme-linked immuno sorbent assay; CT = chemotherapy; IHC = immunohistochemistry; SF2 = surviving fraction at 2 Gray; PPV = positive predictive value; CE or PE = cloning or plating efficiency; NPV = negative predictive value.

were of a non-malignant cell type. In 2000, the same group reported on 156 previously untreated HNC patients (70% culture success rate, 110/156) and evaluated in 54% (84/156) of the patients the prognostic value of SF2 prospectively[43]. Eighty-four patients were mainly treated with neoadjuvant CT plus RT, with or without final surgery. For prognostic analysis, patients were divided in radioresistant (SF2 > 0.40) and radiosensitive (SF2 < 0.40) tumors. After multivariate analysis, tumor SF2 was found an independent prognostic factor for local control (p = 0.036), but not for overall survival (p = 0.20).

Dollner used a colony forming assay without soft-agar, in a 96-well plate format. In 2000, they used monochromatic light sources to avoid flavin-mediated photo-oxidative effects (termed "Flavino-assay") especially during chemosensitivity testing. Fresh tumor biopsies were digested and after 3 days of exposure to various drugs adherent colonies were fixed and counted to determine the IC-50[50,51]. The overall chemoresponse was dominated by stromal cell multidrug resistance[52-54]. Stromal cells were resistant to drug combinations in 98% of the experiments, whereas epithelial colonies were sensitive to cisplatin/5-FU in 16%, to carboplatin/5-FU in 8.3%, to cisplatin/docetaxel in 33% and to carboplatin/docetaxel in 8.3%. In 2010, the assay was correlated to clinical outcome in 18 cultures receiving neoadjuvant TPF (docetaxel, cisplatin and 5-FU) prior to RT[55]. Twelve tumors could be successfully cultured (66.7%) The *in vivo* tumor response to induction CT was correctly predicted by the tumor culture assay in 10 patients (83.3%). However, an *in vitro* prediction of clinical tumor response to the complete treatment regimen was disregarded[55]. These data were only published in a meeting abstract; the full article was not published and thus not fully evaluable. In recent years, this group has used this assay to test CT response to several drugs *in vitro*[56]. However, no reports have been published reporting a proper correlation between predicted outcome based on the Flavino assay and the actual patient outcome in the clinic.

Histocultures

Another way of culturing is to leave tumor tissue intact by only mechanical mincing. This maintains the normal and (largely) unaffected tumor-tumor environment interactions as occurring *in vivo*. The second part of *Table 1* depicts studies using this technique.

The Histoculture Drug Response Assay (HDRA)

In an effort to preserve the three-dimensional (3D) histological structure of the tumor, a method was developed to culture (mouse) breast tumor fragments without further dispersal[57], thereby maintaining cell heterogeneity and cell-cell interactions[58]. These models became the cornerstone of the histoculture drug response assay (HDRA), further

developed by the group of Hoffman for gastric and colorectal cancers[59,60]. Primary tumor material was minced into fragments of about 0.5 mm diameter and placed on 1x1 cm collagen sponge gels in a 24-well plate. One mL of RPMI-1640 medium supplemented with FBS was added and the plate was incubated. RPMI medium was selected rather than (D)MEM, for better preservation of phenotypic heterogeneity[61]. For chemosensitivity assessment, drugs were added to the culture medium and cultured for 7 days. Viability was determined using the MTT assay that measures metabolic activity by a spectrophotometer. When the inhibition rate (absorbance in treated, compared to untreated samples) was 50% or more, tumors were regarded as chemosensitive[62].

Robbins and colleagues were the first to describe the HDRA in HNSCC[63]. They investigated inhibition of tumor proliferation by cisplatin using ^{3}H-thymidine incorporation in tumor cells as an endpoint. In a group of 26 patients with HNC (21 SCC, five with other histological types), 23 (88%) specimens were evaluable. The authors described a positive predictive value (PPV) of 83% and a negative predictive value (NPV) of 64% for partial or complete clinical response in patients treated with cisplatin chemoradiation. Singh observed a correlation between *in vitro* chemosensitivity and 2-year cause-specific survival, for cisplatin, 5-FU and both agents[64]. However, the 41 patients included endured various treatment modalities including CT, surgery and RT. Therefore, no conclusion could be drawn considering chemosensitivity in this study. Another study concerning patients treated for oral cavity SCC showed a PPV of 87% and a NPV of 50% for sensitivity testing with 5-FU, cisplatin, adriamycin, bleomycin and docetaxel[65]. In 2007, Hasegawa *et al.* assessed both primary tumors and lymph node metastases and found a significant correlation between *in vitro* cisplatin sensitivity and clinical response. There was no correlation for 5-FU[62]. Pathak studied a rather homogenous group of oral cavity SCC patients receiving CT regimens resulting in comparable predictive values[66]. The efficacy and utility of the HDRA as a useful predictor for CT response in patients is also described in a number of studies of various pother human solid tumors, including gastric and esophageal cancer[67,68], colorectal cancer[59] and ovarian cancer[69-71].

Recently, Gerlach and colleagues described an adaptation of the HDRA[72]. In this assay, HNSCC fragments of 12 tumors were sliced with a vibratome or tissue chopper and were placed on membranes, rather than a collagen sponge. Tumor slices were incubated with docetaxel, cisplatin, or no drugs and cultured for 5h to 7 days in a flavin-free culture medium. The slices were then fixed, embedded in paraffin and examined using Ki-67 (a proliferation marker), caspase-3 staining (an apoptosis marker) and H2AX (a marker for double-strand DNA breaks). After 7 days of culture, tissue quality decreased in some tumor slices. Increased apoptosis was observed in the slices exposed to drug, compared

to controls. In their publication on this culture method, no correlations to clinical outcomes were done[26]. Recently, more groups have started to generate histocultures of HNSCC to investigate the effect of existing or novel, more targeted drug-based, therapies, such as the PI3K inhibitor LY294002, to investigate the effect of molecular signaling in tumor growth[73,74].

Spheroids, squamospheres and organoids

The spheroid culture technique was developed as well to maintain tumor tissue heterogeneity and 3D architecture (*Table 1*)[75]. Spheroids would ideally resemble the growth pattern of solid tumors *in vivo* as they are composed of an outer layer of proliferating cells closest to nutrient and oxygen supply (capillaries) with inner layers of quiescent and -most central- necrotic cells. This was tested with a variety of cell lines[76,77]. Technically, they can either be grown from cells obtained from monolayer cell cultures after trypsinisation or grown from fresh tumor biopsy fragments[16].

In 2000, Heimdal described malignant and benign "fragment spheroids" in a non-adhesive system[78]. HNSCC fragments were cultured on agar-coated culture flasks and after 10 to 14 days rounded spheroid-like structures were selected for a 2-week co-culture with autologous monocytes derived from peripheral blood samples of the patients. Cytokine IL-6 production of monocytes was significantly higher in case of direct cell-cell (*i.e.*, tumor-monocyte) contact compared to co-cultures where tumor cells and monocytes were separated by a semi-permeable membrane. In 2005, Kross used the same model to study the cytokine secretion, and to describe the number of epithelial cells (cytokeratin positive), fibroblasts (vimentin-positive) and macrophages (CD68 positive) in both malignant HNSCC and benign spheroids[79]. In malignant spheroids, the proportion of epithelial cells during spheroid formation decreased from 28% to 13%. The density of macrophages (2%) and fibroblasts (13%) did not change. Monocytes secreted more IL-6 when co-cultured with malignant compared to benign spheroids. In 2008 they found increased IL-6 cytokine production *in vitro* to be predictive for recurrence and survival (*Table 2*)[80].

A few years later, Lim *et al.* described "squamospheres" resulting from culturing mechanically and enzymatically digested biopsies from 47 HNSCC patients[81]. Single cells were incubated for 2 to 4 weeks to assess sphere forming ability (self-renewal) and other cancer stem cell hallmarks like tumor-initiating capabilities and chemoresistance. A distinction was made between undifferentiated squamospheres (cultured in stem cell medium: serum-free, with N2, B27, EGF and bFGF) and differentiated squamospheres (medium with 10% FBS, without EGF and bFGF). Overall, the success rate of spheroid formation was 6%. Single cells from spheres were assessed for anchorage-independent

growth ability as an indicator for cell transformation *in vitro*; undifferentiated cells that maintained sphere forming capability sustained and differentiated cells diminished in agar. In agreement, tumor formation in nude mice was significantly better for undifferentiated cells. This was later confirmed by Pozzi *et al.*, who found better tumorigenicity in sphere forming cancer stem cell (CSC)-enriched cell populations than in unselected tumor cells[82]. To investigate whether HNSCC CSCs can be expanded in adherent cultures without loss of stem cell properties, Lim *et al.* tested different plate coatings[83]. HNSCC-CSCs grew much faster on type IV collagen-coated plates than in suspension. Adherent CSCs expressed stem cell markers, were chemoresistant, produced tumors in mice and showed less spontaneous apoptotic cell death.

Leong *et al.* described the establishment of three cell lines from primary HNSCC grown as spheroids or monolayers. They confirmed the improved chemoresistance of spheroids when treated with 5FU, cisplatin, etoposide or irradiation[84]. Unfortunately, correlation of the *ex vivo* results with the actual clinical outcome was not one of the aims of this study. On the other hand, while sphere formation or sphere formation capability of CSCs, may increase resistance to some drugs, another group has shown in primary HNSCC spheroid cultures that it is also possible to target these CSCs in particular[85].

Until now, only one group described an "organoid culture assay" of HNSCC[86,87]. Although the authors did not use fresh primary tumor, they aimed for *in vitro* 3D tumor growth allowing to form organized and differentiated structures such as those existing in the organism. After full digestion of a xenografted HNSCC in mice, single cell suspension droplets were seeded on a bridge-like filter in a petri-dish. In this model the tissue grows at the air-medium interface, as medium was added just until the bridge. After 4 weeks solid culture nodules were disaggregated again to assess viability of cells by Trypan Blue. Pathologic evaluation of the nodules showed histological characteristics similar to the original human hypopharyngeal carcinoma up to 3 weeks of culturing. After 3 weeks degeneration was seen.

Other assays

Various other techniques to establish *in vitro* cultures of primary HNSCC were reported, but were only described by a single group and not further popularized. For completeness, these assays are briefly described below.

Flow-cytometric analysis

In 1989, Garozzo presented a different model for short-term culturing of HNSCC in which he acknowledged an equal contribution of all cell populations in the progression of neoplastic disease, and referred to Von Hoff stating that HNC are not very likely to grow on agar[88,89]. Surgical HNSCC specimens were disaggregated into cell suspensions and exposed to various drugs for 24h. The major endpoint was the presence of cell cycle blocks, determined by flow cytometry. Patients were treated with a standardized, undisclosed, regimen of polychemotherapy. Thirteen of the 15 patients showed complete or partial remission. The assay predicted sensitivity to several of the drugs in 11 of these 13 patients (PPV 85%).

Tumor slices grown in test-tubes

Elprana *et al.* described a culture system where human HNSCC fragments, from one patient, floated freely in test tubes containing medium with or without drugs[90,91]. *In vitro*, the tumor was sensitive to cisplatin and 5-fluorouracil. The patient received a combination of these drugs and experienced complete regression in four months, although long-term outcome was not described.

Microdevices

Recently, the group of Greenman cultured HNSCC samples *in vitro* with a microfluidic device. Medium flowed through the device and was collected after drug or irradiation treatment[92-94]. Response to drugs or irradiation is determined by measuring LDH in the effluent. Drug treated samples showed significantly more LDH release than the control groups. No further reports were found that correlated the *in vitro* response to clinical data. This culture technique has been reviewed by Sivagnanam[95].

Micronucleus Assay

Champion *et al.* described an assay that involved establishing a monolayer culture of primary HNSCC tumors and immunohistochemical staining of these cultures after irradiation to identify micronuclei[96]. These micronuclei may be visible in dividing cells and are considered as DNA fragments that cannot be incorporated in daughter cells, due to (radiation) damage. The primary endpoint was the correlation between micronuclei formation and the amount of radiation exposure. After optimizing the assay in cell lines, primary HNSCC specimens were tested. Unfortunately, no correlation between assay outcome and clinical outcome could be established.

DISCUSSION

With this review we aimed to evaluate the most successful *in vitro* culture technique for HNSCC and to discover which model has the best correlation with clinical response. As the chemotherapeutic repertoire increases, a simple and reliable assay to determine the expected patient response becomes critical in making a correct individualized treatment decision.

Monolayer cell line culture is not a proficient method for the use of a preclinical prediction assay. Reasons for this are the long duration of cell line establishment, low culture success rates[12,15] and senescence, the state in which cells no longer divide[13]. Cell line formation is also accompanied with genetic changes like upregulation of oncogenes, and consequently worse clinical outcome[97,98]. Probably for all these reasons a good clinical correlation was never shown[26].

Short-term fresh tumor cultures, however, do not experience clonal evolution of tumor cell (sub)populations[99]. Worsham, Ragin and Bjerkvig found genetic and molecular cytogenetic resemblance between HNSCC cultures and the primary tumor *in vivo*[100-102]. The short duration of culture increases the evaluability of these assays, as these are not influenced by senescence[103-105].

Although tumor biopsies are fully digested in the short-term CAM assay, the assay is thought to allow for restored cell-cell contact within the anchored monolayer. It was probably thought that this anchorage was required to establish the predictive value of SF2 for clinical control, however SF2 was not significantly related to outcome in these studies[29-32]. Only the alpha value (initial slope of radiation curve) had a good clinical correlation with local tumor control in two studies[30,31]. Heppner and colleagues argued that tumor sensitivity to therapeutic agents in a clonal monolayer culture differ to that of *in vivo*-like tissue architectures comprised of heterogeneous cells[106].

Another short-term assay is the soft-agar assay. Von Hoff did a meta-analysis on 54 trials in 1990, using a clonogenic assay, which compared *in vitro* results to clinical outcome in 2300 cases of solid tumors, including a relatively small number of HNSCCs[107]. Overall, they found a 69% true positive rate and a favorable true negative rate of 91%, with a sensitivity and specificity of 79% and 86%, respectively, in predicting outcome. We reviewed several studies using soft-agar showing that plating efficiency of HNSCCs is relatively poor. An explanation may be a rather low subpopulation of stem cells in HNSCC. Moreover, solid HNSCC in these studies were fully digested, likely leading to mechanical trauma to cells. Some authors propose that enzymatic digestion is preferable to maintain viability and growth potential[108]. In addition, the disruption of intercellular attachments may not only irreversibly damage tumor specimens, but may also lead to higher chemosensitivity

of cells, not representing the actual *in vivo* sensitivity[109-113]. For example, this is seen in experiments on mouse mammary tumor cell lines; Miller found that chemoresistance to melphalan and 5-fluorouracil was up to a 1000-fold higher in 3D collagen gel structures than in monolayer cell lines[110,112,113]. Unfortunately, research concerning clonogenic assays also failed to systematically show predictive value for individual clinical outcome, probably due to disruption of the tissue. Namely, four studies investigating clinical correlations involving soft-agar HNSCC colony forming assay, did not find any correlation between *in vitro* and *in vivo* response (*Table 2*)[41,47-49]. In two chemosensitivity studies, plating efficiency was associated with tumor stage, N-class and survival[37] and early mortality[41], however not with therapy response. These studies, nevertheless, described a low number of tumor cells available. Björk performed a radiosensitivity colony forming assay where SF2 was a significant prognostic factor for local control, but not for overall survival[43].

The use of soft-agar should have the advantage of providing support for solid tumor cells, which frequently have difficulties in attaching to the surface of culture dishes. Tumor cells then grow as spherical colonies in agar, while the growth of benign cells such as fibroblast, that require anchorage to a solid substrate, is thought to be reduced[114]. Several groups investigated the impact of stromal cell contamination on culture and treatment sensitivity and concluded that most colonies consisted of fibroblasts. The SF2 is then mainly determined by fibroblast SF2 instead of overall or tumor SF2, and therefore this may contribute as well in not mimicking the correct response *in vivo*[43,44,48,50,51,54,55].

Overall, the number of weeks to culture and the low percentage of evaluable results make the soft-agar clonogenic assay less suitable for use in individual clinical decision making in HNSCC.

In 1994, while other research groups were exploring cultures of fully digested tumor specimens (CAM- and soft-agar assays), Robbins *et al.*, adopted the HDRA model. This short-term, sponge-supported histoculture of HNSCC tissue fragments does not require enzymatic digest, leaving cell-cell adhesions, 3D character, as well as the tumor heterogeneity intact[60,63]. All cells, benign and malignant, are co-cultured together. This method allows for the formation of cell aggregates with identifiable and distinctive tissue patterns simulating the *in vivo* tumor[57]. This probably explains that, for the first time, high culture success rates were reached (88% to 100%). The hypoxic tumor interior, its low pH and relative inaccessibility to chemotherapeutic agents may be the reason for the high predictive values described for *in vivo* correlations, compared to clonogenic or monolayer assays. In addition, the HDRA needs short-term culturing and will therefore have few genetic alterations when compared to longer-term cultures. Finally, the tumor microenvironment in the HDRA may be of importance for a proper clinical correlation, as the presence of tumor-infiltrating lymphocytes seems to determine clinical outcome

in patients with HNSCC[115]. Indeed, the HDRA has been confirmed to be a well feasible culture system for fresh HNSCC tissue, as shown by several other research groups with a good correlation to clinical response[62-66]. Only Singh correlated it with clinical outcome, and found that *in vitro* chemosensitivity was a significant prognostic variable for survival[64]. However, these studies tested only chemosensitivity *in vitro*, while patients received CT often combined with RT. To improve predictive values and to optimize the clinical relevance for predicting the long-term clinical outcome of HNSCC patients, the HDRA model may be tested not only to determine chemosensitivity, but also radiosensitivity. Furthermore, the clinical follow-up duration or the moment of endpoint determination in the identified studies was not always described or it was short (2 to 4 weeks)[62,66]. This might give an overestimate of the chemosensitivity.

Since 2000, several research groups have focused on growing HNSCC "spheres", "squamospheres" and "organoids"[79-81]. As the term suggests, the investigators aimed to establish a 3D arrangement of tumor cells, forming a sphere or organoid, mimicking solid tumor growth *in vivo*. Therefore, the *in vitro* 3D model might better mimic drug response *in vivo*. Heimdal and Kross showed the potential importance of immune cells in culture prediction assays using this model. Increased cytokine production in co-culture was significantly higher in direct cell-cell contact between autologous monocytes and tumor[116], and was found to be predictive for a clinical unfavorable prognosis in HNSCC[80]. However, overall, the reviewed studies did not succeed to systematically generate the intended organoid like structures. In addition, growing spheres and organoids as described here is relatively time-consuming. After 2 weeks of spheroid formation, a prediction assay warrants another 2 weeks of incubation. Within the first weeks a decreasing proportion of epithelial cells was seen[80] and a degeneration of histological characteristics[87].

CONCLUSIONS

Within the treatment of HNSCC, there is a strong need for predicting individual clinical outcome prior to therapy, as the overall patient survival rates are relatively low and reliable biomarkers are not available. Moreover, there is a need to test novel drugs before introduction into clinical practice. A preclinical model that closely resembles the *in vivo* situation would be highly valuable. In this review, we observed that the most successful culture rates and best correlations to clinical response were reported with the HDRA technique. The HDRA assay has the benefit of better representing the tumor and its microenvironment as it does not involve tissue disaggregation, thus maintaining cell heterogeneity, cell-cell interactions and tissue architecture. However, the correlation

to clinical outcome of the HDRA technique has been reported only on a small group of patients and should be validated in larger patient cohorts. Within the HDRA technique it is important to correct for stroma cell response. Another outstanding and obvious point is that the clinical treatment should be resembled *in vitro* as closely as possible, including irradiation. This will ultimately determine the success of this culture-based assay for personalized treatment decisions. As it stands, the HDRA technique appears to be the best model to test and identify novel treatment modalities for HNSCC, which is currently specified by a very poor prognosis.

ACKNOWLEDGMENTS

This work was kindly supported by the Riki Stichting.

REFERENCES

1 Pulte, D. & Brenner, H. Changes in survival in head and neck cancers in the late 20th and early 21st century: a period analysis. *The oncologist* **15**, 994-1001, doi:10.1634/theoncologist.2009-0289 (2010).

2 Surveillance Epidemiology End Results Program. *Cancer of the Larynx - SEER fact sheets*, <http://seer.cancer.gov/statfacts/html/laryn.html> (

3 Surveillance Epidemiology End Results Program. *Cancer of the Oral Cavity and Pharynx - SEER fact sheets*, <http://seer.cancer.gov/statfacts/html/oralcav.html> (

4 Al-Sarraf, M. Treatment of locally advanced head and neck cancer: Historical and critical review. *Cancer Control* **9**, 387-399 (2002).

5 Pignon, J. P., le Maitre, A., Maillard, E., Bourhis, J. & Group, M.-N. C. C. Meta-analysis of chemotherapy in head and neck cancer (MACH-NC): an update on 93 randomised trials and 17,346 patients. *Radiotherapy and oncology: journal of the European Society for Therapeutic Radiology and Oncology* **92**, 4-14, doi:10.1016/j.radonc.2009.04.014; 10.1016/j.radonc.2009.04.014 (2009).

6 Fakhry, C. *et al.* Improved survival of patients with human papillomavirus-positive head and neck squamous cell carcinoma in a prospective clinical trial. *Journal of the National Cancer Institute* **100**, 261-269, doi:10.1093/jnci/djn011 (2008).

7 Forastiere, A. A. *et al.* Long-term results of RTOG 91-11: A comparison of three nonsurgical treatment strategies to preserve the larynx in patients with locally advanced larynx cancer. *Journal of Clinical Oncology* **31**, 845-852, doi:10.1200/JCO.2012.43.6097 (2013).

8 Adelstein, D. J. *et al.* An intergroup phase III comparison of standard radiation therapy and two schedules of concurrent chemoradiotherapy in patients with unresectable squamous cell head and neck cancer. *Journal of clinical oncology: official journal of the American Society of Clinical Oncology* **21**, 92-98, doi:10.1200/JCO.2003.01.008 (2003).

9 Caudell, J. J. *et al.* Locoregionally Advanced Head and Neck Cancer Treated With Primary Radiotherapy: A Comparison of the Addition of Cetuximab or Chemotherapy and the Impact of Protocol Treatment. *International Journal of Radiation Oncology Biology Physics* **71**, 676-681, doi:10.1016/j.ijrobp.2007.10.040 (2008).

10 Ley, J. *et al.* Cisplatin versus cetuximab given concurrently with definitive radiation therapy for locally advanced head and neck squamous cell carcinoma. *Oncology* **85**, 290-296, doi:10.1159/000355194 (2013).

11 Wright, J. C., Cobb, J. P., Gumport, S. L., Golomb, F. M. & Safadi, D. Investigation of the relation between clinical and tissue-culture response to chemotherapeutic agents on human cancer. *The New England journal of medicine* **257**, 1207-1211, doi:10.1056/NEJM195712192572502 (1957).

12 Carey, T. E. (eds R. J. Hay, J. Park, & A. Gazdar) 79-120 (Academic Press, Inc, 1994).

13 Rheinwald, J. G. & Beckett, M. A. Tumorigenic keratinocyte lines requiring anchorage and fibroblast support cultured from human squamous cell carcinomas. *Cancer Research* **41**, 1657-1663 (1981).

14 Easty, D. M., Easty, G. C., Carter, R. L., Monaghan, P. & Butler, L. J. Ten human carcinoma cell lines derived from squamous carcinomas of the head and neck. *British journal of cancer* **43**, 772-785, doi:10.1038/bjc.1981.115 (1981).

15 Sacks, P. G. Cell, tissue and organ culture as in vitro models to study the biology of squamous cell carcinomas of the head and neck. *Cancer metastasis reviews* **15**, 27-51, doi:10.1016/B0-12-227620-5/00124-5 (1996).

16 Lin, C. J. *et al.* Head and neck squamous cell carcinoma cell lines: established models and rationale for selection. *Head & neck* **29**, 163-188, doi:10.1002/hed.20478 (2007).

17 Owen, J. H. *et al.* UM-SCC-103: A Unique Tongue Cancer Cell Line That Recapitulates the Tumorigenic Stem Cell Population of the Primary Tumor. *The Annals of otology, rhinology, and laryngology*, doi:10.1177/0003489414531910 (2014).

18 van Zeeburg, H. J. T. Generation and Molecular Characterization of Head and Neck Squamous Cell Lines of Fanconi Anemia Patients. *Cancer Research* **65**, 1271-1276, doi:10.1158/0008-5472.CAN-04-3665 (2005).

19 Bijman, J. T., Wagener, D. J., van Rennes, H., Wessels, J. M. & van den Broek, P. Flow cytometric evaluation of cell dispersion from human head and neck tumors. *Cytometry* **6**, 334-341 (1985).

20 Ji, Z. W., Oku, N., Umeda, M. & Komori, T. Establishment of an oral squamous cell carcinoma cell line (NOS-1) exhibiting amplification of the erbB-1 oncogene and point mutation of p53 tumor suppressor gene: its biological characteristics and animal model of local invasion by orthotopic transplanta. *Oral oncology* **37**, 386-392 (2001).

21 Kudo, Y. *et al.* Establishment of an oral squamous cell carcinoma cell line with high invasive and p27 degradation activities from a lymph node metastasis. *Oral Oncology* **39**, 515-520, doi:10.1016/S1368-8375(03)00015-0 (2003).

22 Taitz, A. *et al.* Immune parameters of mice bearing human head and neck cancer. *Cancer immunology, immunotherapy: CII* **40**, 283-291 (1995).

23 Kim, S. Y., Chu, K. C., Lee, H. R., Lee, K. S. & Carey, T. E. Establishment and characterization of nine new head and neck cancer cell lines. *Acta oto-laryngologica* **117**, 775-784 (1997).

24 O-Charoenrat, P., Rhys-Evans, P. & Eccles, S. Characterization of ten newly-derived human head and neck squamous carcinoma cell lines with special reference to c-erbB proto-oncogene expression. *Anticancer research* **21**, 1953-1963 (2001).

25 Owen, J. H. *et al.* Novel method of cell line establishment utilizing fluorescence-activated cell sorting resulting in 6 new head and neck squamous cell carcinoma lines. *Head & neck* **55**, 691-696, doi:10.1002/hed.24019 (2015).

26 Grénman, R. *et al.* In vitro radiation resistance among cell lines established from patients with squamous cell carcinoma of the head and neck. *Cancer* **67**, 2741-2747 (1991).

27 Baker, F. L. *et al.* Drug and radiation sensitivity measurements of successful primary monolayer culturing of human tumor cells using cell-adhesive matrix and supplemented medium. *Cancer Research* **46**, 1263-1274 (1986).

28 Brock, W. A., Baker, F. L. & Peters, L. J. Radiosensitivity of human head and neck squamous cell carcinomas in primary culture and its potential as a predictive assay of tumor radiocurability. *International journal of radiation biology* **56**, 751-760, doi:10.1080/09553008914552001 (1989).

29 Brock, W. A., Baker, F. L., Wike, J. L., Sivon, S. L. & Peters, L. J. Cellular radiosensitivity of primary head and neck squamous cell carcinomas and local tumor control. *International journal of radiation oncology, biology, physics* **18**, 1283-1286 (1990).

30 Girinsky, T. *et al.* In vitro parameters and treatment outcome in head and neck cancers treated with surgery and/or radiation: cell characterization and correlations with local control and overall survival. *International journal of radiation oncology, biology, physics* **30**, 789-794, doi:10.1016/0360-3016(94)90350-6 (1994).

31 Girinsky, T. *et al.* Predictive value of in vitro radiosensitivity parameters in head and neck cancers and cervical carcinomas: preliminary correlations with local control and overall survival. *International journal of radiation oncology, biology, physics* **25**, 3-7, doi:10.1016/0360-3016(93)90137-K (1993).

32 Eschwege, F. *et al.* Predictive assays of radiation response in patients with head and neck squamous cell carcinoma: a review of the Institute Gustave Roussy experience. *International journal of radiation oncology, biology, physics* **39**, 849-853 (1997).

33 Puck, T. T. & Marcus, P. I. A rapid method for viable cell titration and clone production with hela cells in tissue culture: the use of x-irradiated cells to supply conditioning factors. *Proceedings of the National Academy of Sciences of the United States of America* **41**, 432-437, doi:10.1073/pnas.41.7.432 (1955).

34 Puck, T. T., Marcus, P. I. & Cieciura, S. J. Clonal growth of mammalian cells in vitro; growth characteristics of colonies from single HeLa cells with and without a feeder layer. *The Journal of experimental medicine* **103**, 273-283, doi:10.1084/jem.103.2.273 (1956).

35 Hamburger, A. W. & Salmon, S. E. Primary bioassay of human tumor stem cells. *Science (New York, N.Y.)* **197**, 461-463, doi:10.1126/science.560061 (1977).

36 Courtenay, V. D. & Mills, J. An in vitro colony assay for human tumours grown in immune-suppressed mice and treated in vivo with cytotoxic agents. *British journal of cancer* **37**, 261-268 (1978).

37 Johns, M. E. The clonal assay of head and neck tumor cells: results and clinical correlations. *The Laryngoscope* **92**, 1-26 (1982).

38 Macpherson, I. & Montagnier, L. Agar suspension culture for the selective assay of cells transformed by polyoma virus. *Virology* **23**, 291-294, doi:10.1016/0042-6822(64)90301-0 (1964).

39 Mattox, D. E. & Von Hoff, D. D. Culture of human head and neck cancer stem cells using soft agar. *Archives of otolaryngology* **106**, 672-674 (1980).

40 Mattox, D. E. & Von Hoff, D. D. In vitro stem cell assay in head and neck squamous carcinoma. *American journal of surgery* **140**, 527-530 (1980).

41 Mattox, D. E., Von Hoff, D. D., Clark, G. M. & Aufdemorte, T. B. Factors that influence growth of head and neck squamous carcinoma in the soft agar cloning assay. *Cancer* **53**, 1736-1740 (1984).

42 Schiff, L. J. & Shugar, M. A. Growth of human head and neck squamous cell carcinoma stem cells in agarose. *Cancer* **53**, 286-290 (1984).

43 Björk-Eriksson, T., West, C., Karlsson, E. & Mercke, C. Tumor radiosensitivity (SF2) is a prognostic factor for local control in head and neck cancers. *International Journal of Radiation Oncology Biology Physics* **46**, 13-19, doi:10.1016/S0360-3016(99)00373-9 (2000).

44 Björk-Eriksson, T. *et al.* The in vitro radiosensitivity of human head and neck cancers. *British journal of cancer* **77**, 2371-2375 (1998).

45 Cobleigh, M. A., Gallagher, P. A., Hill, J. H., Applebaum, E. L. & McGuire, W. P. Growth of human squamous head and neck cancer in vitro. *The American journal of pathology* **115**, 397-402 (1984).

46 Rofstad, E. K., Wahl, A. & Brustad, T. Radiation sensitivity in vitro of cells isolated from human tumor surgical specimens. *Cancer Research* **47**, 106-110 (1987).

47 Stausbøl-Grøn, B. *et al.* In vitro radiosensitivity of tumour cells and fibroblasts derived from head and neck carcinomas: mutual relationship and correlation with clinical data. *British journal of cancer* **79**, 1074-1084, doi:10.1038/sj.bjc.6690172 (1999).

48 Stausbøl-Grøn, B., Nielsen, O. S., Møller Bentzen, S. & Overgaard, J. Selective assessment of in vitro radiosensitivity of tumour cells and fibroblasts from single tumour biopsies using immunocytochemical identification of colonies in the soft agar clonogenic assay. *Radiotherapy and oncology: journal of the European Society for Therapeutic Radiology and Oncology* **37**, 87-99, doi:10.1016/0167-8140(95)98589-D (1995).

49 Stausbøl-Grøn, B. & Overgaard, J. Relationship between tumour cell in vitro radiosensitivity and clinical outcome after curative radiotherapy for squamous cell carcinoma of the head and neck. *Radiotherapy and Oncology* **50**, 47-55, doi:10.1016/S0167-8140(98)00129-7 (1999).

50 Dollner, R. *et al.* Ex vivo responsiveness of head and neck squamous cell carcinoma to glufosfamide, a novel alkylating agent. *Anticancer research* **24**, 2947-2951 (2004).

51 Dollner, R., Granzow, C., Tschop, K. & Dietz, A. Ex vivo responsiveness of head and neck squamous cell carcinoma to vinorelbine. *Anticancer Research* **26**, 2361-2365 (2006).

52 Dollner, R. *et al.* The Impact of Stromal Cell Contamination on Chemosensitivity Testing of Head and Neck Carcinoma. *Anticancer Research* **24**, 325-331 (2004).

53 Dollner, R., Granzow, C., Neudert, M. & Dietz, A. Ex vivo chemosensitivity of head and neck carcinoma to cytostatic drug combinations. *Anticancer Research* **26**, 1651-1655 (2006).

54 Horn, I.-S. *et al.* Heterogeneity of epithelial and stromal cells of head and neck squamous cell carcinomas in ex vivo chemoresponse. *Cancer chemotherapy and pharmacology* **65**, 1153-1163, doi:10.1007/s00280-009-1124-4 (2010).

55 Dietz, A. *et al.* Prediction of outcome of TPF with or without cetuximab induction chemotherapy in head and neck squamous cell carcinoma (HNSCC) using the FLAVINO assay. *Journal of Clinical Oncology* **28**, SUPPL. 1-SUPPL. 1 (2010).

56 Wichmann, G., Körner, C., Boehm, A., Mozet, C. & Dietz, A. Stimulation by Monocyte Chemoattractant Protein-1 Modulates the Ex-vivo Colony Formation by Head and Neck Squamous Cell Carcinoma Cells. *Anticancer research* **35**, 3917-3924 (2015).

57 Leighton, J. A sponge matrix method for tissue culture; formation of organized aggregates of cells in vitro. *Journal of the National Cancer Institute* **12**, 545-561 (1951).

58 Sherwin, R. P., Richters, A., Yellin, A. E. & Donovan, A. J. Histoculture of human breast cancers. *Journal of surgical oncology* **13**, 9-20 (1980).

59 Furukawa, T., Kubota, T. & Hoffman, R. M. Clinical applications of the histoculture drug response assay. *Clinical cancer research: an official journal of the American Association for Cancer Research* **1**, 305-311 (1995).

60 Hoffman, R. M. In vitro sensitivity assays in cancer: a review, analysis, and prognosis. *Journal of clinical laboratory analysis* **5**, 133-143, doi:10.1002/jcla.1860050211 (1991).

61 Burford-Mason, A. P., Dardick, I. & MacKay, A. Collagen gel cultures of normal salivary gland: conditions for continued proliferation and maintenance of major cell phenotypes in vitro. *The Laryngoscope* **104**, 335-340, doi:10.1288/00005537-199403000-00016 (1994).

62 Hasegawa, Y. *et al.* Evaluation of optimal drug concentration in histoculture drug response assay in association with clinical efficacy for head and neck cancer. *Oral Oncology* **43**, 749-756, doi:10.1016/j.oraloncology.2006.09.003 (2007).

63 Robbins, K. T., Connors, K. M., Storniolo, A. M., Hanchett, C. & Hoffman, R. M. Sponge-gel-supported histoculture drug-response assay for head and neck cancer. Correlations with clinical response to cisplatin. *Archives of otolaryngology--head & neck surgery* **120**, 288-292, doi:10.1001/archotol.1994.01880270036007 (1994).

64 Singh, B. *et al.* Prediction of survival in patients with head and neck cancer using the histoculture drug response assay. *Head & neck* **24**, 437-442, doi:10.1002/hed.10066 (2002).

65 Ariyoshi, Y., Shimahara, M. & Tanigawa, N. Study on chemosensitivity of oral squamous cell carcinomas by histoculture drug response assay. *Oral Oncology* **39**, 701-707, doi:10.1016/S1368-8375(03)00082-4 (2003).

66 Pathak, K. A. *et al.* In vitro chemosensitivity profile of oral squamous cell cancer and its correlation with clinical response to chemotherapy. *Indian journal of cancer* **44**, 142-146 (2007).

67 Kubota, T. *et al.* Potential of the histoculture drug-response assay to contribute to cancer patient survival. *Clinical cancer research: an official journal of the American Association for Cancer Research* **1**, 1537-1543 (1995).

68 Suda, S. *et al.* Evaluation of the histoculture drug response assay as a sensitivity test for anticancer agents. *Surgery today* **32**, 477-481, doi:10.1007/s005950200080 (2002).

69 Jung, P.-S. *et al.* Progression-free survival is accurately predicted in patients treated with chemotherapy for epithelial ovarian cancer by the histoculture drug response assay in a prospective correlative clinical trial at a single institution. *Anticancer research* **33**, 1029-1034 (2013).

70 Nakada, S. *et al.* Chemosensitivity testing of ovarian cancer using the histoculture drug response assay: sensitivity to cisplatin and clinical response. *International journal of gynecological cancer: official journal of the International Gynecological Cancer Society* **15**, 445-452, doi:10.1111/j.1525-1438.2005.15307.x.

71 Ohie, S. *et al.* Cisplatin sensitivity of ovarian cancer in the histoculture drug response assay correlates to clinical response to combination chemotherapy with cisplatin, doxorubicin and cyclophosphamide. *Anticancer research* **20**, 2049-2054.

72 Gerlach, M. M. *et al.* Slice cultures from head and neck squamous cell carcinoma: a novel test system for drug susceptibility and mechanisms of resistance. *British journal of cancer* **110**, 479-488, doi:10.1038/bjc.2013.700 (2014).

73 Freudlsperger, C. *et al.* Phosphorylation of AKT(Ser473) serves as an independent prognostic marker for radiosensitivity in advanced head and neck squamous cell carcinoma. *International Journal of Cancer* **136**, 2775-2785, doi:10.1002/ijc.29328 (2015).

74 Peria, M. *et al.* Evaluation of individual sensitivity of Head and Neck Squamous Cell Carcinoma to cetuximab by short-term culture of tumor slices. *Head & neck*, 1-16, doi:10.1002/hed.24126 (2015).

75 Freshney, R. I. in *Culture of Animal Cells: A Manual of Basic Technique and Specialized Applications* Ch. 15 Characterization, (2010).

76 Freyer, J. P. Role of necrosis in regulating the growth saturation of multicellular spheroids. *Cancer research* **48**, 2432-2439 (1988).

77 Schwachofer, J. H. M. *et al.* Oxygen tensions in two human tumor cell lines grown and irradiated as multicellular spheroids. *Anticancer Research* **11**, 273-279 (1991).

78 Heimdal, J. H., Aarstad, H. J. & Olofsson, J. Monocytes secrete interleukin-6 when co-cultured in vitro with benign or malignant autologous fragment spheroids from squamous cell carcinoma patients. *Scandinavian Journal of Immunology* **51**, 271-278, doi:10.1046/j.1365-3083.2000.00680.x (2000).

79 Kross, K. W., Heimdal, J.-H., Olsnes, C., Olofsson, J. & Aarstad, H. J. Head and neck squamous cell carcinoma spheroid- and monocyte spheroid-stimulated IL-6 and monocyte chemotactic

protein-1 secretion are related to TNM stage, inflammatory state and tumor macrophage density. *Acta oto-laryngologica* **125**, 1097-1104, doi:10.1080/00016480510038031 (2005).

80 Kross, K. W., Heimdal, J. H., Olsnes, C., Olofsson, J. & Aarstad, H. J. Co-culture of head and neck squamous cell carcinoma spheroids with autologous monocytes predicts prognosis. *Scandinavian Journal of Immunology* **67**, 392-399, doi:10.1111/j.1365-3083.2008.02072.x (2008).

81 Lim, Y. C. *et al.* Cancer stem cell traits in squamospheres derived from primary head and neck squamous cell carcinomas. *Oral oncology* **47**, 83-91, doi:10.1016/j.oraloncology.2010.11.011 (2011).

82 Pozzi, V. *et al.* Identification and Characterization of Cancer Stem Cells from Head and Neck Squamous Cell Carcinoma Cell Lines. *Cellular Physiology and Biochemistry* **36**, 784-798, doi:10.1159/000430138 (2015).

83 Lim, Y. C., Oh, S.-Y. & Kim, H. Cellular characteristics of head and neck cancer stem cells in type IV collagen-coated adherent cultures. *Experimental Cell Research* **318**, 1104-1111, doi:10.1016/j.yexcr.2012.02.038 (2012).

84 Leong, H. S. *et al.* Targeting Cancer Stem Cell Plasticity Through Modulation of Epidermal Growth Factor and Insulin-Like Growth Factor Receptor Signaling in Head and Neck Squamous Cell Cancer. *Stem Cells Translational Medicine* **3**, 1055-1065, doi:10.5966/sctm.2013-0214 (2014).

85 Sun, S. *et al.* Targeting the c-Met/FZD8 Signaling Axis Eliminates Patient-Derived Cancer Stem-like Cells in Head and Neck Squamous Carcinomas. *Cancer Research* **74**, 7546-7559, doi:10.1158/0008-5472.CAN-14-0826 (2014).

86 Kopf-Maier, P. A new approach for realizing the 'antioncogram'. *Life Sciences* **50**, 1711-1718, doi:10.1016/0024-3205(92)90426-P (1992).

87 Kopf-Maier, P. & Kolon, B. An organoid culture assay (OCA) for determining the drug sensitivity of human tumors. *International Journal of Cancer* **51**, 99-107, doi:10.1002/ijc.2910510119 (1992).

88 Garozzo, A. *et al.* In vitro short-term chemosensitivity test in head and neck tumors. *Journal of chemotherapy (Florence, Italy)* **1**, 59-63 (1989).

89 Von Hoff, D. D. Vol. 308 154-155 (1983).

90 Elprana, D., Schwachöfer, J., Kuijpers, W., Van Den Broek, P. & Wagener, D. J. Cytotoxic drug sensitivity of squamous cell carcinoma as predicted by an in vitro testing model. *Anticancer research* **9**, 1089-1094 (1989).

91 Elprana, D., Schwachöfer, J., Kuijpers, W., van den Broek, P. & Wagener, D. J. In vitro chemosensitivity testing of squamous cell carcinoma of the head and neck. A preliminary report. *Acta oto-laryngologica* **103**, 529-536 (1987).

92 Carr, S. D., Green, V. L., Stafford, N. D. & Greenman, J. Analysis of radiation-induced cell death in head and neck squamous cell carcinoma and rat liver maintained in microfluidic devices. *Otolaryngology--head and neck surgery: official journal of American Academy of Otolaryngology-Head and Neck Surgery* **150**, 73-80, doi:10.1177/0194599813507427 (2014).

93 Hattersley, S. M. *et al.* A microfluidic system for testing the responses of head and neck squamous cell carcinoma tissue biopsies to treatment with chemotherapy drugs. *Annals of Biomedical Engineering* **40**, 1277-1288, doi:10.1007/s10439-011-0428-9 (2012).

94 Sylvester, D., M. Hattersley, S., D. Stafford, N., J. Haswell, S. & Greenman, J. Development of Microfluidic-based Analytical Methodology for Studying the Effects of Chemotherapy Agents on Cancer Tissue. *Current Analytical Chemistry* **9**, 2-8, doi:10.2174/157341113804486446 (2013).

95 Sivagnanam, V. & Gijs, M. A. M. Exploring living multicellular organisms, organs, and tissues using microfluidic systems. *Chemical reviews* **113**, 3214-3247, doi:10.1021/cr200432q (2013).

96 Champion, A. R., Hanson, J. A., Venables, S. E., McGregor, A. D. & Gaffney, C. C. Determination of radiosensitivity in established and primary squamous cell carcinoma cultures using the micronucleus assay. *European Journal of Cancer Part A* **33**, 453-462, doi:10.1016/S0959-8049(97)89022-3 (1997).

97 Köhler, G. *et al.* Oncogene and HSP-70 expression in primary tumor cell cultures of renal cell carcinoma compared to their corresponding cell line. *Anticancer research* **17**, 3225-3231.

98 Liu, C. & Tsao, M. S. Proto-oncogene and growth factor/receptor expression in the establishment of primary human non-small cell lung carcinoma cell lines. *The American journal of pathology* **142**, 413-423 (1993).

99 Shapiro, J. R. & Shapiro, W. R. The subpopulations and isolated cell types of freshly resected high grade human gliomas: Their influence on the tumor's evolution in vivo and behavior and therapy in vitro. *Cancer and Metastasis Review* **4**, 107-124, doi:10.1007/BF00050691 (1985).

100 Bjerkvig, R. *Spheroid Culture in Cancer Research*. First edit edn, (CRC Press, 1992).

101 Ragin, C. C. R., Reshmi, S. C. & Gollin, S. M. Mapping and analysis of HPV16 integration sites in a head and neck cancer cell line. *International journal of cancer. Journal international du cancer* **110**, 701-709, doi:10.1002/ijc.20193 (2004).

102 Worsham, M. J. *et al.* Chromosomal aberrations identified in culture of squamous carcinomas are confirmed by fluorescence in situ hybridisation. *Molecular pathology: MP* **52**, 42-46, doi:10.1136/mp.52.1.42 (1999).

103 Gisselsson, D. *et al.* Centrosomal abnormalities, multipolar mitoses, and chromosomal instability in head and neck tumours with dysfunctional telomeres. *British journal of cancer* **87**, 202-207, doi:10.1038/sj.bjc.6600438 (2002).

104 Jin, Y. *et al.* Chromosome abnormalities in eighty-three head and neck squamous cell carcinomas: influence of culture conditions on karyotypic pattern. *Cancer research* **53**, 2140-2146 (1993).

105 Leess, F. R., Bredenkamp, J. K., Lichtenstein, A. & Mickel, R. A. Lymphokine-activated killing of autologous and allogeneic short-term cultured head and neck squamous carcinomas. *The Laryngoscope* **99**, 1255-1261 (1989).

106 Heppner, G. H. & Miller, B. E. Therapeutic implications of tumor heterogeneity. *Seminars in oncology* **16**, 91-105 (1989).

107 Von Hoff, D. D. He's not going to talk about in vitro predictive assays again, is he? *Journal of the National Cancer Institute* **82**, 96-101 (1990).

108 Moscona, A. Vol. 3 535-539 (1952).

109 Kobayashi, H. *et al.* Acquired multicellular-mediated resistance to alkylating agents in cancer. *Proceedings of the National Academy of Sciences of the United States of America* **90**, 3294-3298, doi:10.1073/pnas.90.8.3294 (1993).

110 Lawler, E. M., Miller, F. R. & Heppner, G. H. Significance of three-dimensional growth patterns of mammary tissues in collagen gels. *In vitro* **19**, 600-610, doi:10.1007/BF02619573 (1983).

111 Miller, B. E., Miller, F. R. & Heppner, G. H. Interactions between tumor subpopulations affecting their sensitivity to the antineoplastic agents cyclophosphamide and methotrexate. *Cancer Research* **41**, 4378-4381 (1981).

112 Miller, B. E., Miller, F. R. & Heppner, G. H. Assessing tumor drug sensitivity by a new in vitro assay which preserves tumor heterogeneity and subpopulation interactions. *Journal of cellular physiology. Supplement* **3**, 105-116 (1984).

113 Miller, B. E., Miller, F. R. & Heppner, G. H. Factors affecting growth and drug sensitivity of mouse mammary tumor lines in collagen gel cultures. *Cancer Research* **45**, 4200-4205 (1985).

114 Lawton, P. A., Hodgkiss, R. J., Eyden, B. P. & Joiner, M. C. Growth of fibroblasts as a potential confounding factor in soft agar clonogenic assays for tumour cell radiosensitivity. *Radiotherapy and oncology: journal of the European Society for Therapeutic Radiology and Oncology* **32**, 218-225, doi:10.1016/0167-8140(94)90021-3 (1994).

115 Balermpas, P. *et al.* CD8+ tumour-infiltrating lymphocytes in relation to HPV status and clinical outcome in patients with head and neck cancer after postoperative chemoradiotherapy: A multicentre study of the German cancer consortium radiation oncology group (DKTK-ROG). *International journal of cancer. Journal international du cancer*, doi:10.1002/ijc.29683 (2015).

116 Heimdal, J. H., Aarstad, H. J., Olsnes, C. & Olofsson, J. Human autologous monocytes and monocyte-derived macrophages in co-culture with carcinoma F-spheroids secrete IL-6 by a non-CD 14-dependent pathway. *Scandinavian Journal of Immunology* **53**, 162-170, doi:10.1046/j.1365-3083.2001.00853.x (2001).

SUPPLEMENTAL DATA

Literature search strategy for question 1 and 2.

Question 1:

(((head[Tiab] OR neck[Tiab] OR tongue[Tiab] OR lip[Tiab] OR cheek[Tiab] OR oral[Tiab] OR oropharyn*[Tiab] OR pharyng*[Tiab] OR pharynx[Tiab] OR larynge*[Tiab] OR larynx[Tiab] OR throat[Tiab] OR glotti*[Tiab] OR nasopharyn*[Tiab] OR hypopharyn*[Tiab] OR "Floor of mouth"[Tiab] OR palate[Tiab] OR retromolar[Tiab] OR gingiva*[Tiab] OR mouth[Tiab] OR ent[Tiab] OR "upper aerodigestive tract"[Tiab] OR UADT[Tiab] OR tonsil*[Tiab]) AND ("squamous cell carcinoma"[Tiab] OR scc[Tiab] OR "carcinoma, squamous cell"[MeSH Terms])) OR (hnscc[Tiab] OR scchn[Tiab] OR "carcinoma, squamous cell of head and neck" [Supplementary Concept])) AND (histoculture[Tiab] OR HDRA[Tiab] OR "cell culture"[Tiab] OR "cells, cultured"[MeSH Terms] OR "single-cell suspension"[Tiab] OR "single-cell suspensions"[Tiab] OR "single cell suspensions"[Tiab] OR "suspension cultures"[Tiab] OR cell-line[Tiab] OR cell-lines[Tiab] OR "cell line"[Tiab] OR "cell lines"[Tiab] OR xenograf*[Tiab] OR "tumor line"[Tiab] OR "tumor lines"[Tiab] OR "primary cell cultures"[Tiab] OR "in vitro model"[Tiab] OR "tissue samples"[Tiab] OR "clonogenic assay"[Tiab] OR tca[Tiab] OR (cells[Tiab] AND culture[Tiab]) OR squamospheres[Tiab] OR "cell culture techniques"[MeSH Terms])

Question 2:

(((head[Tiab] OR neck[Tiab] OR tongue[Tiab] OR lip[Tiab] OR cheek[Tiab] OR oral[Tiab] OR oropharyn*[Tiab] OR pharyng*[Tiab] OR pharynx[Tiab] OR larynge*[Tiab] OR larynx[Tiab] OR throat[Tiab] OR glotti*[Tiab] OR nasopharyn*[Tiab] OR hypopharyn*[Tiab] OR Floor of mouth[Tiab] OR palate[Tiab] OR retromolar[Tiab] OR gingiva*[Tiab] OR mouth[Tiab] OR ENT[Tiab] OR "upper aerodigestive tract"[Tiab] OR UADT[Tiab] OR tonsi*[Tiab]) AND ("squamous cell carcinoma"[Tiab] OR SCC[Tiab] OR "carcinoma, squamous cell"[MeSH Terms])) OR (HNSCC[Tiab] OR SCCHN[Tiab] OR "Carcinoma, squamous cell of head and neck" [Supplementary Concept]))AND (chemoresistan*[tiab] OR chemosensitivity[Tiab] OR chemotoleran*[tiab] OR radiotoleran*[tiab] OR radioresistan*[tiab] OR radiosensitivity[Tiab] OR chemoradiosensitivity[Tiab] OR "Radiation Tolerance"[Mesh terms] OR ((resistanc*[Tiab] OR susceptibility[Tiab] OR sensitivity[Tiab]) AND (cisplatin [Tiab] OR CDDP [Tiab] OR docetaxel [Tiab] OR taxol [Tiab] OR chemotherapy[Tiab] OR radiotherapy[Tiab])))

CHAPTER 4

Sponge-supported cultures of primary head and neck tumors for an optimized preclinical model

A.J.C. Dohmen
J. Sanders
S. Canisius
E.S. Jordanova
E.A. Aalbersberg
M.W.M. van den Brekel
J. Neefjes
C.L. Zuur

Oncotarget. May 2018, 9(38), 25034-25047

ABSTRACT

Treatment of advanced head and neck cancer is associated with low survival, high toxicity and a widely divergent individual response. The sponge-gel-supported histoculture model was previously developed to serve as a preclinical model for predicting individual treatment responses. We aimed to optimize the sponge-gel-supported histoculture model and provide more insight in cell specific behaviour by evaluating the tumor and its microenvironment using immunohistochemistry. We collected fresh tumor biopsies from 72 untreated patients and cultured them for 7 days. Biopsies from 57 patients (79%) were successfully cultured and 1451 tumor fragments (95.4%) were evaluated. Fragments were scored for percentage of tumor, tumor viability and proliferation, EGF-receptor expression and presence of T-cells and macrophages. Median tumor percentage increased from 53% at day 0 to 80% at day 7. Viability and proliferation decreased after 7 days, from 90% to 30% and from 30% to 10%, respectively. Addition of EGF, folic acid and hydrocortisone can lead to improved viability and proliferation, however this was not systematically observed. No patient subgroup could be identified with higher culture success rates. Immune cells were still present at day 7, illustrating that the tumor microenvironment is sustained. EGF supplementation did not increase viability and proliferation in patients overexpressing EGF-Receptor.

INTRODUCTION

Seventy percent of head and neck squamous cell carcinoma (HNSCC) patients present with advanced stage disease. Avast majority of these patients is treated with surgery and/or high-dose cisplatin chemoradiotherapy (CCRT) or cetuximab based bioradiation. Despite these intensive treatment modalities, clinical outcome is characterized by a relatively low overall 5-year survival of 35-63% [1-3]. Furthermore, CCRT is associated with substantial toxicity, namely 89% of patients receiving CCRT for grade III and IV HNSCC, endured grade 3 or worse toxicity (CTCAEv3.0), compared to 52% of patients treated with single modality radiation [4]. A limited absolute overall survival benefit of 6.5% at 5 years for HNSCC patients treated with CCRT compared to RT alone is observed [5]. The choice between different strategies is mainly based on patient comorbidity, age and doctor preferences. Consequently, there is a strong need for a predictive test to select the optimal treatment. A pretreatment method could be a short-term culture model assessing *in vitro* response to different modalities. Ultimately, patients would then undergo individualized treatment regimens based on the *in vitro* tumor response.

Tumor culture assays have the potential to mimic the *in vivo* sensitivity, especially when the microenvironment and the heterogeneity of the tumor is maintained. A recent review summarized all preclinical models in HNSCC [6]. Our group performed a systematic review on primary HNSCC culture models and their ability to predict clinical response. We found that the most successful culture rates and best clinical correlations are obtained with the sponge-gel-supported histoculture, used as the histoculture drug response assay (HDRA) [7]. Leighton *et al.* developed this technique in 1951 in an effort to resemble a patient's tumor more accurately [8]. The technique preserves the 3D histological structure by using tumor fragments instead of cell lines. Furthermore, the sponge-gel-supported histoculture does not require additional enzymatic digestion, thus maintaining cell-cell interactions within the tumor tissue [8, 9]. This short-term assay hinders clonal evolution of tumor cell (sub)populations [10–13] and senescence [14, 15]. All cells, benign and malignant, are co-cultured together, supported by a sponge that allows for the formation of cell clusters with identifiable and distinctive tissue patterns. These are prerequisites to arrive at a preclinical culture model comparable to the *in vivo* tumor environment [8]. The group of Hoffman further developed this assay, in gastric and colorectal cancer, for clinical response applications [16, 17]. Robbins *et al.*, however, were the first to test the HDRA technique on HNSCC tissue in 1994 [18]. Later, the HDRA model was adopted by several authors for preclinical chemosensitivity correlations in patients with head and neck cancer [7, 19–22].

Overall culture success rates of HNSCC with HDRA, are quite high; ranging from 88% to 100% [18, 19, 21, 22] with a culture duration varying from 2 to 11 days [18–21]. The main cause of culture failure is bacterial contamination. Looking at the correlation between *in vitro* chemosensitivity and clinical outcome in these studies, positive predictive values of 69% to 90% and negative predictive values of 50% to 100% were reported [18–21]. Interestingly, one study found improved predictive values by excluding patients that received adjuvant radiotherapy [19]. Despite these promising results, overall, the preclinical model did not allow individual clinical decision making and was therefore not taken into routine clinical practice.

To improve the HNSSC histoculture system, several aspects should be taken into account. Firstly, literature has reported that preclinical chemoresponses and radiation responses are dependent on the response of stromal cells surrounding the malignant cells. These studies indicated that chemosensitivity tests should be corrected for stromal cell content since they are more resistant for cytostatic drugs and radiation [23–25]. Secondly, the abundance of immune cells in the tumor microenvironment (TME) has not been evaluated in previous reports. Extracellular matrix, endothelial, stromal and infiltrating immune cells make up the bulk of the tumor environment and continuously interacts with cancer cells to sustain tumor progression and therapy resistance [26]. The TME affects treatment response and the prognosis of patients. An increased number of immune cells has been shown to correlate to an increased disease-free and overall survival [27, 28]. Thirdly, mainly fetal calf serum has been added to the medium in HDRAs of HNSCC [19–22], which could provide or deplete essential factors for healthy maintenance of the tumors in this culture system. The predictive value of the HDRA system for HNSCC may be improved by adding growth factors and other medium supplements sustaining viability of the cancer and stromal cells. Finally, so far, the HDRA assay in HNSCC has been performed with a metabolic cell viability read-out (MTT or tritiated thymidine incorporation). Using a metabolic read-out, one cannot differentiate between the various cells types present in the tissue.

With our research, we aim to evaluate the short-term sponge-gel-supported tumor histoculture for its abundance, viability and proliferation of malignant cells and surrounding stromal and immune cells using immunohistochemistry. In addition, we aim to test various supplements in the culture medium to support an optimal *in vitro* growth of HNSCC fragments. With these adaptations, we aim to optimize the histoculture for its potential use as an individual preclinical model to select the best individualized treatment regimens for HNSCC patients.

RESULTS

Patient, tumor and histoculture characteristics

Biopsies of 72 patients were taken under routine general anaesthesia and transported to our laboratory. After microscopic assessment of the fragments, we excluded 2 patients in which >50% of the fragments were contaminated with bacteria and fungi (70% and 86%) and 3 patients with >50% of the fragments containing mostly benign cells (67%, and two times 100%). Consequently, 93% of patient biopsies were successfully taken into culture. Furthermore, 6 patients were excluded in which a reliable day 0 statistical calculation was not possible since less than 3 fragments survived the procedure.

Table 1. Patient and tumor characteristics

Characteristics	Number of patients (*n* = 57)
Gender	
Male	36
Female	21
Age	
Age (years, median)	64
Range (years)	45–86
Operating room	
EUA*	38
Surgical resection	19
Anatomical site	
Oral cavity	16
Oropharynx	24
Hypopharynx	7
Larynx	10
T-stage	
T1/T2	27
T3/T4	30
N-stage	
N0	19
N1	5
N2	31
N3	2
Stage	
I/II	11
III/IV	46

**Examination under anaesthesia.*

Four patients with less than 3 fragments at day 7 for our control measurement, standard 'RPMI' medium, were also excluded. In total, 57 of 72 patients (79%) were included for analysis. For further details on patient and tumor characteristics, see Table 1. Of the 24 patients with oropharyngeal tumors tested, 16 tumors were HPV negative and 8 tumors were HPV positive. Fragments were fixated at day 5 for 2 patients and at day 8 for one patient, while all other patient samples were fixed at day 7. For readability, we will further refer to 7 days for all patients.

From the biopsies of 57 patients, we cultured 1451 tumor fragments in total. After microscopic assessment, 104 single fragments (7.2%) were of benign origin (gland or muscle tissue) and therefore excluded from further analysis. From the 1451 tumor fragments we excluded 35 fragments (2.4%) due to bacteria or fungi contamination and 32 fragments (2.2%) due to technical issues (tissue had disintegrated in culture, no tissue in cassette after the tissue processor machine, no tissue found in the paraffin block). Fragments taken from the hypopharynx site had the lowest successful culture efficiency, namely 83.2%, due to a high bacteria or fungi contamination rate of 13.8%. The total evaluability rate of the included 1451 fragments was 95.4% (see Table 2).

Table 2. Overview of tumor fragments per tumor site

	Number of patients	Number of tumor fragments	Contamination	Technical problem	Total succes
Oral cavity	16 (28.1%)	429 (29.6%)	2 (0.5%)	8 (1.9%)	419 (97.7%)
Oropharynx	24 (42.1%)	633 (43.6%)	4 (0.6%)	15 (2.4%)	614 (97.0%)
Hypopharynx	7 (12.3%)	167 (11.5%)	23 (13.8%)	5 (3.0%)	139 (83.2%)
Larynx	10 (17.5%)	222 (15.3%)	6 (2.7%)	4 (1.8%)	212 (95.5%)
Total	**57**	**1451**	**35 (2.4%)**	**32 (2.2%)**	**1384 (95.4%)**

Culture efficacy in view of state, site and tumor proportion

Tumor viability and proliferation at day 7 did not relate to tumor stage or tumor site of origin, see Table 3. Also, we wondered whether a high percentage of cancer cells (raw median ≥70%) in the tissue sample at day 0 would benefit the culture efficacy. However, tumor viability and proliferation during culturing did not relate to the abundance of cancer cells at the start of culture, see Table 3. With ≥70% tumor cells at day 0 a median of 42% viability and 33% proliferation was seen, compared to respectively 30% and 25% with tissue with <70% tumor cells at day 0. As seen in Table 3, the results in the various samples vary widely and no significant differences could be extracted.

Table 3. Culture efficacy in view of state, site and tumor proportion

Variable	% Viability		% Proliferation		# of patients	Statistics	
	Day 7	Range	Day 7	Range			
Stage I	10	5–80	35	1–50	*n* = 2		
Stage II	42	0–300	29	0–167	*n* = 9	Viability	*p = 0.263*[‡]
Stage III	25	11–89	25	0–100	*n* = 6	Proliferation	*p = 0.881*[‡]
Stage IV	36	0–150	29	0–160	*n* = 40		
Oral cavity	27	0–95	33	0–160	*n* = 16		
Oropharynx	31	0–300	25	0–156	*n* = 24	Viability	*p = 0.051*[‡]
Hypopharynx	47	0–100	22	0–133	*n* = 7	Proliferation	*p = 0.272*[‡]
Larynx	44	0–400	33	0–167	*n* = 10		
≥70% Tumor day 0	42	0–150	33	0–167	*n* = 18	Viability	*p = 0.559**
<70% Tumor day 0	30	0–400	25	0–160	*n* = 39	Proliferation	p = 0.053*

*Median normalized percentages of viability and proliferation at day 7 for RPMI fragments, and its range (min – max), in view of stage of disease, tumor site and abundance of cancer cells present at day 0. ([‡]Kruskal–Wallis test; *Mann–Whitney U test.).*

Culture efficacy with RPMI condition

Using the standard 'RPMI' culture condition, the median tumor percentage increased from 53% at day 0 to 80% at day 7. The median viability of these cancer cells decreased from 90% at day 0 to 30% at day 7. The proliferation rate of the viable cancer cells also decreased, from 30% at day 0 to 10% at day 7. When comparing the normalized values of day 0 and 7 the same trend was observed (Figure 1).

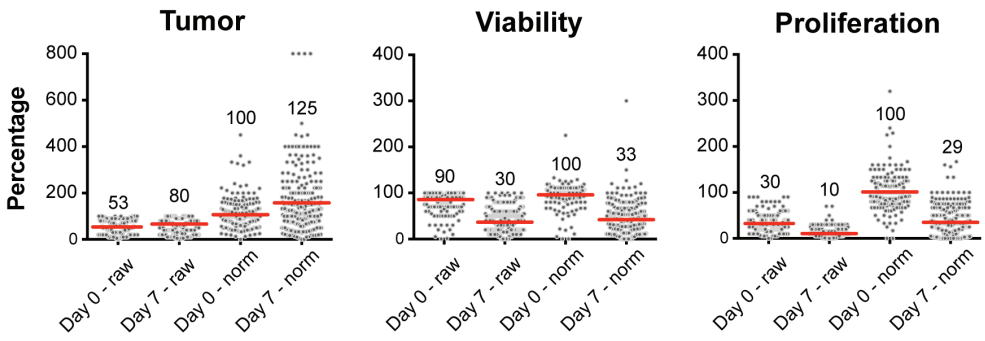

Figure 1. Culture efficacy data from all single tumor fragments (dots) at day 0 and day 7 cultured with standard RPMI. Depicted are the raw and normalized values for each tumor fragment. Values shown in the graph correspond to the horizontal bar which depicts the median from all included fragments.

Optimization conditions

To optimize the histoculture efficacy in terms of tumor viability and proliferation, we tested various optimization conditions and compared the results to the standard 'RPMI' (Figure 2). In Figure 2A normalized percentages of viability and proliferation are shown for all tumor fragments taken together (not per patient), cultured with a specific supplement versus standard RPMI. RPMI reached a median viability of 33% at day 7. EGF 50 ng/ml (34%), hydrocortisone + EGF 50 ng/ml (38%) and folic acid 6 mg/L (42%) increased the median viability of the cultured fragments in comparison to RPMI. Concerning proliferation, various conditions increased the median proliferation rate (RPMI, 28%). However, the best conditions were EGF 50 ng/ml (38%), hydrocortisone (44%) and hydrocortisone + EGF 20 ng/ml (50%) (Figure 2A). The Mann–Whitney *U* test only revealed one significant improvement, namely for hydrocortisone + EGF 20 ng/ml ($p = 0.04$) on proliferation.

However, it could be that data averaged over all tumor fragments (Figure 2A), mask a significantly improved viability or proliferation at the individual patient level. Therefore, data were also analyzed per patient (Figure 2B). The absolute (not relative) median difference between the tested conditions and standard RPMI at day 7, of all fragments from one patient, is plotted in Figure 2B. Value '0' stands for no difference between RPMI and the optimization condition. Addition of EGF 50 ng/ml (9%), hydrocortisone (5%) and folic acid 6 mg/L (5%) improved viability when compared to RPMI. Addition of hydrocortisone + EGF 20 ng/ml (5%), folic acid 6 mg/L (4%) and hydrocortisone (3%) improved proliferation of tumor cells in the tissue fragments.

Data from Figure 2A and 2B suggest that optimization conditions containing hydrocortisone, EGF 50 ng/ml or folic acid 6 mg/L supplements would be optimal to improve viability and proliferation of HNSCC cultures. In Figure 2C these three conditions are shown as normalized median values for all fragments per patient at day 7 and related to standard RPMI. Heterogeneity within individual patient biopsies concerning tumor viability and proliferation in response to supplements EGF, hydrocortisone and folic acid, is observed. Also, data suggest EGF 50 ng/ml and folic acid 6 mg/L to be beneficial for individual tumor viability and not proliferation. Hydrocortisone may be beneficial for individual tumor proliferation, however not for tumor viability.

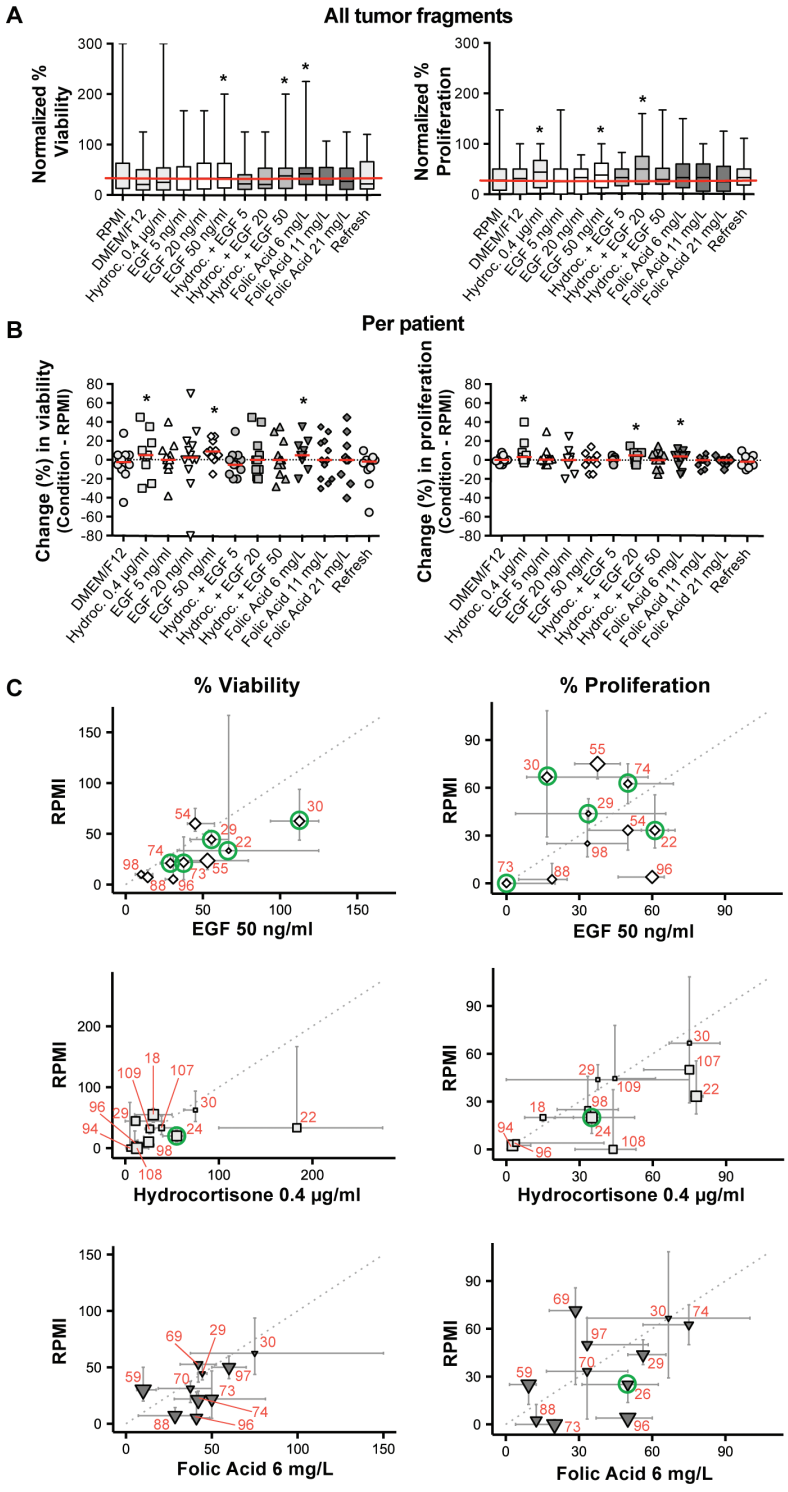
A
All tumor fragments
Normalized % Viability
Normalized % Proliferation
RPMI
DMEMF12
Hydroc. 0.4 µg/ml
EGF 5 ng/ml
EGF 20 ng/ml
EGF 50 ng/ml
Hydroc. + EGF 5
Hydroc. + EGF 20
Hydroc. + EGF 50
Folic Acid 6 mg/L
Folic Acid 11 mg/L
Folic Acid 21 mg/L
Refresh
B
Per patient
Change (%) in viability (Condition - RPMI)
Change (%) in proliferation (Condition - RPMI)
C
% Viability
% Proliferation
RPMI
EGF 50 ng/ml
Hydrocortisone 0.4 µg/ml
Folic Acid 6 mg/L

Figure 2. The effect of the culture optimization conditions on tumor viability and proliferation in comparison to standard RPMI, at day 7. (**A**) Boxplot of normalized viability and proliferation (median and range) of all tumor fragments cultured with the various optimization conditions. The horizontal red line delineates the median value for the standard RPMI. (˚Best conditions.) (**B**) Scatter plot of raw median viability and proliferation percentages per optimization condition when compared to standard RPMI, depicted per individual patient. A single data point represents the difference between the median individual percentage of an optimization condition and the standard RPMI. The red bar indicates the median of all these single data points within that specific condition. (˚Best conditions.) (**C**) Scatter plot of normalized data per patient for the three best selected optimization conditions (EGF 50 ng/ml ◊, Hydrocortisone 0.4 µg/ml and Folic Acid 6 mg/L ▼) versus standard RPMI. One symbol resembles the median of all fragments per individual patient; error bars around the symbols range from the first to the third quartiles. The size of the symbol is inversely proportional to the *p*-value of a two-sided Mann–Whitney *U* test comparing the RPMI and the tested optimization condition within one patient. The green circles indicate the selected samples for EGFR and immune cell IHC. For comparison between figures and tables, red numbers indicate individual patients. (Mind the axes that vary between the graphs.)

EGF-Receptor (EGFR)

In head and neck cancer the EGFR is frequently overexpressed [29]. Therefore, we analyzed whether, the supplementation of EGF would increase viability and proliferation of EGFR positive tissue samples. To study this, we cut additional sections from fragments of 7 patients with EGFR positive tumors (green circles, Figure 2C). Five individual patient fragments were cultured with EGF 50 ng/ml (Histocultures 22, 29, 30, 73 and 74) and 1 fragment with hydrocortisone and folic acid 6 mg/L, both to serve as control. We selected 1 to 2 fragments at day 0 and day 7, see Table 4. Surprisingly, addition of EGF at 50 ng/ml did not further improve viability and proliferation of the EGFR positive tumours in the fragments.

Table 4. EGF-Receptor expression

Patient	Culture condition	EGFR (%)		Viability (%)	Proliferation (%)
		Day 0	Day 7	Day 7	Day 7
22	EGF 50	90	100	30	70
			80	60	50
24	Hydrocortisone	80	70	70	10
		40	80	60	25
26	Folic acid 6	80	70	30	30
		80			
29	EGF 50	50	20	50	30
		40	10	90	2
30	EGF 50	90	10	50	0
		90	5	30	30

Patient	Culture condition	EGFR (%)		Viability (%)	Proliferation (%)
		Day 0	Day 7	Day 7	Day 7
73	EGF 50	100	80	70	10
		90	5	30	0
74	EGF 50	95	40	30	30
			50	40	20

Raw percentage of positive EGFR expression at day 0 and day 7.

Integrity tumor microenvironment during culture

To assess the integrity of the tumor microenvironment during histoculture, we performed additional immune stainings on the same sections previously selected for EGFR. One fragment at day 0 and one at day 7 was selected for multiparameter fluorescent immune cell IHC, an example is shown in Figure 3A and 3B. From these immune cell marker stainings, the raw numbers of positive stained immune cell classes per mm^2 were scored, at day 0 and day 7 (Table 5). Immune cells remained in the tissue of most fragments over the 7-day culture period. There is some variability with some fragments showing a decrease and others showing an increase of immune cell subpopulations when comparing day 0 to day 7 (highlighted cells, Table 5). $CD68^+/CD163^+$ macrophages at day 0 might shift to more $CD68^-/CD163^+$ macrophages at day 7. The number of $CD8^+$ cells may decrease during histoculture. There are no significant differences between the total macrophage and T-cell population when comparing day 0 to day 7 (nonparametric unpaired Mann–Whitney *U* test; p = 0.073 – 1.000).

Table 5. Quantification of immune cell expression

Patient	CD68CD163		CD163		CD68		CD3FoxP3		CD3		CD3CD8		CD3CD8FoxP3	
	Day 0	Day 7	Day 0	Day 7	Day 0	Day 7	Day 0	Day 7	Day 0	Day 7	Day 0	Day 7	Day 0	Day 7
22	3.7	42.5	3.7	10.6	3.7	9.7	38.7	19.4	10.6	7.8	0.0	0.0	0.0	0.0
24	36.7	22.5	2.5	7.0	5.1	9.8	78.8	15.9	36.1	0.0	32.8	0.0	9.9	0.0
26	54.6	20.3	7.1	0.0	2.4	10.1	217.1	41.2	130.3	13.7	111.6	20.6	24.8	0.0
29	0.0	0.0	0.0	0.0	2.2	0.0	6.5	16.1	19.6	32.2	19.6	0.0	0.0	0.0
30	16.7	0.0	0.0	0.0	5.6	11.0	31.1	48.8	56.1	32.5	24.9	16.3	12.5	0.0
73	54.4	58.7	0.0	4.5	38.1	97.9	392.4	222.6	654.1	585.8	697.1	304.6	34.9	11.7
74	33.6	88.7	1.2	7.2	0.0	64.4	6.5	47.7	58.5	160.4	149.6	86.7	0.0	0.0

Values shown are the raw numbers of positive stained immune cells per mm^2, at day 0 and day 7. The highlighted cells point out an increase of immune cells at day 7 when compared to day 0.

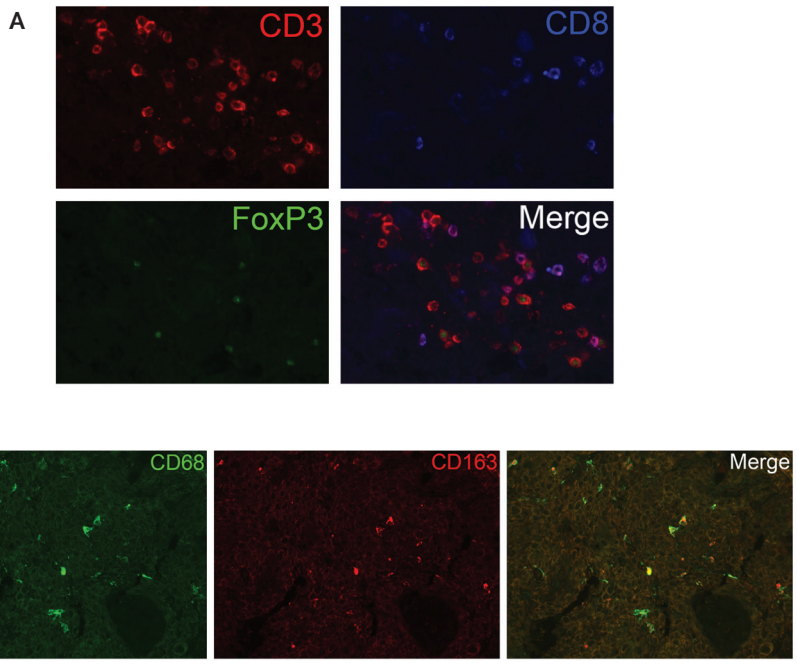

Figure 3. The presence of immune cells during histoculture. (**A**) Visualization of CD3, CD8 and FoxP3 T-cell staining at day 7. In the merged image, one can distinguish between T helper cells (CD3+), cytotoxic T cells (CD3+, CD8+) and regulatory T cells (CD3+, FoxP3+). (**B**) Visualization of CD68 and CD163 macrophage staining at day 0. In the merged image, one can distinguish M2 macrophages (CD68/CD163).

DISCUSSION

Advanced HNSCC is characterized by an unfavourable 5-year overall survival rate of 35–63% [1–3]. Furthermore, there is a widely divergent individual response to CCRT regimens. Consequently, there is a strong need for a preclinical assay to identify the best treatment for individual patients but also to test novel drugs and drug combinations for these patients.

Since the 1990s various culture models to allow for individualized treatment tests in HNSCC patients, have been published. As HNSCC patients need to start their treatment within 5–6 weeks after diagnosis, *in vitro* screening should be performed preferably within 1–2 weeks to guide decision making. The HDRA assay has led to a culture model most comparable to the *in vivo* tumor with successful culture rates, with a read-out after 7–8 days, and the best correlation between *in vitro* and *in vivo* treatment responses [7]. Despite these promising results, the HDRA is not taken into routine clinical practice, likely for various reasons. First, it is difficult to culture tumor tissue. A laboratory within the hospital is needed in order

to quickly transport the fresh biopsies and put them into culture. Secondly, the process of culturing and investigating biopsies is laborious and costly. Thirdly, the specificity and sensitivity of correlating *in vivo* tumor response to *in vitro* HDRA chemosensitivity is relatively low, ranging from 57–78% and 71–91% respectively [18–21]. This could be due the metabolic read-out, used to detect the response of the tumor fragments, as this includes stromal cells and immune cells as well, which might camouflage the specific cancer cell response.
We included immunohistochemistry in our strategy to better determine culture effects on tumor viability and proliferation, and also on the tumor microenvironment which is related to tumor progression, therapy resistance and ultimately patient survival [26, 27]. We also tested various supplements to the standard medium to improve culture conditions.

In our study, 93% of the patient biopsies was successfully cultured. This culture success rate is in agreement with previous literature reporting 88–100% [18, 19, 21, 22]. Hypopharyngeal tumors were more difficult to culture due to a high contamination rate of 13.8% of the fragments. In previous studies [18, 19, 21, 22], the tumor site was never mentioned when patients were excluded due to contamination. We noticed, after microscopic analysis, that more fragments were contaminated with bacteria and fungi than expected. We also noted the culture of benign cells instead of tumor cells, another point not considered in previous studies. Knowing the exact composition of the culture fragments is critical for any conclusion, as illustrated by observations showing that stromal cells are more resistant for cytostatic drugs and radiation *in vitro* [23–25]. When no distinction is made, any chemosensitivity response could represent the response of the tumor microenvironment, benign cells or maybe even contaminations, rather than the tumor cells themselves. By analyzing tumor fragments through immunohistochemistry, we could distinguish tumor cells from benign cells, and also exclude fragments having contaminations. Interestingly, although biopsies were taken from primary tumor sites, 3 patients were excluded since 67% and 100% of the fragments contained mostly benign cells. Furthermore, from the 1451 included tumor fragments we excluded another 104 fragments (7.2%) because of benign tissue presence. The immunohistochemistry read-out also enabled us to see whether a cut-off, arbitrary set to 70% of cancer cells at day 0, would have improved effects on viability and proliferation rates of tumor cells in culture. No significant differences were observed, although tumor fragments containing ≥ 70% tumor cells at day 0 usually showed higher proliferation rates ($p = 0.053$). There is, however, no evidence that the immunohistochemical read-out provides better correlation with regards to *in vitro* chemosensitivity and clinical response. Nevertheless, immunohistochemical read-out of tumor samples is essential to interpret culture results, as our data show.

Using the standard RPMI medium, the percentage of tumor cells increased from 53% at day 0 to 80% at day 7, while the viability and proliferation of the tumor cells decreased from 90% to 30% and from 30% to 10%, respectively. In order to increase the *in vitro* tumor viability and proliferation at day 7 we tested various optimization conditions. EGF 50 ng/ml, folic acid 6 mg/L and hydrocortisone appeared to improve the viability or proliferation, but there was a patient-to-patient variability between the samples and one condition active for all patients was not identified. We also did not find evidence that EGF is more beneficial in tumor samples overexpressing EGFR. It is unclear whether the EGF recombinant protein is able to penetrate or diffuse efficiently into the tumor tissue when cultured on a sponge.

The wide variety in responses in the culture system could be due to the fact that HNSCCs possess a large degree of intra-tumor genetic heterogeneity [30]. This heterogeneity could lead to a selection bias when culturing HNSCC cells. It is plausible that only the more aggressive subclones stay vital and proliferative during culture. Yet, in a 7-day culture, these subclones will most likely not overgrow the other subclones, only become more dominant [31]. Fact is that the culture does not select for one single subclone –as is the case for organoids and tissue culture cell lines- and therefore can be expected to show a more reliable reflection of the individual patient's tumor. Drug responses in sponge-gel-supported histoculture are therefore expected to better predict drug responses *in vivo*.

There are indeed marked variabilities in the tumor behaviour in the tissue culture system, variabilities that can only be observed by microscopic analysis. In our study, tumor viability and proliferation at day 7 did not significantly relate to stage of disease, tumor site, the abundance of cancer cells at day 0 or the percentage of EGFR expression. However, our comparison of viability and proliferation by stage and tumor was descriptive in nature, rather than testing a specific a priori hypothesis. In this perspective, the *p*-value should be interpreted as indicators of the strength of heterogeneity, given the data we have collected. We interpret the fact that none of the *p*-values are significant as evidence that viability and proliferation are relatively similar within categories of stage and tumor site, given the variability of viability and proliferation within each category. The power of the study did not allow selection of a subgroup of patients with tumor tissue growing more successfully in histoculture. In order to potentially use the histoculture as preclinical individual drug-response assay, a larger window in terms of tumor viability and proliferation at day 7 may be required to assess the efficacy of drugs and/or irradiation. We choose a 7-day read-out in line with earlier HDRA studies in HNC [7], showing good culture success rates and relatively good correlation to the clinic. It could be that shortening of the culture period from 7 to 3–5 days demonstrates higher viability and proliferation rates. On the other hand, cancer cells *in vivo* do not grow at rates as described in cell lines or organoids and

have growth rates more similar to those observed in our cultures. But there are still many other variations to test for optimizing the culture system. For example, tumor fragments from one patient (nr 22) were cultured for 5 days. These fragments showed higher rates of viability and proliferation when cultured with EGF. However, reviewing the tumor, it turned out to be an oropharynx tumor with a basaloid SCC histology type, which could be a more rare and aggressive type of cancer [32]. This illustrates that different tumors may have different characteristics in culture, which represents another variable where the pathologist is critical in the assessment of the data.

One obvious advantage of our system over other tumor culture models is that the normal tumor microenvironment is preserved. T-cells and macrophages remain present during 7 days of culture, but again with some variability. Some patients showed a higher number of infiltrating immune cells during culture, and in others the number decreased. Remarkably, in the day 0 fragments almost all macrophages are CD163/CD68 double positive, however after culturing, there is a higher expression of markers for single CD163 and CD68 macrophages. Macrophages exhibiting predominately the anti-inflammatory CD163/CD68 phenotype are known to be tumor-associated M2 macrophages, supporting the tumor, whereas M1 macrophages (CD68) act against the tumor [33]. This switch in phenotype could oppose the grow of tumor cells *in vitro* but this has not been further tested. Although it is an important finding that immune cells are still present after 7 days of culture, we do not have data showing that they are still functionally active or viable. Any such model system limits conclusion on these given the small number of cells and the heterogeneity in the immune cell components observed. Fact is that immune cells do not migrate out of the cultured tissue and be lost for analyses, as our data show. Nevertheless, we have carefully observed the morphology of the macrophages and T-cells infiltrating the tissue before and after culture, and we believe these cells to be still viable as we do not observe any morphological differences: T-cells had a normal rounded shape and FoxP3 expression was very bright in the nucleus. Macrophages had also retained their normal shape and dendrites and had a bright and clear CD68/CD163 staining. So, based on the morphology, we believe that the macrophages were viable, without differences between day 0 and day 7.

In conclusion, the implementation of immunohistochemistry in the sponge-gel-supported histoculture method has provided valuable insights in the quality and interpretation of culturing cancer cells. The histocultures showed decreases in viability and proliferation of tumor cells with marked variation between samples from different patients. This could reflect the natural variability in tumor aggressiveness and tumor type. Our data also show that the tumor microenvironment remains intact although some immune cell types

change during the 7-day culture. We report a series of conditions that appear to improve these variations, but a great variability between tumors remains.

In the future, *in vitro* testing of chemotherapeutical agents or irradiation is the next step, preferably in a preclinical setting with tumor tissue from patients derived before treatment. When a good correlation with individual clinical treatment response is found, the histoculture may allow for personalized treatment selection. Also, the assay allows testing of novel treatment agents for this cancer type with a relatively poor prognosis. The heterogeneity of tumors and their microenvironment is preserved which comes closer to reality than cell lines or even organoids. It is in line of these that we expect that our histocultures will allow a better prediction of the optimal treatment for individual HNSCC patients.

MATERIALS AND METHODS

Patient selection

The Institutional Review Board of the Netherlands Cancer Institute NKI approved the study and informed consent was obtained from all patients. Tumor samples were obtained from 72 patients with HNSCC in the operating room undergoing either surgery or examination under general anaesthesia, between August 2012 and September 2014. None of the patients received prior chemotherapy or radiotherapy treatment. Only patients with histologically proven squamous cell carcinoma were included.

Sponge-gel-supported histoculture method

The method used in this study, is based on the collagen sponge-gel-supported histoculture utilized before to develop the HDRA, as described by Furukawa in 1995 [16]. Immediately after excision the freshly isolated tumor biopsies were placed in a 15 ml plastic tube containing 10 ml 37˚ C pre-warmed culture medium (RPMI 1640, Biochrom, cat. no. F1275, without phenol red) supplemented with 10% FBS (Sigma-Aldrich, F7524), L-glutamine (Gibco, 2mM), HEPES (Gibco, 14 mM) and with antibiotics and antimycotics: Amikacin (Sigma-Aldrich, A2324, 20 µg/ml), penicillin and streptomycin (Gibco, 15070, 50 Units/ml and 50 µg/ml), Metronidazole (Sigma-Aldrich, M3761, 25 µg/ml) and Fluconazole (Sigma-Aldrich, F8929, 10 µg/ml). This culture medium was our standard medium, further referred to as 'RPMI' in our data. The biopsies were transported to the laboratory within 1 hour after excision. Subsequently, the tumor tissue was placed on a Petri Dish (BD Falcon, 100 x 20 mm) and rinsed twice with PBS to minimize microbial contamination. Next, the

biopsies were mechanically minced with scalpels into 1-2 mm^3 fragments. From each biopsy, three to six fragments were immediately fixated in 4% formalin to determine 'day 0' control values. The remaining fragments were each placed on individual sponges (Pfizer, Gelfoam absorbable gelatin sponge, 12-7 mm, Brocacef, cut into 0.5 cm squares), which were first placed into individual wells (BD Falcon, 12-well Multiwell plate) with 1 ml medium and cultured at 37˚ C in 5% CO_2 atmosphere. Three to six fragments were cultured in the above-mentioned standard 'RPMI' control medium, the remaining fragments were used to test various culture conditions. A simplification of the culture method is shown in Figure 4A. The cultured fragments were harvested after completion of the 7-day culture period. These fragments were removed from the sponges with forceps and every single fragment was placed into an individual biopsy cassette (Klinipath), which was then immediately transported into a 4% formalin fixation solution (Klinipath, 4090-9010, diluted with demi-water) for at least 24 hours.

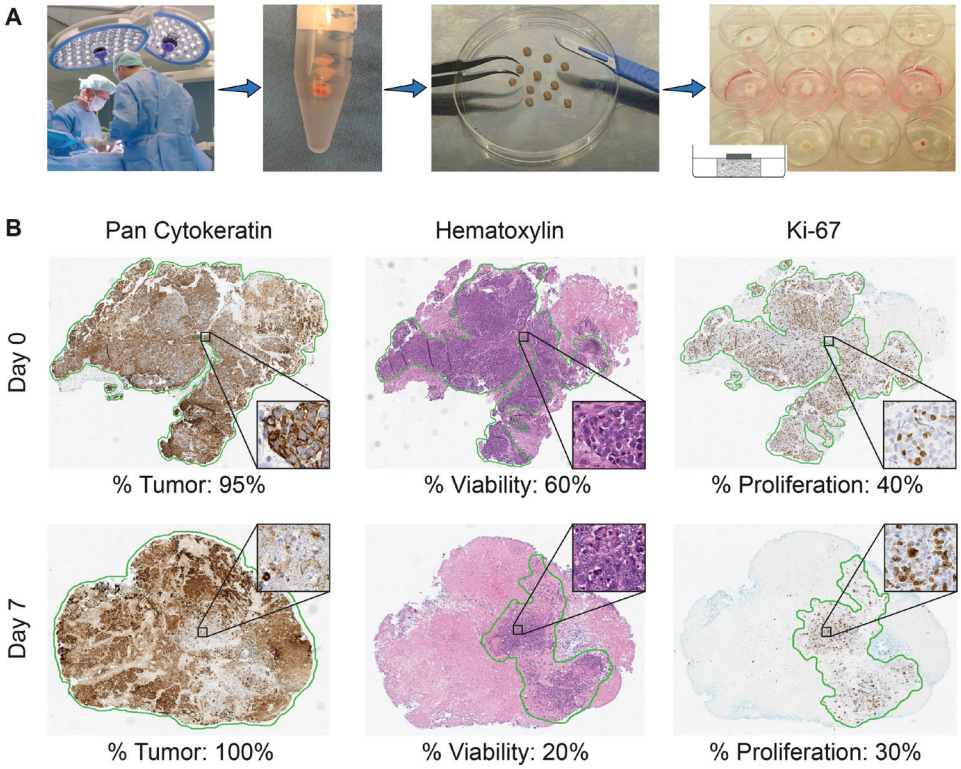

Figure 4. Illustration of the sponge-gel-supported histoculture method and immunohistochemistry read-out. (**A**) Biopsies from previously untreated HNSCC patients are taken under general anaesthesia after informed consent. Biopsies are transported to the laboratory within 1 hour and cut into single fragments. Each single fragment is cultured on a sponge drenched into medium in a 12-well plate. The fragment is placed on the sponge in such a way

that it is surrounded by air and attached to the sponge enabling it to absorb medium. Using this method, the *in-vivo* situation is simulated. (**B**) Illustration of the pathological scoring system. Of each single tumor fragment, at day 0 and 7, three slides are cut and stained for pan-Cytokeratin, Hematoxylin and Eosin (H&E) and Ki-67. With the H&E and pan-Cytokeratin staining the percentage of tumor is scored (% Tumor, cancer cells). With the H&E staining the percentage of viable cancer cells in relation to the total amount of tumor (including areas of necrosis) is determined (% Viability). The Ki-67 staining is used to determine the proliferation rate of the viable cancer cells (% Proliferation).

Optimization conditions

A variety of conditions were tested aiming to potentially improve the above-mentioned standard 'RPMI' culture condition. 'RPMI' was compared to the following optimization conditions: Hydrocortisone supplement (Sigma, H4001): 0.4 µg/ml; Epidermal growth factor supplement (EGF, PeproTech, AF-100-15): 5 ng/ml, 20 ng/ml and 50 ng/ml; Folic acid supplement (Sigma-Aldrich, F8758): 6 mg/L, 11 mg/L and 21 mg/L; DMEM/F-12 + GlutaMax medium (Gibco, 31331) with all the supplements of our standard RPMI medium; and refresh medium every 2 days. All conditions were tested in tissue samples derived from at least 10 patients (involving 30 to 60 tumor fragments).

Immunohistochemical analysis

After formalin fixation, the samples were processed via a Tissue Processor machine (Excelsior, Thermo Scientific. Reagents: formaldehyde, alcohol, xylene and paraffin) and thereafter embedded in paraffin, sectioned and placed onto slides. Immunohistochemistry was performed on the BenchMark Ultra automated staining instrument (Ventana Medical Systems). Paraffin sections were cut at 3 µm and heated at 75˚ C for 28 minutes and deparaffinized in the instrument with EZ prep solution. Sections were treated with Cell Conditioning 1 buffer (CC1, Ventana Medical Systems) for 36 minutes (Ki-67, pan-Cytokeratin) or 64 minutes (EGFR) at 95˚ C before incubation with the primary antibodies (Ventana Medical Systems).

To analyze tumor characteristics we used the standard Hematoxylin and Eosin (H&E) staining and the immunohistochemical stainings Ki-67 (nuclear staining) and pan-Cytokeratin (cytoplasmic staining). For the Ki-67 staining, sections were incubated in a 1:250 dilution of the primary antibody (clone MIB-1, DAKO) for 32 minutes at RT. For the pan-Cytokeratin staining, sections were incubated in a 1:100 dilution of the primary antibody (clone AE1/ AE3, Thermo Scientific) for 32 minutes at RT. Bound primary antibody was detected using the Universal DAB Detection Kit (Ventana Medical Systems) and slides were counterstained with Hematoxylin. To investigate tumor infiltrating immune cells we used multiplex fluorescent immunohistochemistry stained slides for CD4+ helper T-cells (CD3+,

CD8-, FoxP3-), regulatory T-cells (CD3+, FoxP3+), CD8+ cytotoxic T-cells (CD3+, CD8+) and CD8+ regulatory T-cells (CD3+, CD8+, FoxP3+). We also stained for M1 macrophages ($CD68^+$) and M2 macrophages ($CD68^+$/ $CD163^+$). Two different primary antibody combinations were used for overnight incubation: CD3 (1:100, ab828 rabbit polyclonal antibody; Abcam, Cambridge, UK), CD8 (1:100, mouse monoclonal IgG2b, 4B11; Novocastra, Newcastle-upon-Tyne, UK), FoxP3 (1:100, mouse monoclonal IgG1, clone 236A/E7; Abcam) and CD163 (clone 10D6, Novocastra NCL-CD163) / CD68 (clone 514H12; ab49777; Abcam). Alexa Fluor labeled Goat-anti-rabbit-A546 (red), Goat-anti-mouse-IgG2b-A647 (blue) and Goat-anti-mouse-IgG1-A488 (green) (Invitrogen, Life Technologies, Carlsbad, USA) were used for visualizing the T-cell markers. Alexa Fluor labelled Goat-anti-mouse-IgG2a-A488 and Goat-anti-mouse-IgG1-A546 (Invitrogen-Molecular Probes, Eugene, OR) were used for CD68 and CD163 detection. Slides were mounted using VectaShield mounting medium containing DAPI (Vector Laboratories, Burlingame, USA). Immunofluorescent images were acquired with an LSM700 confocal laser scanning microscope equipped with an LCI Plan-Neofluar 25x/0.8 Imm Korr DIC M27 objective (Zeiss, Göttingen, Germany) and analyzed with the LSM software.

EGF-Receptor (EGFR) was detected using clone 5B7 (ready-to-use dispenser, 16 minutes at 37° C, Roche). Bound antibody was detected using the UltraView DAB Detection Kit (Ventana Medical Systems). Slides were counterstained with Hematoxylin II and Bluing Reagent (Ventana Medical Systems).

At our institute, HPV status of oropharyngeal tumors is determined with the surrogate IHC markers p53 and $p16^{ink4a}$ as described in literature [34].

Pathologist scoring read-out

The immunohistochemistry slides were analyzed by experienced research pathologists (JS, EJ), blinded for the conditions. In order to make a reliable calculation we took a cut-off of at least 3 available fragments for the day 0 control, the standard 'RPMI' day 7 control and for the various tested conditions. Consequently, for each biopsy, three to six fragments were used to determine 'day 0' values, and three to six fragments were used at day 7 per culture condition. Per cultured tumor fragment three histological slides were cut, stained and scored for percentage of tumor, viability and proliferation.

The percentage of tumor (abundance of cancer cells in the tissue fragment) was assessed using the H&E staining. This was subsequently verified with the pan-Cytokeratin staining (see % Tumor, Figure 4B). Of note, while scoring for % Tumor, stromal tissue and infiltrate were always excluded. The pathologist also scored for tumor viability using the H&E slides (see % Viability, Figure 4B) by estimating the percentage of viable cancer cells within the total amount of cancer cells. Cells were scored viable when specific signs and characteristics

of cell death (like pyknosis, karyorrhexis, karyolysis and eventually disappearance of the cell nucleus) were absent. The percentage of viability assessed, is solely the viability of the total number of all cancer cells, while excluding again stromal tissue and infiltrate. Ki-67 was used to determine the proliferation rate of the viable cancer cells (see % Proliferation Figure 4B). Therefore, for each successfully cultured fragment, three percentages were scored. An example of our scoring system is shown in Figure 4B. The EGFR expression was scored as percentage of positive tumor cells. The T-cell and macrophage subpopulations, as determined by multiparameter fluorescent IHC, were scored as number of cells per mm^2 in the total tumor section.

Analyses and statistics

The scoring results are presented in this manuscript as either raw or normalized data. Raw data were used to present the actual success of the histoculture technique. Normalized data were used for the analyses between patients. To normalize the data per patient, median percentages (tumor, viability and proliferation) at day 0 were calculated. Consequently, all single fragment scoring percentages at day 0 and day 7, were normalized against this median value at day 0. These data will further be referred to as the 'normalized data'. This analysis method was done in order to deal with the tissue heterogeneity issues that exist within HNSCC and therefore this method corrects for the variability between the fragments at day 0. Beside this, we were now also capable of comparing data between patients.
To see whether we were able to optimize our standard 'RPMI' medium by adding various supplements, the 'RPMI' condition served as the control condition to which the optimization conditions were compared. This was done by comparing the normalized median percentage of each condition, which was calculated as the median percentage of all normalized percentages per tested condition.
Descriptive statistics were gathered using GraphPad Prism 4.0b. Data were analyzed using IBM SPSS Statistics 23.0. Figure 2C was conducted using R version 3.1.3. Overall, p values < 0.05 were considered significant.

ACKNOWLEDGMENTS

The author(s) would like to acknowledge the NKI-AVL Core Facility Molecular Pathology & Biobanking (CFMPB) for performing the immunohistochemical stainings and lab support. We would like to thank the Riki Foundation for their financial support.

CONFLICTS OF INTEREST

The authors declare no potential conflicts of interest.

FUNDING

This work was supported by the Riki Foundation awarded to CZ and MB, and by a NWO TOP grant awarded to JN and HO.

REFERENCES

1 Pulte D, Brenner H. Changes in survival in head and neck cancers in the late 20th and early 21st century: a period analysis. Oncologist. 2010; 15:994–1001. https://doi. org/10.1634/ theoncologist.2009-0289.

2 Surveillance Epidemiology and End Results (SEER) Program. Oral Cavity and Pharynx Cancer.

3 Surveillance Epidemiology and End Results (SEER) Program. Larynx Cancer.

4 Adelstein DJ, Li Y, Adams GL, Wagner H Jr, Kish JA, Ensley JF, Schuller DE, Forastiere AA. An intergroup phase III comparison of standard radiation therapy and two schedules of concurrent chemoradiotherapy in patients with unresectable squamous cell head and neck cancer. J Clin Oncol. 2003; 21:92–98. https://doi.org/10.1200/ JCO.2003.01.008.

5 Pignon JP, le Maître A, Maillard E, Bourhis J, and MACH-NC Collaborative Group. Meta-analysis of chemotherapy in head and neck cancer (MACH-NC): an update on 93 randomised trials and 17,346 patients. Radiother Oncol. 2009; 92:4–14. https://doi.org/10.1016/j. radonc.2009.04.014.

6 Méry B, Rancoule C, Guy JB, Espenel S, Wozny AS, Battiston-Montagne P, Ardail D, Beuve M, Alphonse G, Rodriguez-Lafrasse C, Magné N. Preclinical models in HNSCC: A comprehensive review. Oral Oncol. 2017; 65:51– 56. https://doi.org/10.1016/j.oraloncology.2016.12.010.

7 Dohmen AJ, Swartz JE, Van Den Brekel MW, Willems SM, Spijker R, Neefjes J, Zuur CL. Feasibility of Primary Tumor Culture Models and Preclinical Prediction Assays for Head and Neck Cancer: A Narrative Review. Cancers (Basel). 2015; 7:1716–42. https://doi.org/10.3390/cancers7030858.

8 Leighton J. A sponge matrix method for tissue culture; formation of organized aggregates of cells *in vitro*. J Natl Cancer Inst. 1951; 12:545–61.

9 Sherwin RP, Richters A, Yellin AE, Donovan AJ. Histoculture of human breast cancers. J Surg Oncol. 1980; 13:9–20. https://doi.org/10.1002/jso.2930130103.

10 Ragin CC, Reshmi SC, Gollin SM. Mapping and analysis of HPV16 integration sites in a head and neck cancer cell line. Int J Cancer. 2004; 110:701–09. https://doi.org/10.1002/ ijc.20193.

11 Worsham MJ, Wolman SR, Carey TE, Zarbo RJ, Benninger MS, Van Dyke DL. Chromosomal aberrations identified in culture of squamous carcinomas are confirmed by fluorescence *in situ* hybridisation. Mol Pathol. 1999; 52:42– 46. https://doi.org/10.1136/mp.52.1.42.

12 Shapiro JR, Shapiro WR. The subpopulations and isolated cell types of freshly resected high grade human gliomas: their influence on the tumor's evolution *in vivo* and behavior and therapy *in vitro*. Cancer Metastasis Rev. 1985; 4:107–24. https://doi.org/10.1007/BF00050691.

13 Bjerkvig R. Spheroid Culture in Cancer Research. Boca Raton (FL): CRC Press; 1992.

14 Leess FR, Bredenkamp JK, Lichtenstein A, Mickel RA. Lymphokine-activated killing of autologous and allogeneic short-term cultured head and neck squamous carcinomas. Laryngoscope. 1989; 99:1255–61. https://doi. org/10.1288/00005537-198912000-00009.

15 Gisselsson D, Jonson T, Yu C, Martins C, Mandahl N, Wiegant J, Jin Y, Mertens F, Jin C. Centrosomal abnormalities, multipolar mitoses, and chromosomal instability in head and neck tumours with dysfunctional telomeres. Br J Cancer. 2002; 87:202–07. https://doi. org/10.1038/sj.bjc.6600438.

16 Furukawa T, Kubota T, Hoffman RM. Clinical applications of the histoculture drug response assay. Clin Cancer Res. 1995; 1:305–11.

17 Hoffman RM. *In vitro* sensitivity assays in cancer: a review, analysis, and prognosis. J Clin Lab Anal. 1991; 5:133–43. https://doi.org/10.1002/jcla.1860050211.

18 Robbins KT, Connors KM, Storniolo AM, Hanchett C, Hoffman RM. Sponge-gel-supported histoculture drug-response assay for head and neck cancer. Correlations with clinical response to cisplatin. Arch Otolaryngol Head Neck Surg. 1994; 120:288–92. https://doi.org/10.1001/archotol.1994.01880270036007.

19 Ariyoshi Y, Shimahara M, Tanigawa N. Study on chemosensitivity of oral squamous cell carcinomas by histoculture drug response assay. Oral Oncol. 2003; 39:701– 07. https://doi.org/10.1016/S1368-8375(03)00082-4.

20 Hasegawa Y, Goto M, Hanai N, Ijichi K, Adachi M, Terada A, Hyodo I, Ogawa T, Furukawa T. Evaluation of optimal drug concentration in histoculture drug response assay in association with clinical efficacy for head and neck cancer. Oral Oncol. 2007; 43:749–56. https://doi.org/10.1016/j.oraloncology.2006.09.003.

21 Pathak KA, Juvekar AS, Radhakrishnan DK, Deshpande MS, Pai VR, Chaturvedi P, Pai PS, Chaukar DA, D'Cruz AK, Parikh PM. *In vitro* chemosensitivity profile of oral squamous cell cancer and its correlation with clinical response to chemotherapy. Indian J Cancer. 2007; 44:142– 46. https://doi.org/10.4103/0019-509X.39376.

22 Singh B, Li R, Xu L, Poluri A, Patel S, Shaha AR, Pfister D, Sherman E, Goberdhan A, Hoffman RM, Shah J. Prediction of survival in patients with head and neck cancer using the histoculture drug response assay. Head Neck. 2002; 24:437– 42. https://doi.org/10.1002/hed.10066.

23 Dollner R, Granzow C, Helmke BM, Ruess A, Schad A, Dietz A. The impact of stromal cell contamination on chemosensitivity testing of head and neck carcinoma. Anticancer Res. 2004; 24:325–31.

24 Dollner R, Granzow C, Tschop K, Dietz A. *Ex vivo* responsiveness of head and neck squamous cell carcinoma to vinorelbine. Anticancer Res. 2006; 26:2361–65.

25 Stausbøl-Grøn B, Nielsen OS, Møller Bentzen S, Overgaard J. Selective assessment of *in vitro* radiosensitivity of tumour cells and fibroblasts from single tumour biopsies using immunocytochemical identification of colonies in the soft agar clonogenic assay. Radiother Oncol. 1995; 37:87–99. https://doi.org/10.1016/0167-8140(95)98589-D.

26 Schmitz S, Machiels JP. Targeting the Tumor Environment in Squamous Cell Carcinoma of the Head and Neck. Curr Treat Options Oncol. 2016; 17:37. https://doi.org/10.1007/ s11864-016-0412-6.

27 Fridman WH, Pagès F, Sautès-Fridman C, Galon J. The immune contexture in human tumours: impact on clinical outcome. Nat Rev Cancer. 2012; 12:298–306. https://doi. org/10.1038/nrc3245.

28 Gentles AJ, Newman AM, Liu CL, Bratman SV, Feng W, Kim D, Nair VS, Xu Y, Khuong A, Hoang CD, Diehn M, West RB, Plevritis SK, Alizadeh AA. The prognostic landscape of genes and infiltrating immune cells across human cancers. Nat Med. 2015; 21:938–45. https://doi. org/10.1038/nm.3909.

29 Maiti GP, Mondal P, Mukherjee N, Ghosh A, Ghosh S, Dey S, Chakrabarty J, Roy A, Biswas J, Roychoudhury S, Panda CK. Overexpression of EGFR in head and neck squamous cell carcinoma is associated with inactivation of SH3GL2 and CDC25A genes. PLoS One. 2013; 8:e63440. https://doi. org/10.1371/journal.pone.0063440.

30 Mroz EA, Tward AD, Hammon RJ, Ren Y, Rocco JW. Intra-tumor genetic heterogeneity and mortality in head and neck cancer: analysis of data from the Cancer Genome Atlas. PLoS Med. 2015; 12:e1001786. https://doi.org/10.1371/ journal.pmed.1001786.

31 Janik K, Popeda M, Peciak J, Rosiak K, Smolarz M, Treda C, Rieske P, Stoczynska-Fidelus E, Ksiazkiewicz M. Efficient and simple approach to *in vitro* culture of primary epithelial cancer cells. Biosci Rep. 2016; 36:e00423. https:// doi.org/10.1042/BSR20160208.

32 Ereño C, Gaafar A, Garmendia M, Etxezarraga C, Bilbao FJ, López JI. Basaloid squamous cell carcinoma of the head and neck: a clinicopathological and follow-up study of 40 cases and review of the literature. Head Neck Pathol. 2008; 2:83–91. https://doi.org/10.1007/s12105-008-0045-6.

33 Almatroodi SA, McDonald CF, Darby IA, Pouniotis DS. Characterization of M1/M2 Tumour-Associated Macrophages (TAMs) and Th1/Th2 Cytokine Profiles in Patients with NSCLC. Cancer Microenviron. 2016; 9:1–11. https://doi.org/10.1007/s12307-015-0174-x.

34 van Monsjou HS, van Velthuysen ML, van den Brekel MW, Jordanova ES, Melief CJ, Balm AJ. Human papillomavirus status in young patients with head and neck squamous cell carcinoma. Int J Cancer. 2012; 130:1806–12. https://doi. org/10.1002/ijc.26195.

PART II

Drug screens to identify novel radiosensitizers for HNSCC

CHAPTER 5

A drug screening assay identifies mTOR inhibitors and SERMs as novel radiosensitizers for head and neck cancer

A.J.C. Dohmen
R.H. Wijdeven
C. Lieftink
B. Morris
P. Halonen
B. Rodenko
M.C. de Jong
J.P. de Boer
H. Ovaa
M.W.M. van den Brekel
J. Neefjes
C.L. Zuur

INTRODUCTION

In locally advanced head and neck squamous cell carcinoma (HNSCC), the addition of high-dose cisplatin to RT since the early 1980s[1] has yielded a moderate absolute overall survival benefit of 6.5% at 5 years[2]. Cisplatin chemoradiotherapy (CCRT, concomitant) is therefore considered the standard treatment for these patients, and is often combined with surgery. Despite this survival response, high recurrence rates of up to 50% of patients are seen[2]. Moreover, CCRT is accompanied with a substantial increase in severe, partially irreversible adverse events, including mucositis, dysphagia, nephrotoxicity, neurotoxicity and hematologic toxicity[3]. More recently, the radiosensitizers cetuximab and olaparib have been advocated to treat locally advanced HNSCC as well. However, cetuximab does not show benefit over cisplatin[4] and no clinical data are available for olaparib yet[5-8]. Therefore, there is still an unmet need to improve radiosensitization strategies for HNSCC. We hypothesized that there should be a more efficacious radiosensitizer available than cisplatin, ideally with greater anticancer efficacy and lower toxicity.

In order to identify novel radiosensitizers and/or anti-cancer drugs for HNSCC, the number of potential drugs and corresponding (if known) targets to test is fairly unlimited. If anti-cancer drugs are tested that are already FDA approved, their radiosensitizing activities can be swiftly applied in the clinic, creating a fast introduction of 'old' drugs into novel HNSCC treatment. Another class of drugs that are popular in cancer treatment nowadays are drugs targeting kinases. Kinases are enzymes that modify their targets by phosphorylation, thereby controlling most aspects of cellular function, including cell proliferation and ultimately cancer as well[9]. Kinase signaling pathways have been shown to drive many hallmarks of tumor biology[10] and currently, more than 25 oncology drugs that target kinases have been approved[9]. Furthermore, there are radiosensitizing kinase inhibitors known that target ATM, ATR and DNA-PKcs, kinases critical for DNA repair[11]. Testing and identifying other radiosensitizing kinase inhibitors for HNSCC would therefore be very interesting. Finally, we considered a third class of drugs that received more interest as drug targets recently; deubiquitinating enzymes (DUBs). Ubiquitination is a process in which ubiquitin, a small protein, is conjugated to a target/substrate protein. This modification is also critical in multiple cellular processes including DNA repair, mitosis and intracellular vesicular transport. DUBs remove ubiquitin from targets and thus control these processes as well. Some DUBs are associated with cancer and can be used as targets for novel inhibitors in anti-cancer therapy[12-16]. DUBs involved in DNA damage response include USP1, USP4 and USP7[17]; targeting these DUBs could result in radiosensitization. Consequently, we performed drug screens using three compound libraries containing either FDA-approved oncology drugs, Roche kinase inhibitors or DUB inhibitors. Compounds were compared to currently used clinical radiosensitizers.

MATERIALS AND METHODS

Cell culture

The human HNSCC cell lines UT-SCC-2, UT-SCC-8, UT-SCC-24a, UT-SCC-36 and UT-SCC-40 were kindly provided by Prof. R. Grénman (University of Turku, Finland). These cell lines were harvested from previously untreated HPV negative HNSCC patients and show various sensitivities to irradiation (IR)[18,19]. Cell line characteristics are listed in *Table 1*. Cells were cultured in Dulbecco's Modified Eagle Medium (DMEM) high glucose, GlutaMAX™, pyruvate (Invitrogen) supplemented with 10% FBS, 1% non-essential amino acids (Sigma), penicillin and streptomycin (Gibco 15070, 50 Units/ml and 50 µg/ml) as previously described[20,21]. The cell lines were cultured at 37°C with 5% CO_2.

Table 1. HNSCC cell line characteristics

Cell line	Gender	Primary tumor location	TNM	Type of lesion	Histol. grade	Radiosens. (SF_2 ± SD)	HPV	P53	Ref
UT-SCC-2	Male	Floor of mouth	T4N1M0	Primary	2	0.35 ± 0.05	Neg	Mut	[18,19,21]
UT-SCC-8	Male	Supraglottic larynx	T2N0M0	Primary	1	0.37 ± 0.03	Neg	Mut	[18,21]
UT-SCC-24a	Male	Tongue	T2N0M0	Primary	2	0.51 ± 0.06	Neg	Mut	[19,21]
UT-SCC-36	Male	Floor of mouth	T4N1M0	Primary	3	0.72 ± 0.07*	Neg	Mut	[21]
UT-SCC-40	Male	Tongue	T3N0M0	Primary	1	0.45 ± 0.02[†]	Neg	ND	[21]

*TNM status of primary tumors according to the International Union against Cancer (1997). Histologic grade: 1, well differentiated; 2, moderately differentiated; 3, poorly differentiated. Radiosens.: radiosensitivity. *Determined in this manuscript. [†]Unpublished data from Prof. R. Grénman. SF_2: Survival fraction at 2 Gy, measured by clonogenic survival HPV Neg: human papillomavirus negative P53 Mut: mutated, ND: not detectable*

Compound libraries and individual compounds

We exposed the cell lines to three compound libraries. Firstly, the FDA-approved Oncology Drugs ("FDA screen"), consisting of 114 anticancer drugs (NCI, set V, plate 4803 and 4804, Maryland, USA)[10]. The second library consisted of 218 Roche kinase inhibitors ("Roche screen") (Hofmann-La Roche Inc., Nutley, New Jersey). The third library was the NKI DUB-targeted small molecule drug library v1.3 ("DUB screen"). This home-made library consisted of a proprietary collection of 536 inhibitors reported in literature and structural analogs thereof, either synthesized in-house or purchased from various suppliers. Olaparib was obtained from Syncom (dissolved in DMSO, Groningen, The Netherlands), cisplatin from Selleck Chemicals (dissolved in water, Houston, USA).

Screening and validation method

For all three screens, cells were automatically seeded into 384-well plates at day 0 using the Multidrop Combi (Thermo Scientific). Seeding density for each specific cell line was continuously optimized to reach approximately 80% confluency on day 4 or 7. At day 1, compounds were robotically added to the cell plates using the Microlab STARlet liquid handling workstation (Hamilton). DMSO (final concentration depending on and equal to final compound DMSO concentration) and phenylarsine oxide (PAO, 20 μM final concentration) were used as a negative and positive control for cell viability, respectively. In some experiments individual compounds or controls were automatically added to the plates with the Digital Dispenser (Tecan, HP D300 Digital Dispenser, Switzerland). One plate is treated with drugs only (IRneg), the other (identical) plate is treated with drugs + 4 Gy IR (Best Theratronics Gammacell® 40 Exactor, 0.95 Gy/min, Ottawa, Ontario, Canada) (IRpos). Irradiation was performed 20-50 minutes after compound addition. At day 4 or 7, cell viability was determined using the CellTiter-Blue (CTB) assay, in which cells were incubated with CellTiter-Blue® (Promega, final 1:20) followed by fluorescence intensity measurement using the EnVision plate reader (Perkin Elmer).

The FDA and Roche screens were performed in cell lines UT-SCC-24a, UT-SCC-36 and UT-SCC-40. Concentration ranges of 50 nM - 5 μM and 10 nM to 10 μM, at 10-fold dilutions, were used for the FDA and Roche screen, respectively. Olaparib was added to the FDA library, cisplatin was added to the Roche library. At day 7, the cell viability was measured. Both screens were done in three independent experiments, yielding a total number of 54 plates and 72 plates for the FDA and Roche screen, respectively.

The DUB screen was performed in UT-SCC-2, UT-SCC-8, UT-SCC-24a, UT-SCC-36 and UT-SCC-40 cell lines. The screen with compounds only, and with compounds combined with irradiation, were executed separately, using final concentrations at 10-fold dilutions of 100 pM - 1 μM and of 10 nM - 10 μM, respectively. CTB read-out was done at day 4. Both screens were performed in two independent experiments, with a total number of 50 and 84 plates, respectively.

Data analysis

Analysis of the screening data was done using Excel and R version 3.1.2. The CTB viability data were normalized using the normalized percent inhibition (NPI) method, to correct for plate effects and thus allow direct comparison of plates[22]. This NPI method uses the formula: ((average PAO - compound measurement) / (average PAO - average DMSO)). This way, the positive PAO control value is set to '0' corresponding to complete cell death. The negative DMSO control value is set to '1' corresponding to high viability. Normalizing

to the DMSO controls on IRneg plates sets 'cells + DMSO' to 1. Normalizing to the DMSO controls on IRpos plates sets 'cells + DMSO + 4Gy IR' to 1. When a compound then yielded identical viability in the absence and presence of IR, there is no enhanced effect. When a compound in the IRpos group induced decreased cell viability when compared to the compound alone at the same concentration, this may reflect a potential radiosensitizing effect.

For both the FDA and Roche screen, potential radiosensitization was determined by calculating the difference between IRpos and IRneg NPI values (see *Figure 1,* both ranging from 0 to 1) gathered for each compound, per tested condition (three cell lines, four concentrations and three replicates). We compared the distribution of these compound difference values to the distribution of the negative control difference values. The comparison was done using the Wilcoxon test. The resulting *p*-value was corrected for multiple testing using the Benjamini-Hochberg method[23]. Adjusted *p*-values ≤ 0.1 were considered significant. A ranked list was made of leading candidates showing the largest mean difference (on a relative scale from -1 to 0 normalized viability, meaning from potential radiosensitization to no radisensitization, respectively) between IRpos and IRneg for all conditions.

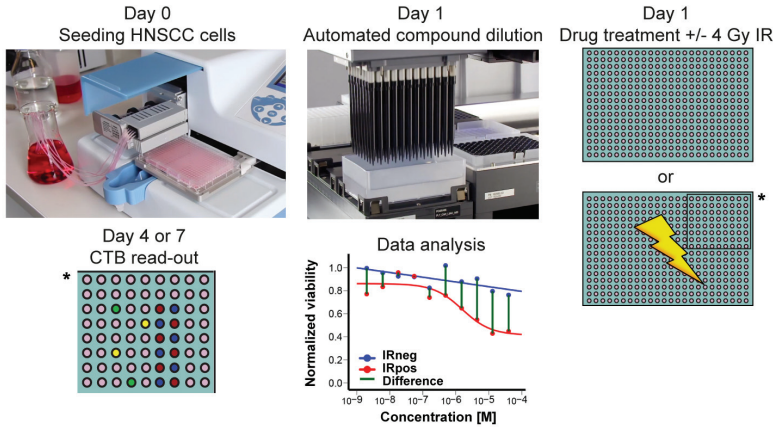

Figure 1. Schematic overview of the performed screening method and analysis. (HNSCC: head and neck squamous cell carcinoma; IR: irradiation, *magnification of plate segment, CTB: CellTiter-Blue®)

For the DUB screen, candidates were selected based on the 1 µM and 10 µM conditions only. For the 1 µM condition, IRpos values showing < 50% viability, compared to > 70% viability for IRneg values, were selected for validation. For the 10 µM condition, IRpos values showing < 50% viability, without showing < 50% viability in the 1 µM condition were

also selected for validation. These compounds could possibly be radiosensitizers as well, however less specific, if they did not already show decreased viability in the 1 µM condition.

Validation experiments were additionally analyzed using Graphpad Prism version 6.0h. Normalized NPI data were fitted using nonlinear regression dose-response curves. To calculate the absolute IC_{50} from the fitted curves, we determined the interpolation of Y = 0.5 with the corresponding X-value of the curve. We determined ratios to define the enhanced effect of combined treatments. The radiation enhancement ratio (RER) was defined as: IC_{50} (drug alone) / IC_{50} (drug + 4 Gy IR); with a RER value of > 1 being indicative for radiosensitization.

RESULTS

FDA-approved oncology drugs

To identify novel radiosensitizing drugs for HNSCC, we robotically screened the FDA-approved oncology drugs library in three HNSCC cell lines exposed to either 4 Gy IR (IRpos) or not (IRneg) *(Figure 1,* general screening method). From the primary screen, drugs were selected showing the highest mean difference, between IRpos and IRneg (See *Table 2).* Olaparib was identified as the top compound (mean difference -0.320), showing that known radiosensitizers [24] are detected by this assay and thereby validating our method. Candidate compounds showing half the effect of the mean difference of olaparib were selected for validation. This was the case for compounds raloxifene, rapamycin and tamoxifen showing a mean difference of -0.193, -0.186, -0.179, respectively. Cisplatin was poorly ranked at position 78 (mean difference -0.026). We hypothesized that this could be an underestimation of the real effect of cisplatin, since all compounds in the library are dissolved in DMSO but in case of cisplatin it is known that this results in adduct formation with reduced toxicity[25]. The relative inactivity of cisplatin as a radiosensitizer in this experiment can thus be attributed to the adduct formation rather than the inactivity of the combination treatment. We do not know if this holds true for other compounds as well.

We then validated the top three drugs (after olaparib) over a wider concentration range in 96-well plates, with irradiation 1 hour after compound addition and CTB read-out at day 7 and related their efficacy to olaparib *(Figure 2).* At higher concentrations, raloxifene and tamoxifen showed radiosensitization *(Figure 2B,* RER 1.51 – 1.65 and RER 1.23 – 1.54, respectively). However, both IRneg and IRpos conditions are quite toxic at high concentrations, with a steep decline in viability *(Figure 2A).* The radiosensitizing effect of olaparib was more pronounced (RER 5.64 – 15.58). Rapamycin was highly toxic

at low concentrations in the first two experiments. Therefore, in the third experiment the concentration of rapamycin was reduced (1:4 dilutions, 95 pM to 25 µM). Even at 95 pM concentration the drug decreased the viability of cells by 20 to 55% (IRneg, rapamycin corr., *Figure 2A).* Of note, rapamycin produced good radiosensitization effects with RERs of 8.33 and 333 in UT-SCC-40 and UT-SCC-24a, respectively *(Figure 2B).* Indeed, previous literature has described rapamycin as a well-known radiosensitizer in various cancers[26-28], also in HNSCC. Again, this finding validates our method for detecting radiosensitizers.

Table 2. Top 10 radiosensitizing candidates from the FDA-approved oncology screen

Compound	Action	All.IRneg. Mean	All.IRpos. Mean	All.Diff. Mean	All.Diff.w .pval	All.Diff.w .padj
1. Olaparib	PARP	0.695	0.375	**-0.320**	0.000	0.000
2. Raloxifene	SERM	0.889	0.696	**-0.193**	0.000	0.000
3. Rapamycin	mTOR	0.536	0.350	**-0.186**	0.000	0.000
4. Tamoxifen	SERM	0.823	0.644	**-0.179**	0.000	0.000
5. Nilotinib	BCR-ABL	0.811	0.657	**-0.154**	0.000	0.002
6. Temsirolimus	mTOR	0.516	0.365	**-0.151**	0.000	0.000
7. Vismodegib	SMO	0.935	0.785	**-0.150**	0.002	0.011
8. Etoposide	Topoisomerase II	0.449	0.308	**-0.141**	0.000	0.001
9. Retinoic acid	RAR	0.833	0.697	**-0.136**	0.000	0.000
10. Everolimus	mTOR	0.547	0.425	**-0.122**	0.000	0.004
78. Cisplatin	*Alkylating*	*0.990*	*0.964*	***-0.026***	*0.061*	*0.133*

PARP: poly(ADP-ribose) polymerase. SERM: selective estrogen receptor modulator. mTOR: mechanistic target of rapamycin. BCR-ABL: breakpoint cluster region – Abelso. SMO: smoothened homologue. RAR: retinoic acid receptor. All.IRneg.Mean: the mean of normalized values of non-radiated compounds for all variables (UT-SCC-24a, UT-SCC-36, UT-SCC-40, 50 nM, 500 nM, 5 µM). All.IRpos.Mean: the mean of normalized values of radiated compounds for all variables. All.Diff.Mean: the mean of all single difference values. Difference values were determined by subtracting IRpos from IRneg for every single variation. All.Diff.w.pval: compare the distribution of all single difference values to the distribution of the difference values of the negative controls using the Wilcoxon test, and calculate a p-value. All.Diff.w. padj: the resulting p-value was corrected for multiple testing using the Benjamin-Hochberg method. Adjusted p-values ≤ 0.1 were considered significant. (Of note, in the library cisplatin was dissolved in DMSO resulting in reduced toxicity.)

Additionally, we also observed the effect of FDA oncology drugs in the IRneg situation from the primary screen (*Table 3*). These observations could refer to new treatment options for recurrent / metastatic HNSCC patients, currently being treated with cisplatin, carboplatin, 5-fluorouracil, paclitaxel, methotrexate, cetuximab, immune checkpoint inhibitors[29] or a combination thereof (NCCN guidelines version 2.2014). In our screen these chemotherapeutics did not end up in the top 10 oncology drugs screened in the absence of irradiation (*Table 3,* with the exception of immune checkpoint inhibitors and cetuximab which were not included in the library). Depsipeptide, bortezomib and idarubicin were the most cytotoxic oncology drugs, with mean IRneg values of -0.0013, 0.0007 and 0.0023, respectively.

A

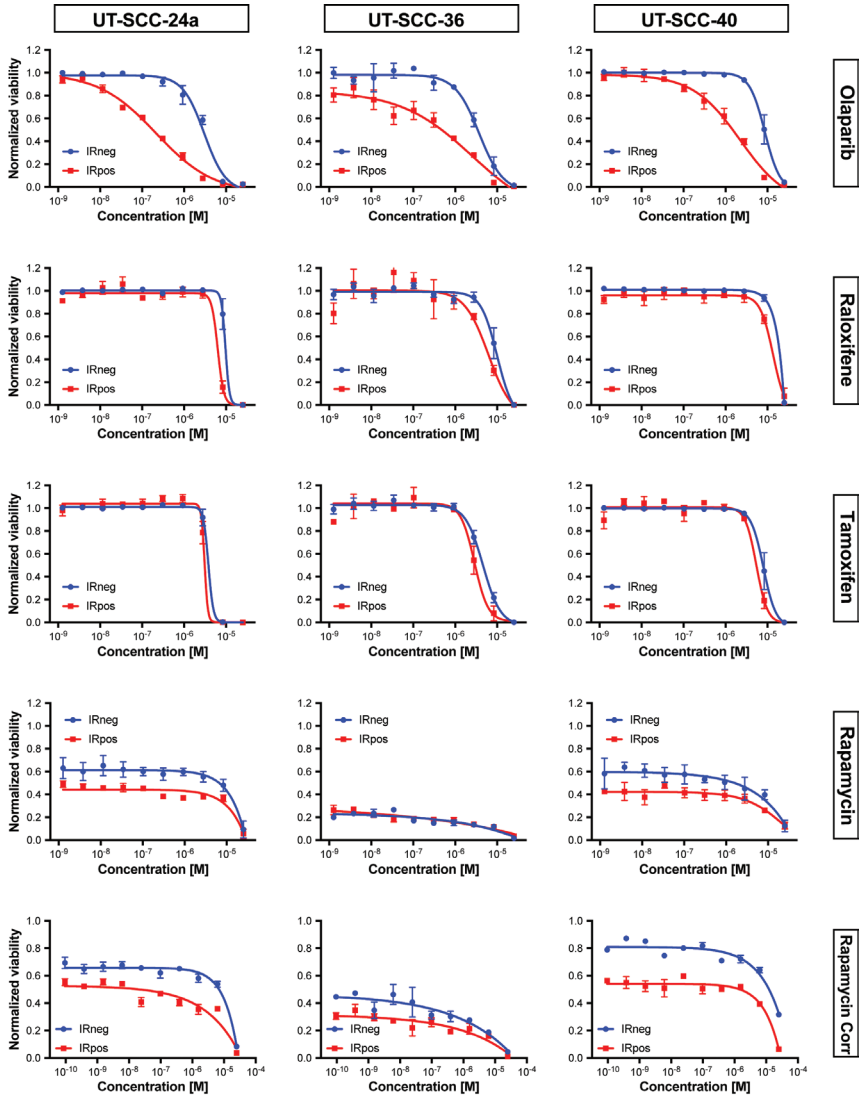

B

Compound	UT-SCC-24a			UT-SCC-36			UT-SCC-40		
	IRneg	IRpos	RER	IRneg	IRpos	RER	IRneg	IRpos	RER
Olaparib	2.81	0.18	**15.58**	3.44	0.48	**7.19**	8.40	1.49	**5.64**
Raloxifene	9.67	6.28	**1.54**	8.93	5.40	**1.65**	18.89	12.54	**1.51**
Tamoxifen	3.80	3.09	**1.23**	4.59	2.98	**1.54**	7.79	5.43	**1.44**
Rapamycin	6.65	-	**> 1**	-	-	**-**	1.59	-	**> 1**
Rapamycin corr	6.95	0.02	**333.5**	-	-	**-**	12.29	1.48	**8.33**

Figure 2. Validation of top three radiosensitizing candidates (raloxifene, tamoxifen and rapamycin) of the FDA library, in view of olaparib efficacy. **A**, Shown are dose-response curves of the compounds in the absence (IRneg)

and presence (IRpos) of 4 Gy radiation in UT-SCC-24a, UT-SCC-36 and UT-SCC-40. The IR-effect was eliminated by normalizing to negative controls that received IR. For rapamycin two curves are depicted. The upper curve shows the effect of the first two independent experiments. The bottom curve represents the effect of the third experiment (error bars shows the difference between the two technical replicates within only one experiment) with adjusted, lower, concentrations on the x-axis. (Other data shown as mean from three independent experiments, using two technical replicates per experiment, with SEM.) **B**, Depicted are the corresponding calculated IC50 values (μM) for IRneg and IRpos from the nonlinear regression curve fitted in A and the determined radiation enhancement ratio (RER).

Table 3. Top 20 FDA-approved oncology drugs without irradiation

Compound	All.IRneg. Mean	All.Diff.w. pval	All.Diff.w. padj
1. Depsipeptide	-0.0013	0.0001	0.0015
2. Bortezomib	0.0007	0.1620	0.2890
3. Idarubicin	0.0020	0.9030	1.0000
4. Daunorubicin	0.0023	0.9970	1.0000
5. Carfilzomib	0.0023	0.9820	1.0000
6. Gemcitabine	0.0024	0.1050	0.2100
7. Dactinomycin	0.0026	0.9960	1.0000
8. Mitoxantrone	0.0026	0.9650	1.0000
9. Plicamycin	0.0030	0.9940	1.0000
10. Ixabepilone	0.0033	0.8550	1.0000
11. Paclitaxel	*0.0045*	*0.9960*	*1.0000*
12. Doxorubicin	0.0058	0.9950	1.0000
13. Vincristine	0.0077	1.0000	1.0000
14. Cabazitaxel	0.0088	0.9990	1.0000
15. Docetaxel	0.0088	0.9940	1.0000
16. Vinorelbine	0.0110	1.0000	1.0000
17. Vinblastine	0.0122	1.0000	1.0000
18. Mitomycin C	0.0182	0.1340	0.2440
19. Topotecan	0.0193	0.9970	1.0000
20. Omacetaxine	0.0343	0.9070	1.0000
25. Methotrexate	*0.0115*	*0.9960*	*1.0000*
48. 5-Fluorouracil	*0.6260*	*0.3140*	*0.4830*
74. Carboplatin	*0.9300*	*0.0001*	*0.0014*
102. Cisplatin	*0.9900*	*0.0613*	*0.1330*

In italic font style: drugs routinely used in the clinic for locally advanced HNSCC patients. For description table headings, see footnotes of Table 2. (Of note, in the library cisplatin was dissolved in DMSO resulting in reduced toxicity.)

Roche kinase inhibitors

We proceeded screening by testing the Roche library in the hope to detect novel radiosensitizers. Again, data from the primary screen were analyzed by determining the

mean difference between IRpos and IRneg for all variables (*Table 4*). Cisplatin, added manually to the library as reference compound (dissolved in water), was the top compound in the result list, with a mean difference of -0.158. Compound RO3303724 had a mean difference of -0.122 and compound RO0506220 of -0.091 with *p*-values and adjusted *p*-values <0.05 and <0.1 respectively. The dose-response curve (*Figure 3*), simplified because only 4 concentrations have been tested in the primary screen, did not show relevant radiosensitizing effects. Since the main goal of our screening efforts was to find better radiosensitizers than cisplatin, no candidates were selected for further validation.

Table 4. Top 10 radiosensitizing drugs from the Roche kinase inhibitor screen

Compound	All.IRneg. Mean	All.IRpos. Mean	All.Diff. Mean	All.Diff. w.pval	All.Diff. w.padj
1. Cisplatin	0.740	0.582	**-0.158**	0.000	0.000
2. RO3303724	0.514	0.392	**-0.122**	0.000	0.000
3. RO0506220	0.638	0.548	**-0.090**	0.006	0.045
4. RO4624208	0.867	0.795	**-0.072**	0.167	0.422
5. RO0317476	0.909	0.846	**-0.063**	0.086	0.259
6. RO0317471	0.806	0.745	**-0.062**	0.028	0.146
7. RO0317886	0.873	0.815	**-0.058**	0.130	0.358
8. RO4509407	0.977	0.928	**-0.048**	0.021	0.126
9. RO4498484	0.676	0.630	**-0.046**	0.712	0.851
10. RO4582641	0.710	0.668	**-0.041**	0.180	0.431

For description table headings see footnotes of Table 2.

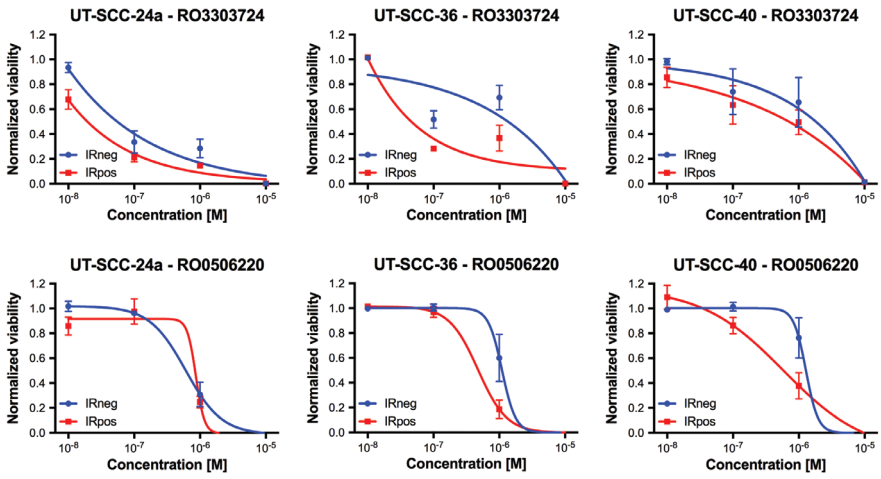

Figure 3. The two lead radiosensitizing drugs from the Roche library. Shown are dose-response curves of the two compounds in the absence (IRneg) and presence (IRpos) of 4 Gy radiation in UT-SCC-24a, UT-SCC-36 and UT-SCC-40 HNSCC. The IR-effect was eliminated by normalizing to negative controls that received IR. (Data shown as mean from three independent experiments, with SEM.)

DUB inhibitors

We continued screening by testing the DUB library as well, in 5 HNSCC cell lines. Since the lower concentrations of drugs (from 100 pM to 100 nM) did not show any relevant reduced viability, we analyzed the 1 µM condition in the IRneg and IRpos screen, and the 10 µM condition in the IRpos screen. Six compounds showed IRpos viability values < 50%, compared to > 70% viability for IRneg values, in the 1 µM condition. Forty-six compounds showed IRpos values with < 50% viability in the 10 µM condition, without showing < 50% viability in the 1 µM condition. For better candidate selection these 52 compounds were retested in the same 5 HNSCC cell lines over a wider concentration range. From this experiment, only two compounds were selected based on their IRpos-IC50 and IRneg-IC50: compound 2X-0324 and compound AM-807/13614750 *(Figure 4).* Their potential radiosensitization was subsequently validated in two HNSCC cell lines, with a read-out at day 7, and compared to cisplatin (in water) and olaparib *(Figure 5).* Compound 2X-0324 in UT-SCC-36 showed less viability *(Figure 5A)* due to plate evaporation edge effects, being positioned in the upper row of the plate. This was avoided in the subsequent experiments. In UT-SCC-40 cells, 2X-0324 has minimal radiosensitizing effects (RER 1.86) *(Figure 5B).* AM-807 did not show explicit radiosensitizing effects in both HNSCC cell lines (RER 0.88 and 1.48). Olaparib, showed a RER of 2.50 and 28.80 in UT-SCC-36 and UT-SCC-40, respectively. Cisplatin again was less effective as a radiosensitizer (RER 1.32 and 1.90).

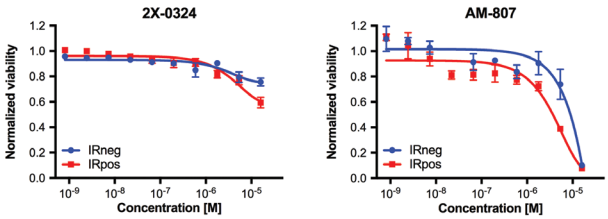

Figure 4. The DUB screen identified two compounds (2X-0324 and AM-807) with potential radiosensitizing effect. Shown are dose-response curves of 2X-0324 and AM-807 in the absence (IRneg) and presence (IRpos) of 4 Gy radiation in UT-SCC-40 HNSCC. The IR-effect was eliminated by normalizing to negative controls that received IR. (Data shown as mean from four dependent technical replicates, with SEM.)

A

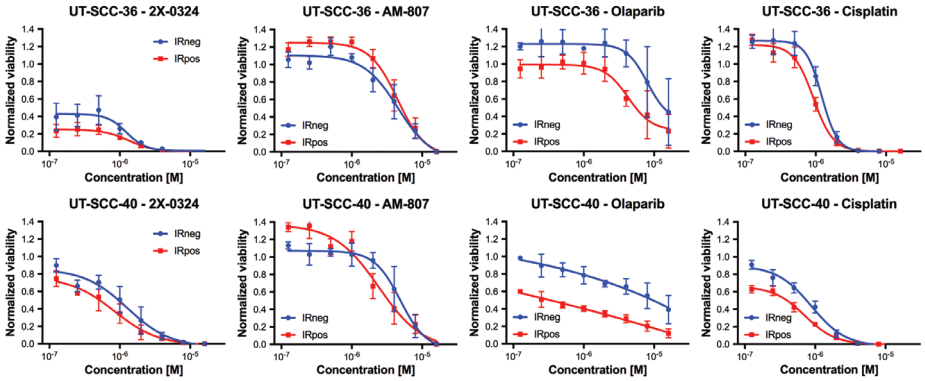

B

Cell line	2X-0324			AM-807			Olaparib			Cisplatin		
	IRneg	IRpos	RER	IRneg	IRpos	RER	IRneg	IRpos	RER	IRneg	IRpos	RER
UT-SCC-36	-	-	**> 1**	4.55	5.15	**0.88**	13.67	5.48	**2.50**	1.22	0.93	**1.32**
UT-SCC-40	0.96	0.52	**1.86**	4.93	3.33	**1.48**	9.52	0.33	**28.80**	0.76	0.40	**1.90**

Figure 5. Validation of the top 2 radiosensitizing DUBs compounds 2X-0324 and AM-807. A, Shown are dose-response curves of the two compounds in the absence (IRneg) and presence (IRpos) of 4 Gy radiation in UT-SCC-36 and UT-SCC-40 HNSCC cells. Their effect was compared to olaparib en cisplatin. The IR-effect was eliminated by normalizing to negative controls that received IR. (Data shown as mean from three independent experiments, with a technical duplicate per experiment, with SEM.) **B**, Depicted are the corresponding calculated IC50 values (μM) for IRneg and IRpos from the nonlinear regression curve fitted in A and the determined radiation enhancement ratio (RER).

Compound 2X-0324 showed radiosensitizing effects after validation (RER 1.86). Thereafter, we aimed at improving this compound by performing structure-activity relationship (SAR) analyses. This is a powerful concept in drug discovery which allows drug optimization[30]. By modifying the chemical structure of a drug, one can determine the chemical group responsible for evoking the biological effect (*i.e.* radiosensitization). Thirteen analog compounds were generated with chemical structures related to the structure of 2X-0324 (*Figure 6A* and *6B*). We created variants devoid of the toxic side effects (compound 7T-0319, STK-870832, 4T-0286, 4T-0296, 8X-0929, 8X-0931 and 8X-0933). Other variants still showed toxicity (compound 3X-0226, AK-454, 2X-0324, 4T-0332, 9T-0336, *Figure 6A* and *6B*), however no systematic improvement in radiosensitization was observed compared to compound 2X-0324 (RER 1.60 – 1.76) (*Figure 6C*). Olaparib showed the best radiosensitizing capacities (RER average 7.90, range 3.69 – 12.97).

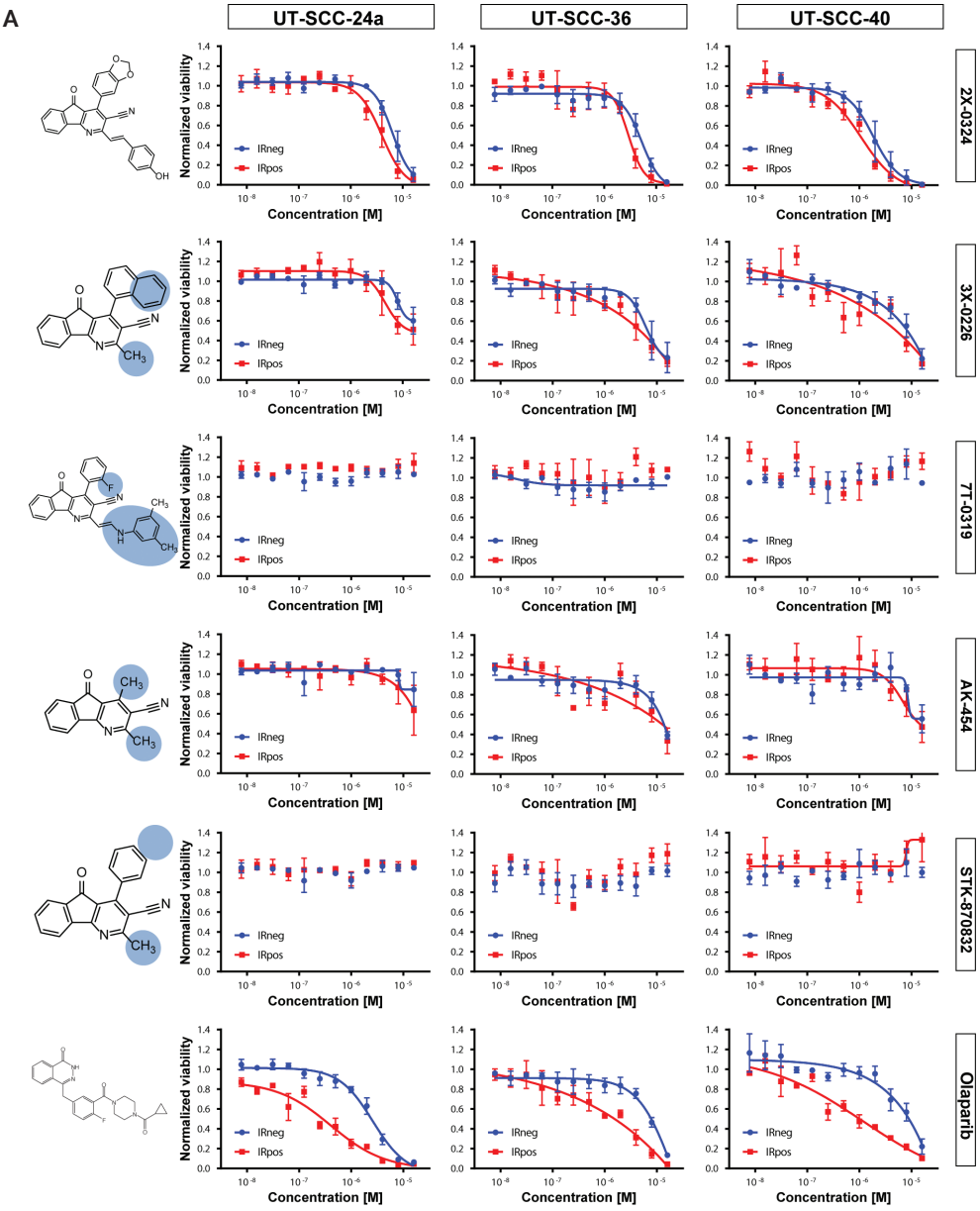
A
UT-SCC-24a
UT-SCC-36
UT-SCC-40
2X-0324
3X-0226
7T-0319
AK-454
STK-870832
Olaparib
Normalized viability
Concentration [M]
IRneg
IRpos

B

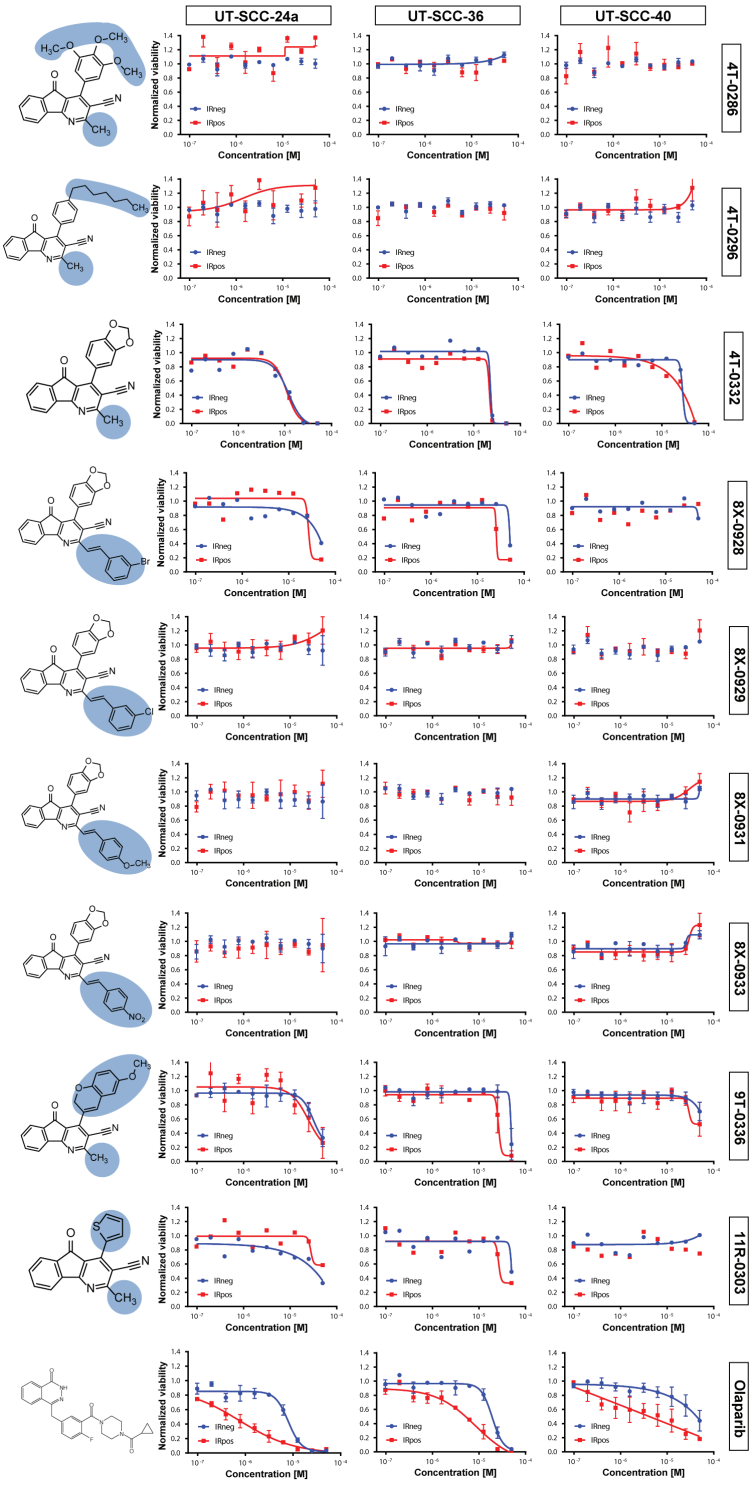
UT-SCC-24a
UT-SCC-36
UT-SCC-40
4T-0286
4T-0296
4T-0332
8X-0928
8X-0929
8X-0931
8X-0933
9T-0336
11R-0303
Olaparib
Normalized viability
Concentration [M]
IRneg
IRpos

C

Compound	UT-SCC-24a			UT-SCC-36			UT-SCC-40		
	IRneg	IRpos	RER	IRneg	IRpos	RER	IRneg	IRpos	RER
2X-0324	6.62	3.98	**1.66**	4.70	2.93	**1.60**	1.82	1.03	**1.76**
3X-0226	-	14.45	**> 1**	6.71	4.86	**1.38**	8.43	5.18	**1.63**
7T-0319	-	-	**< 1**	-	-	**< 1**	-	-	**< 1**
AK-454	-	20.56	**> 1**	13.71	12.74	**1.08**	-	14.83	**> 1**
STK-870832	-	-	**< 1**	-	-	**< 1**	-	-	**< 1**
Olaparib	2.59	0.41	**6.38**	7.80	1.53	**5.08**	8.93	1.00	**8.89**
4T-0286	-	-	**< 1**	-	-	**< 1**	-	-	**< 1**
4T-0296	-	-	**< 1**	-	-	**< 1**	-	-	**< 1**
4T-0332	10.61	10.31	**1.03**	22.86	21.42	**1.07**	27.41	24.99	**1.10**
8X-0928	44.49	27.33	**1.63**	49.12	25.39	**1.94**	-	-	**<1**
8X-0929	-	-	**< 1**	-	-	**< 1**	-	-	**< 1**
8X-0931	-	-	**< 1**	-	-	**< 1**	-	-	**< 1**
8X-0933	-	-	**< 1**	-	-	**< 1**	-	-	**< 1**
9T-0336	35.94	29.11	**1.23**	48.52	26.32	**1.84**	-	-	**< 1**
11R-0303	34.23	-	**<1**	49.94	27.88	**1.79**	-	-	**< 1**
Olaparib	7.23	0.56	**12.97**	18.99	5.14	**3.69**	42.84	4.12	**10.40**

Figure 6. Radiosensitizing effect of 2X-0324, 13 analogs, cisplatin and olaparib. Shown are dose-response curves of the compounds in the absence (IRneg) and presence (IRpos) of 4 Gy radiation in UT-SCC-24a, UT-SCC-36 and UT-SCC-40. On the left the chemical structures are shown. The IR-effect was eliminated by normalizing to negative controls that received IR. **A** and **B** are two different experiments, with other concentration ranges. (Data shown as mean from one to three independent experiments, depending on the amount of compound available, with SEM.) **C**, Depicted are the corresponding calculated IC50 values (μM) for IRneg and IRpos from the nonlinear regression curve fitted in A and B and the determined radiation enhancement ratio (RER).

DISCUSSION

In the treatment of locally advanced head and neck cancer there is still an unmet need to improve clinical outcome of combined chemoradiotherapy. Despite very recent developments in immunotherapy[29], patients with recurrent metastatic HNSCC suffer relatively poor perspectives. In order to improve prospects after radiotherapy, irradiation could be combined with drugs that enhance irradiation efficacy, known as radiosensitizers. Ideally, a radiosensitizer should specifically target cancer cells and not normal tissues, thereby enhancing the therapeutic ratio. This would lead to improved locoregional tumor control and overall survival rates with lower morbidity. In this research, we have performed screens of various drugs/compounds with and without concurrent irradiation to identify novel radiosensitizing drugs.

Our assay is reliable in detecting potential radiosensitization since we were able to identify known radiosensitizers as top hits in every screen and validation experiments. This finding is very important for future drug discovery activities for cancers treated with RT, including HNSCC. This assay is able to test for radiosensitivity in high drug throughput, in a short timeframe (7 days) and with relatively limited effort (cell viability measurement, multiple drugs on one plate) compared to the conventional colony forming clonogenic assay. The latter takes at least 14 days, is very laborious since every single condition has to be tested in a different plate and renders time-consuming counting of colonies[31]. Potential radiosensitizers identified with this assay can be further validated with a colony forming assay to confirm and prove their radiosensitizing effect (IR vs IR + drug).

Screening the FDA-approved oncology drugs library yielded some interesting radiosensitizing compounds. The most pronounced effect was reached with rapamycin (RER 8.33 and 333; generic name: sirolimus). It is a (first generation) mTOR inhibitor, inhibiting mTORC1 activity, with immunosuppressant function, mainly used in preventing the rejection of kidney transplants or as coating in coronary stents. mTOR plays a pivotal role in cell growth and proliferation being located downstream in the PI3K-Akt pathway, which is activated in most cancer types[32]. At the moment, rapalogs (analogs of rapamycin) have been developed (everolimus, temsirolimus and ridaforolimus) in order to improve pharmacokinetics and stability of rapamycin[33]. Two of these (temsirolimus and everolimus) were ranked at position 6 and 10 respectively in our FDA-approved oncology drug screen (see Table 2). Rapalogs are approved for the treatment of a few cancers (renal cell carcinoma, mantle cell lymphoma), but not for the majority of solid tumors[33]. It has been hypothesized that their mechanism of action is probably mediated by a direct cytostatic (anti-proliferative) effect of the drugs itself, rather than a cytotoxic (inducing cell death) effect. To overcome this limitation, rapalogs are combined with cytotoxic agents, hormonal therapy and DNA-damaging agents. Many studies reported increased radiosensitivity in several cancer types when an mTOR inhibitor was combined with radiation[27,34-39], also in head neck cancer[40-42]. In HNSCC, the EGFR-PI3K-Akt-mTOR pathway is by far the most altered pathway as > 80% of the tumors have alterations in components of this pathway[40,43-46]. Several phase I and II studies including an mTOR inhibitor have been performed in head and neck cancer patients[47-53]. However, only one phase I study combined everolimus (and concurrent cisplatin) with radiotherapy; this combination treatment appeared to be tolerable with acceptable toxicities[54]. However, everolimus+RT has not been compared to cisplatin+RT in a phase II/III trial, and it is unclear whether our experimental results can be extrapolated to patients. However, our results indicate that there are excellent reasons to start testing this combination. Also *in vitro* and *in vivo* mice studies in lung and head and neck cancer cells show cancer specific radiosensitization for rapamycin and

radioprotection in normal lung cells and oral keratinocytes[39,55], suggesting low toxicities. In conclusion, combining an mTOR inhibitor with RT could be an interesting therapy for locally advanced HNSCC patients.

Besides rapamycin, raloxifene (RER 1.51 - 1.64) and tamoxifen (RER 1.23 – 1.54) were identified as radiosensitizers. Both drugs are known as selective estrogen receptor modulators (SERMs). SERMs have been investigated for their efficacy in combination with RT, mainly in breast cancer. Two studies, summarizing literature of estrogen application in RT, showed ambiguous results in *in vitro* and *in vivo* radiosensitivity studies, and a possible increased risk of fibrosis[56,57]. The underlying mechanism for radiosensitization remains unclear, but targeting the estrogen receptor (ER) could lead to irreparable double strand breaks by affecting components of the non-homologous end-joining (NHEJ) DNA repair pathway, de-regulating of homologous recombination (HR) repair and altering cell cycle progression via c-Myc and Cyclin D1[57]. Inhibiting estrogen could also decrease cell proliferation and radioresistance via growth factor signaling pathways (EGFR, MAPK, PI3K)[57]. Interestingly, there could also be a possible role for ER during HNSCC carcinogenesis. HNSCC cells show prominent ERß expression[58], ERß overexpression is related to radioresistance and unfavorable survival in HNSCC[59] and estradiol stimulation induces invasion of HNSCC cells together with EGF[60]. Thus, combining SERMS with RT could give rise to a novel therapy to treat locally advanced HNSCC.

Screening the Roche Kinase inhibitor library did not identify drugs that were more potent in radiosensitization than cisplatin. Screening the DUBs inhibitor library, compound 2X-0324 was identified with potential radiosensitizing efficacy (RER (>1 – 1.86) and was extensively tested, even with 13 analog compounds, however no compounds were identified with better radiosensitization than olaparib.

Interestingly, preliminary screening data suggest that some FDA-approved drugs (*Table 3*) could outperform the oncology drugs currently used to treat recurrent / metastatic HNSCC patients. These FDA drugs include depsipeptide (a histone deacetylase (HDAC) inhibitor), bortezomib (proteasome inhibitor) and anthracycline drugs inhibiting topoisomerase II (idarubicin, daunorubicin). Further *in vitro* and *in vivo* testing is needed to investigate whether these drugs could indeed serve as novel and more potent anti-cancer drugs.

We describe an assay that is robust, reliable and easy for identifying drugs with radiosensitizing capacities. Our results suggest that mTOR inhibitors and SERMs could be of value as radiosensitizers for definitive treatment in locally advanced HNSCC. While new drugs may be identified with this assay as well, the FDA-approved drugs will more easily enter clinical trials as their toxicities are known. The route to *in vivo* testing of our findings is defined.

REFERENCES

1 Al-Sarraf, M. Treatment of locally advanced head and neck cancer: Historical and critical review. *Cancer Control* **9**, 387-399 (2002).

2 Pignon, J. P., le Maitre, A., Maillard, E., Bourhis, J. & Group, M.-N. C. C. Meta-analysis of chemotherapy in head and neck cancer (MACH-NC): an update on 93 randomised trials and 17,346 patients. *Radiotherapy and oncology: journal of the European Society for Therapeutic Radiology and Oncology* **92**, 4-14, doi:10.1016/j.radonc.2009.04.014; 10.1016/j.radonc.2009.04.014 (2009).

3 Adelstein, D. J. *et al.* An intergroup phase III comparison of standard radiation therapy and two schedules of concurrent chemoradiotherapy in patients with unresectable squamous cell head and neck cancer. *Journal of clinical oncology: official journal of the American Society of Clinical Oncology* **21**, 92-98, doi:10.1200/JCO.2003.01.008 (2003).

4 Gyawali, B., Shimokata, T., Honda, K. & Ando, Y. Chemotherapy in locally advanced head and neck squamous cell carcinoma. *Cancer Treat Rev* **44**, 10-16, doi:10.1016/j.ctrv.2016.01.002 (2016).

5 Chatterjee, P. *et al.* PARP inhibition sensitizes to low dose-rate radiation TMPRSS2-ERG fusion gene-expressing and PTEN-deficient prostate cancer cells. *PLoS One* **8**, e60408, doi:10.1371/journal.pone.0060408 (2013).

6 Nowsheen, S., Bonner, J. A. & Yang, E. S. The poly(ADP-Ribose) polymerase inhibitor ABT-888 reduces radiation-induced nuclear EGFR and augments head and neck tumor response to radiotherapy. *Radiother Oncol* **99**, 331-338, doi:10.1016/j.radonc.2011.05.084 (2011).

7 Powell, C. *et al.* Pre-clinical and clinical evaluation of PARP inhibitors as tumour-specific radiosensitisers. *Cancer Treat Rev* **36**, 566-575, doi:10.1016/j.ctrv.2010.03.003 (2010).

8 Senra, J. M. *et al.* Inhibition of PARP-1 by olaparib (AZD2281) increases the radiosensitivity of a lung tumor xenograft. *Mol Cancer Ther* **10**, 1949-1958, doi:10.1158/1535-7163.MCT-11-0278 (2011).

9 Gross, S., Rahal, R., Stransky, N., Lengauer, C. & Hoeflich, K. P. Targeting cancer with kinase inhibitors. *J Clin Invest* **125**, 1780-1789, doi:10.1172/JCI76094 (2015).

10 Hanahan, D. & Weinberg, R. A. Hallmarks of cancer: the next generation. *Cell* **144**, 646-674, doi:10.1016/j.cell.2011.02.013 (2011).

11 Weber, A. M. & Ryan, A. J. ATM and ATR as therapeutic targets in cancer. *Pharmacol Ther* **149**, 124-138, doi:10.1016/j.pharmthera.2014.12.001 (2015).

12 Mofers, A., Pellegrini, P., Linder, S. & D'Arcy, P. Proteasome-associated deubiquitinases and cancer. *Cancer Metastasis Rev* **36**, 635-653, doi:10.1007/s10555-017-9697-6 (2017).

13 Kumari, N. *et al.* The roles of ubiquitin modifying enzymes in neoplastic disease. *Biochim Biophys Acta* **1868**, 456-483, doi:10.1016/j.bbcan.2017.09.002 (2017).

14 Gallo, L. H., Ko, J. & Donoghue, D. J. The importance of regulatory ubiquitination in cancer and metastasis. *Cell Cycle* **16**, 634-648, doi:10.1080/15384101.2017.1288326 (2017).

15 Singh, N. & Singh, A. B. Deubiquitinases and cancer: A snapshot. *Crit Rev Oncol Hematol* **103**, 22-26, doi:10.1016/j.critrevonc.2016.04.018 (2016).

16 McClurg, U. L. & Robson, C. N. Deubiquitinating enzymes as oncotargets. *Oncotarget* **6**, 9657-9668, doi:10.18632/oncotarget.3922 (2015).

17 He, M. *et al.* The emerging role of deubiquitinating enzymes in genomic integrity, diseases, and therapeutics. *Cell Biosci* **6**, 62, doi:10.1186/s13578-016-0127-1 (2016).

18 Pekkola-Heino, K., Jaakkola, M., Kulmala, J. & Grenman, R. Comparison of cellular radiosensitivity between different localizations of head and neck squamous-cell carcinoma. *J Cancer Res Clin Oncol* **121**, 452-456 (1995).

19 Pekkola-Heino, K., Servomaa, K., Kiuru, A. & Grenman, R. Increased radiosensitivity is associated with p53 mutations in cell lines derived from oral cavity carcinoma. *Acta Otolaryngol* **116**, 341-344 (1996).

20 de Jong, M. C. *et al.* Pretreatment microRNA Expression Impacting on Epithelial-to-Mesenchymal Transition Predicts Intrinsic Radiosensitivity in Head and Neck Cancer Cell Lines and Patients. *Clin Cancer Res* **21**, 5630-5638, doi:10.1158/1078-0432.CCR-15-0454 (2015).

21 Lansford, C. D. *et al.* in *Human Cell Culture Vol 2, Cancer Cell Lines Part 2* (eds John R.W. Masters & B Palsson) 185-255 (Kluwer Academic Publishers, 1999).

22 Boutros, M., Bras, L. P. & Huber, W. Analysis of cell-based RNAi screens. *Genome Biol* **7**, R66, doi:10.1186/gb-2006-7-7-R66 (2006).

23 Benjamini, Y. & Hochberg, Y. Controlling the False Discovery Rate: A Practical and Powerful Approach to Multiple Testing *Journal of the Royal Statistical Society* **57**, 289-300 (1995).

24 Verhagen, C. V. *et al.* Extent of radiosensitization by the PARP inhibitor olaparib depends on its dose, the radiation dose and the integrity of the homologous recombination pathway of tumor cells. *Radiother Oncol* **116**, 358-365, doi:10.1016/j.radonc.2015.03.028 (2015).

25 Fischer, S. J., Benson, L. M., Fauq, A., Naylor, S. & Windebank, A. J. Cisplatin and dimethyl sulfoxide react to form an adducted compound with reduced cytotoxicity and neurotoxicity. *Neurotoxicology* **29**, 444-452, doi:10.1016/j.neuro.2008.02.010 (2008).

26 Chen, H. *et al.* The mTOR inhibitor rapamycin suppresses DNA double-strand break repair. *Radiat Res* **175**, 214-224 (2011).

27 Nagata, Y. *et al.* Effect of rapamycin, an mTOR inhibitor, on radiation sensitivity of lung cancer cells having different p53 gene status. *Int J Oncol* **37**, 1001-1010 (2010).

28 Albert, J. M., Kim, K. W., Cao, C. & Lu, B. Targeting the Akt/mammalian target of rapamycin pathway for radiosensitization of breast cancer. *Mol Cancer Ther* **5**, 1183-1189, doi:10.1158/1535-7163.MCT-05-0400 (2006).

29 Ferris, R. L. *et al.* Nivolumab for Recurrent Squamous-Cell Carcinoma of the Head and Neck. *N Engl J Med* **375**, 1856-1867, doi:10.1056/NEJMoa1602252 (2016).

30 McKinney, J. D., Richard, A., Waller, C., Newman, M. C. & Gerberick, F. The practice of structure activity relationships (SAR) in toxicology. *Toxicol Sci* **56**, 8-17 (2000).

31 Buch, K. *et al.* Determination of cell survival after irradiation via clonogenic assay versus multiple MTT Assay--a comparative study. *Radiat Oncol* **7**, 1, doi:10.1186/1748-717X-7-1 (2012).

32 Klumpen, H. J., Beijnen, J. H., Gurney, H. & Schellens, J. H. Inhibitors of mTOR. *Oncologist* **15**, 1262-1269, doi:10.1634/theoncologist.2010-0196 (2010).

33 Zheng, Y. & Jiang, Y. mTOR Inhibitors at a Glance. *Mol Cell Pharmacol* **7**, 15-20 (2015).

34 Dai, Z. J. *et al.* Targeted inhibition of mammalian target of rapamycin (mTOR) enhances radiosensitivity in pancreatic carcinoma cells. *Drug Des Devel Ther* **7**, 149-159, doi:10.2147/DDDT.S42390 (2013).

35 Holler, M. *et al.* Dual Targeting of Akt and mTORC1 Impairs Repair of DNA Double-Strand Breaks and Increases Radiation Sensitivity of Human Tumor Cells. *PLoS One* **11**, e0154745, doi:10.1371/journal.pone.0154745 (2016).

36 Lai, Y., Yu, X., Lin, X. & He, S. Inhibition of mTOR sensitizes breast cancer stem cells to radiation-induced repression of self-renewal through the regulation of MnSOD and Akt. *Int J Mol Med* **37**, 369-377, doi:10.3892/ijmm.2015.2441 (2016).

37 Liu, Z. G. *et al.* The novel mTORC1/2 dual inhibitor INK128 enhances radiosensitivity of breast cancer cell line MCF-7. *Int J Oncol* **49**, 1039-1045, doi:10.3892/ijo.2016.3604 (2016).

38 Zhang, D. *et al.* Inhibition of mammalian target of rapamycin by rapamycin increases the radiosensitivity of esophageal carcinoma Eca109 cells. *Oncol Lett* **8**, 575-581, doi:10.3892/ol.2014.2186 (2014).

39 Zheng, H. *et al.* Inhibition of mTOR enhances radiosensitivity of lung cancer cells and protects normal lung cells against radiation. *Biochem Cell Biol* **94**, 213-220, doi:10.1139/bcb-2015-0139 (2016).

40 Horn, D., Hess, J., Freier, K., Hoffmann, J. & Freudlsperger, C. Targeting EGFR-PI3K-AKT-mTOR signaling enhances radiosensitivity in head and neck squamous cell carcinoma. *Expert Opin Ther Targets* **19**, 795-805, doi:10.1517/14728222.2015.1012157 (2015).

41 Leiker, A. J. *et al.* Radiation Enhancement of Head and Neck Squamous Cell Carcinoma by the Dual PI3K/mTOR Inhibitor PF-05212384. *Clin Cancer Res* **21**, 2792-2801, doi:10.1158/1078-0432.CCR-14-3279 (2015).

42 Wang, D., Gao, L., Liu, X., Yuan, C. & Wang, G. Improved antitumor effect of ionizing radiation in combination with rapamycin for treating nasopharyngeal carcinoma. *Oncol Lett* **14**, 1105-1108, doi:10.3892/ol.2017.6208 (2017).

43 Agrawal, N. *et al.* Exome sequencing of head and neck squamous cell carcinoma reveals inactivating mutations in NOTCH1. *Science* **333**, 1154-1157, doi:10.1126/science.1206923 (2011).

44 Iglesias-Bartolome, R., Martin, D. & Gutkind, J. S. Exploiting the head and neck cancer oncogenome: widespread PI3K-mTOR pathway alterations and novel molecular targets. *Cancer Discov* **3**, 722-725, doi:10.1158/2159-8290.CD-13-0239 (2013).

45 Lui, V. W. *et al.* Frequent mutation of the PI3K pathway in head and neck cancer defines predictive biomarkers. *Cancer Discov* **3**, 761-769, doi:10.1158/2159-8290.CD-13-0103 (2013).

46 Stransky, N. *et al.* The mutational landscape of head and neck squamous cell carcinoma. *Science* **333**, 1157-1160, doi:10.1126/science.1208130 (2011).

47 Bauman, J. E. *et al.* A phase II study of temsirolimus and erlotinib in patients with recurrent and/or metastatic, platinum-refractory head and neck squamous cell carcinoma. *Oral Oncol* **49**, 461-467, doi:10.1016/j.oraloncology.2012.12.016 (2013).

48 Fury, M. G. *et al.* A phase I study of temsirolimus plus carboplatin plus paclitaxel for patients with recurrent or metastatic (R/M) head and neck squamous cell cancer (HNSCC). *Cancer Chemother Pharmacol* **70**, 121-128, doi:10.1007/s00280-012-1894-y (2012).

49 Fury, M. G. *et al.* A phase 1 study of everolimus plus docetaxel plus cisplatin as induction chemotherapy for patients with locally and/or regionally advanced head and neck cancer. *Cancer* **119**, 1823-1831, doi:10.1002/cncr.27986 (2013).

50 Geiger, J. L. *et al.* Phase II trial of everolimus in patients with previously treated recurrent or metastatic head and neck squamous cell carcinoma. *Head Neck* **38**, 1759-1764, doi:10.1002/hed.24501 (2016).

51 Grunwald, V. *et al.* TEMHEAD: a single-arm multicentre phase II study of temsirolimus in platin- and cetuximab refractory recurrent and/or metastatic squamous cell carcinoma of the head and neck (SCCHN) of the German SCCHN Group (AIO). *Ann Oncol* **26**, 561-567, doi:10.1093/annonc/mdu571 (2015).

52 Massarelli, E. *et al.* Phase II trial of everolimus and erlotinib in patients with platinum-resistant recurrent and/or metastatic head and neck squamous cell carcinoma. *Ann Oncol* **26**, 1476-1480, doi:10.1093/annonc/mdv194 (2015).

53 Saba, N. F. *et al.* Phase 1 and pharmacokinetic study of everolimus in combination with cetuximab and carboplatin for recurrent/metastatic squamous cell carcinoma of the head and neck. *Cancer* **120**, 3940-3951, doi:10.1002/cncr.28965 (2014).

54 Fury, M. G. *et al.* A phase 1 study of everolimus + weekly cisplatin + intensity modulated radiation therapy in head-and-neck cancer. *Int J Radiat Oncol Biol Phys* **87**, 479-486, doi:10.1016/j.ijrobp.2013.06.2043 (2013).

55 Iglesias-Bartolome, R. *et al.* mTOR inhibition prevents epithelial stem cell senescence and protects from radiation-induced mucositis. *Cell Stem Cell* **11**, 401-414, doi:10.1016/j.stem.2012.06.007 (2012).

56 Chargari, C., Toillon, R. A., Macdermed, D., Castadot, P. & Magne, N. Concurrent hormone and radiation therapy in patients with breast cancer: what is the rationale? *Lancet Oncol* **10**, 53-60, doi:10.1016/S1470-2045(08)70333-4 (2009).

57 Rong, C., Meinert, E. & Hess, J. Estrogen Receptor Signaling in Radiotherapy: From Molecular Mechanisms to Clinical Studies. *Int J Mol Sci* **19**, doi:10.3390/ijms19030713 (2018).

58 Shatalova, E. G., Klein-Szanto, A. J., Devarajan, K., Cukierman, E. & Clapper, M. L. Estrogen and cytochrome P450 1B1 contribute to both early- and late-stage head and neck carcinogenesis. *Cancer Prev Res (Phila)* **4**, 107-115, doi:10.1158/1940-6207.CAPR-10-0133 (2011).

59 Grunow, J. *et al.* Regulation of submaxillary gland androgen-regulated protein 3A via estrogen receptor 2 in radioresistant head and neck squamous cell carcinoma cells. *J Exp Clin Cancer Res* **36**, 25, doi:10.1186/s13046-017-0496-2 (2017).

60 Egloff, A. M. *et al.* Cross-talk between estrogen receptor and epidermal growth factor receptor in head and neck squamous cell carcinoma. *Clin Cancer Res* **15**, 6529-6540, doi:10.1158/1078-0432.CCR-09-0862 (2009).

CHAPTER 6

Identification of a novel ATM inhibitor with cancer cell specific radiosensitization activity

A.J.C. Dohmen
X. Qiao
A.M. Duursma
R.H. Wijdeven
C. Lieftink
F. Hageman
B. Morris
P. Halonen
C. Vens
M.W.M. van den Brekel
H. Ovaa
J. Neefjes
C.L. Zuur

Adapted from Oncotarget. May 2017, 8(43), 73925-73937

ABSTRACT

Treatment of advanced head and neck squamous cell carcinoma (HNSCC) is plagued by low survival and high recurrence rates, despite multimodal therapies. Presently, cisplatin or cetuximab is used in combination with radiotherapy which has resulted in minor survival benefits but increased severe toxicities relative to RT alone. This underscores the urgent need for improved tumor-specific radiosensitizers for better control with lower toxicities. In a small molecule screen targeting kinases, performed on three HNSCC cell lines, we identified GSK635416A as a novel radiosensitizer. The extent of radiosensitization by GSK635416A outperformed the radiosensitization observed with cisplatin and cetuximab in our models, while exhibiting virtually no cytotoxicity in the absence of radiation and in normal fibroblast cells. Radiation induced phosphorylation of ATM was inhibited by GSK635416A. GSK63541A increased DNA double strand breaks after radiation and GSK63541A mediated radiosensitization was lacking in ATM-mutated cells thereby further supporting the ATM inhibiting properties of GSK63541A. As a novel ATM inhibitor with highly selective radiosensitizing activity, GSK635416A holds promise as a lead in the development of drugs active in potentiating radiotherapy for HNSCC and other cancer types.

INTRODUCTION

Of the estimated 686,000 new head and neck cancer cases per year worldwide[1], seventy percent of HNSCC patients enter the clinic with advanced stage disease and exhibit an overall 5-year survival rate of only 35-60%[2-4]. Radiotherapy (RT) serves as a backbone of first-line local therapy offered to nearly 75% of HNSCC patients. However, the success of this approach is limited on a number of fronts. First, HNSCC is associated with high rates of locoregional and distant recurrences. Second, RT is given at high doses (up to 70 Gy), which can cause considerable morbidity, such as loss of organ integrity and function (i.e. speech and swallowing). In an effort to improve cure rates and functional outcomes of locally advanced HNSCC, high-dose cisplatin chemotherapy has been integrated into the RT treatment regimens (CCRT) since the early 1980s[5]. The concurrent CCRT regimen is thought to sensitize tumor cells to RT by virtue of obstructing repair of radiation-induced DNA breaks. However, meta-analysis of randomized trials has indicated only a moderate absolute overall survival benefit of 6.5% at 5 years for HNSCC patients upon addition of cisplatin to locoregional RT[6]. Furthermore, in addition to the high local recurrence rate in more than 50% of patients, CCRT is accompanied with a substantial increase in severe adverse events, including mucositis, dysphagia, nephrotoxicity and hematologic toxicity[7]. As an alternative to cisplatin, cetuximab —a humanized monoclonal antibody against the epidermal growth factor (EGF) receptor—has been administered before RT. To date, only one trial reported efficacy of cetuximab-RT in HNSCC[8], while a recent phase 2 randomized trial, comparing RT with concomitant cisplatin versus cetuximab, showed that cetuximab increased acute toxicity rates without a corresponding clinical benefit[9]. While CCRT is presently favoured over cetuximab-RT in routine care[10], it is clear that many HNSCC patients are not receiving benefits from the currently available treatments, highlighting an urgent need for alternatives. Among novel targeted drugs, PARP inhibitors (such as olaparib) emerged as potential radiosensitizers. Pre-clinical studies show efficient sensitization to RT in various tumor types[11-14].

Aiming to identify novel and better radiosensitizers for the treatment of HNSCC, we performed a screen to test compounds in a higher scale, with structural diversities and a broader range of targets. Compound screening allows for identification of compounds with a certain biological effect without the need for prior knowledge of the mechanism or the target, which facilitates the identification of critical targets[15]. To this end, we performed a kinase inhibitor screen on HNSCC cell lines in the absence and presence of ionizing radiation (IR). We identified GSK635416A as a novel radiosensitizer with radiosensitization efficacy superior to that of cisplatin or cetuximab, and comparable to olaparib. Furthermore, as single agent in the absence of IR, GSK635416A showed lower cytotoxicity compared

to the other three drugs, and it did not radiosensitize normal fibroblast cells, indicating tumor-selectivity. We further characterized GSK635416A as a novel ATM inhibitor capable of impairing ATM activation following DNA damage. When used in combination with olaparib, GSK635416A's induced radiosensitization was additive to olaparib induced radiosensitization, while showing no increased cytotoxicity. This combination treatment showed no increased radiosensitization or cytotoxicity in normal fibroblast cells. Takn together, our findings provide a basis to further explore new RT combination options with GSK635416A.

RESULTS

Identification of a novel radiosensitizing compound

To identify novel radiosensitizing compounds for HNSCC, we screened the GSK-PKIS kinase library consisting of 356 kinase inhibitors, in three HNSCC cell lines (UT-SCC-24a, -36 and -40) in the presence (IRpos) and absence (IRneg) of 4 Gy IR *(Figure 1A).* Cell viability was measured at day 7. Values were normalized to negative controls and IRpos values of each compound were then compared to IRneg to determine the radiosensitizing effects. A cell viability heat-map example, that visualizes the leading compound candidates at 500 nM ranked by the largest mean difference between IRneg and IRpos for the three cell lines and each replicate, is shown in *Figure 1B.* The *p*-values and adjusted *p*-values for these differences were all significant (< 0.00016 and < 0.00077, respectively).

Next, we validated the 17 leading candidates (the top 5 compounds in the following categories: 50 nM, 500 nM and 5 μM separately, and all concentrations taken together) over a wide concentration range. This yielded a single outstanding compound, GSK635416A, exhibiting the greatest mean difference between IRpos and IRneg for all variables (see *Supplementary Table S1).* The dose-response curve of GSK635416A in three cell lines *(Figure 1C)* showed significant IR-dependent cell kill in IRpos. However, the cytotoxicity of GSK635416A, i.e. decrease in cell viability in the absence of IR, is limited. This consequently produces a large window between the two curves, hence depicting the potential radiosensitization. Taken together, these results suggest that GSK635416A can act as a radiosensitizer with limited cytotoxicity. To further assay for radiosensitizing properties, we performed a colony forming assay (CFA) at 2 μM GSK635416A and various IR doses, in UT-SCC-36 *(Figure 1D).* This concentration was chosen based on the viability assay results, at which 2 μM GSK635416A showed a significant decrease in cell viability only when combined with IR. Plating efficiencies (PE) in the CFA were not different and did not decrease under 2 μM of GSK635416A treatment compared to vehicle treated controls,

thereby confirming a lack of clonogenic cell death at this drug concentration without IR *(Supplementary Figure S1A).* The results of the CFA showed a strong radiosensitizing activity of GSK635416A with a radiation dose enhancement factor (DEF) of 1.99 (DEF_{37} 1.99, ± SD: 0.19) *(Figure 1D).* For comparison, a DEF_{37} of 1.90 for cisplatin in a UT-SCC cell line[16] and a DEF_{37} of 1.08-1.61 for olaparib in various cancer cell types[11,17,18] have been reported for similar conditions. The structure of GSK635416A is shown in *Figure 1E* and is unrelated to olaparib or cisplatin.

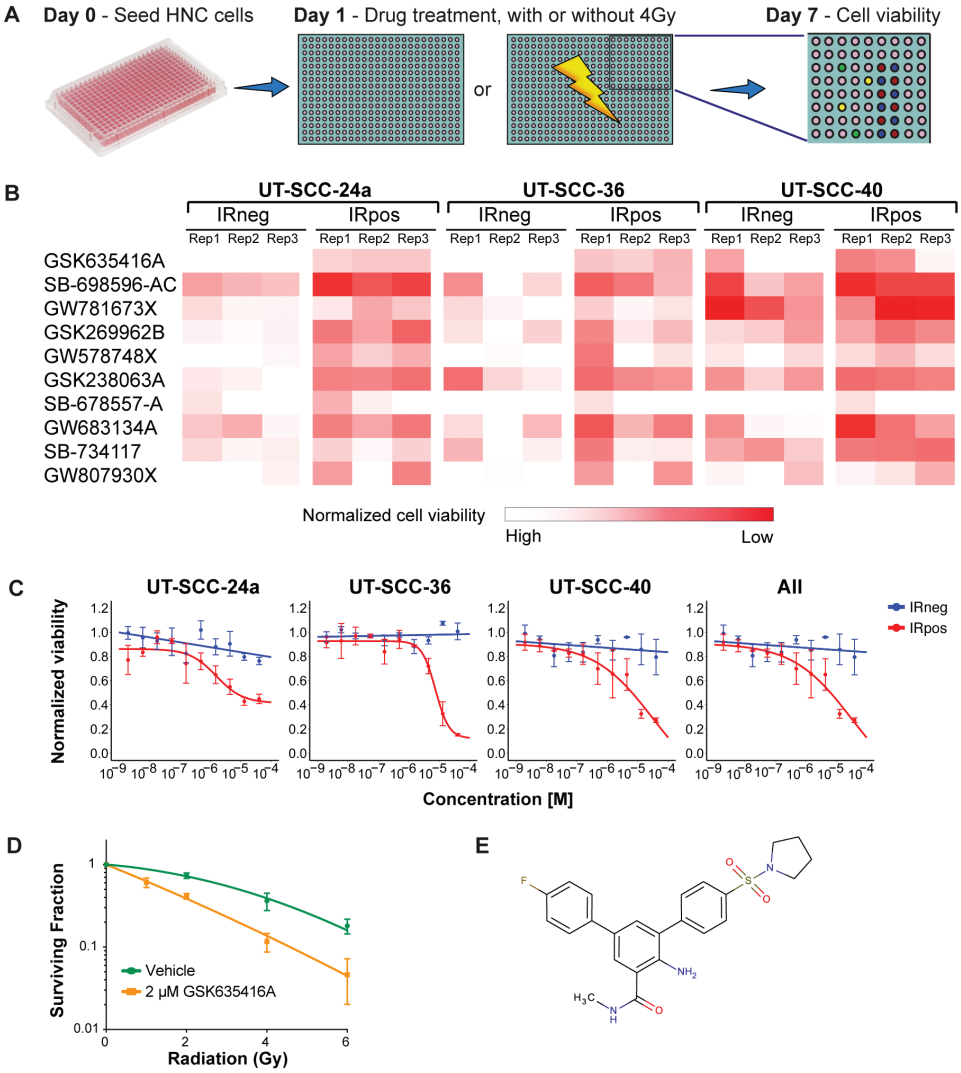

Figure 1. A kinase inhibitor screen identifies GSK635416A as a potential novel radiosensitizer for head and neck cancer. **A**, Schematic overview of the screening procedure. **B**, Top 10 compounds as identified in the primary

screen performed in triplicate. The heat map is a graphic representation of normalized cell viability at day 7 at a concentration of 500 nM, depicted by colour intensity. The three replicate values depict the reproducibility of the effect of the compound on cell viability in three HNSCC cell lines. IRneg is the effect on non-radiated cells; IRpos is the effect in combination with 4 Gy radiation. **C**, Validation of top hit GSK635416A library compound. Shown are dose-response curves of GSK635416A for IRneg and IRpos in UT-SCC-24a, UT-SCC-36, UT-SCC-40 cells, and a graph representing the effect on all three cell lines. The IR-effect was eliminated by normalizing to negative controls that received IR. (Data shown as mean from three independent experiments, with SEM.) **D**, CFA on UT-SCC-36 cultured in the presence or absence of 2 μM GSK635416A and exposed to different doses of radiation. (Data shown are the mean of three independent experiments, with SD.) **E**, Structure of GSK635416A.

Comparing GSK635416A to radiosensitizers currently used in HNSCC

To compare GSK635416A to the radiosensitizers cisplatin, cetuximab and olaparib that are presently used or tested in the clinic, we generated dose-response curves using a 7-day cell viability assay. During this 7-day assay, cells were continuously exposed to the drugs. This was done since wash-out experiments revealed the highest cell kill with long drug exposures *(Supplementary Figure S2).* Significant differences between IRneg and IRpos data points were observed for GSK635416A and olaparib *(Figure 2A),* but not for cisplatin *(Figure 2A)* and cetuximab *(Supplementary Figure S3A).* This implies that cisplatin and cetuximab exhibits poor radiosensitizing effects in the three HNSCC cell lines tested. Although olaparib treatment showed a robust reduction of cell viability when combined with IR, it also resulted in cytotoxicity at higher concentrations. In contrast, the IRneg curve of GSK635416A did not reach the IC_{50} in any of the three cell lines, reported as '> 25 μM' in *Figure 2B,* illustrating again limited cytotoxicity of GSK635416A. To quantify these observations, we calculated the radiation enhancement ratio (RER) from the reported IC_{50}'s, which reflects the shift in the IC_{50} introduced by 4 Gy IR in the presence of the drug, as a measure of potential radiosensitizing activity. Cisplatin showed a low RER of 1.28 – 1.51 in all cell lines that were tested *(Figure 2B).* The RER of cetuximab was determined as > 1.00 in UT-SCC-24a and 0.86 in UT-SCC-36, indicating lack of radiosensitization under our experimental conditions *(Supplementary Figure S3B).* Therefore, we did not investigate cetuximab any further in this manuscript.

Although olaparib showed a similar or somewhat higher RER (11.56) than GSK635416A (> 7.67) in UT-SCC-24a cells, GSK635416A acted as a considerably stronger radiosensitizer in the other two cell lines. Importantly, the reported IC_{50} (IRneg) values of '> 25 μM' underestimates the radiosensitizing capabilities of GSK635416A since 25 μM is the highest concentration that was tested; as the actual IC_{50} is higher, a higher RER would be a consequence.

To improve the radiosensitizing activity of GSK635416A structure-activity relationship (SAR) analyses can be performed. This is a powerful concept in drug discovery which allows drug optimization. By modifying the chemical structure of a drug, one can determine the chemical group responsible for evoking the biological effect *(i.e.* radiosensitization). Nine analog compounds were generated with chemical structures related to the structure of GSK635416A *(Supplementary Figure S4).* We created variants devoid of the toxic side effects (analog AZ-210, AZ-215-I/II, AZ-224, AZ-225), with increased toxicity (analog AZ-210, AZ-232, AZ-226, AZ-238). No systematic improvement in radiosensitization was observed compared to GSK635416A.

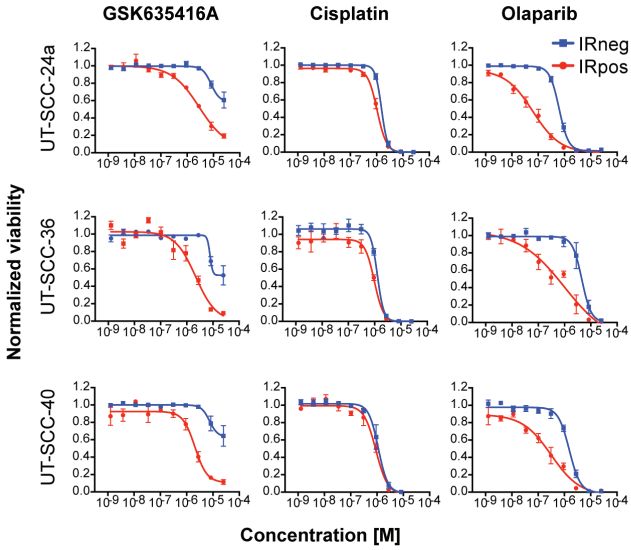

B

UT-SCC-24a			
Inhibitor	IRneg	IRpos	RER
GSK635416A	> 25	3.26	> 7.67
Cisplatin	1.53	1.01	1.51
Olaparib	0.62	0.05	11.56

UT-SCC-36			
Inhibitor	IRneg	IRpos	RER
GSK635416A	> 25	2.28	> 10.97
Cisplatin	1.31	0.91	1.44
Olaparib	4.50	0.56	8.04

UT-SCC-40			
Inhibitor	IRneg	IRpos	RER
GSK635416A	> 25	2.16	> 11.57
Cisplatin	1.13	0.88	1.28
Olaparib	1.49	0.21	7.10

Figure 2. Comparison of GSK635416A to the current clinical radiosensitizers cisplatin and olaparib in various HNSCC cell lines. Shown on the left (**A**) are the dose-response curves of (resynthesized) GSK635416A, cisplatin and olaparib in UT-SCC-24a, UT-SCC-36 and UT-SCC-40. The IRneg line (grey) represents the cytotoxicity effect of the compound alone. The IRpos line (black) represents the effect of the compound combined with 4 Gy radiation. The IR-effect was eliminated by normalizing to negative controls that received IR. Depicted on the right (**B**) are the corresponding calculated IC_{50} values (μM) for IRneg and IRpos and the determined radiation enhancement ratio (RER). (Data shown are the mean of three independent experiments, with SEM.)

GSK635416A sensitized a variety of cancer cell lines to radiation

To assess the breadth of impact of our new radiosensitizer, we also tested GSK635416A in two additional HNSCC cell lines (UT-SCC-2 and UT-SCC-8) and two tumor cell lines originating from cervical and long tissues (HeLa and A549) *(Table 1).* GSK635416A shows virtually no cytotoxicity in all tested cell lines (IC_{50} [IRneg] > 25 μM in UT-SCC-2, UT-SCC-8

and HeLa; 6.95 µM in A549), but effectively sensitized all cell lines to IR (RER 1.49 – 9.23). Once again, olaparib was found to be an efficient radiosensitizer (RER 2.90 – 13.46), while cisplatin only produced a limited radiosensitizing effect (RER 1.10 – 1.62). Of note, the RERs of cisplatin, olaparib and GSK635416A could not be directly compared to each other, as the RER for GSK635416A was underestimated given its limited cytotoxicity on non-radiated cells (the IC_{50} [IRneg] value of '> 25 µM' underestimates the calculated ratio).

Table 1. The effect of GSK635416A on various cell lines, compared to cisplatin and olaparib.

	UT-SCC-2			UT-SCC-8			HeLa			A549		
Inhibitor	**IRneg**	**IRpos**	**RER**	**IRneg**	**IRpos**	**RER**	**IRneg**	**IRpos**	**RER**	**IRneg**	**IRpos**	**RER**
GSK635416A	>25	4.32	**5.79**	>25	9.93	**2.52**	>25	2.71	**9.23**	6.95	4.68	**1.49**
Cisplatin	0.61	0.39	**1.56**	2.39	1.63	**1.47**	0.36	0.22	**1.62**	1.21	1.10	**1.10**
Olaparib	5.98	2.06	**2.90**	9.42	0.70	**13.46**	2.04	0.16	**12.75**	1.24	0.22	**5.64**

Calculated IC_{50} values (in µM) for IRneg and IRpos and the determined radiation enhancement ratio (RER) from dose-response curves of GSK635416A, cisplatin and olaparib in UT-SCC-2, UT-SCC-8, HeLa and A549 cells, as measured in a cell viability assay at day 7. (Data shown are the mean of three independent experiments, with SEM.)

In keeping with the importance of selectivity for cancer cells during treatment, we subjected a normal fibroblast cell line (BJ-ET) to various radiosensitizing drugs *(Figure 3A).* Interestingly, GSK635416A showed significantly higher cell viability in these cells when compared to cisplatin or olaparib. Also, GSK635416A showed only modest radiosensitization (DEF_{37} 1.11, ± 0.16) at a concentration of 2 µM in these cells when measured in the CFA *(Figure 3B).* Additionally, PE was similar between vehicle and GSK6535416A treatments, implying no apparent cytotoxicity of this drug on these cells *(Supplementary Figure S1B).* Taken together, these data suggest that GSK635416A's radiosensitization is tumor-specific in a variety of cancer cell lines with limited cytotoxicity in non-radiated cells and in non-transformed cells.

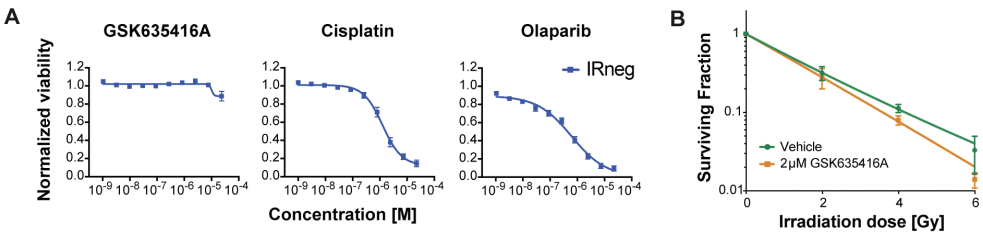

Figure 3. The effect of GSK635416A on normal BJ-ET fibroblast cells. A, Cytotoxicity of GSK635416A, cisplatin and olaparib treatment in a normal fibroblast cell line, BJ-ET. (Data shown are the mean of three independent experiments, with SEM.) **B,** Clonogenic survival of BJ-ET cells cultured in the presence or absence of 2 µM GSK635416A and exposed to different doses of radiation. (Data shown are the mean of five independent experiments, with SD.)

GSK635416A targets ATM kinase

Our screen identified a novel and unique radiosensitizer given its selectivity to cancer cells with limited cytotoxicity to non-radiated as well as normal cells. To identify the underlying biology and target for this compound, we first determined the timing of GSK635416A administration (i.e. prior to or following IR) that resulted in the most prominent radiosensitizing effect on HNSCC cells. GSK635416A exhibited a higher radiosensitizing effect when added prior to IR (0.5, 3 and 6 hours pre-IR; UT-SCC-36 *Figure 4A,* UT-SCC-24a *Supplementary Figure S5A)* than when added to cells post-IR, which suggested that GSK635416A targets the immediate DNA damage response (DDR). Given that the ataxia-telangiectasia mutated (ATM) kinase is an important early sensor of DNA double-strand breaks (DSBs) generated by IR, we examined IR-induced activation of the ATM pathway overtime in the presence or absence of GSK635416A. We assayed phosphorylation of ATM and its key downstream target CHK2 as read-outs for activation of ATM signaling (UT-SCC-36 *Figure 4B,* UT-SCC-24a *Supplementary Figure S5B).* A marked decrease in phosphorylation of both ATM and CHK2 was observed in the presence of GSK635416A. Since phosphorylation of ATM is the result of autophosphorylation, this suggested that GSK635416A acts as a direct inhibitor of the ATM kinase. To test target specificity, we generated replication stress using Hydroxyurea (instead of DNA damage following IR) to activate ATM-related ataxia telangiectasia and Rad3 related (ATR) kinase *(Figure 4C)* and tested phosphorylation of its downstream target CHK1 in response to GSK635416A treatment. Notably, GSK635416A exhibited no effect on CHK1 phosphorylation, excluding the ATR kinase as a possible target of GSK635416A and further cementing specificity of this inhibitor for the ATM signaling pathway. Additionally, we tested 10 μM GSK635416A *in vitro* against a panel of 456 kinases (not including ATM) in a competition binding assay *(Materials and Methods, Supplementary text),* which did not reveal any additional targets *(Supplementary Table S2A* and *S2B).* Due to its large molecular weight of around 350 kDa the associated challenges of expression and purification were difficult, therefore we chose to address whether ATM constitutes a valid target of GSK635416A by testing the radiosensitizing effect in the H23 cell line, that lacks ATM [19]. Of note, H23 cells were radiated with only 1 Gy instead of 4 Gy, because they are highly radiosensitive. The radiosensitizing activity of GSK635416A was lost in ATM deficient H23 cells upon 1 Gy of IR *(Figure 4D).* The lack of radiosensitization in two ATM deficient HNSCC cell lines (UPCI-SCC-040 and UPCI-SCC-131)[20] further supports ATM specificity of the radiosensitization by GSK635416A *(Supplementary Figure S6).* The established ATM-inhibitor KU-60019 also failed to radiosensitize H23 cells at 1 Gy, supporting the role of ATM deficiency of this cell line *(Figure 4E),* while exhibiting radiosensitizing activity in UT-SCC-24a and UT-SCC-36 cell lines at 4 Gy *(Figure 4F).* Notably, KU-60019, was not able to radiosensitize cells to the same extend as GSK635416A, and showed higher cytotoxicity

(compare *Figure 4F* to *Figure 2A;* UT-SCC-24a and UT-SCC-36). Collectively, the above data indicate that IR-dependent cell kill incurred by GSK635416A requires ATM and suggests that the mechanism of GSK635416A action proceeds via inhibition of the DDR. We therefore assessed DSB formation by radiation with constant-field gel electrophoresis techniques and showed increased DSBs after radiation when combined with GSK635416A *(Supplementary Figure S7).* Together, this further supports GSK635416A's role in DDR and as ATM inhibitor.

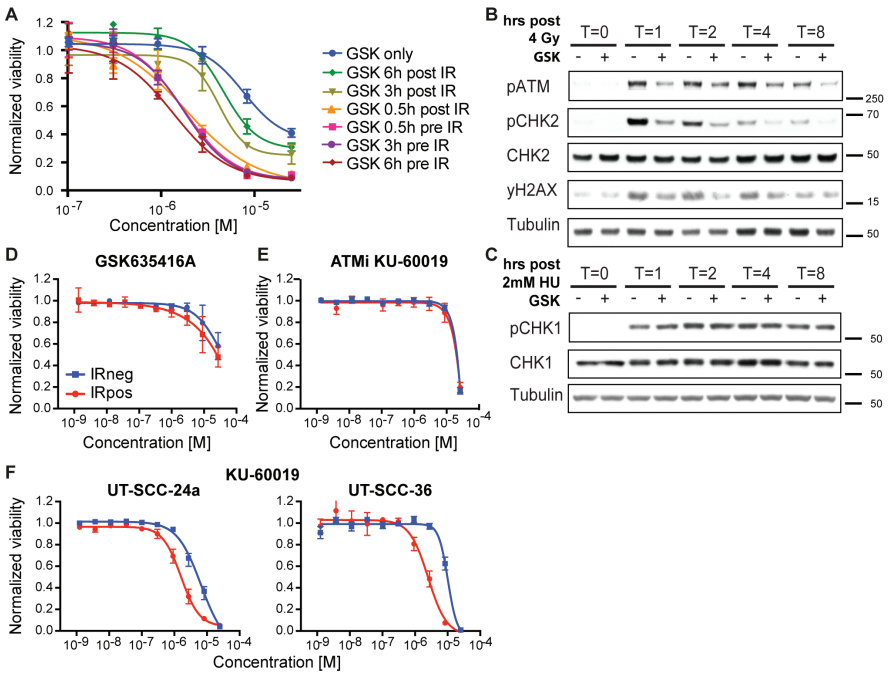

Figure 4. GSK635416A targets the DDR pathway. A, Tested timeframes of GSK635416A administration post- or pre-radiation in UT-SCC-36. **B**, **C**, Western blot of UT-SCC-36, showing subunits of the DDR pathway. Cells were exposed to 4 Gy IR for ATM pathway activation (**B**), and with 2 mM Hydroxyurea for ATR pathway activation (**C**). Cells were treated in the presence (+) or absence (-) of 2 μM GSK635416A, and subsequently harvested 0, 1, 2, 4 or 8 hours following treatment. **D**, GSK635416A in H23 ATM-deficient cells shows a loss of radiosensitization (1 Gy). **E**, Lack of radiosensitization by the ATM inhibitor KU-60019 in H23, confirming ATM defect (1 Gy). **F**, ATM inhibitor KU-60019 dose-response curves of UT-SCC-24a and UT-SCC-36 (4 Gy). (Data shown in A, D, E and F were measured with cell viability read-out at day 7 and shown as mean of at least three independent experiments with SEM).

GSK635416A and olaparib interplay

While both olaparib and GSK635416A sensitize cells to radiation, they target different aspects of the DDR. While olaparib inhibits PARP, GSK635416A targets the ATM kinase. Here

we tested whether combined inhibition of both pathways could improve radiosensitization without further increasing cytotoxicity of cells that are not exposed to IR. UT-SCC-24a and UT-SCC-36 were treated with or without 2 μM GSK635416A and with increasing olaparib concentrations up to 10 μM in combination with IR *(Figure 5A).* The RER for olaparib as a single drug is 14.22 and 7.41 in UT-SCC-24a and UT-SCC-36, respectively, while the combined enhancement ratio (CER) for olaparib and 2 μM GSK635416A increased 14- and 320-fold increase in the same cell lines (CER 177.50 and 2650.50 in UT-SCC-24a and UT-SCC-36, respectively; *Figure 5B).*

A different presentation of the data in *Supplementary Figure S8A* shows that olaparib radiosensitization is largely unaffected by GSK635416A addition. Simulating an additive effect by adding the effect of 2 μM GSK635416A (at the lowest olaparib concentration) to the non-GSK635416A treated olaparib viability values at different olaparib doses shows a "theoretical" curve line that is not different from the measured values when combining with GSK635416A. Comparing the IRneg profile of olaparib monotherapy to the IRneg curve of olaparib plus 2 μM GSK635416A revealed no increased cytotoxicity on non-radiated UT-SCC-36 cells *(Figure 5A,* IC_{50} [IRneg] 6.78 and 5.30, respectively) and increased cytotoxicity on non-radiated UT-SCC-24a cells *(Figure 5A,* IC_{50} [IRneg] 1.44 and 0.36, respectively). Most importantly and consistent with a lack of radiosensitization of GSK635416A in this cell line, the combination treatment did not show marked additional effects on cell viability in normal BJ-ET cells *(Figure 5A)* as ratio values remained low (RER 0.04 for olaparib and CER 0.01 for olaparib with GSK635416A) *(Figure 5B).*

The combination of GSK635416A with olaparib was also tested at 0.3 μM and 5 μM of GSK635416A *(Supplementary Figures S8B* and *S8C),* revealing a clear dose-dependent effect of GSK635416A in combination with olaparib with respect to radiosensitization. Although some cytotoxicity of GSK635416A was observed at 5 μM, as deduced from the IRneg curves starting at a cell viability below 1.0 *(Supplementary Figure S8A,* UT-SCC-24a and UT-SCC-36), no additional cytotoxicity of 0.3, 2 or 5 μM GSK635416A was observed for normal BJ-ET cells *(Figure 5A* and *Supplementary Figure S8B)* compared to olaparib alone. The CER in BJ-ET cells only increased when olaparib was combined with 5 μM GSK635416A *(Supplementary Figure S8C,* CER 0.58) due to the additional combination with IR. Collectively, these data suggest that GSK635416A increases radiation induced tumor cell death and maintains this property also in combination with olaparib, while preserving the low cytotoxicity profile in non-radiated and normal cells.

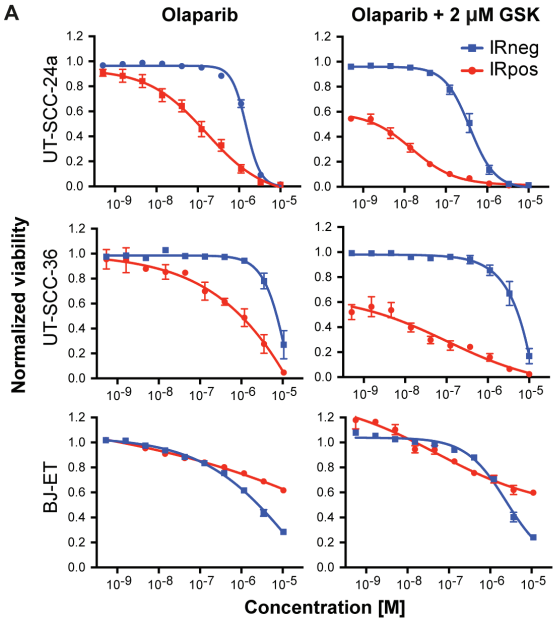

B

UT-SCC-24a			
Inhibitor	**IRneg**	**IRpos**	**R/CER**
Olaparib	1.436	0.101	14.22
Olaparib + 2 µM GSK	0.355	0.002	177.50

UT-SCC-36			
Inhibitor	**IRneg**	**IRpos**	**R/CER**
Olaparib	6.778	0.915	7.41
Olaparib + 2 µM GSK	5.301	0.002	2,650.50

BJ-ET			
Inhibitor	**IRneg**	**IRpos**	**R/CER**
Olaparib	2.448	69.823	0.04
Olaparib + 2 µM GSK	0.355	370.304	0.01

Figure 5. GSK635416A combined with olaparib enhances IR effect in radiosensitizing HNSCC cell lines but not in normal fibroblast BJ-ET cells. A, Dose-response curves of olaparib in the presence or absence of 2 µM GSK635416A in UT-SCC-24a, UT-SCC-36 and BJ-ET, measured by cell viability read-out at day 7. **B**, Corresponding IC_{50} values (µM) for IRneg and IRpos, and the RER and CER were determined to compare the treatments. (Data are shown as mean of three to five independent experiments, with SEM).

6

DISCUSSION

In spite of various treatment attempts, advanced HNSCC is poised by poor prognoses, with RT constituting the best available therapy option next to surgery, despite its limited benefits when administered on its own. The addition of cisplatin or cetuximab to RT regimens has shown only limited survival benefit and substantial systemic toxicity compared to RT alone[6,7,9,10]. While immunotherapy and newer drugs are under development for HNSSC, RT will remain an important part of the treatment protocol. Development of better and more specific radiosensitizers is crucial and may have substantial therapeutic effects on HNSCC patients. To identify novel radiosensitizers, we performed a screen with the GSK kinase inhibitor library to identify compounds capable of sensitizing HNSCC cells to IR, while excluding compounds targeting non-radiated cells. This approach was aimed at selecting compounds capable of improving current treatment efficacy and avoiding adverse effects. Using this approach, we identified one compound, GSK635416A, as a novel tumor-specific radiosensitizer.

GSK635416A, with a DEF37 of 1.99 in HNSCC cells, compares favourably to established radiosensitizers, including cisplatin (DEF37 of 1.90 in UT-SCC-24a[16]) and olaparib (DEF37 of 1.25 (+0.18) and 1.61 (± 0.55) in 6 other UT-SCC cell lines at 1 μM and 3.3 μM, respectively[18]). Direct comparison to cetuximab was not assessed, as no DEF_{37} for this drug has been reported. In addition to its IR-dependent effects, an ideal radiosensitizer would be expected to display tumor-specific activity, resulting in limited systemic toxicities as well as sparing normal cells within the radiation field. Our data indicate that GSK635416A outperforms cisplatin, cetuximab and olaparib, as it did not affect viability of non-radiated HNSCC cells, was not cytotoxic to normal BJ-ET fibroblast and barely radiosensitized BJ-ET cells (DEF 1.11). High cytotoxicity of cisplatin, cetuximab and olaparib treatment was observed when these drugs were administered as single agents to a variety of cell lines, including BJ-ET cells. On the basis of these comparisons, GSK635416A has the potential for development into a highly effective and tumor-specific radiosensitizing compound applicable to difficult to treat head and neck cancers that often fail to respond to even high doses of radiotherapy.

Given the severe limitations of radiosensitizers currently administered in the clinic and the urgent need for new RT-compatible therapies, there has been substantial discussion on the topic. It has been proposed that inhibitors of the DDR pathway may present a suitable source of novel targeted anticancer treatments[21-26]. Interestingly, we found that GSK635416A appeared to inhibit DDR by targeting the ATM kinase. There are multiple arguments for this. First, GSK635416A must be present during, and not after, exposure to IR to act as a radiosensitizer, suggesting an effect on early cellular events resulting from IR. Second, because ATM acts upstream of the double-strand DNA repair pathway, inhibition of this master kinase in DDR could thus explain the strong radiosensitizing effects of GSK635416A. Indeed, exposure of HNSCC cells to GSK635416A markedly reduced activation of ATM and its downstream target CHK2 in response to IR. Thirdly, a cell line lacking ATM failed to be radiosensitized by GSK635416A. Furthermore, GSK635416A seems remarkably specific for ATM kinase as we failed to detect any other target for GSK635416A in an *in vitro* competition binding assay screen with 456 kinases. This may explain why GSK635416A hardly affects cells unless radiated, as the drug has few detectable off-targets. Of note, we compared the effects of GSK635416A to an established ATM inhibitor (KU-60019), which also displayed radiosensitizing activity, but was more toxic to non-radiated cells. It is possible that GSK635416A is simply more selective for ATM than other reported ATM inhibitors[24,27], since GSK635416A has a distinct chemical structure. In literature, only a handful of selective ATM inhibitors have been reported, all in the interest of finding novel radiosensitizers. These ATM inhibitors have not been tested on HNSCC cell lines and did not progress into the clinical practice due to their poor bioavailability and selectivity[24,27].

Deciphering the molecular targets of bioactive molecules is a key step towards understanding their clinical potential, particularly in designing effective combination therapies while mitigating compounding side effects. As ATM is critical in DNA double strand break repair, attenuating this repair by inhibiting ATM could simply explain the molecular basis for GSK635416A as a radiosensitizer. As an inhibitor of ATM, GSK635416A affects the DDR pathway. Simplified, the DDR pathway is activated by single (SSB) and double-strand DNA breaks (DSB). SSBs are recognized mainly by PARP[28], and ATM is activated by DSBs[29]. Olaparib inhibits PARP and thus plays an important role in the base-excision repair (BER) pathway and in the repair of SSBs. The radiosensitizing effect of olaparib requires DNA replication which implies selectivity of rapidly dividing and/or DNA repair defective tumor cells. Bryant *et al.* showed that PARP inhibitors selectively kill homologous recombinant (HR)-deficient (BRCA2) cancers cells[30]. In addition, Verhagen *et al.* and Wurster *et al.* showed that olaparib has stronger synergistic interaction in HR-deficient than in HR-proficient HNSCC once combined with IR[18,31]. Unfortunately, in HNSCC mutations in HR genes are rare[31]. However, by inhibiting ATM, GSK635416A also inhibits HR. The accumulation of SSBs in the absence of PARP activity, leads to replication fork collapse and DSBs, which require HR factors to repair. IR produces DNA damage and SSBs that the replication fork encounters but perhaps may have controlled if the DDR would not have been inhibited by GSK635416A. This provides a rationale to explore the combined effect of PARP and ATM inhibitors as radiosensitizers. We show that the radiosensitizing effect of the combination of 2 μM GSK635416A and olaparib follows an additive effect. This effect could be further investigated in the future by varying concentrations of GSK635416A and by performing colony forming assays and *in vivo* experiments. Importantly, GSK635416A differs from olaparib in that it is considerably less cytotoxic in the absence of IR and less cytotoxic in healthy normal fibroblasts both in the presence or absence of additional IR. Therefore, we still believe that GSK635416A is an excellent lead for further development towards a radiosensitizing drug, either as single compound or in combination with olaparib, being a starting point for medicinal chemistry on its chemical structure with a corresponding target and biological mechanism. Furthermore, GSK635416A displayed radiosensitizing effects in cervical HeLa and lung A549 cancer cells, implying therapeutic potential against other cancer types. We expect that additional medicinal SAR-chemistry efforts, to optimize GSK635416A, may fuel a much needed improvement in treatment options for HNSCC patients, as well as other cancer patients that respond poorly to standard chemoradiotherapy.

MATERIALS AND METHODS

Cell culture

The human HNSCC cell lines UT-SCC-2, UT-SCC-8, UT-SCC-24a, UT-SCC-36 and UT-SCC-40 were kindly provided by Prof. R. Grénman (University of Turku, Finland). We primarily selected p53 mutated and HPV negative cell lines since 74% of HNSCC tumors are HPV negative and have poor prognosis[32]. Of these, the majority (75 to 85%) have TP53 mutations[33]. Cell lines with these characteristics were therefore chosen. These cell lines were harvested from previously untreated HPV negative patients and have various sensitivities to IR [34,35]. Cell line characteristics are listed in *Table 2*. These cells were cultured in Dulbecco's Modified Eagle Medium high glucose, GlutaMAX™, pyruvate (Invitrogen) supplemented with 10% FBS, 1% non-essential amino acids (Sigma), penicillin and streptomycin (Gibco 15070, 50 Units/ml and 50 µg/ml), as previously described[36,37]. The characterization of these cell lines was further confirmed by immunohistochemistry staining of hematoxylin-eosin, Cytokeratin AE1/3, Cam 5.2, p63 and Vimentin. Two human lung cancer cell lines (A549 and H23 [ATCC CRL-5800]), a human cervical cancer cell line (HeLa), and a human normal fibroblast cell line (BJ-ET [ATCC CRL-2522, overexpressing hTERT][38]) were cultured in DMEM (Invitrogen) supplemented with 10% FBS and penicillin and streptomycin. The cell lines were cultured at 37˚C with 5% CO_2.

Table 2. HNSCC cell line characteristics

Cell line	Gender	Primary tumor location	TNM	Type of lesion	Histol. grade	Radiosens. (SF_2 ± SD)	HPV	P53	Ref
UT-SCC-2	Male	Floor of mouth	T4N1M0	Primary	2	0.35 ± 0.05	Neg	Mut	34,35,37
UT-SCC-8	Male	Supraglottic larynx	T2N0M0	Primary	1	0.37 ± 0.03	Neg	Mut	34,37
UT-SCC-24a	Male	Tongue	T2N0M0	Primary	2	0.51 ± 0.06	Neg	Mut	35,37
UT-SCC-36	Male	Floor of mouth	T4N1M0	Primary	3	0.72 ± 0.07*	Neg	Mut	37
UT-SCC-40	Male	Tongue	T3N0M0	Primary	1	0.45 ± 0.02[‡]	Neg	ND	37

*TNM status of primary tumors according to the International Union against Cancer (1997). Histologic grade: 1, well differentiated; 2, moderately differentiated; 3, poorly differentiated. Radiosens.: radiosensitivity. *Determined in this manuscript. [‡]Unpublished data from Prof. R. Grénman. SF_2: Survival fraction at 2 Gy, measured by clonogenic survival. HPV Neg: human papillomavirus negative. P53 Mut: mutated, ND: not detectable.*

Compounds

We exposed the cell lines to the open-source GlaxoSmithKline Published Kinase Inhibitor Set (GSK PKIS) containing 356 defined and potential protein kinase inhibitors, representing 31 chemical chemotypes[39]. The majority of kinase inhibitors in this screening library compete with ATP for binding to the common enzyme active site.

The following individual compounds were used. Olaparib was obtained from Syncom (Groningen, The Netherlands). Cisplatin and ATM-inhibitor KU-60019 were obtained from Selleck Chemicals (Houston, USA). Cetuximab (Erbitux, 5 mg/ml, buffer) was obtained from Merck Serono (Darmstadt, Germany). GSK635416A was synthesized as described[40], and stock solution was dissolved in 20% DMSO and 80% Ethanol at 10 mM. Compounds dissolved in solely DMSO were added automatically to the plates with the HP D300 Digital Dispenser. Hydroxyurea (HU, a ribonucleotide reductase inhibitor) was obtained from Sigma.

Screening

Using a robotic liquid handling platform system, we screened the compound library in three ten-fold dilutions (50 nM to 5 µM) in three cell lines (UT-SCC-24a, UT-SCC-36 and UT-SCC-40) with or without 4 Gy IR). All experiments were performed in independent biological triplicates. On day 0, cells were seeded automatically (Thermo Scientific Multidrop Combi Reagent Dispenser) in 384-well plates in 45 µl medium. Seeding densities were previously optimized to reach approximately 80% confluency on day 7. The outer two rows and columns of the 384-well plates did not include any experimental or control compounds to exclude potential evaporation and edge effects. At day 1, compounds were administered with the 'Hamilton STARlet Liquid Handler' robot, and DMSO and phenylarsine oxide (PAO, 20 µM) were used as a negative and positive control for cell viability, respectively. Furthermore, olaparib was taken along as a control for detecting radiosensitizing effects[18]. Half an hour after compound addition, the plates were either subjected to 4 Gy IR (Best Theratronics Gammacell® 40 Exactor, 0.95 Gy/min, Ottawa, Ontario, Canada) (IRpos) or left non-radiated (IRneg). At day 7, cell viability was determined by CellTiter-Blue assay. In short, cells were incubated with CellTiter-Blue® (Promega, final 1:20) for 4 hours, then the fluorescence intensity was measured using the EnVision plate reader (Perkin Elmer).

Hit validation

Lead candidates showing the largest mean difference with significant adjusted *p*-values, were selected for validation. We picked the best 5 compounds from the following four categories: dataset at 50 nM, 500 nM, 5 µM and all concentrations combined. The efficacy of the 17 selected compounds was validated using freshly dissolved compounds. This was done in 3-fold dilutions with 10 concentrations ranging from 2 nM to 40 µM on UT-SCC-24a, UT-SCC-36 and UT-SCC-40 cell lines, in triplicate in 384-well plates.

Thereafter, we selected the top hit, GSK635416A, based on the largest window between IRneg and IRpos. We resynthesized GSK635416A[40] to chemically validate for purity by

High-performance liquid chromatography and for structure by mass spectrometry. Subsequently, we biologically validated its activity on our panel of cell lines (UT-SCC-2, -8, -24a, -36 and -40, HeLa, A549, and BJ-ET) in 3-fold dilutions with 10 concentrations ranging from 1.3 nM to 40 μM. All subsequent validation experiments were performed with the resynthesized GSK635416A in 96-well format routinely.

Colony formation assay

To validate the efficacy of our lead candidate, we assessed clonogenic survival after radiation using the colony formation assay, as described[41]. Briefly, single-cell suspensions of proliferating UT-SCC-36 and BJ-ET cells were seeded into 10-cm dishes at different cell densities in triplicate and radiated 6 hours after plating. Cells were exposed to a single radiation dose, varying from 2 to 6 Gy. GSK635416A was added 1 hour prior to IR at 2 μM. Controls were treated with the vehicle (drug solvent, DMSO/ethanol) at equal concentration as the GSK635416A treated cells. After 2 weeks (for UT-SCC-36) or 3 weeks (for BJ-ET) of incubation, colonies were fixed and stained with 0.5% crystal violet/6.0% glutaraldehyde. Only colonies consisting of more than 100 cells were counted. GSK635416A treated samples did not require longer incubation times as GSK635416A did not influence colony formation or size at this concentration. Plating efficiencies were not significantly altered by GSK635416A treatment *(Supplementary Figure S1).* Survival after radiation of vehicle or GSK635416A treated cells was calculated relative to the plating efficiency of non-radiated controls, vehicle or GSK635416A treated cells, respectively. Survival data points are the mean of the averages of three to five independent experiments. Dose enhancement factors (DEF) values were calculated as the ratio of radiation doses to produce 37% survival (DEF_{37}) without GSK635416A to those with GSK635416A. These doses were calculated from the linear quadratic fits through the radiation dose response data.

Western blot analysis

Western blot analysis was performed using standard protocols, to determine the target of GSK635416A. In brief, UT-SCC-24a and UT-SCC-36 cells were lysed directly with Laemmli sample buffer. Samples were separated by SDS-PAGE and proteins transferred to PVDF membranes (Millipore). The PVDF membranes were subsequently blocked by 5% milk in TBS. Antibody blotting was done in TBS supplemented with 0.05% Tween and 2% milk. Antibodies used for Western blotting: pCHK1-Ser345 (Cell Signaling; 133D3), CHK1 (Santa Cruz Biotechnology; G-4), pCHK2-Thr68 (Cell Signaling), CHK2 (Santa Cruz; H-300), pATM-S1981 (Rockland Immunochemicals for research), H2AX-Ser139P (Upstate) and Tubulin-α (Sigma).

Data analysis and radiosensitization

Analysis of the screening data was done using R version 3.1.2. Cell viability data were analyzed using the normalized percent inhibition (NPI) method, to correct for plate effects and allow direct comparison of plates[42]. This NPI method divides the difference between the average of the positive controls and the compound measurement, by the difference between the averages of the positive and negative controls. This way, the value '0' corresponds to complete cell death and the value '1' to no treatment. Correlation plots of the replicates showed consistent correlation between the three replicates. The effect of IR was eliminated by normalizing to negative controls that received IR, which allowed us to evaluate the enhanced effects of compounds with IR. If a compound showed identical viability in the absence and presence of IR, there would be no enhanced effect. If a compound in the IRpos group showed decreased viability compared to compound alone at the same concentration, potential radiosensitizing effect would be identified. Therefore, potential radiosensitization was determined by the difference between IRpos and IRneg NPI values gathered for each compound, for all tested conditions (three cell lines, three concentrations and three replicates). We then compared the distribution of the difference values of a compound to the distribution of the difference values of the negative controls. The comparison was done using the Wilcoxon test. The resulting *p*-value was corrected for multiple testing using the Benjamini-Hochberg method. Adjusted *p*-values ≤ 0.1 were considered significant.

All other analyses, such as compound potency determination, were performed using Graphpad Prism version 6.0h. Normalized data were fitted using nonlinear regression dose-response curves. To calculate the absolute IC_{50} from the fitted curve we determined the interpolation of Y = 0.5 with the corresponding X-value of the curve. We determined ratios to define the enhanced effect of combined treatments. The radiation enhancement ratio (RER) was defined as: IC_{50} (drug alone) / IC_{50} (drug + 4 Gy IR); with a RER value of > 1 being indicative for radiosensitization. The combined enhancement ratio (CER) was defined as: IC_{50} (olaparib + 2 μM GSK635416A) / IC_{50} (olaparib + 2 μM GSK635416A + 4 Gy IR).

ACKNOWLEDGMENTS

The authors are grateful for the kind gift of the HNSCC cell lines by Prof. dr R. Grenman. We thank Anass Znabet for the SAR-chemistry support and Ilana Berlin for her critical reading of the manuscript. This work was supported by the Riki Foundation awarded to CZ and MB, and by a NWO TOP grant awarded to JN and HO.

REFERENCES

1 Stewart, B. W. & Wild, C. P. World Cancer Report 2014. *WHO*, 609-625 (2014).

2 Pulte, D. & Brenner, H. Changes in survival in head and neck cancers in the late 20th and early 21st century: a period analysis. *The oncologist* **15**, 994-1001, doi:10.1634/theoncologist.2009-0289 (2010).

3 Surveillance, Epidemiology, and End Results Program. Cancer of the Larynx - SEER fact sheets. https://seer.cancer.gov/statfacts/html/laryn.html.

4 Surveillance, Epidemiology, and End Results Program. Cancer of the Larynx - SEER fact sheets. https://seer.cancer.gov/statfacts/htl/oralcav.html.

5 Al-Sarraf, M. Treatment of locally advanced head and neck cancer: Historical and critical review. *Cancer Control* **9**, 387-399 (2002).

6 Pignon, J. P., le Maitre, A., Maillard, E., Bourhis, J. & Group, M.-N. C. C. Meta-analysis of chemotherapy in head and neck cancer (MACH-NC): an update on 93 randomised trials and 17,346 patients. *Radiotherapy and oncology: journal of the European Society for Therapeutic Radiology and Oncology* **92**, 4-14, doi:10.1016/j.radonc.2009.04.014; 10.1016/j.radonc.2009.04.014 (2009).

7 Adelstein, D. J. *et al.* An intergroup phase III comparison of standard radiation therapy and two schedules of concurrent chemoradiotherapy in patients with unresectable squamous cell head and neck cancer. *Journal of clinical oncology: official journal of the American Society of Clinical Oncology* **21**, 92-98, doi:10.1200/JCO.2003.01.008 (2003).

8 Bonner, J. A. *et al.* Radiotherapy plus cetuximab for locoregionally advanced head and neck cancer: 5-year survival data from a phase 3 randomised trial, and relation between cetuximab-induced rash and survival. *Lancet Oncol* **11**, 21-28, doi:10.1016/S1470-2045(09)70311-0 (2010).

9 Magrini, S. M. *et al.* Cetuximab and Radiotherapy Versus Cisplatin and Radiotherapy for Locally Advanced Head and Neck Cancer: A Randomized Phase II Trial. *J Clin Oncol* **34**, 427-435, doi:10.1200/JCO.2015.63.1671 (2016).

10 Gyawali, B., Shimokata, T., Honda, K. & Ando, Y. Chemotherapy in locally advanced head and neck squamous cell carcinoma. *Cancer Treat Rev* **44**, 10-16, doi:10.1016/j.ctrv.2016.01.002 (2016).

11 Senra, J. M. *et al.* Inhibition of PARP-1 by olaparib (AZD2281) increases the radiosensitivity of a lung tumor xenograft. *Mol Cancer Ther* **10**, 1949-1958, doi:10.1158/1535-7163.MCT-11-0278 (2011).

12 Powell, C. *et al.* Pre-clinical and clinical evaluation of PARP inhibitors as tumour-specific radiosensitisers. *Cancer Treat Rev* **36**, 566-575, doi:10.1016/j.ctrv.2010.03.003 (2010).

13 Nowsheen, S., Bonner, J. A. & Yang, E. S. The poly(ADP-Ribose) polymerase inhibitor ABT-888 reduces radiation-induced nuclear EGFR and augments head and neck tumor response to radiotherapy. *Radiother Oncol* **99**, 331-338, doi:10.1016/j.radonc.2011.05.084 (2011).

14 Chatterjee, P. *et al.* PARP inhibition sensitizes to low dose-rate radiation TMPRSS2-ERG fusion gene-expressing and PTEN-deficient prostate cancer cells. *PLoS One* **8**, e60408, doi:10.1371/journal.pone.0060408 (2013).

15 Macarron, R. *et al.* Impact of high-throughput screening in biomedical research. *Nat Rev Drug Discov* **10**, 188-195, doi:10.1038/nrd3368 (2011).

16 Zhang, N. *et al.* Concurrent cetuximab, cisplatin, and radiation for squamous cell carcinoma of the head and neck in vitro. *Radiother Oncol* **92**, 388-392, doi:10.1016/j.radonc.2009.04.019 (2009).

17 Dungey, F. A., Loser, D. A. & Chalmers, A. J. Replication-dependent radiosensitization of human glioma cells by inhibition of poly(ADP-Ribose) polymerase: mechanisms and therapeutic potential. *Int J Radiat Oncol Biol Phys* **72**, 1188-1197, doi:10.1016/j.ijrobp.2008.07.031 (2008).

18 Verhagen, C. V. *et al.* Extent of radiosensitization by the PARP inhibitor olaparib depends on its dose, the radiation dose and the integrity of the homologous recombination pathway of tumor cells. *Radiother Oncol* **116**, 358-365, doi:10.1016/j.radonc.2015.03.028 (2015).

19 Vendetti, F. P. *et al.* The orally active and bioavailable ATR kinase inhibitor AZD6738 potentiates the anti-tumor effects of cisplatin to resolve ATM-deficient non-small cell lung cancer in vivo. *Oncotarget* **6**, 44289-44305, doi:10.18632/oncotarget.6247 (2015).

20 Sankunny, M. *et al.* Targeted inhibition of ATR or CHEK1 reverses radioresistance in oral squamous cell carcinoma cells with distal chromosome arm 11q loss. *Genes Chromosomes Cancer* **53**, 129-143, doi:10.1002/gcc.22125 (2014).

21 O'Connor, M. J. Targeting the DNA Damage Response in Cancer. *Mol Cell* **60**, 547-560, doi:10.1016/j.molcel.2015.10.040 (2015).

22 Lord, C. J. & Ashworth, A. The DNA damage response and cancer therapy. *Nature* **481**, 287-294, doi:10.1038/nature10760 (2012).

23 Raleigh, D. R. & Haas-Kogan, D. A. Molecular targets and mechanisms of radiosensitization using DNA damage response pathways. *Future Oncol* **9**, 219-233, doi:10.2217/fon.12.185 (2013).

24 Weber, A. M. & Ryan, A. J. ATM and ATR as therapeutic targets in cancer. *Pharmacol Ther* **149**, 124-138, doi:10.1016/j.pharmthera.2014.12.001 (2015).

25 Curtin, N. J. DNA repair dysregulation from cancer driver to therapeutic target. *Nat Rev Cancer* **12**, 801-817, doi:10.1038/nrc3399 (2012).

26 Goldstein, M. & Kastan, M. B. The DNA damage response: implications for tumor responses to radiation and chemotherapy. *Annu Rev Med* **66**, 129-143, doi:10.1146/annurev-med-081313-121208 (2015).

27 Min, J. *et al.* Optimization of a Novel Series of Ataxia-Telangiectasia Mutated Kinase Inhibitors as Potential Radiosensitizing Agents. *J Med Chem* **59**, 559-577, doi:10.1021/acs.jmedchem.5b01092 (2016).

28 Javle, M. & Curtin, N. J. The role of PARP in DNA repair and its therapeutic exploitation. *Br J Cancer* **105**, 1114-1122, doi:10.1038/bjc.2011.382 (2011).

29 Guleria, A. & Chandna, S. ATM kinase: Much more than a DNA damage responsive protein. *DNA Repair (Amst)* **39**, 1-20, doi:10.1016/j.dnarep.2015.12.009 (2016).

30 Bryant, H. E. *et al.* Specific killing of BRCA2-deficient tumours with inhibitors of poly(ADP-ribose) polymerase. *Nature* **434**, 913-917, doi:10.1038/nature03443 (2005).

31 Wurster, S. *et al.* PARP1 inhibition radiosensitizes HNSCC cells deficient in homologous recombination by disabling the DNA replication fork elongation response. *Oncotarget* **7**, 9732-9741, doi:10.18632/oncotarget.6947 (2016).

32 Kreimer, A. R., Clifford, G. M., Boyle, P. & Franceschi, S. Human papillomavirus types in head and neck squamous cell carcinomas worldwide: a systematic review. *Cancer Epidemiol Biomarkers Prev* **14**, 467-475, doi:10.1158/1055-9965.EPI-04-0551 (2005).

33 Zhou, G., Liu, Z. & Myers, J. N. TP53 Mutations in Head and Neck Squamous Cell Carcinoma and Their Impact on Disease Progression and Treatment Response. *J Cell Biochem* **117**, 2682-2692, doi:10.1002/jcb.25592 (2016).

34 Pekkola-Heino, K., Jaakkola, M., Kulmala, J. & Grenman, R. Comparison of cellular radiosensitivity between different localizations of head and neck squamous-cell carcinoma. *J Cancer Res Clin Oncol* **121**, 452-456 (1995).

35 Pekkola-Heino, K., Servomaa, K., Kiuru, A. & Grenman, R. Increased radiosensitivity is associated with p53 mutations in cell lines derived from oral cavity carcinoma. *Acta Otolaryngol* **116**, 341-344 (1996).

36 de Jong, M. C. *et al.* Pretreatment microRNA Expression Impacting on Epithelial-to-Mesenchymal Transition Predicts Intrinsic Radiosensitivity in Head and Neck Cancer Cell Lines and Patients. *Clin Cancer Res* **21**, 5630-5638, doi:10.1158/1078-0432.CCR-15-0454 (2015).

37 Lansford, C. D. *et al.* in *Human Cell Culture Vol 2, Cancer Cell Lines Part 2* (eds John R.W. Masters & B Palsson) 185-255 (Kluwer Academic Publishers, 1999).

38 Voorhoeve, P. M. & Agami, R. The tumor-suppressive functions of the human INK4A locus. *Cancer Cell* **4**, 311-319 (2003).

39 Drewry, D. H., Willson, T. M. & Zuercher, W. J. Seeding collaborations to advance kinase science with the GSK Published Kinase Inhibitor Set (PKIS). *Curr Top Med Chem* **14**, 340-342 (2014).

40 Christopher, J. A. *et al.* The discovery of 2-amino-3,5-diarylbenzamide inhibitors of IKK-alpha and IKK-beta kinases. *Bioorg Med Chem Lett* **17**, 3972-3977, doi:10.1016/j.bmcl.2007.04.088 (2007).

41 Franken, N. A., Rodermond, H. M., Stap, J., Haveman, J. & van Bree, C. Clonogenic assay of cells in vitro. *Nat Protoc* **1**, 2315-2319, doi:10.1038/nprot.2006.339 (2006).

42 Boutros, M., Bras, L. P. & Huber, W. Analysis of cell-based RNAi screens. *Genome Biol* **7**, R66, doi:10.1186/gb-2006-7-7-R66 (2006).

SUPPLEMENTAL DATA

Supplementary Table S1. Results from validation of the 17 leading candidates

Compound	All.IRneg. Mean	All.IRpos. Mean	All.Diff. Mean	All.Diff. w.pval	All.Diff. w.padj
GSK635416A	0.917	0.720	**−0.197**	0.000	0.000
SB-698596-AC	0.654	0.554	**−0.100**	0.000	0.000
GSK619487A	0.654	0.573	**−0.081**	0.000	0.000
GW578748X	0.869	0.791	**−0.078**	0.010	0.026
GW781673X	0.722	0.647	**−0.076**	0.004	0.014
GW683134A	0.735	0.664	**−0.071**	0.004	0.014
SB-678557-A	0.774	0.706	**−0.068**	0.005	0.014
SB-675259-M	0.534	0.467	**−0.066**	0.005	0.014
GSK269962B	0.737	0.675	**−0.062**	0.001	0.006
GSK238063A	0.768	0.707	**−0.060**	0.002	0.009
GW620972X	0.636	0.597	**−0.039**	0.252	0.359
GW810576X	0.484	0.446	**−0.039**	0.341	0.439
GSK1007102B	0.381	0.344	**−0.038**	0.042	0.096
GSK238583A	0.725	0.692	**−0.034**	0.072	0.127
GW806290X	0.396	0.383	**−0.013**	0.230	0.345
GW771127A	0.816	0.809	**−0.007**	0.949	0.949
GSK571989A	0.307	0.341	**0.034**	0.802	0.830

GSK635416A significantly shows the largest mean difference between IRpos and IRneg for all variables (cell line, concentration, replicate) included. All.IRneg.Mean: the mean of normalized values of non-radiated compounds for all variables (UT-SCC-24a, UT-SCC-36, UT-SCC-40, 50 nM, 500 nM, 5 µM). All.IRpos.Mean: the mean of normalized values of radiated compounds for all variables. All.diff.Mean: the mean of all single difference values. Difference values were determined by subtracting IRpos from IRneg for every single variation. All.Diffw.pval: compare the distribution of all single difference values to the distribution of the difference values of the negative controls using the Wilcoxon test, and calculate a p-value. All.Diff.w.padj: the resulting p-value was corrected for multiple testing using the Benjamin-Hochberg method. Adjusted p-values ≤ 0.1 were considered significant.

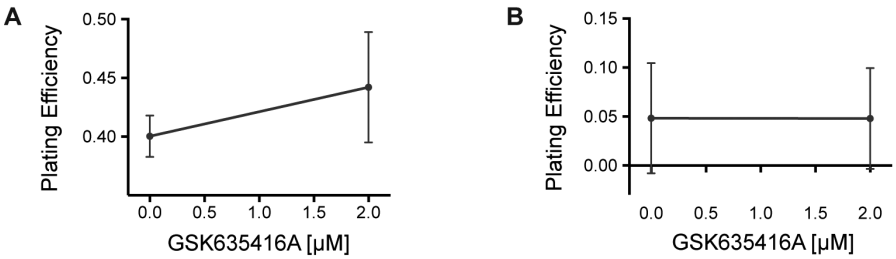

Supplementary Figure S1. GSK635416A cytotoxicity as determined with a colony forming assay. Plating efficiency did not decrease at 2 µM GSK635416A in UT-SCC-36 (**A**) and BJ-ET (**B**) cells. These results suggest that 2 µM GSK635416A does not affect clonogenic survival. (Data are shown as mean of three (UT-SCC-36) and five (BJ-ET) experiments, with SD.)

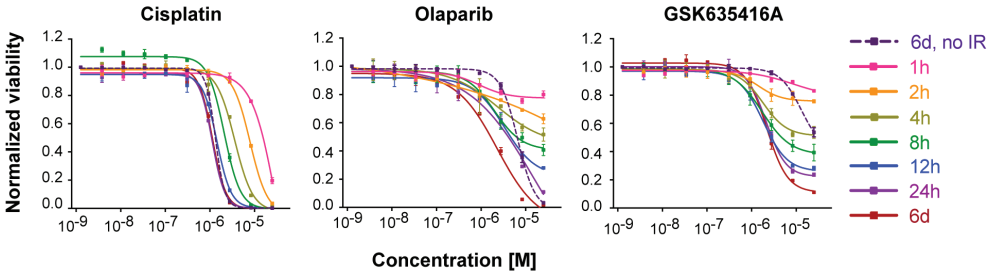

Supplementary Figure S2. Drug wash-out experiment in UT-SCC-36. At Day 1 UT-SCC-36 cells were treated for half an hour with cisplatin, olaparib or GSK635416A and subsequently irradiated with 4 Gy. At the indicated time points post irradiation, the drugs were removed by washing twice with medium. Data from cells treated with drug, but without IR, are plotted with a dash line. (Data are cell viability read-outs at day 7 and shown as mean of two independent experiments with SD).

A

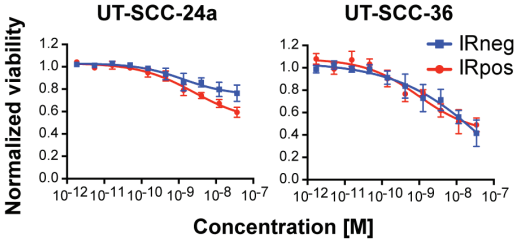

B

Cetuximab			
Inhibitor	IRneg	IRpos	RER
UT-SCC-24a	> 34	>34	1.00
UT-SCC-36	0.018	0.021	0.86

Supplementary Figure S3. Radiosensitizing properties of cetuximab. A, Dose-response curves of cetuximab in UT-SCC-24a and UT-SCC-36, measured with cell viability read-out at day 7. **B**, IC_{50} values (nM) for IRneg and IRpos were calculated from the corresponding dose-response curves and the RER was determined. (Data are shown as mean of three independent experiments, with SEM).

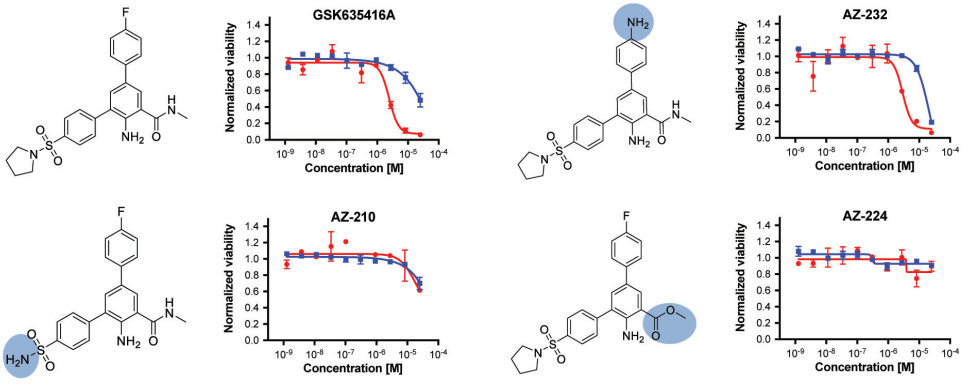

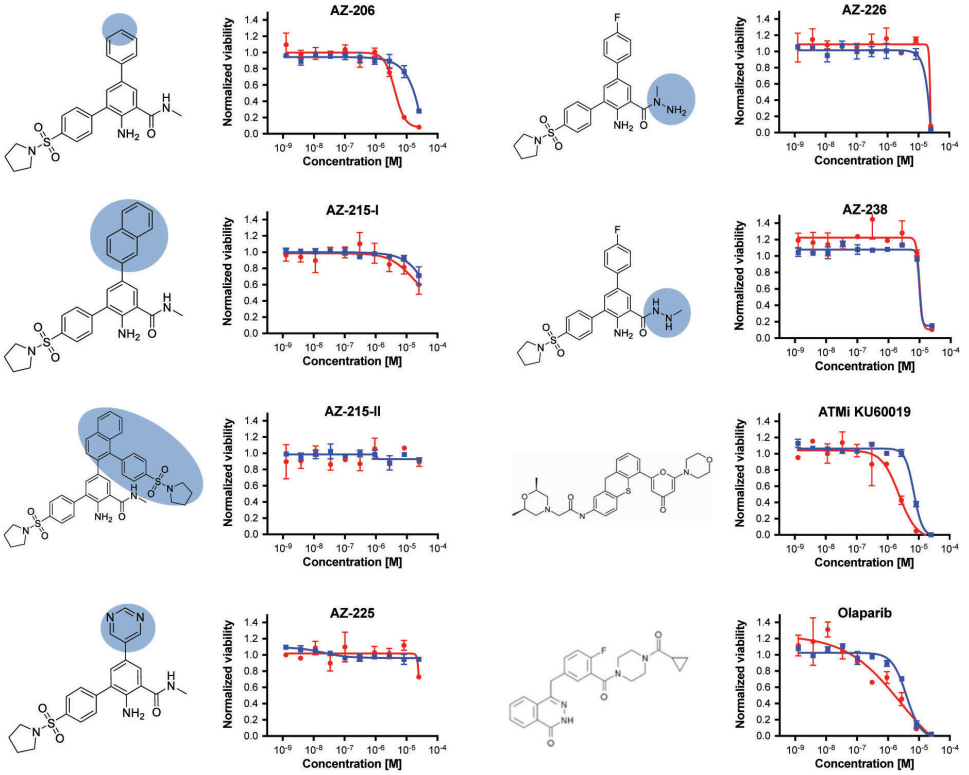

Supplementary Figure S4. Radiosensitizing effect of GSK635416A, 9 SAR-analogs, KU60019 and olaparib. Shown are dose-response curves of the compounds in the absence (IRneg, blue) and presence (IRpos, red) of 4 Gy radiation in UT-SCC-36. The IR-effect was eliminated by normalizing to negative controls that received IR. On the left side of the curves the chemical SAR-structures are shown. (Data shown as mean from one experiment, with two technical replicates, with SEM.)

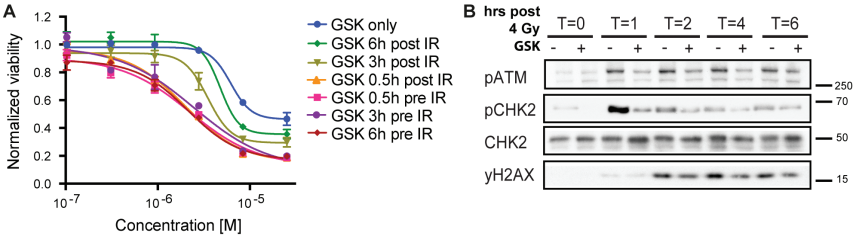

Supplementary Figure S5. GSK635416A targets the DNA damage response pathway. A, Tested timeframes of GSK635416A administration pre- and post-radiation in UT-SCC-24a. (Data shown are measured with cell viability read-out at day 7 and presented as mean of at least three independent experiments, with SEM.) **B**, Western blot of UT-SCC-24a, showing various proteins involved in the DDR pathway. Cells were treated with 4 Gy IR in the presence (+) or absence (-) of 2 µM GSK635416A, and subsequently harvested 0, 1, 2, 4 or 6 hours following treatment. Western blots are probed with antibodies detecting the proteins or phosphoproteins indicated. The position of molecular weight standards is indicated on the right side. A marked inhibition of the ATM pathway components is observed.

Supplementary Table S2. Results from competition binding assay with GSK635416A

A

#	Target Gene	%Ctrl at 10 µM GSK615416A	#	Target Gene	%Ctrl at 10 µM GSK615416A	#	Target Gene	%Ctrl at 10 µM GSK615416A
1	AAK1	96	153	FAK	100	305	PCTK2	92
2	ABL1(E155K)-phosphorylated	86	154	FER	94	306	PCTK1	100
3	ABL1(F317I)-nonphosphorylated	98	155	FES	83	307	PDGFRA	84
4	ABL1(F317I)-phosphorylated	89	156	FGFR1	100	308	PDGFRB	78
5	ABL1(F317L)-nonphosphorylated	97	157	FGFR2	89	309	PDPK1	84
6	ABL1(F317L)-phosphorylated	87	158	FGFR3	99	310	PFCDPK1(P.falciparum)	91
7	ABL1(H396P)-nonphosphorylated	83	159	FGFR3(G697C)	69	311	PFPK5(P.falciparum)	96
8	ABL1(H396P)-phosphorylated	95	160	FGFR4	100	312	PFTAIRE2	96
5	ABL1(M351T)-phosphorylated	94	161	FGR	87	313	FKK1	100
10	ABL1(Q252H)-nonphosphorylated	96	162	FLT1	94	314	PHKG1	100
11	ABL1(Q252H)-phosphorylated	89	163	FLT3	70	315	PHKG2	90
12	ABL1(T315I)-nonphosphorylated	92	164	FLT3(D835H)	85	316	PIK3C2B	100
13	ABL1(T315I)-phosphorylated	88	165	FLT3(D835V)	98	317	PIK3C2G	75
14	ABL1(Y253F)-phosphorylated	81	166	FLT3(ITD)	83	318	PIK3CA	100
15	ABL1-nonphosphorylated	84	167	FLT3(K663Q)	100	319	PIK3CA(C420R)	78
16	ABL1-phosphorylated	95	168	FLT3(N841I)	92	320	PIK3CA(E542K)	84
17	ABL2	100	169	FLT3(R834Q)	94	321	PIK3CA(E545A)	81
18	ACVR1	100	170	FLT3-autoinhibited	69	322	PIK3CA(E545K)	83
19	ACVR1B	100	171	FLT4	85	321	PIK3CA(H1047L)	97
20	ACVR2A	90	172	FRK	88	324	PIK3CA(H1047Y)	100
21	ACVR2B	100	173	FYN	100	325	PIK3CA(I800L)	100
22	ACVRL1	89	174	GAK	99	326	PIK3CA(M1043I)	69
23	ADCK3	98	175	GCN2(Kin.Dom.2,S808G)	79	327	PIK3CA(Q546K)	79
24	ADCK4	98	176	GRK1	98	328	PIK3CB	76
25	AKT1	84	177	GRK4	82	329	PIK3CD	98
26	AKT1	84	178	GRK7	100	330	PIK3CG	98
27	AKT3	99	179	G5K3A	94	331	PIK4CB	96
28	ALK	69	180	G5K3B	73	332	PIM1	77
29	ALK(C1156Y)	71	181	HASPIN	100	333	PIM2	72
30	ALK(L1196M)	74	182	HCK	100	334	PIM3	85
31	AMPK-alpha1	100	183	HIPK1	96	335	PIP5K1A	100
32	AMPK-alpha2	77	184	HIPK2	93	336	PIP5K1C	96
33	ANKK1	75	185	HIPK3	97	337	PIP5K2B	100
34	ARK5	74	186	HIPK4	93	338	PIP5K2C	100
35	ASK1	92	187	HPK1	93	339	PKAC-alpha	82
36	ASK2	75	188	HUNK	89	340	PKAC-beta	97
37	AURKA	76	189	ICK	89	341	PKMVT1	99
38	AURKB	88	190	IGF1R	96	342	PKN1	100
39	AURKC	68	191	IKK-alpha	81	343	PKN2	83
40	AXL	58	192	IKK-beta	100	344	PKNB(M.tuberculosis)	78
41	BIKE	77	193	IKK-epsilon	84	345	PLK1	100
42	BLK	100	194	INSR	90	346	PLK2	74
43	BMPR1A	97	195	INSRR	91	347	PLK3	76
44	BMPR1B	82	196	IRAK1	82	348	PLK4	87
45	BMPR2	88	197	IRAK3	95	349	PRKCD	100
46	BMX	92	198	IRAK4	100	350	PRKCE	95
47	BRAF	96	199	ITK	98	351	PRKCH	77
43	BRAF(V600E)	85	200	JAK1(JH1domain-catalytic)	91	352	PRKCI	98
49	BRK	95	201	JAK1 (JH2domain-pseudokinase)	100	353	PRKCQ	72
50	BRSK1	100	202	JAK2 (JH1domain-catalytic)	100	354	PRKD1	94
51	BRSK2	95	203	JAK3 (JH1domain-catalytic)	94	355	PRKD2	82
52	BTK	98	204	JNK1	97	356	PRKD3	100
53	BUB1	83	205	JNK2	79	357	PRKG1	91
54	CAMK1	94	206	JNK3	91	358	PRKG2	95
55	CAMK1D	100	207	KIT	80	359	PRKR	74
56	CAMK1G	95	208	KIT(A829P)	94	360	PRKX	98
57	CAMK2A	98	209	KIT(D816H)	96	361	PRP4	76
58	CAMK2B	100	210	KIT(D816V)	97	362	PYK2	95
59	CAMK2D	96	211	KIT(L576P)	82	361	QSK	66
60	CAMK2G	86	212	KIT(V559D)	77	364	RAF1	100
61	CAMK4	92	213	KIT(V559D,T670I)	77	365	RET	80
62	CAMKK1	89	214	KIT(V559D,V654A)	90	366	RET(M918T)	83
63	CAMKK2	94	215	KIT-autoinhibited	100	367	RET(VS04L)	88
64	CASK	100	216	LATS1	97	368	RET(V804M)	100
65	CDC2L1	95	217	LATS2	83	369	RIOK1	81
66	CDC2L2	100	218	LCK	95	370	RIOK1	78
67	CDC2L5	97	219	LIMK1	100	371	RIOK1	86
68	CDK11	100	220	LIMK2	100	372	RIPK1	91
69	CDK2	100	221	LKB1	100	373	RIPK2	100
70	CDK3	98	222	LOK	100	374	RIPK4	91
71	CDK4-cyclinD1	97	223	LRRK2	100	375	RIPK5	73
72	CDK4-cyclinD3	95	224	LRRK2(G2019S)	92	376	ROCK1	99
73	CDK5	70	225	LTK	100	377	ROCK2	100
74	CDK7	92	216	LYN	94	378	ROS1	90
75	CDK8	58	227	LZK	88	379	RPS6KA4(Kin.Dom.1-N-terminal)	93

#	Target Gene	%Ctrl at 10 µM GSK615416A
76	CDK9	89
77	CDKL1	98
78	CDKL2	73
79	CDKL3	100
80	CDKL5	88
81	CHEK1	100
82	CHEK2	85
83	CIT	97
84	CLK1	78
85	CLK2	100
86	CLK3	94
87	CLK4	76
88	CSF1R	82
89	CSF1R-autoinhibited	97
90	CSK	100
91	CSNK1A1	96
92	CSNK1A1L	100
93	CSNK1D	100
94	CSNK1E	77
95	CSNK1G1	96
96	CSNK1G2	84
97	CSNK1G3	90
98	CSNK2A1	88
99	CSNK2A2	56
100	CTK	78
101	DAPK1	100
102	DAPK2	83
103	DAPK3	96
104	DCAMKL1	76
105	DCAMKL2	100
106	DCAMKL3	100
107	DDR1	100
108	DDR2	83
109	DLK	98
110	DMPK	100
111	DMPK2	78
112	DRAK1	100
113	DRAK2	98
114	DYRK1A	76
115	DYRK1B	88
116	DYRK2	88
117	EGFR	69
118	EGFR(E746-A750del)	75
119	EGFR(G719C)	99
120	EGFR(G719S)	97
121	EGFR(L747-E749del, A750P)	66
122	EGFR(L747-S752del, P753S)	66
123	EGFR(L747-T751del,Sins)	71
124	EGFR(L858R)	68
125	EGFR(L858R,T790M)	84
126	EGFR(L861Q)	86
127	EGFR(S752-1759del)	68
128	EGFR(T790M)	100
129	EIF2AK1	73
130	EPHA1	71
131	EPHA2	81
132	EPHA3	93
133	EPHA4	95
134	EPHA5	66
135	EPHA6	90
136	EPHA7	100
137	EPHA8	98
138	EPHB1	100
139	EPHB2	89
140	EPHB3	91
141	EPHB4	84
142	EPHB6	72
143	ERBB2	99
144	ERBB3	100
145	ERBB4	100
146	ERK1	98
147	ERK2	68
148	ERK3	85
149	ERK4	98
150	ERK5	100
151	ERK8	82
152	ERN1	100
228	MAK	100
229	MAP3K1	93
230	MAP3K15	70
231	MAP3K2	84
232	MAP3K3	96
233	MAP3K4	73
234	MAP4K2	103
235	MAP4K3	103
236	MAP4K4	89
237	MAP4K5	88
238	MAPKAPK2	89
239	MAPKAPK5	94
240	MARK1	100
241	MARK2	86
242	MARK3	85
243	MARK4	100
244	MAST1	97
245	MEK1	96
246	MEK2	92
247	MEK3	92
248	MEK4	100
249	MEK5	82
250	MEK6	94
251	MELK	93
252	MERTK	96
253	MET	100
254	MET(M1250T)	96
255	MET(Y1235D)	92
256	MINK	82
257	MKK7	71
258	MKNK1	61
259	MKNK2	83
260	MLCK	100
261	MLK1	103
262	MLK2	103
263	MLK3	86
264	MRCKA	100
265	MRCKB	94
266	MST1	100
267	MST1R	100
268	MST2	71
269	MST3	77
270	MST4	84
271	MTOR	100
272	MUSK	84
273	MYLK	80
274	MYLK2	103
275	MYLK4	96
276	MY03A	94
277	MY03B	94
278	NDR1	66
279	NDR2	65
280	NEK1	95
281	NEK10	100
282	NLK11	93
283	NEK2	98
284	NEK3	67
285	NEK4	90
286	NEKS	77
287	NEK6	76
288	NEK7	100
289	NEK9	99
290	NIK	81
291	NIM1	97
292	NLK	100
293	OSR1	78
294	p38-alpha	94
295	938-beta	88
296	p38-delta	100
297	p38-gamma	82
298	PAK1	103
299	PAK2	100
300	PAK3	98
301	PAK4	83
302	PAK6	100
303	PAK7	92
304	PCTK1	96
380	RPS6KA4(Kin.Dom.2-C-terminal)	80
381	RPS6KA5(Kin.Dom.1-N-terminal)	80
382	RPS6KAS(Kin.Dom.2-C-termiinal)	66
383	RSK1(Kin.Dom.1-N-terminal)	93
384	RSK1(Kin.Dom.2-C-terminal)	100
385	RSK2(Kin.Dom.1-N-terminal)	87
386	RSK2(Kin.Dom.2-C-terminal)	100
387	RSK3(Kin.Dom.1-N-terminal)	97
388	RSK3(Kin.Dom.2-C-terminal)	100
389	RSK4(Kin.Dom.1-N-terminal)	100
390	R5K4(Kin.Dom.2-C-terminal)	92
391	S6K1	96
392	SBK1	81
393	SGK	83
394	Sgk110	96
395	SGK2	62
396	SGK3	69
397	SIK	83
398	SIK2	100
339	SLK	97
400	SNARK	77
401	SNRK	81
402	SRC	86
403	SRMS	87
404	SRPK1	92
405	SRPK2	91
406	SRPK3	100
407	STK16	98
408	STK33	100
409	STK35	100
410	STK36	99
411	STK39	98
412	SYK	100
413	TAK1	96
414	TAOK1	99
415	TAOK2	87
416	TAOK3	92
417	TBK1	95
418	TEC	100
419	TESK1	85
420	TGFBR1	94
421	TGFBR2	98
422	TIE1	100
423	TIE2	100
424	TLK1	100
425	TLK2	86
426	TNIK	100
427	TNK1	100
428	TNK2	100
429	TNNI3K	99
430	TRKA	98
431	TRKB	100
432	TRKC	100
433	TRPM6	80
434	TSSK1B	94
435	TTK	100
436	TXK	82
437	TYK2(JH1domain-catalytic)	91
438	TYK2(JH2domain-pseudokinase)	84
439	TYRO3	100
440	ULK1	59
441	ULK2	100
442	ULK3	96
443	VEGFR2	64
444	VRK2	68
445	WEE1	100
446	WEE2	96
447	WNK1	77
448	WNK3	84
449	VANK1	80
450	VANK2	73
451	YANK3	83
452	YES	100
453	YSK1	93
454	YSK4	100
455	ZAK	72
456	ZAP70	100

B

Compound	Selectivity score type	Number of hits	Number of non-mutant kinases	Screening concentration (nM)	Selectivity score
GSK635416A	S(35)*	0	**395**	10000	0
GSK635416A	S(10)*	0	**395**	10000	0
GSK635416A	S(1)*	0	**395**	10000	0

Competition binding assay to quantitatively measure interactions between GSK635416A and 456 human kinases and disease relevant mutant. **A**. *The binding interactions are reported as '% Ctrl', where lower numbers (preferably between <0.1% and 35%) indicate stronger hits. Our % Ctrl results revealed no hits (average % Ctrl = 90, range 56 – 100).* **B**, *Selectivity Score results showed no hits as well.*
**S(35) = (number of non-mutant kinases with %Ctrl < 35)/(number of non-mutant kinases tested)*
**S(10) = (number of non-mutant kinases with %Ctrl < 10)/(number of non-mutant kinases tested)*
**S(1) = (number of non-mutant kinases with %Ctrl < 1)/(number of non-mutant kinases tested)*

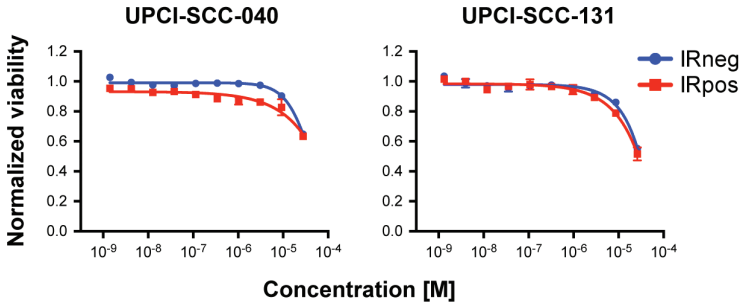

Supplementary Figure S6. Loss of GSK635416A-mediated radiosensitization in ATM deficient HNSCC cell lines, namely UPCI-SCC-040 and UPCI-SCC-131 as indicated. Cells were radiated with 2.5 Gy, IRpos, and compared to non-radiated plates, IRneg. (Data shown are collected form cell viability read-outs at day 7 and shown as mean of two independent experiments with SD).

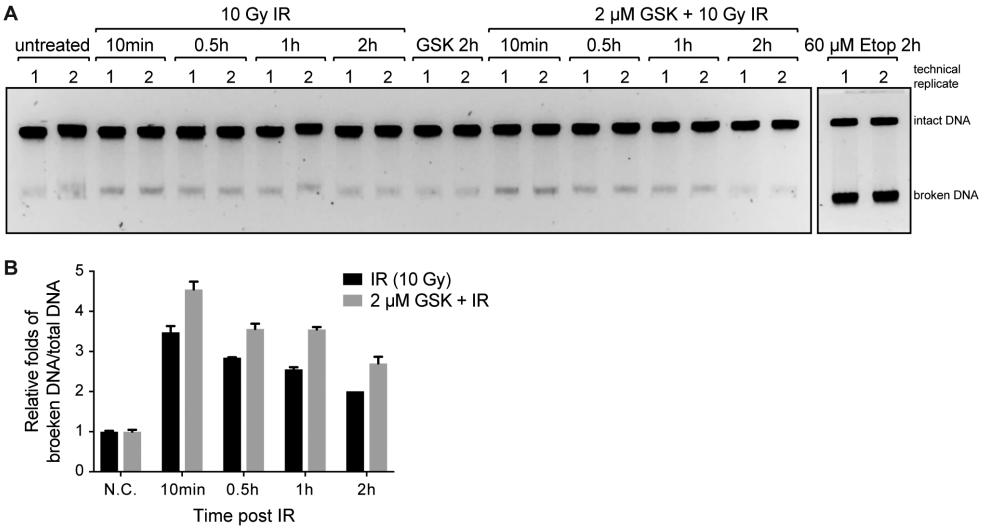

Supplementary Figure S7. Constant-field gel electrophoresis data show increased radiation induced DNA damage in the presence of GSK635416A. A, Constant-field gel electrophoresis in UT-SCC-36 cells, collected at the indicated time points post 10 Gy IR in the presence and absence of 2 μM GSK635416A. Lower bands represent the broken DNA and the top bands the intact DNA. **B**, Quantification of the broken DNA relative to intact DNA after scanning the gel, followed by calculation with ImageJ. (Data shown is a representative figure of two independent experiments).

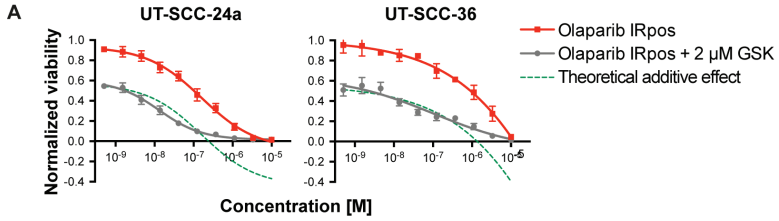

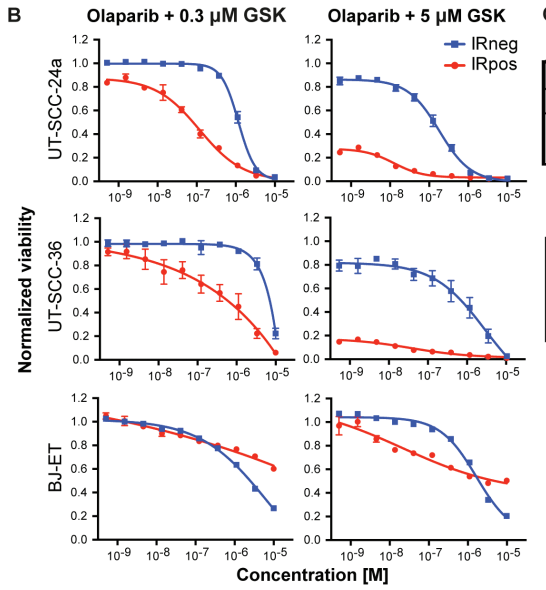

C

UT-SCC-24a			
Inhibitor	**IRneg**	**IRpos**	**CER**
Olaparib + 0.3 μM GSK	1.131	0.072	15.71
Olaparib + 5 μM GSK	0.129	< 0.0005	258.00

UT-SCC-36			
Inhibitor	**IRneg**	**IRpos**	**CER**
Olaparib + 0.3 μM GSK	6.873	0.503	13.66
Olaparib + 5 μM GSK	0.641	< 0.0005	1,282.00

BJ-ET			
Inhibitor	**IRneg**	**IRpos**	**CER**
Olaparib + 0.3 μM GSK	2.463	79.035	0.03
Olaparib + 5 μM GSK	1.811	3.107	0.58

Supplementary Figure S8. Radiosensitization by combining GSK635416A with olaparib. A, This figure is related to the dose response curves in Figure 5 and includes an additional theoretical line that plots the calculated (in contrast to the tested) effect of 2 μM GSK635416A in combination with olaparib and IR, assuming additivity. The same IRpos of olaparib and olaparib + 2 μM GSK635416A from Figure 5 is plotted. The dotted theoretical line depicts the additional effect of 2 μM GSK635416A at data point 0.5 nM olaparib (lowest concentration). This effect was subtracted from every data point of the 'Olaparib IRpos' curve, creating the parallel dotted theoretical line. This calculated line is similar to the 'Olaparib IRpos + 2 μM GSK635416A' curve, suggesting an additive effect. **B**, Shown on the left are the dose-response curves of olaparib in the constant presence of 0.3 or 5 μM GSK635416A in UT-SCC-24a, UT-SCC-36 and BJ-ET. Depicted on the right (**C**) are the corresponding calculated IC_{50} values (μM) for IRneg and IRpos and the determined RER. The figure shows that GSK635416A should be included at proper concentrations as 0.3 μM GSK635416A did not show an additive effect when compared to olaparib alone (see Figure 5). The combination of 5

μM GSK635416A with olaparib has increased radiosensitization effects when compared to olaparib as a single drug in Figure 5. (Data are shown as mean of three to five independent experiments, with SEM).

SUPPLEMENTAL MATERIALS AND METHODS

Competition binding assay

GSK635416A was send to DiscoveRx UK for MAX KINOMEscan analysis. This scan included 456 human kinases and disease relevant mutant variants. GSK635416A was screened at 10 μM. A percentage of control ([test compound signal – positive control signal]/[negative control signal – positive control signal] *100) was determined for every kinase. Lower %Ctrl were associated with tighter binding. A Selectivity Score, excluding mutant variants, was determined as a quantitative measure of compound selectivity. This was calculated by dividing the number of kinases with affinity for the compound, by the total number of distinct kinases tested.

Cell culture

UPCI-SCC-040 and UPCI-SCC-131 (DSMZ, Germany) were cultured in MEM supplemented with FBS, L-glutamine and non-essential amino acids, at 37˚C under 5% CO_2.

Constant-field gel electrophoresis

To directly detect DNA double-strand breaks induced by IR or by the combination of IR and GSK635416A, DNA from UT-SCC-36 cells was analyzed by Constant-field gel electrophoresis [1] was performed on UT-SCC-36 cells. Cells were collected at various indicated time points post 10 Gy IR in the presence and absence of 2 μM GSK635416A. Cells exposed to 2 μM GSK635416A were first treated for 0.5 hour and consequently irradiated with 10 Gy. 2 h cell exposure to 60 μM Etoposide served as a positive control for drug induced DNA breaks. Quantification of the broken DNA was done with ImageJ. The percentage of broken DNA was normalized to untreated (N.C., negative control) samples.

REFERENCES

1. Wlodek D, Banath J, Olive PL. Comparison between pulsed- field and constant-field gel electrophoresis for measurement of DNA double-strand breaks in irradiated Chinese hamster ovary cells. Int J Radiat Biol. 1991; 60:779–90.

CHAPTER 7

Summary and general discussion

SUMMARY AND GENERAL DISCUSSION

This thesis describes a significant translational step forward in the improvement of the prognosis of advanced head and neck squamous cell carcinoma (HNSCC) patients. In an effort to achieve higher survival rates with decreased morbidity, we aimed to optimize a predictive preclinical patient-derived tumor culture model and we aimed to identify novel radiosensitizers that are specific for cancer cells.

Chapter 1 provides a general introduction into cancer development, the current state of HNSCC treatment and prognosis and stating the background of our research questions. 70% of HNSCC patients are diagnosed with an advanced stage disease at presentation (stage III or IV). They are treated with multi-modality approaches including a combination of chemotherapy (CT), radiotherapy (RT) and surgery. Despite these treatments, the prognosis of these patients is relatively poor due to a high local recurrence rate or development of a second primary tumor. Cisplatin and cetuximab CT are usually combined with concurrent RT (CRT) to improve survival outcome. However, the survival benefit of CRT in comparison to RT alone, is low; while patients do endure a substantial increase in toxicity in case of CRT. Furthermore, the currently available treatments result in a great variety in clinical outcome, illustrating the significant intrinsic sensitivity variability of individual tumors to anti-cancer treatment. Currently, it is impossible to predict - prior to treatment - which patient is likely to respond to the intended treatment regimen, as there are no reliable individual predictive biomarkers available. The above-mentioned problems of a poor prognosis, high toxicity and a heterogenous interpatient treatment response has led to our principal thesis goals.

Part I: Preclinical fresh tumor histoculture models of HNSCC

The goal of this thesis part is to search for the best performing preclinical, patient-derived, short-term fresh tumor culture model. There is a critical need for such a model to assist in individualized treatment decision-making, prior to therapy, enabling to identify patients who will (or will not) respond to their intended treatment regimen. Furthermore, ideally, this model could also be used for future testing of potential novel drugs. It seems essential for such a model to mimic the original tumor as closely as possible, thereby maintaining tumor heterogeneity and the tumor microenvironment (TME), in order to reliably translate *in vitro* findings to clinical results in patients.

In Chapter 2, we summarized literature concerning preclinical HNSCC culture model systems, including cancer cell lines, *in vivo* animal models and primary (freshly isolated

from human tissue) tumor cultures. The use of cancer cell lines has important advantages including their wide availability, ease of use, indefinite growth, low costs, well applicability in high-throughput screens and their suitability for genetic modification. However, this model also has critical limitations such as a monolayer flat growth and thereby loss of the normal 3D structure, the lack of a tumor microenvironment, selective growth and failure to phenotypically and genetically resemble the native tumor when passaged. When generating a cell line, usually only homogenous cell type grows out to form a cell line, while the original tumor is quite heterogeneous. This illustrates the difficulty for cancer cells to survive and adapt to *in vitro* conditions.[1] Besides these limitations, cell lines are an important and preferred starting point for assessing various cell biological mechanisms.

Animal experiments have the advantage of offering a culture model in which the TME and 3D structure is maintained, while also offering physiological conditions such as nutrients and blood supply. This provides the opportunity to investigate pharmacokinetics and toxicity of drugs. The use of mice models has also limitations. Mice share a highly similar set of genes compared to humans, however, gene expression is evolutionary substantially diverging between the two species. This is especially the case for immune-system-related genes, which have undergone more rapid evolution, resulting in extensive differences in the immune systems of humans and mice.[2] Additionally, mice primarily develop cancers in mesenchymal tissue (lymphomas, sarcomas) while cancers in humans are of epithelial origin (carcinomas). Furthermore, mice have a distinct, higher metabolism resulting in a shorter life span.[1] These differences impact the predictive value of this model. Successful translation from results in animal models to results in clinical trials remains challenging and as little as 8% of animal tested drugs pass phase I trials.[3-5]

Primary tumor cultures (summarized in Chapter 2 and investigated in Chapter 3) include models culturing fresh primary human tumor tissue, like the cell-adhesive matrix assay, soft-agar clonogenic assay, histocultures, spheroids and organoids. Primary cultures that reflect the tumor *in vivo* and its microenvironment more closely are preferred. In our review, Chapter 3, we found that the most successful culture rates and best correlation to clinical response were reported with the sponge-gel-supported histoculture model, often used in the histoculture drug response assay (HDRA). This histoculture model has the benefit of better representing the tumor and its microenvironment, mostly because it does not involve enzymatic tissue disaggregation, thereby preserving cell heterogeneity, cell-cell interactions and the 3D tissue architecture. Furthermore, this model has the ability to mimic the human situation as closely as possible since the tumor fragments are cultured on a sponge partly drenched in medium and partly exposed and surrounded by air, thereby simulating the air-mucosa interface of tumor growth in head and neck cancer.

These above-mentioned characteristics of the sponge-gel-supported histoculture model probably explains the high overall culture success rates reported in literature, ranging from 88% to 100%, with culture durations varying from 2 to 11 days. Additionally, a good correlation between *in vitro* chemosensitivity and clinical outcome was reported with positive predictive values of 69% to 90% and negative predictive values of 50% to 100%.

Encouraged by these data, we aimed to optimize the sponge-gel-supported histoculture model as a potential model for future drug testing and individualized medicine. Despite the promising reported results, this model is not used routinely in clinical practice yet. We hypothesized that, to improve this system, several aspects could be investigated and optimized. Firstly, it could be beneficial to use an immunohistochemistry (IHC) analysis, instead of a metabolic viability read-out. IHC enables a separate analysis of all cell types present. This, we thought, is important since we know that tumor cells and tumor stromal cells respond differently to drugs and irradiation (stromal cells are more resistant to cytostatic drugs and irradiation).[6-8] With IHC, one can also investigate the presence of tumor microenvironment cells, such as stromal cells and immune cells. It is reported that these cells can affect clinical treatment response.[9-11] Secondly, we tested various medium supplements to potentially further improve culture efficacy (viability, proliferation, culture success rate and clinical correlation). Hence, to test our, we cultured fresh tumor biopsies of 72, previously untreated, patients (Chapter 4). Biopsies from 57 patients (79%) were included for analysis, cut in small fragments (1451 fragments in total), cultured for 7 days and immunohistochemically scored for percentage of tumor, percentage of tumor viability and tumor proliferation, EGFR expression and presence of T-cells and macrophages. Firstly, we observed that both malignant, stroma and immune cells sustain during culture. The median tumor percentage increased from 53% at day 0 to 80% at day 7. Within these tumor cells, the viability and proliferation decreased after 7 days, from 90% to 30% and from 30% to 10%, respectively. Secondly, we showed that the addition of EGF, folic acid and hydrocortisone to the culture medium led to improved viability and proliferation. However, this phenomenon was not systematically observed. Thirdly, unfortunately, no patient subgroup could be identified with higher culture success rates. Interestingly, EGF supplementation did not increase viability and proliferation in patients' tumors overexpressing EGF-receptor. Overall, a wide heterogeneity in results was observed between patients' tumors and within individual patient tumor fragments. Therefore, no firm conclusions could be drawn. Nevertheless, in our opinion, this variety in results does reflect the known genetic tumor heterogeneity in HNSCC.[12]

With our study, we have tried to optimize the sponge-gel-supported histoculture model for HNSCC to allow predicting individual treatment responses and to allow future novel drug

testing to improve clinical outcome in our patients. However, regarding above-mentioned results, the question is to what extend this model could be used for drug testing? First of all, it may be that *in vivo* treatment response is still, despite our hypothesis, not dependent on the histologic characterization *in vitro*. After all, correlations between *in vitro* metabolic chemosensitivity and clinical outcome was successful in earlier studies.[13-16] However, their treatment *in vitro* did not resemble the clinical treatment regarding the specific drugs used and regarding the combination with RT. Furthermore, only small groups of patients were investigated with a very short follow-up. Second of all, it is yet unclear whether the heterogeneity of our results, even within single patient tumor biopsies, may or may not be troublesome for unambiguous interpretation of results and/or defining cut-offs for a potential correlation with clinical outcome in patients. Finally, the window for detecting differences in treatment response is relatively small. The median percentages of tumor, tumor viability and tumor proliferation at day 7 was 80%, 30% and 10%, respectively. Maybe, one is able to detect a difference between control/RPMI and a cytotoxic treatment, but one is probably not able to distinguish between various drug treatments and to select the most optimal treatment. Therefore, for future perspectives, the sponge-gel-supported histoculture model with IHC read-out could be further refined to test cisplatin CRT and correlate that to the response of CRT in the clinic, to see if we are able to correlate the results, and to see if we could identify and predict the patients that are prone to treatment response. However, testing novel drugs with this model, as a method between cell lines and mice experiments, will be difficult. We may be able to identify cytotoxic compounds, but comparison between them will be very hard.

A novel method is the *in vitro* formation of patient-derived tumor organoids. An organoid is developed from stem cells or organ progenitors, originating from a collection of multiple organ-specific cell types from fresh tumor tissue[17]. Organoid cultures have been established from esophagus, stomach, pancreas, liver, colon, prostate and breast cancer biopsy samples. An organoid develops and self-organizes to form an organ-like 3D tissue structure in a 3D matrix with properties as those *in vivo*.[17] For example, mini-guts can be formed with epithelial architecture of small intestine and colon. Organoids can be expanded, cryopreserved, genetically modified and they remain genetically and phenotypical stable.[18] This culture method allows for a wide range of application in cancer research.[18] For example, one can test drugs on normal and cancer organoids to see if there are cancer-specific drugs and one can test for intratumor heterogeneity. Regarding head and neck tissue, no primary HNSCC or normal HNSC organoids have been formed yet, only organoids of primary parotid pleomorphic adenoma[19] and primary normal parotid epithelial cells.[19-21] Intrinsic limitations of organoid cultures are the degradation of tumor

biopsies into single-cell-suspension by enzyme digestion, selection for usually one subclone and the exclusion of TME cells.[18,22]

In summary, all previous mentioned models, from cell lines, histocultures and organoids to mice models, only partly resemble the original tumor. It is impossible to display all *in vivo* human features in one model. However, all models represent valuable "bridge models" between the use of cell lines and clinical patient trials. Yet, histoculture of tumor fragments enables the most natural tumor environment. We think that our improved histoculture model could potentially be used to test treatment response and correlation to clinical response, as a potential future individual predictive model. However, regarding the heterogeneity of the tumors, which is reflected in our data, it will be difficult to draw usable conclusions.

Part II: Drug screens to identify novel radiosensitizers for HNSCC

The second part of this thesis focusses on our research goal regarding the improvement of clinical outcome and the reduction of high toxicity rates in advanced HNSCC patients, treated with the current (C)RT regimens. RT is a key component in the treatment of advanced HNSCC, however its efficacy can be limited by toxicity to normal tissues or resistance of tumor cells. Irradiation can be combined with 'radiosensitizers'. Radiosensitizers can achieve the same therapeutic effect while lowering the irradiation dose or they can enhance RT efficacy in resistant tumors. Improving survival rates while limiting toxicity can be achieved by a radiosensitizer that specifically targets cancer cells while not affecting normal tissue, known as the therapeutic window. To identify novel radiosensitizers we performed high-throughput drug screens of various compound libraries.

In Chapter 5, we describe the screening of three compound libraries, namely the FDA-approved Oncology Drugs set, the Roche kinase inhibitor library and the NKI DUB-targeted small molecule drug library. The screens were performed on several head and neck cancer cell lines (UT-SCC-24a, -36 and -40), in absence and presence of irradiation, with cell viability as outcome measurement. Potential compounds were compared to the currently used clinical chemotherapeutics for advanced HNSCC as cisplatin, cetuximab and olaparib in trial. From the FDA screen, the most distinct potential radiosensitizing effect was reached with rapamycin with radiation enhancement ratios (RERs) of 8.33 and 333.5, in comparison to RERs of 5.64 – 15.58 of olaparib. Besides rapamycin, raloxifene and tamoxifen (both selective estrogen receptor modulators, SERMs) were also identified as radiosensitizers (RER 1.51 – 1.65 and RER 1.23 – 1.54, respectively), but not as strong as olaparib.

Rapamycin (sirolimus) is an indirect inhibitor of mTORC1 activity, located downstream in the PI3K-Akt-mTOR pathway. This pathway is activated in most cancer types[23] as well as in HNSCC, where > 80% of the tumors have alterations in components of the EGFR-PI3K-Akt-mTOR pathway[24-28]. Besides rapamycin, first generation rapalogs (analogs of rapamycin: temsirolimus, everolimus and ridaforolimus) have been developed with improved pharmacokinetics and stability.[29] However, clinical application of rapalogs as monotherapy in cancer treatment is only limited and restricted to a few cancers due to their cytostatic rather than cytotoxic effect, as a result of incomplete inhibition of mTORC1 and inactivity against mTORC2, resulting in compensatory feedback loops.[29,30] Therefore, combination treatments are used and second/third generation mTOR inhibitors were developed with dual PI3K/mTOR targets or targeting mTOR directly (blocking both mTORC1 and mTORC2). *In vitro*, mTOR inhibitors are widely described as radiosensitizers in various cancers[31-39], also in head neck cancer[25,40,41]. *In vitro* and *in vivo* mice studies in lung and head and neck cancer cells showed cancer specific radiosensitization for rapamycin, and radioprotection in normal lung cells and oral keratinocytes[39,42]; suggesting low toxicities. In HNSCC patients, several phase I and II studies including mTOR inhibitors have been performed,[43-49] however only one phase I study reported on the combination with RT[50]. In this trial, 13 advanced HNSCC patients were treated with a combination of everolimus and concurrent cisplatin with RT. Two patients had recurrent disease and 1 patient died. The treatment combination appeared to be tolerable with acceptable toxicities: >30% of the patients had treatment-related adverse events of which lymphopenia (92%) and mucositis (62%) were the most common grade ≥3 adverse events. The 2-year progression-free survival was 85% and overall survival was 92%.
For future perspectives, we recommend further preclinical experiments that may result in a phase II/III trial combining an FDA-approved mTOR inhibitor+RT and compare this to cisplatin+RT, or olaparib+RT. It would be interesting to test novel dual PI3K/mTOR-inhibitors in combination with RT for HNSCC as well, first *in vitro* and *in vivo*.

The Roche screen and DUB screen did not detect potential compounds with increased radiosensitization efficacy when compared to cisplatin or olaparib. Interestingly, the preliminary FDA screen data without irradiation showed several compounds to outperform the drugs currently used for recurrent / metastatic HNSCC: cell viability of HNSCC cell lines decreased substantially when depsipeptide, bortezomib and idarubicin were administered, when compared to cisplatin, carboplatin, 5-fluorouracil, paclitaxel and methotrexate (cetuximab was not included in the library). Further *in vitro* and *in vivo* testing is needed to investigate whether these drugs could indeed serve as novel and more potent drugs for patients with recurrent / metastatic HNSCC in the future.

Chapter 6 addresses the screening of library 'GlaxoSmithKline Published Kinase Inhibitor Set' (GSK PKIS). This screen identified GSK635416A as a novel radiosensitizer (RER >7.67 - >11.57). The extent of radiosensitization by GSK635416A outperformed the radiosensitization observed with cisplatin (RER 1.28 – 1.51) and cetuximab (RER 0.86 and >1.00) and was equal or somewhat higher than olaparib (RER 7.10 – 11.56). A colony forming assay was done confirming the radiosensitizing activity of GSK635416A (DEF_{37} 1.99, ± SD: 0.19). In comparison with data in previous literature (DEF_{37} of 1.90 for cisplatin[51] and a DEF_{37} of 1.08-1.61 for olaparib[52-54]), the radiosensitization of GSK635416A is very promising. The radiosensitization was also observed in other HNSCC cell lines (UT-SCC-2 and -8) and in HeLa cervix and A549 lung cancer cell lines (RER: GSK635416A 1.49 – 9.23, cisplatin 1.10 – 1.62, olaparib 2.90 – 13.46). Of equivalent importance, GSK635416A showed significant lower cytotoxicity in the absence of irradiation and virtually no cytotoxicity in a normal fibroblast cell line (BJ-ET), when compared to cisplatin or olaparib. We claimed GSK635416A to be a novel ATM inhibitor as it increased DNA double strand breaks (DSBs) after irradiation, it inhibited the irradiation induced phosphorylation of ATM and its mediated radiosensitization was lacking in ATM-mutated cells.

After all our screening efforts, we were successful in identifying GSK635416A as a novel ATM inhibitor, with tumor-specific radiosensitization and limited cytotoxicity. This makes GSK635416A an ideal novel radiosensitizer to improve survival rates and reduce side effects in patients. Classified as an ATM-inhibitor, GSK635416A falls in a category of known radiosensitizers. ATM plays a central role in maintaining genome integrity by regulating the detection and repair of DNA DSBs. Loss of ATM kinase activity causes a significant increase in the sensitivity of cells to irradiation, making it an attractive target for clinical radiosensitization[55]. In literature, only a handful of selective ATM inhibitors have been reported, all in the interest of finding novel clinical radiosensitizers[55,56]. They have never been tested on HNSCC cell lines. Despite structure-activity relationship (SAR) studies, these ATM inhibitors did not progress into the clinical practice yet due to their pharmalogical and biological characteristics[55,56]. Currently, a novel ATM inhibitor[57] is being tested in combination with RT in a phase I trial concerning patients with brain tumors (clincaltrials.gov: NCT03423628). The lack of clinically available selective ATM inhibitors highlights the urgent need to develop alternative inhibitors. In this view, the identification of GSK635416A gives crucial new insights in alternative ATM inhibitors as it has a distinctive chemical structure. Additionally, GSK635416A seems to be remarkably specific as we failed to detect any other targets in an *in vitro* competition binding assay with 456 kinases. Therefore, GSK635416A holds promise as a lead in the development of drugs active in potentiating RT for HNSCC and other cancer types. In perspective, towards clinical implementation, we have performed pharmacokinetic studies of GSK635416A in

mice which showed good tissue retention, especially in the tumors (preliminary data, not shown). Future experiments will be based on assessing the radiosensitivity in mice and in optimizing GSK635416A efficacy by performing SAR studies to even further improve the therapeutic window.

Our assay has proven to be reliable in detecting potential radiosensitizers. In every screen and validation experiment we identified known radiosensitizers (e.g. olaparib, rapamycin) as one of our top hits, validating our method. This finding is very important for future drug discovery activities for cancers treated with RT, including HNSCC. Our assay is able to test for potential radiosensitizers, in a high-throughput setting, in a short timeframe (7 days) and with relatively limited effort (cell viability measurement, multiple drugs on one plate) compared to the conventional colony forming assay. The latter takes at least 14 days, is very laborious since every single condition has to be tested in a different plate and renders time-consuming counting of colonies.[58] We would propose to use our assay to identify potential radiosensitizers and then further validate them with a colony forming assay to confirm and prove their radiosensitizing effect.

In conclusion, the identification of GSK635416A and rapamycin provides a promising step forward in the identification of a novel radiosensitizer for advanced HNSCC patients. GSK635416A seems to be a very potent radiosensitizer as its radiosensitizing is especially observed in cancers cells and far less in normal cells. Further *in vitro* and *in vivo* (mice) testing should be performed in comparison to the current clinical radiosensitizers. This will hopefully yield a novel future treatment with improved survival rates and decreased toxicity.

REFERENCES

1 Unger, F. T., Witte, I. & David, K. A. Prediction of individual response to anticancer therapy: historical and future perspectives. *Cell Mol Life Sci* **72**, 729-757, doi:10.1007/s00018-014-1772-3 (2015).

2 Yue, F. *et al.* A comparative encyclopedia of DNA elements in the mouse genome. *Nature* **515**, 355-364, doi:10.1038/nature13992 (2014).

3 Johnson, J. I. *et al.* Relationships between drug activity in NCI preclinical in vitro and in vivo models and early clinical trials. *Br J Cancer* **84**, 1424-1431, doi:10.1054/bjoc.2001.1796 (2001).

4 Mak, I. W., Evaniew, N. & Ghert, M. Lost in translation: animal models and clinical trials in cancer treatment. *Am J Transl Res* **6**, 114-118 (2014).

5 Voskoglou-Nomikos, T., Pater, J. L. & Seymour, L. Clinical predictive value of the in vitro cell line, human xenograft, and mouse allograft preclinical cancer models. *Clin Cancer Res* **9**, 4227-4239 (2003).

6 Dollner, R. *et al.* The impact of stromal cell contamination on chemosensitivity testing of head and neck carcinoma. *Anticancer research* **24**, 325-331 (2004).

7 Dollner, R., Granzow, C., Tschop, K. & Dietz, A. Ex vivo responsiveness of head and neck squamous cell carcinoma to vinorelbine. *Anticancer research* **26**, 2361-2365 (2006).

8 Stausbol-Gron, B., Nielsen, O. S., Moller Bentzen, S. & Overgaard, J. Selective assessment of in vitro radiosensitivity of tumour cells and fibroblasts from single tumour biopsies using immunocytochemical identification of colonies in the soft agar clonogenic assay. *Radiother Oncol* **37**, 87-99 (1995).

9 Fridman, W. H., Pages, F., Sautes-Fridman, C. & Galon, J. The immune contexture in human tumours: impact on clinical outcome. *Nat Rev Cancer* **12**, 298-306, doi:10.1038/nrc3245 (2012).

10 Gentles, A. J. *et al.* The prognostic landscape of genes and infiltrating immune cells across human cancers. *Nat Med* **21**, 938-945, doi:10.1038/nm.3909 (2015).

11 Schmitz, S. & Machiels, J. P. Targeting the Tumor Environment in Squamous Cell Carcinoma of the Head and Neck. *Curr Treat Options Oncol* **17**, 37, doi:10.1007/s11864-016-0412-6 (2016).

12 Mroz, E. A. & Rocco, J. W. Intra-tumor heterogeneity in head and neck cancer and its clinical implications. *World J Otorhinolaryngol Head Neck Surg* **2**, 60-67, doi:10.1016/j.wjorl.2016.05.007 (2016).

13 Ariyoshi, Y., Shimahara, M. & Tanigawa, N. Study on chemosensitivity of oral squamous cell carcinomas by histoculture drug response assay. *Oral oncology* **39**, 701-707 (2003).

14 Hasegawa, Y. *et al.* Evaluation of optimal drug concentration in histoculture drug response assay in association with clinical efficacy for head and neck cancer. *Oral oncology* **43**, 749-756, doi:10.1016/j.oraloncology.2006.09.003 (2007).

15 Pathak, K. A. *et al.* In vitro chemosensitivity profile of oral squamous cell cancer and its correlation with clinical response to chemotherapy. *Indian journal of cancer* **44**, 142-146 (2007).

16 Robbins, K. T., Connors, K. M., Storniolo, A. M., Hanchett, C. & Hoffman, R. M. Sponge-gel-supported histoculture drug-response assay for head and neck cancer. Correlations with clinical response to cisplatin. *Archives of otolaryngology--head & neck surgery* **120**, 288-292 (1994).

17 Lancaster, M. A. & Knoblich, J. A. Organogenesis in a dish: modeling development and disease using organoid technologies. *Science* **345**, 1247125, doi:10.1126/science.1247125 (2014).

18 Drost, J. & Clevers, H. Organoids in cancer research. *Nat Rev Cancer*, doi:10.1038/s41568-018-0007-6 (2018).

19 Steiner, M. G. *et al.* Characterization of novel cell lines from pleomorphic adenomas of the parotid gland established in a collagen gel system. *Laryngoscope* **107**, 654-660 (1997).

20 Ozdemir, T. *et al.* Bottom-up assembly of salivary gland microtissues for assessing myoepithelial cell function. *Biomaterials* **142**, 124-135, doi:10.1016/j.biomaterials.2017.07.022 (2017).

21 Shin, H. S. *et al.* Functional spheroid organization of human salivary gland cells cultured on hydrogel-micropatterned nanofibrous microwells. *Acta Biomater* **45**, 121-132, doi:10.1016/j.actbio.2016.08.058 (2016).

22 Drost, J. *et al.* Organoid culture systems for prostate epithelial and cancer tissue. *Nat Protoc* **11**, 347-358, doi:10.1038/nprot.2016.006 (2016).

23 Klumpen, H. J., Beijnen, J. H., Gurney, H. & Schellens, J. H. Inhibitors of mTOR. *Oncologist* **15**, 1262-1269, doi:10.1634/theoncologist.2010-0196 (2010).

24 Agrawal, N. *et al.* Exome sequencing of head and neck squamous cell carcinoma reveals inactivating mutations in NOTCH1. *Science* **333**, 1154-1157, doi:10.1126/science.1206923 (2011).

25 Horn, D., Hess, J., Freier, K., Hoffmann, J. & Freudlsperger, C. Targeting EGFR-PI3K-AKT-mTOR signaling enhances radiosensitivity in head and neck squamous cell carcinoma. *Expert Opin Ther Targets* **19**, 795-805, doi:10.1517/14728222.2015.1012157 (2015).

26 Iglesias-Bartolome, R., Martin, D. & Gutkind, J. S. Exploiting the head and neck cancer oncogenome: widespread PI3K-mTOR pathway alterations and novel molecular targets. *Cancer Discov* **3**, 722-725, doi:10.1158/2159-8290.CD-13-0239 (2013).

27 Lui, V. W. *et al.* Frequent mutation of the PI3K pathway in head and neck cancer defines predictive biomarkers. *Cancer Discov* **3**, 761-769, doi:10.1158/2159-8290.CD-13-0103 (2013).

28 Stransky, N. *et al.* The mutational landscape of head and neck squamous cell carcinoma. *Science* **333**, 1157-1160, doi:10.1126/science.1208130 (2011).

29 Zheng, Y. & Jiang, Y. mTOR Inhibitors at a Glance. *Mol Cell Pharmacol* **7**, 15-20 (2015).

30 Vilar, E., Perez-Garcia, J. & Tabernero, J. Pushing the envelope in the mTOR pathway: the second generation of inhibitors. *Mol Cancer Ther* **10**, 395-403, doi:10.1158/1535-7163.MCT-10-0905 (2011).

31 Albert, J. M., Kim, K. W., Cao, C. & Lu, B. Targeting the Akt/mammalian target of rapamycin pathway for radiosensitization of breast cancer. *Mol Cancer Ther* **5**, 1183-1189, doi:10.1158/1535-7163.MCT-05-0400 (2006).

32 Chen, H. *et al.* The mTOR inhibitor rapamycin suppresses DNA double-strand break repair. *Radiat Res* **175**, 214-224 (2011).

33 Dai, Z. J. *et al.* Targeted inhibition of mammalian target of rapamycin (mTOR) enhances radiosensitivity in pancreatic carcinoma cells. *Drug Des Devel Ther* **7**, 149-159, doi:10.2147/DDDT.S42390 (2013).

34 Holler, M. *et al.* Dual Targeting of Akt and mTORC1 Impairs Repair of DNA Double-Strand Breaks and Increases Radiation Sensitivity of Human Tumor Cells. *PLoS One* **11**, e0154745, doi:10.1371/journal.pone.0154745 (2016).

35 Lai, Y., Yu, X., Lin, X. & He, S. Inhibition of mTOR sensitizes breast cancer stem cells to radiation-induced repression of self-renewal through the regulation of MnSOD and Akt. *Int J Mol Med* **37**, 369-377, doi:10.3892/ijmm.2015.2441 (2016).

36 Liu, Z. G. *et al.* The novel mTORC1/2 dual inhibitor INK128 enhances radiosensitivity of breast cancer cell line MCF-7. *Int J Oncol* **49**, 1039-1045, doi:10.3892/ijo.2016.3604 (2016).

37 Nagata, Y. *et al.* Effect of rapamycin, an mTOR inhibitor, on radiation sensitivity of lung cancer cells having different p53 gene status. *Int J Oncol* **37**, 1001-1010 (2010).

38 Zhang, D. *et al.* Inhibition of mammalian target of rapamycin by rapamycin increases the radiosensitivity of esophageal carcinoma Eca109 cells. *Oncol Lett* **8**, 575-581, doi:10.3892/ol.2014.2186 (2014).

39 Zheng, H. *et al.* Inhibition of mTOR enhances radiosensitivity of lung cancer cells and protects normal lung cells against radiation. *Biochem Cell Biol* **94**, 213-220, doi:10.1139/bcb-2015-0139 (2016).

40 Leiker, A. J. *et al.* Radiation Enhancement of Head and Neck Squamous Cell Carcinoma by the Dual PI3K/mTOR Inhibitor PF-05212384. *Clin Cancer Res* **21**, 2792-2801, doi:10.1158/1078-0432.CCR-14-3279 (2015).

41 Tonlaar, N. *et al.* Antitumor activity of the dual PI3K/MTOR inhibitor, PF-04691502, in combination with radiation in head and neck cancer. *Radiother Oncol* **124**, 504-512, doi:10.1016/j.radonc.2017.08.001 (2017).

42 Iglesias-Bartolome, R. *et al.* mTOR inhibition prevents epithelial stem cell senescence and protects from radiation-induced mucositis. *Cell Stem Cell* **11**, 401-414, doi:10.1016/j.stem.2012.06.007 (2012).

43 Bauman, J. E. *et al.* A phase II study of temsirolimus and erlotinib in patients with recurrent and/or metastatic, platinum-refractory head and neck squamous cell carcinoma. *Oral oncology* **49**, 461-467, doi:10.1016/j.oraloncology.2012.12.016 (2013).

44 Fury, M. G. *et al.* A phase I study of temsirolimus plus carboplatin plus paclitaxel for patients with recurrent or metastatic (R/M) head and neck squamous cell cancer (HNSCC). *Cancer Chemother Pharmacol* **70**, 121-128, doi:10.1007/s00280-012-1894-y (2012).

45 Fury, M. G. *et al.* A phase 1 study of everolimus plus docetaxel plus cisplatin as induction chemotherapy for patients with locally and/or regionally advanced head and neck cancer. *Cancer* **119**, 1823-1831, doi:10.1002/cncr.27986 (2013).

46 Geiger, J. L. *et al.* Phase II trial of everolimus in patients with previously treated recurrent or metastatic head and neck squamous cell carcinoma. *Head Neck* **38**, 1759-1764, doi:10.1002/hed.24501 (2016).

47 Grunwald, V. *et al.* TEMHEAD: a single-arm multicentre phase II study of temsirolimus in platin- and cetuximab refractory recurrent and/or metastatic squamous cell carcinoma of the head and neck (SCCHN) of the German SCCHN Group (AIO). *Ann Oncol* **26**, 561-567, doi:10.1093/annonc/mdu571 (2015).

48 Massarelli, E. *et al.* Phase II trial of everolimus and erlotinib in patients with platinum-resistant recurrent and/or metastatic head and neck squamous cell carcinoma. *Ann Oncol* **26**, 1476-1480, doi:10.1093/annonc/mdv194 (2015).

49 Saba, N. F. *et al.* Phase 1 and pharmacokinetic study of everolimus in combination with cetuximab and carboplatin for recurrent/metastatic squamous cell carcinoma of the head and neck. *Cancer* **120**, 3940-3951, doi:10.1002/cncr.28965 (2014).

50 Fury, M. G. *et al.* A phase 1 study of everolimus + weekly cisplatin + intensity modulated radiation therapy in head-and-neck cancer. *Int J Radiat Oncol Biol Phys* **87**, 479-486, doi:10.1016/j.ijrobp.2013.06.2043 (2013).

51 Senra, J. M. *et al.* Inhibition of PARP-1 by olaparib (AZD2281) increases the radiosensitivity of a lung tumor xenograft. *Mol Cancer Ther* **10**, 1949-1958, doi:10.1158/1535-7163.MCT-11-0278 (2011).

52 Dungey, F. A., Loser, D. A. & Chalmers, A. J. Replication-dependent radiosensitization of human glioma cells by inhibition of poly(ADP-Ribose) polymerase: mechanisms and therapeutic potential. *Int J Radiat Oncol Biol Phys* **72**, 1188-1197, doi:10.1016/j.ijrobp.2008.07.031 (2008).

53 Verhagen, C. V. *et al.* Extent of radiosensitization by the PARP inhibitor olaparib depends on its dose, the radiation dose and the integrity of the homologous recombination pathway of tumor cells. *Radiother Oncol* **116**, 358-365, doi:10.1016/j.radonc.2015.03.028 (2015).

54 Zhang, N. *et al.* Concurrent cetuximab, cisplatin, and radiation for squamous cell carcinoma of the head and neck in vitro. *Radiother Oncol* **92**, 388-392, doi:10.1016/j.radonc.2009.04.019 (2009).

55 Min, J. *et al.* Optimization of a Novel Series of Ataxia-Telangiectasia Mutated Kinase Inhibitors as Potential Radiosensitizing Agents. *J Med Chem* **59**, 559-577, doi:10.1021/acs.jmedchem.5b01092 (2016).

56 Weber, A. M. & Ryan, A. J. ATM and ATR as therapeutic targets in cancer. *Pharmacol Ther* **149**, 124-138, doi:10.1016/j.pharmthera.2014.12.001 (2015).

57 Durant, S. T. *et al.* The brain-penetrant clinical ATM inhibitor AZD1390 radiosensitizes and improves survival of preclinical brain tumor models. *Sci Adv* **4**, eaat1719, doi:10.1126/sciadv.aat1719 (2018).

58 Buch, K. *et al.* Determination of cell survival after irradiation via clonogenic assay versus multiple MTT Assay--a comparative study. *Radiation oncology (London, England)* **7**, 1, doi:10.1186/1748-717x-7-1 (2012).

CHAPTER 8

Samenvatting

Author contributions

Author affiliations

Curriculum vitae

List of publications

Dankwoord / Acknowledgments

SAMENVATTING

Dit proefschrift beschrijft een translationele stap voorwaarts ter verbetering van de prognose van patiënten met een gevorderd plaveiselcelcarcinoom in het hoofd-halsgebied. Om voor deze patiënten hogere overlevingskansen te bereiken met minder bijwerkingen, streefden wij ernaar om een voorspellend preklinisch, patiënt-afgeleid, tumorkweekmodel te vinden en streefden we naar het identificeren van nieuwe radiosensitizers die gericht zijn op kankercellen en gezonde cellen zoveel mogelijk ongemoeid laten.

Hoofdstuk 1 geeft een algemene inleiding in de ontwikkeling van kanker, de huidige behandeling en prognose van gevorderde hoofd-halskanker en vermeldt de achtergrond van onze onderzoeksvragen. 70% van de patiënten met hoofd-halskanker wordt gediagnosticeerd met de ziekte in een vergevorderd stadium (stadium III of IV). Zij worden behandeld met multimodale benaderingen, waaronder een combinatie van chemotherapie (CT), radiotherapie (RT, bestraling) en chirurgie. Ondanks deze behandelingen is de prognose van deze patiënten relatief slecht vanwege een hoog recidiefpercentage of de ontwikkeling van een tweede primaire tumor. Cisplatinum en cetuximab chemotherapie worden gecombineerd met radiotherapie (CRT) om de overleving te verbeteren. Echter, het overlevingsvoordeel van CRT in vergelijking met RT is laag, terwijl patiënten wel een aanzienlijke toename in toxiciteit (bijwerkingen) ervaren in geval van CRT. Bovendien reageren individuele patiënten met een soortgelijke tumor heel anders op dezelfde CRT-behandeling. Dit illustreert dat elke individuele tumor een andere intrinsieke gevoeligheid heeft, wat ervoor zorgt dat er een grote variëteit is in respons en dus ook in prognose. Momenteel is het onmogelijk om – voorafgaand aan de behandeling – te voorspellen welke patiënt zal reageren op het beoogde behandelingsregime, omdat er geen betrouwbare individuele voorspellende biomarkers beschikbaar zijn. De bovenvermelde problemen (relatief slechte prognose, hoge toxiciteit en interpatiënt-heterogeniteit in behandelingsrespons) hebben geleid tot onze belangrijkste onderzoeksvragen.

Deel I: Preklinisch kweken van vers hoofd-halstumor materiaal

Het doel van dit gedeelte van het proefschrift is onderzoek doen naar het best presterende preklinisch, patiëntafgeleide, verse tumorkweekmodel. Er is een sterke behoefte aan een dergelijk *in vitro* model, om voorafgaand aan de behandeling te kunnen voorspellen welke individuele patiënt goed zal reageren op de beoogde therapie. Bovendien zou dit model, idealiter, ook kunnen worden gebruikt voor het testen van toekomstige nieuwe geneesmiddelen. Het lijkt van essentieel belang voor een dergelijk model om de oorspronkelijke tumor zo nauwkeurig mogelijk na te bootsen, waardoor de

tumorheterogeniteit (verscheidene celtypes in de tumor) en de tumor micro-omgeving (ook omliggende cellen zoals stroma- en immuuncellen) behouden blijven. Dit met het oog op een betrouwbare vertaling van *in vitro* laboratoriumbevindingen naar klinische resultaten in patiënten.

In Hoofdstuk 2 hebben we de literatuur samengevat van de bestaande preklinische tumorkweekmodellen waaronder kankercellijnen, *in vivo* diermodellen en primaire (vers geïsoleerd uit tumoren van patiënten) tumorkweken. Het gebruik van kankercellijnen heeft belangrijke voordelen zoals de brede beschikbaarheid, het gebruiksgemak, de ongelimiteerde groei, de lage kosten, de goede toepasbaarheid in high-throughput screens en hun geschiktheid voor genetische modificatie. Dit model heeft echter ook kritische beperkingen, zoals de één-lagige vlakke groei en daardoor verlies van de normale 3D-tumorstructuur, het ontbreken van een tumor micro-omgeving, selectieve groei en de afwezigheid van fenotypische en genetische overeenkomsten met de originele tumor na meerdere passages. Bij het maken van een cellijn groeit er vaak maar één homogeen celtype uit, terwijl de oorspronkelijk tumor juist heel heterogeen was. Dit illustreert de moeilijkheid voor kankercellen om te overleven en zich aan te passen aan *in vitro* omstandigheden. Naast deze beperkingen zijn cellijnen een belangrijk en geprefereerd startpunt voor het beoordelen van celbiologische mechanismen.

Dierproeven hebben het voordeel dat ze een kweekmodel bieden waarin de tumor een 3D-structuur en micro-omgeving kan behouden, en kan groeien onder fysiologische omstandigheden met voedingsstoffen en bloedtoevoer. Dit biedt de mogelijkheid om *in vivo* de farmacokinetiek en toxiciteit van geneesmiddelen te onderzoeken. Beperkingen van het muismodel zijn een ander immuunsysteem, de ontwikkeling van andere type tumoren (voornamelijk lymfomen en sarcomen, in plaats van carcinomen) en het snellere metabolisme en daarmee een kortere levensduur van de muis. Deze verschillen hebben invloed op de voorspellende waarde van dit model. Succesvolle vertaling van diermodelresultaten naar resultaten in klinische studies blijft een uitdaging, slechts 8% van de op dieren geteste medicijnen passeert fase I trials in mensen.

Primaire tumorkweken (samengevat in Hoofdstuk 2 en onderzocht in Hoofdstuk 3) is een model dat vers menselijk tumorweefsel kweekt door middel van o.a. de zogenaamde 'cell-adhesive matrix assay', 'soft-agar clonogenic assay', 'histocultures', 'spheroids' en 'organoids'. Primaire tumorkweken die de *in vivo* tumor en zijn micro-omgeving het beste reflecteren, hebben de voorkeur. In onze review (Hoofdstuk 3), concludeerden wij dat de meest succesvolle kweek en de beste correlatie met klinische resultaten werden gerapporteerd met het zogenoemde 'spons-gel-ondersteunende histoculture'

kweekmodel. Dit model heeft als voordeel dat de tumor en zijn micro-omgeving beter wordt nagebootst, voornamelijk omdat er geen gebruik wordt gemaakt van enzymatische digestie van de tumor (zoals bij het maken van cellijnen), waardoor de celheterogeniteit, de celcel interactie en de 3D-architectuur behouden blijven. Bovendien reflecteert dit model de menselijke situatie zo nauwkeurig mogelijk doordat de tumorfragmenten worden gekweekt op een spons die gedeeltelijk doordrenkt is in medium en gedeeltelijk omgeven wordt door lucht. Dit simuleert de lucht-slijmvliessituatie van tumorgroei in het hoofd-halsgebied. Deze bovengenoemde kenmerken van het spons-gel-ondersteunende kweekmodel verklaart waarschijnlijk het feit dat hoge succesvolle kweekpercentages worden beschreven in de literatuur, variërend van 88% tot 100%, met een kweekduur van 2 tot 11 dagen. Bovendien worden er goede correlaties gerapporteerd tussen *in vitro* chemosensitiviteit en klinische uitkomst, met positief voorspellende waarden van 69% tot 90% en negatief voorspellende waarden van 50% tot 100%.

Deze bevindingen hebben ons ertoe gebracht om dit preklinische tumorkweekmodel te selecteren als mogelijk model voor het toekomstig testen van medicijnen en voor geïndividualiseerde therapiebepaling. Ondanks de veelbelovende resultaten wordt het model echter nog niet routinematig gebruikt in de klinische praktijk. We stelden de hypothese dat, om dit model te verbeteren, verschillende aspecten grondiger zouden kunnen worden onderzocht en geoptimaliseerd. Ten eerste zou het nuttig kunnen zijn om een immunohistochemische analyse (IHC) te gebruiken als read-out in plaats van een metabole assay. IHC maakt het mogelijk om de aanwezigheid van verschillende celtypen afzonderlijk te analyseren. Dit is volgens ons belangrijk, omdat we weten dat stroma-en tumorcellen anders reageren op geneesmiddelen en bestraling. Men kan met IHC ook de aanwezigheid van immuuncellen onderzoeken, waarvan bekend is dat zij van invloed zijn op de klinische behandelingsrespons. Ten tweede hebben we verschillende mediumsupplementen getest om de effectiviteit van de kweek (bijvoorbeeld levensvatbaarheid en proliferatie van tumorcellen) mogelijk nog verder te verbeteren.

Om deze twee hypothesen te testen kweekten we, middels het spons-gel-ondersteunende kweekmodel, verse tumorbiopten van 72, voorheen onbehandelde, patiënten (Hoofdstuk 4). De biopten van 57 patiënten (79%) werden geïncludeerd voor analyse, in kleine fragmenten gesneden (1451 fragmenten in totaal), gedurende 7 dagen gekweekt en immunohistochemisch beoordeeld op percentage tumor, percentage vitaliteit en proliferatie van de tumor, EGFR-expressie en aanwezigheid van T-cellen en macrofagen. Ten eerste hebben we waargenomen dat zowel tumor-, stroma- en immuuncellen inderdaad behouden blijven tijdens de kweek. Het mediane tumorpercentage steeg van 53% op dag 0 tot 80% op dag 7. De vitaliteit en proliferatie van de tumorcellen namen

af na 7 dagen, respectievelijk van 90% tot 30% en van 30% tot 10%. Ten tweede toonden we aan dat toevoeging van EGF, foliumzuur en hydrocortison aan het kweekmedium leidde tot verbeterde vitaliteit en proliferatie. Dit fenomeen werd echter niet systematisch waargenomen. Ten derde konden we helaas geen patiënten-subgroep identificeren met een hoger kweek succespercentage. Interessant genoeg verhoogde EGF-suppletie de vitaliteit en proliferatie niet bij tumoren van patiënten die de EGF-receptor tot overexpressie brachten. Over het algemeen werd een grote heterogeniteit in de resultaten waargenomen zowel tussen tumoren van patiënten als binnen tumorfragmenten van individuele patiënten. Daarom konden er geen systematische conclusies worden getrokken.

Samenvattend, alle eerdergenoemde modellen, van cellijnen en tumor-'histoculture'-kweken tot muizenmodellen, lijken slechts gedeeltelijk op de oorspronkelijke humane tumor. Het is onmogelijk om alle *in vivo* menselijke kenmerken in één model weer te geven. Alle modellen vertegenwoordigen echter waardevolle 'overbruggingsmodellen' tussen het gebruik van cellijnen en klinische patiëntentrials. Toch maakt het kweken van tumorfragmenten een natuurlijke tumoromgeving mogelijk. We denken dat ons verbeterde kweekmodel mogelijk kan worden gebruikt om de respons van de behandeling en de correlatie met de klinische respons te testen, als potentieel individueel voorspellend model. Gezien de heterogeniteit van de tumor, die in onze resultaten duidelijk wordt weerspiegeld, kan het echter moeilijk zijn om harde conclusies te trekken.

Deel II: Drug screens om nieuwe radiosensitizers tegen hoofd-halskanker te identificeren

Het tweede deel van dit proefschrift heeft als onderzoeksdoel om de klinische uitkomst te verbeteren en om de bijwerkingen van behandelingen te verminderen bij patiënten met gevorderde hoofd-halskanker. Radiotherapie is een belangrijk onderdeel van de behandeling van patiënten met hoofd-halskanker, maar de werkzaamheid kan worden beperkt door de toxiciteit op normale weefsels of door de resistentie van tumorcellen. Bestraling kan worden gecombineerd met 'radiosensitizers'. Radiosensitizers kunnen hetzelfde therapeutische effect bereiken maar met een verlaging van de bestralingsdosis of ze kunnen de RT-werkzaamheid in resistente tumoren verbeteren. Het verbeteren van de overlevingskansen met beperkte toxiciteit kan worden bereikt met een radiosensitizer die specifiek op kankercellen is gericht zonder het normale weefsel te schaden, ook wel 'het therapeutisch bereik' genoemd. Met als doel nieuwe en betere radiosensitizers te identificeren, hebben we drugscreens uitgevoerd bestaande uit het grootschalig testen van samengestelde bibliotheken met allerlei verschillende chemische verbindingen of bekende medicijnen.

In Hoofdstuk 5 beschrijven we het screenen van drie drugbibliotheken, bestaande uit 1) klinisch goedgekeurde anti-kanker medicijnen, 2) de Roche kinaseremmers en 3) de remmers van zogenoemde deubiquitinerende enzymen (DUBs). De screens werden uitgevoerd op verschillende hoofd-halskankercellijnen, in aan- en afwezigheid van bestraling, waarbij als resultaat de vitaliteit van de cellen werd gemeten. Deze stoffen werden vergeleken met de momenteel gebruikte klinische radiosensitizers voor gevorderde hoofd-halskanker, namelijk cisplatinum, cetuximab en olaparib. Bij het screenen van de bekende anti-kanker medicijnen werd het meest significante potentiële radiosensitizing effect bereikt met rapamycine, raloxifen en tamoxifen. Het screenen van de Roche en DUB bibliotheken resulteerden niet in radiosensitizers die meer potentie hadden dan cisplatinum of olaparib.

Interessant is nog te vermelden dat voorlopige resultaten uit de screen met bekende anti-kankermedicijnen, in de groep zonder bestraling, verschillende verbindingen detecteerden die beter presteerden dan de geneesmiddelen die momenteel worden gebruikt voor recidiverende of gemetastaseerde hoofd-halskanker. De vitaliteit van de kankercellijnen nam namelijk aanzienlijk meer af wanneer depsipeptide, bortezomib en idarubicine werden toegediend, in vergelijking met cisplatinum, carboplatin, 5-fluorouracil, paclitaxel en methotrexaat (cetuximab was niet opgenomen in de bibliotheek). Verder *in vitro* en *in vivo* onderzoek is nodig om te onderzoeken of deze geneesmiddelen inderdaad zouden kunnen dienen als nieuwe en krachtigere medicijnen voor patiënten met recidiverend of gemetastaseerd hoofd-halskanker.

Hoofdstuk 6 behandelt het screenen van de GlaxoSmithKline (GSK) kinase bibliotheek. Deze screen identificeerde GSK635416A als een nieuwe radiosensitizer. De mate van radiosensitisatie door GSK635416A was hoger dan de radiosensitisatie die werd waargenomen met cisplatinum en cetuximab en was gelijk of enigszins hoger dan gemeten met olaparib. Een kolonievormende groeitest werd uitgevoerd en bevestigde de radiosensitizing activiteit van GSK635416A. In vergelijking met gegevens over cisplatinum en olaparib uit eerdere literatuur, lijkt de radiosensitisatie van GSK635416A veelbelovend. De radiosensitisatie werd ook waargenomen in andere hoofd-halskankercellijnen en in cervix- en longkankercellijnen. Van equivalent belang is dat GSK635416A een significant lagere toxiciteit vertoonde in afwezigheid van bestraling en vrijwel geen toxiciteit in een normale fibroblastcellijn, in vergelijking met cisplatinum of olaparib. We toonden aan dat GSK635416A een nieuwe ATM-remmer is, omdat het DNA-dubbelstrengsbreuken verhoogt na bestraling, het de door bestraling geïnduceerde fosforylering van ATM remde en de gemedieerde radiosensitisatie van GSK635416A ontbrak in ATM-gemuteerde cellen.

Een belangrijke bevinding binnen dit gedeelte van mijn proefschrift is dat onze assay betrouwbaar is in het detecteren van potentiële radiosensitizers. In elk screen en validatie-experiment identificeerden we bekende radiosensitizers (bijvoorbeeld olaparib en rapamycine) als een van onze tophits, hetgeen onze methode valideerde. Deze bevinding is belangrijk voor toekomstige onderzoeken die erop gericht zijn nieuwe medicijnen te identificeren voor tumoren die tevens met bestraling worden behandeld, waaronder hoofd-halskanker. Onze methode kan potentiële radiosensitizers testen, in groten getale, in een kort tijdsbestek (7 dagen) en met een relatief beperkte inspanning (meting van de vitaliteit van de cellen, meerdere medicijnen op één plaat). We stellen dan ook voor om onze assay te gebruiken om potentiële radiosensitizers te identificeren en ze vervolgens verder te valideren in de conventionele, maar meer tijdrovende, kolonievormende test, om hun radiosensitisatie-effect te bevestigen en te bewijzen.

Concluderend, de identificatie van GSK635416A en rapamycine biedt een veelbelovende stap voorwaarts in het vinden van een nieuwe radiosensitizer voor patiënten met gevorderde hoofd-halskanker. GSK635416A lijkt daarbij een zeer potente radiosensitizer te zijn, dit omdat het radiosensitizing-effect specifiek lijkt te werken op kankercellen en niet op normale cellen. Dit resulteert in de toekomst hopelijk in een nieuwe behandeling met een hogere overlevingskans en minder bijwerkingen.

AUTHOR CONTRIBUTIONS

Chapter 2 **Preclinical models in head and neck squamous cell carcinoma**

C.L. Zuur, A.J.C. Dohmen, M.W.M. van den Brekel, X.J. Wang, S.P. Malkoski

CZ: Principal investigator, acquired data, wrote the manuscript. AD, MB and XW: Critical input and final approval of the manuscript. SM: Co-principal investigator, acquired data, wrote the manuscript

Chapter 3 **Feasibility of primary tumor culture models and preclinical prediction assays for head and neck cancer: a narrative review**

A.J.C. Dohmen, J.E. Swartz, M.W.M. van den Brekel, S.M. Willems, R. Spijker, J. Neefjes, C.L. Zuur

AD: Acquired the data, analyzed and interpreted data, layout, design, and wrote the manuscript. JS: Contributed to the collection of literature and writing of the manuscript. MB: Critical input and final approval of the manuscript. SW: Critical input and final approval of the manuscript. RS: Contributed to the design of the search strategy, collection of the literature and final approval of the manuscript. JN: Critical input and final approval of the manuscript. CZ: Principal investigator, contributed to writing the manuscript, critical input and final approval of the manuscript.

Chapter 4 **Sponge-supported cultures of primary head and neck tumors for an optimized preclinical model**

A.J.C. Dohmen, J. Sanders, S. Canisius, E.S. Jordanova, E.A. Aalbersberg, M.W.M. van den Brekel, J. Neefjes, C.L. Zuur

AD: Acquired the data, analyzed and interpreted data, layout, design and wrote the manuscript. JS: scored all patients tumor sections. SC: Statistically analyzed and interpreted data. EJ: Scored immune cells and macrophages, critical input in discussion. EA: Acquired data. MB: Critical input and final approval of the manuscript. JN and CZ: principal investigators with critical input during the study, constructing the experiments and drafting the final manuscript.

Chapter 5 **A drug screening assay identifies mTOR inhibitors and SERMs as novel radiosensitizers for head and neck cancer**

A.J.C. Dohmen, R.H. Wijdeven, C. Lieftink, B. Morris, P. Halonen, B. Rodenko, M.C. de Jong, M.W.M. van den Brekel, J.P. de Boer, H. Ovaa, J. Neefjes, C.L. Zuur

AD: Acquired the data, analyzed and interpreted data, layout, design and wrote the manuscript. RW and CF: Critical support and discussion. BM, PH and BR: Supported within screening facility, analyzing screening data and discussion. MJ and JB: Approval part of manuscript. HO: chemistry support and final approval manuscript. MB: Critical input and final approval of the manuscript. JN and CZ: principal investigators with critical input during the study, constructing the experiments and drafting the final manuscript.

Chapter 6 **Identification of a novel ATM inhibitor with cancer cell specific radiosensitization activity**

A.J.C. Dohmen, X. Qiao, A.M. Duursma, R.H. Wijdeven, C. Lieftink, F. Hageman, B. Morris, P. Halonen, C. Vens, M.W.M. van den Brekel, H. Ovaa, J. Neefjes, C.L. Zuur

AD: Acquired the data, analyzed and interpreted data, layout, design and wrote the manuscript. XQ, AD and RW: Contributed to acquiring data and discussion. FH: Performed colony forming assay. CL, BM and PH: Supported within screening facility, analyzing screening data and discussion. CV and MB: Critical input and final approval of the manuscript. HO: chemistry support and final approval manuscript. JN and CZ: principal investigators with critical input during the study, constructing the experiments and drafting the final manuscript.

AUTHOR AFFILIATIONS

E.A. Aalbersberg
Department of Head and Neck Oncology and Surgery, Netherlands Cancer Institute – Antoni van Leeuwenhoek, Amsterdam, The Netherlands.

J.P. de Boer
Department of Medical Oncology, Antoni van Leeuwenhoek Hospital, Amsterdam, The Netherlands

M.W.M. van den Brekel
Department of Head and Neck Oncology and Surgery, Netherlands Cancer Institute – Antoni van Leeuwenhoek, Amsterdam, The Netherlands. Department of Oral and Maxillofacial Surgery, Academic Medical Center, Amsterdam, The Netherlands

S. Canisius
Department of Computational Cancer Biology, Netherlands Cancer Institute, Amsterdam, The Netherlands

A.M. Duursma
Division of Cell Biology, Netherlands Cancer Institute, Amsterdam, The Netherlands

F. Hageman
Division of Biological Stress Response, Netherlands Cancer Institute, Amsterdam, The Netherlands

P. Halonen
NKI Robotics and Screening Center, Netherlands Cancer Institute, Amsterdam, The Netherlands

M.C. de Jong
Department of Radiation Oncology, Netherlands Cancer Institute - Antoni van Leeuwenhoek Hospital, Amsterdam, The Netherlands

E.S. Jordanova
Center for Gynecological Oncology Amsterdam, VUmc, Amsterdam, The Netherlands

C. Lieftink
NKI Robotics and Screening Center, Netherlands Cancer Institute, Amsterdam, The Netherlands

S.P. Malkoski
Department of Medicine, Medicine – Pulmonary Sciences and Critical Care, University of Colorado Hospital, Aurora, CO, USA

B. Morris
NKI Robotics and Screening Center, Netherlands Cancer Institute, Amsterdam, The Netherlands

J. Neefjes
Division of Cell Biology, Netherlands Cancer Institute, Amsterdam, The Netherlands. Department of Chemical Immunology, Leiden University Medical Center, Leiden, The Netherlands

H. Ovaa
Division of Cell Biology, Netherlands Cancer Institute, Amsterdam, The Netherlands. Department of Chemical Immunology, Leiden University Medical Center, Leiden, The Netherlands

X. Qiao
Division of Cell Biology, Netherlands Cancer Institute, Amsterdam, The Netherlands

B. Rodenko
Division of Cell Biology, Netherlands Cancer Institute, Amsterdam, The Netherlands

J. Sanders
Department of Pathology, Netherlands Cancer Institute - Antoni van Leeuwenhoek, Amsterdam, The Netherlands

R. Spijker
Medical Library, Academic Medical Center, Amsterdam, The Netherlands

J.E. Swartz
Department of Head and Neck Oncology and Surgery, Netherlands Cancer Institute – Antoni van Leeuwenhoek, Amsterdam, The Netherlands.

C. Vens
Division of Biological Stress Response, Netherlands Cancer Institute, Amsterdam, The Netherlands

X.J. Wang
Department of Pathology, University of Colorado, Aurora, CO, USA

R.H. Wijdeven
ivision of Cell Biology, Netherlands Cancer Institute, Amsterdam, The Netherlands

S.M. Willems
Department of Pathology, University Medical Center Utrecht, Utrecht, The Netherlands

C.L. Zuur
Department of Head and Neck Oncology and Surgery, Netherlands Cancer Institute – Antoni van Leeuwenhoek, Amsterdam, The Netherlands

CURRICULUM VITAE

Amy Dohmen was born on the 10th of October 1985 in Eindhoven. There she enjoyed her secondary school at the Augustinianum and passed her VWO/Atheneum exams in 2004. In the same year she moved to Maastricht to start medical school at the University of Maastricht. She followed internships abroad in Reykjavik – Iceland and Pretoria – South-Africa. During her Master's degree she clinically participated at the otorhinolaryngology department of the Maastricht University Medical Center in the group of Prof. dr. Robert Stokroos. There she gained her enthusiasm for medical research as she participated in projects regarding the effect of radiotherapy on vestibular schwannomas. After receiving her Master's degree in 2010, Amy worked as a surgical resident in Sittard. To further pursue medical research and her fascination with head and neck oncology and radiotherapy, she moved to Amsterdam and started working at the Netherlands Cancer Institute in Amsterdam, as a PhD-student in the lab of Prof. Dr. Jacques Neefjes. Here, she combined the expertise of the cell biology and chemistry (Prof. Dr. Huib Ovaa) research groups, with the clinical research group of Prof. Dr. Michiel van den Brekel and Dr. Lotje Zuur. The results of this scientific collaboration are presented in this thesis. While finishing her thesis, Amy worked as an otorhinolaryngology resident (ANIOS) at the OLVG in Amsterdam and at the Waterlandziekenhuis in Purmerend.

LIST OF PUBLICATIONS

2018 **A.J.C. Dohmen**, R. H. Wijdeven, C. Lieftink, B. Morris, P. Halonen, B. Rodenko, M.C. de Jong, M.W.M. van den Brekel, J.P. de Boer, H. Ovaa, J. Neefjes, C.L. Zuur. A screening assay identifies mTOR inhibitors and SERMs as novel radiosensitizers for head and neck cancer. To be submitted.

2018 **A.J.C. Dohmen**, J. Sanders, S. Canisius, E.S. Jordanova, E. Aalbersberg, M.W.M. van den Brekel, J. Neefjes, C.L. Zuur. Sponge-supported cultures of primary head and neck tumors for an optimized preclinical model. Oncotarget, May 2018.

2017 **A.J.C. Dohmen**, X. Qiao, A. Duursma, R. H. Wijdeven, C. Lieftink, F. Hageman, B. Morris, P. Halonen, C. Vens, M.W.M. van den Brekel, H. Ovaa, J. Neefjes, C.L. Zuur. Identification of a novel ATM inhibitor with cancer cell specific radiosensitization activity. Oncotarget, May 2017.

2016 C.L. Zuur, **A.J.C. Dohmen**, M.W.M. van den Brekel, X.J. Wang and S.P. Malkoski. Preclinical models of head and neck squamous cell carcinoma. Chapter 10 in "Head and Neck Cancer: Multimodality Management", 2nd edition, J. Bernier (ed.), 2016.

2015 **A.J.C. Dohmen**, J.E. Swartz, M.W.M. van den Brekel, S.M. Willems, R. Spijker, J. Neefjes, C.L. Zuur. Feasibility of primary tumor culture models and preclinical prediction assays for head and neck cancer: a narrative review. Cancers, Aug 2015.

2012 R. van de Langenberg, **A.J.C. Dohmen**, B.G. Baumert, B.J. de Bondt, P.J. Nelemans, R.J. Stokroos. Volume changes after stereotactic LINAC radiotherapy in vestibular schwannoma: control rate and growth patterns. Int J of Radiat Oncol Biol Phys, Feb 2012.

2011 R. van de Langenberg, P.E.J. Hanssens, H.B. Verheul, J.J. van Overbeeke, P.J. Nelemans, **A.J.C. Dohmen**, B.J. de Bondt, R.J. Stokroos. Management of large vestibular schwannoma Part II: primary Gamma-Knife radiosurgery: radiological and clinical aspects. Journal of Neurosurgery, Nov 2011.

2011 R. van de Langenberg, R.B.J. de Bondt, P.J. Nelemans, **A.J.C. Dohmen**, B.G. Baumert, R.J. Stokroos. Predictors of volumetric growth and auditory deterioration in vestibular schwannomas followed in a wait and scan policy. Otology & Neurotology, Feb 2011.

2010 R. van de Langenberg, B.J. de Bondt, P.J. Nelemans, **A.J.C. Dohmen**, B.G. Baumert, R.J. Stokroos. Correlation of vestibular schwannoma volume with growth and auditory function in a wait and scan policy. Neuro-oncology, Sep 2010.

DANKWOORD

Ik kan mij nog goed mijn eerste werkdag herinneren, 7 jaar geleden. Ik stond buiten en keek omhoog naar de gevel van het ziekenhuis. Bij het zien van het Antoni van Leeuwenhoek logo overheerste een gevoel van enorme trots. Nu, aan het einde van de rit, ben ik nog steeds enorm trots. Trots op het resultaat en vooral ook trots op alles wat ik geleerd heb. Ik ben blij met alle bijzondere mensen die ik heb ontmoet en ontzettend dankbaar voor iedereen die mij geholpen heeft gedurende mijn promotie. Zonder jullie was het nooit gelukt! Dit gezegd hebbende, wil ik enkele mensen nog persoonlijk bedanken:

Beginnende bij **Lotje Zuur** en **Sjaak Neefjes**, mijn copromotor en promotor, en beiden ook mijn directe begeleiders. De combi-begeleiding van een hoofd-halschirurg en een rasechte celbioloog heeft mij geregeld kopzorgen bezorgd. Maar met een flinke dosis doorzettingsvermogen en een fantastische groep, hebben we mooi translationeel onderzoek neer kunnen zetten.

Lotje, ik ben jou enorm dankbaar voor alles. Jij bent een groot voorbeeld voor mij door jouw baan als chirurg te combineren met jouw passie voor wetenschap. Jij kijkt over de grenzen van jouw eigen vakgebied en je bent onuitputbaar gemotiveerd om ook door middel van onderzoek iets voor patiënten te kunnen betekenen. Dit laatste was voor mij de voornaamste reden om te promoveren. Jij bent altijd heel prettig en laagdrempelig bereikbaar geweest. Daarnaast ben jij kritisch en precies, wat vaak gewaardeerd werd, maar soms ook kon botsen met mij als ik bijvoorbeeld voor de zoveelste keer mijn grafieken en data normalisatie moest uitleggen. Dat ik het schrijven voor mij uitschoof en liever in het lab werkte, frustreerde jou wellicht. Sorry daarvoor, ik ben nu eenmaal een echte doener, geen schrijver. Achteraf kan ik er natuurlijk ook om lachen; en ik hoop jij ook. Bedankt voor alles wat jij mij geleerd hebt, de extra betaalde schrijftijd om dit boekje af te ronden, jouw enthousiasme, steun, vertrouwen en tevens jouw geduld. Succes met al jouw (nieuwe) projecten. Hopelijk krijgt onze radiosensitizer een mooi vervolg in de toekomst!

Sjaak, bij mijn sollicitatie op jouw kantoor was er één voorwaarde: ik moest kunnen voetballen. Wat waren dat goede tijden, ik zie jouw bril nog over het gras vliegen of jouw lange lijf tegen de muur knallen. Dank dat jij mijn promotor en mentor bent geweest en mij hebt geënthousiasmeerd voor de celbiologie. Jouw gedrevenheid en enthousiasme zijn aanstekelijk en jouw ideeën vooruitstrevend en inspirerend. Wetenschap moet vooral ook leuk zijn, en dat zie je duidelijk terug in jouw groep. Hier draaide het namelijk altijd om lol en gezelligheid (tafelvoetbal/tennis in de seminarroom, gekke kerstfeesten, pannenkoeken happen en labuitjes). Er is geen moment geweest dat ik twijfelde aan mijn keuze om bij jou te promoveren. Dat ik vooralsnog besloten heb om dokter te blijven, doet niets af aan mijn liefde voor wetenschap. Ons vak als dokter is nu eenmaal ook machtig mooi! Ons vak

is echter nog mooier als we het kunnen combineren met gekke wetenschappers zoals jij. Hopelijk heb ik het HBO-dokter-karakter iets overstegen in jouw ogen.

Daarnaast wil ik mijn andere promotor **Michiel van den Brekel** bedanken. Michiel, jouw groep is een fijne omgeving om te werken. De groep is open, laagdrempelig, gezellig en ook kritisch. Jouw betrokkenheid bij alle projecten is mooi om te zien en jouw nieuwsgierigheid voor basaal onderzoek erg prettig. Ik bewonder jou voor het leiden van de afdeling en voor het verzamelen van funding om al het onderzoek mogelijk te maken. Bedankt dat ik bij jou mocht promoveren, voor alles wat ik geleerd heb en voor de open gesprekken.
Mijn andere copromotor, **Huib Ovaa**, wil ik bedanken voor de mooie samenwerking met jouw groep, het meedenken met mijn projecten en het aanleveren van de compounds. Chemie is voor mij een stap te ver om te begrijpen, maar ik vond het interessant om te zien wat jij allemaal kan betekenen in translationeel onderzoek.

Naast mijn compromotoren en promotoren zijn er uiteraard meer mensen van essentieel belang geweest voor het realiseren van mijn PhD.
Ten eerste, met name **B6.** Wat heb ik een toptijd gehad met jullie in het lab! Ook al had ik vaak het idee dat ik als dokter 100 stappen achterliep op kennis en kunde, jullie sfeer en openheid zorgden er altijd voor dat ik mij thuis voelde. Bedankt voor alle gezelligheid: wintersport, wijnproeverijen, pubquizen (waneer gaan we weer?), vrimibo's, labuitjes en kerstfeesten. **Tiziana**, thank you for showing me around in the lab and learning me about cell cultures and using a pipetboy. The dinners and the holiday in Sardinia were amazing. **Ilana**, my other lab-mommy, thank you for all the epic ;) times and conversations together. Thank you for all your advices about work, bosses and life. I am so happy that everything turned out fine for you. **Jeroen**, onze toffe festivalmomentjes zijn onvergetelijk. Ik mis ze nog. Jouw relaxte houding en jouw hulp in het lab was altijd erg fijn. **Lennert**, ook jij stond altijd voor mij klaar (met jouw grapjes) op vele fronten. Jij blijft maar meegaan met al die jonkies die in het lab verschijnen, goed zo ouwe! Fijn dat er nu een paar leuke mensen blijven. **Baoxu**, thank you for all the fun: soccer, table tennis, dinner and our time in SF (sorry for the brakes). You are an amazing and clever guy, keep up the good work. **Xiaohang**, when everyone left you were still around to help me out, I can not thank you enough for that. I hope you can further improve my GSK-baby. **Rik**, **Sjoerd**, **Sabina**, **Menno**, **Jolien** (neefjes-weesje), **Bo**, **Izhar**, **Laurel**, **Hans**, **Robbert**, **Marlieke**, **Petra**, **Inge**, **Gosia** en **Lin-en** écht enorm bedankt voor de onvergetelijke toptijd met jullie allemaal. Ik ben erg blij dat ik jullie allemaal heb leren kennen. Alle **Ovaa's** van B6, jullie ook bedankt voor alle lol, inspiratie en hulp. **Anne**, wat was het fijn om jou erbij te krijgen als 'secretaresse': veel lol (wat ERRUGGG), steun en goede gesprekken om onze 'ellllllende' te delen.

Mijn allergrootste dank gaat uit naar jou, **Ruud**, ut beste pert van de stal. Jij was er gewoon echt altijd voor mij (sowieso voor iedereen), met hulp, adviezen en jouw kalmte. Als ik het weer eens niet wist of begreep, of vast zat met Lotje en Sjaak, was jij er voor mij om het rustig uit te leggen. Toen iedereen weg was en het aardig stil werd bleef jij contact houden. Je bent een lieve, gezellige en bovenal ook slimme gast. Bedankt voor alles: het voetballen (incl toernooitjes), mij opzoeken in het ziekenhuis, het delen van onze blessures (en krukken), PSV in de kroeg, festivals en alle andere leuke momenten. Ik ben blij dat jij op de dag naast mij wil staan als paranimf. Bedankt, hopelijk goan we dur vaak nog eene vatten.

Ten tweede, al die andere toegewijde mensen binnen het **NKI**. Wat was het mooi om in het NKI te werken met zoveel goede, lieve mensen en de fijne laagdrempeligheid tussen verschillende disciplines. **Cor**, **Ben**, **Pasi** en **Roderick** bedankt voor jullie kritische blik en hulp met alle screens en data. **Joyce**, **Ingrid**, **Katja**, **Cindy C** en alle anderen bij de pathologie die mij geholpen hebben; zonder jullie was het kweekproject onmogelijk. Ik kan jullie niet genoeg bedanken daarvoor. Cindy jouw speelsheid en positiviteit maakten mij altijd aan het lachen. Ik was blij met onze twinsie vriendschap (kokosnoot, skylounge, piano, let it goooo) toen we het beiden moeilijk hadden. Jouw creativiteit is een super gave, bedankt voor jouw ontwerp van mijn cover! **Conchita** en **Anja**, bedankt dat jullie zo intensief hebben geholpen met mijn radiosensitizer project. Jullie kennis en ervaring waren onmisbaar. Conchita, thank you for all your critical support. Anja, bedankt dat jij in het PBA zat toen ik mijn praatje hield en het bijna had opgegeven om mijn target te vinden. Jouw passie en enthousiasme waren aanstekelijk, bedankt voor al jouw hulp. **Don**, haha zonder jou was er sowieso geen boekje, bedankt voor het altijd oplossen van mijn Mac-problemen en de leuke gesprekken. Mijn **studenten**, bedankt voor jullie hulp door de jaren heen.

En verder, alle mensen van de hoofd-hals afdeling, bedankt voor de gezelligheid. **Chirurgen**, voor het nemen van de biopten. **Baris**, het was altijd zo fijn en leuk om met jou te praten. Bedankt voor jouw adviezen en geloof in mij, en voor het ongelofelijke zeil-verzuip-tripje. Als je nog zo'n avontuur wil, geef even een seintje! Alle **mede-onderzoekers** bedankt voor de ongelofelijk leuke tijd en gedeelde smart. **Sharon**, bedankt dat jij mij in huis nam en voor de leuke tijd samen. **Cindy B**, bedankt voor jouw KNO-steun. **Renske**, bedankt voor al jouw hulp en steun, dit boekje, en de oh-zo erge wintersport. **Marion** en **Henny**, bedankt voor al het administratieve geregel.

Lieve artsen en assistentes van **KNO Waterlandziekenhuis**, bij jullie werken was een verademing. Wat een gezellig clubje is het daar. Ik voelde mij enorm thuis. Echt onwijs

bedankt voor alles wat jullie mij geleerd hebben en voor alle lol die ik heb gehad! Ik zal jullie niet vergeten.

Hard werken is niet mogelijk zonder goede ontspanning, zowel van sport als van vrienden. Beste **voetbal** (kampioenuh!) en **surf** maatjes, zonder jullie was mijn promotie ook nooit gelukt. Wat was het altijd heerlijk als ik met jullie buiten mocht spelen en mijn hoofd weer leeg kon maken. Bedankt voor de gezellige drankjes en leuke tripjes. **Johanna**, bedankt voor de leuke biermomentjes en jouw Nederlandse feedback. **Kim**, bedankt voor jouw gezelligheid en ritjes op weg naar het surfen. **Remadora's**, wat een toptijd in Maastricht hadden wij bij Saurus, en wat fijn dat we elkaar soms nog zien en ik van jullie promoties heb kunnen leren. **Frans**, wat fijn dat ik jou nog geregeld zie als jij weer een bezoekje brengt aan NL. Jouw nuchterheid en humor zijn altijd een welkome afwisseling.
Lieve **Renate** en **Marjolein**, onmisbaar om jullie erbij te hebben. De borrels in Walters, wijntjes, weekendjes, eten, gesprekken, wandelen (met James), wintersport en ook de suffe spelletjes (haha) waren een welkome afwisseling van de dagelijkse rompslomp. Thanks lieverds! (PS, Marjolein, inderdaad belachelijk dat jij naar Groningen bent verhuisd! ;))
Lieve **Manon** en **Bertine**, bedankt dat ik altijd welkom ben bij jullie, bedankt voor onze tripjes. Manon, wat ben ik blij met jou in mijn leventje, rustig en beheerst, mijn ultieme maatje om te relativeren en voor alle outdoor activiteiten: those days are always the best with…you! Ik voel mij vereerd dat ik jouw getuige mag zijn. Lang leve T…..!
En dan mijn beste vriendinnetjes, **Tineke**, **Dani**, **Gwen**, **Anne** en **Leonie**. We zijn al bijna 15 jaar vriendinnen, bedankt voor de geweldige tijd! Ik weet dat ik altijd op jullie terug kan vallen. Ik zou denk ik altijd willen dat we elkaar vaker zagen, maar als geneesko's verspreid over het land is dat niet gemakkelijk. Toch ben ik onbeschrijfelijk blij met ieder van jullie. Dani, wat fijn dat ik altijd bij jou en Libbe terecht kan. Jouw visies en open houding geven mij altijd een beter gevoel. Gwen, ik ben blij voor alles wat wij hebben meegemaakt in onze mooie jaren samen en dat we dit promotie-avontuur samen zijn begonnen. Van de bieb in Maastricht tot promoveren in het AVL, ik ben trots op jou! Anne, jouw belletjes vanuit Maastricht zijn altijd erg fijn, bedankt dat jij er op afstand voor mij bent. Leo, onze enige specialist, tussen ons is het altijd goed als we elkaar zien, en dat is heel fijn. Ik weet dat jij er altijd voor mij bent. Tineke, waar jij ook bent, wij zien elkaar altijd. Van wekelijks Grey's Anatomy op de bank naar her en der in Nederland, weekendjes weg en radioberichtjes (I'll be there for you, cause you're there for me too). Bedankt voor jouw onvoorwaardelijke steun en belangrijke vriendschap. Fijn dat jij als paranimf naast mij wil staan.

Naast mijn vrienden heb ik natuurlijk ook nog mijn **familie** in Brabant. Lieve ooms en tantes, neefjes en nichtjes, bedankt voor jullie interesse en warmte als we elkaar zagen. Lieve **Kees** en **Tineke**, bedankt voor al jullie liefde, steun en gezelligheid. Ik voelde mij

altijd thuis bij jullie, of het nu bij ons was, bij jullie thuis of in een tentje bij Nice. Jullie zijn hele fijne mensen.
Lieve **Guy**, mijn echte twinsie, bedankt voor jouw steun en belletjes. Ik maakte mij op afstand altijd wel een beetje ongerust over jou, maar ik zie dat het goed met je gaat en daar ben ik heel blij om. Je bent een goeie kerel, heb vertrouwen in jezelf. Lieve **Mathijs**, ik ben trots op wat jij bereikt hebt. Jouw leventje is gelukkig aardig op orde. Bedankt voor de leuke bezoekjes bij jou thuis. **Heidy**, **Floris** en **Vera**, jullie maken mij altijd aan het lachen en doen mij beseffen hoe fijn simpele dingen kunnen zijn. Heidy, bedankt voor jouw altijd lieve woorden en begrip.
Pap en **mam**, bedankt voor jullie onvoorwaardelijke steun, ook al waren mijn keuzes soms moeilijk voor jullie. Dank je wel dat jullie er altijd voor mij zijn; mam, ik weet dat jij altijd aan me denkt. Jullie nieuwe huisje en goede zorgen voelen altijd een beetje als vakantie, dank daarvoor. Ik hou van jullie.

Merel, lieve schat, jij bent de afgelopen jaren de állerbelangrijkste geweest voor mij. Altijd was jij er. Jij hield mij op de been bij alle tegenslagen. Bedankt voor jouw liefde, steun, grapjes, hulp bij het afronden van het boekje, goede zorgen, culinaire dingetjes, onze reizen en zoveel meer. Bij jou thuiskomen was het beste van elke dag. Dat maakte mij intens gelukkig, wat er ook speelde. Ik hoop dat de toekomst voor ons beiden brengt wat onze hartjes begeren... Ik hou van jou, gewoon zoals je bent.